The use of nanofiltration membrane in desalinating brackish water

A thesis submitted to the University of Manchester for the degree of Doctor of Philosophy in the Faculty of Engineering and Physical Sciences and School of Chemical Engineering and Analytical Science

2010

Rasha Amer Hajarat

School of Chemical Engineering and Analytical Science

List of Contents

Total word count 76,336

Table of figures

Nomenclature

a	the solute radius.
a	the uncharged solute activity (mol/m³).
a_i	the activity of ion (i) in the solution (dimensionless).
a_i	the activities of ionic species (i) in the membrane.
$a_{i,m}$	the activity of ion (i) in the membrane (dimensionless).
a_i°	the activities of ionic species (i) in the solution.
a_p	the activity coefficient of the penetrate.
a_i	the activity of ion (i) (mol/m³).
A	the membrane surface area.
A_m	the membrane area.
A_{int}	the internal surface area.
A_o	the pore area where the solvent passes through it.
A	the membrane area (cm²).
A_f	the free area that depends on the size and the shape of penetrate molecules.
b	the friction factor.
B	the constant related to the minimum local free volume necessary to allow displacement.
c	the equilibrium concentration of the solute in the solution (mmol/l).
c	the uncharged solute concentration within the pore (mol/m^3).
c_b	the solute concentration in the bulk concentration.
c_b^+	the cation concentration in the bulk solution.
c_{BL}	the solute concentration in the boundary layer.
c_c	the concentrate solute concentration.
c_d	the solute dialysate inlet concentration.
c_f	the solute concentration in the feed (mol/l).
$c_{f,A}$	the concentration of component (A) in the feed.
$c_{f,B}$	the concentration of component (B) in the feed.
$c_{f,d}$	the solute dialysate inlet concentration.
$c_{f,i}$	the concentration of component (i) in the feed.
c_g	the gel concentration.
c_G	the gel layer concentration.
c_i	the concentration of component (i).
c_i	the concentration of ion (i) within the pore (mol/m³).
c_i	the concentration of component (i) in the membrane (mol/m³).
c_{ib}	the concentration of component (i) in the bulk-feed solution.
$c_{i,o}$	the concentration of component (i) in the feed solution.
$c_{i,1}^m$	the concentration of component (i) in the membrane where (1) is for feed/membrane phase.
$c_{i,1}^m$	the concentration of solute in the membrane and (1) is for solvent.
$c_{i,1}^x$	the concentration of component (i) in the solution or the solvent where (1) is for feed/membrane phase.
$c_{i,2}^m$	the concentration of component (i) in the membrane where (2) is for membrane/permeate phase.
c_i^+	the cation concentration in the concentrate solution.
$c_{i,o,(m)}$	the concentration of component (i) at the membrane-feed interface.
$c_{i,p}$	the concentration of component (i) in permeate.
$c_{i,p,(m)}$	the concentration of component (i) at the permeate-feed interface.

c_{im}	the concentration of component (*i*) at the feed-membrane interface.
c_{im}/c_{ib}	the concentration polarisation module.
c_m	the concentration at the membrane interface.
c^m_+	the concentration of positively charged ions in the membrane.
c^m_-	the concentration of negatively charged ions in the membrane.
c^m_{X-}	the concentration of membrane fixed charge.
c_o^+	the cation concentration in the dilute solution adjacent to the membrane surface.
c_p	the solute concentration in permeate (mol/l).
$c_{p,A}$	the concentration of component (*A)* in the permeate.
$c_{p,B}$	the concentration of component (*B)* in the permeate.
c_s	the solvent concentration.
c_t	the concentration at time *t*.
c_w	the solute concentration at the membrane/water (solvent) interface.
$\bar{c_w}$	the solute mean logarithmic concentration.
c_0	the concentration when time equal zero.
c'_i	the concentration of a hypothetical bulk phase in equilibrium with the interfacial concentrations inside the membrane at the boundary between two layers.
c_1°	the concentration of a single substance, a gas or the only permeating component of a solution in the first reservoir.
c_2°	the concentration of a single substance, a gas or the only permeating component of a solution in the second reservoir.
c°	the concentration of pure liquid in the reservoir.
c_1	the surface concentration.
$\bar{c}$	the mean logarithmic concentration.
c_+	the concentration of positively charged ions in the solution.
c_-	the concentration of negatively charged ions in the solution.
C_i	the ion concentration in the solution (mol/m³).
C_i	the concentration in the bulk concentration (mol/m³).
C_p	the solute concentration in permeate.
C_f	the solute concentration in the feed.
C_O	the feed concentration at time 0.
C_t	the feed concentration at time t, and *t* is the time.
$C_{i,p}$	the concentration of ion (*i*) in the permeate (mol/m³).
$C_{i,f}$	the concentration of ion (*i*) in the feed (mol/m³).
C_p	the uncharged solute bulk permeate concentration (mol/m³).
C_f	the uncharged solute bulk feed concentration (mol/m³).
Δc	the concentration difference between feed and permeate.
Δc_w	the solute concentration difference between the feed and permeate.
D	the diffusion coefficient.
d_{gas}	the gas molecule diameter.
D_i	the diffusion coefficient of component (*i*).
D_i	the diffusion coefficient of ion (*i*).
D_i	the diffusion coefficient of species (*i*) at concentration (*c*).
$D_{i,p}$	the hindered diffusivity (m²/s).
$D_{i,\infty}$	the bulk diffusivity (m^2/s).
D_o	the diffusion at zero concentration where it is small for small molecules and large for large molecules.
$D_{o,i}$	the diffusion coefficient of species (*i*) when its concentration is equal to zero.

D_p	the uncharged solute pore diffusion coefficient (m^2/s).
$D_{i,p}$	the pore diffusion coefficient of ion (i) (m^2/s).
D_s	the solvent diffusion coefficient.
D_s	the solute diffusivity.
D_T	the thermodynamic diffusion coefficient.
D_w	the solute diffusion coefficient.
D^+	the diffusion coefficient of the cation in solution.
Δd	the difference between the volume of the thermal expansion coefficient above the glass transition temperature and below it.
dc_i/dx	the concentration gradient of component (i).
dp/dx	the pressure gradient in the porous medium.
E	the electrical potential.
E	the measured potential in the solution (V).
E_{don}	the Donnan potential.
E^m	the measured potential in the membrane (V).
ΔE	the electrical potential difference.
$\Delta \tilde{E}_a$	the Arrhenius activation energy.
F	the Faraday number (96487 C/mol).
f	the fractional coefficient.
$f_{r,i}$	the frictional resistance for component (i).
F`	the friction force.
F'_{wm}	the viscous flow.
f_{wm}	the friction coefficient of the solute and the membrane.
f_{ws}	the friction coefficient of the solute and the solvent.
G_{11}	the cluster integral.
G	the hydrodynamic drag coefficient.
ΔG_{min}	the minimum free enthalpy of mixing.
h	the step-size.
ΔH_{min}	the minimum enthalpy of mixing.
$\Delta \tilde{H}^\circ$	the standard enthalpy.
i	the electrical current density.
I	the electrical current.
J	the flux.
J	the water flux (solvent).
J_c	the flux after cleaning.
j_i	the flux of ion (i) based on the membrane area ($mol/m^2.s$).
j_i	the factor mole increase due to dissociation for solute (i).
j_i	the ionic flux of ion (i) ($mol/m^2.s$).
J_i	the mass flux of component (i).
$J_{m,i}$	the mass flux for species (i).
$J_{n,i}$	the trans-membrane molar flux of species (i).
J_o	the original flux of the unfouled membrane.
J_O	the initial water flux.
J_{Oa}	the clean water flux after feed filtration.
J_{Ob}	the clean water flux before feed filtration.
j_s	the uncharged solute flux ($mol/m^2.s$).
J_s	the solute flux.
J_s	the solvent flux.
$J_{s,m}$	the solvent volumetric flux in the membrane.
J_v	the volumetric flux.

J_v	the volumetric flux in the boundary layer.
J_v	the volumetric flux through the membrane.
J_v	the volume flux based on the membrane area (m/s).
J_w	the solute flux.
k	the mass transfer coefficient.
k_{bl}	the fluid boundary layer mass transfer coefficient.
k_d	Henry's coefficient.
k_f	the mass transfer resistance in the feed boundary layer.
k_m	the membrane mass transfer coefficient.
k_{ov}	the overall mass transfer coefficient.
k_p	the mass transfer coefficient in the permeate boundary layer.
k_s	the solute mass transfer coefficient.
k_W	the solvent mass transfer coefficient that depends on Reynolds number.
k_w	the solubility or distribution coefficient.
k_0	the overall mass transfer coefficient.
(k_1 and k_{-1})	are rate constants.
K	the Kozeny-Carman constant.
K	the semi-empirical constant that depends on the permeate flux and ion diffusivity.
K	the hydrodynamic drag coefficient.
K	the partitioning coefficient between the membrane and the bulk solution.
K_{eq}	the equilibrium constant.
$K^G{}_i$	the gas phase sorption coefficient.
$K^L{}_i$	the sorption coefficient of component (i) in the liquid phase.
$K^L{}_i$	the liquid-phase sorption coefficient.
$K_{i,c}$	the hindrance factor for convection of ion (i) (dimensionless).
$K_{i,d}$	the hindrance factor for diffusion.
K`	the uptake of the solute by the membrane from the feed.
K'	the coefficient reflecting the membrane nature.
l	the membrane thickness (m).
L_i	the proportionality or phenomenological coefficient of component (i).
L_p	the permeability coefficient.
L_p	the solvent permeability coefficient ($m^3/m^2.s.bar$).
$L^\circ{}_p$	the standard permeability coefficient.
L_s	the local solute permeability ($L_s = L_s' \Delta x$).
L_s'	the solute permeability (m/s).
L_{11}	the hydrodynamic permeability or the solvent permeability coefficient, and is referred to as L_p.
L_{22}	the osmotic permeability or the solute permeability coefficient and is referred to as ϖ.
m_i	the molal concentration.
m_i	the molecular weight of component (i) (g/mol).
M	the average molar mass of organic/polymer.
M	the molar mass of the adsorbing compound (g/mol).
$\dot{M}$	the mass transfer.
n	the number of permeate samples.
n	the number of moles.
n_i	the composition of the gas material (i).
n_i	the molar fraction of component (i) (mol/mol).
$n_{i,o}$	the molar fraction of component (i) in the feed solution.

$n_{i,o,(m)}$	the molar fraction of component (i) at the feed-membrane interface.
n_p	the number of pores.
n_w	the number of moles for the solute.
$n`$	an integer.
N	the number of charged membranes pairs.
p	the pressure.
p_i	the partial pressure of species (i).
p_{ii}	the partial pressure of component (i) at the permeate side.
$p_{i,h}$	the partial pressure of component (i) at high pressure side.
$p_{i,l}$	the partial pressure of component (i) at the low pressure side.
p_i^o	the reference pressure of component (i).
p_i^o	the saturation pressure of component (i).
$p_{i,o}$	the partial pressure of component (i) at the feed side.
$p_{i,sat}$	the vapour saturation pressure.
$p_{i,sat}$	the saturation pressure of component (i).
$p_{i,v}$	the vapour pressure of component (i).
p_l	the pressure at the permeate side.
p_o	the applied pressure at the feed side.
P	the permeability.
P	the pressure (bar).
P	the permeability coefficient.
P^+	the cation permeability through the membrane.
P^-	the whole membrane permeability.
$P^L{}_i$	the permeability coefficient in the liquid phase.
P_{const}	the permeability constant that contains structural factors such as porosity and pore size.
Pe	the Peclet number.
$P^G{}_i$	the permeability coefficient.
P_i	the permeability of substance (i).
P_j	the permeability of substance (j).
$P°$	the vapour pressure (bar).
P_m	the permeability of membrane parts.
Δp	the pressure difference.
ΔP	the trans-membrane pressure difference.
ΔP_e	the effective pressure driving force (N/m).
Q	the volume flow rate.
Q_d	the dialysate volumetric flow rate.
Q_i	the volumetric flow rate of component (i).
Q_t	the volumetric flow rate of penetrate.
r	the pore radius (m).
r	the molecule radius.
r_i	stokes radius of component (i).
r_k	the Kelvin radius (m).
r_p	the effective pore radius (m).
r_p	the pore radius (m).
R	the rejection of ion (i).
R	the ideal gas constant (8.314 J/mol.K).
R	the total membrane stack resistance.
R_A	the resistance due to adsorption.
R_{am}	the resistance of the anion-exchange membrane.

R_{bl}	the boundary layer resistance.
R_c	the cake formation resistance.
R_{cm}	the resistance of cation-exchange membranes.
R_{cp}	the resistance of cell pairs.
R_{cp}	the concentration polarisation resistance.
R_{fc}	the resistance of the feed compartment.
R_G	the gel layer resistance.
R_{int}	the intrinsic retention.
R_m	the hydrodynamic membrane resistance.
R_m	the membrane resistance.
R_M	the clean membrane resistance.
R_O	the real retention.
R_{OBS}	the observed retention.
R_p	the internal pore fouling resistance.
R_{pc}	the resistance of the permeate compartment.
S	the entropy.
s	the solubility coefficient.
$\Delta\tilde{S}^\circ$	the standard entropy.
ΔS_{min}	the minimum entropy of mixing.
t_m^+	the membrane transport number for cations.
t^+	the cation transport number.
t	the time.
T	the temperature in Kelvin.
T_g	the transition temperature.
T	the absolute temperature (K).
ΔT_m	the temperature polarisation.
u_c	convective flow.
v	the relative velocity.
v_D	the diffusion flow.
$v_f(0,T)$	the free volume of the polymer at temperature (T) and in the absence of penetrate.
v_i	the partial specific volume of component (i).
V	the molar volume.
V	the solvent velocity (m/s).
V_c	the concentrate volume.
V_f	the free volume in the membrane.
V_i	the molar volume of species (i).
$\tilde{V}_i$	the partial molar volume of species (i).
V_i	the partial molar volume of ion (i) (m^3/mol).
V_s	the uncharged solute partial molar volume (m^3/mol).
V_{mol}	the molar volume (mol/m^3).
V_o	the membrane volume occupied by molecules at zero temperature.
V_p	the permeate volume.
V_s	the molar volume of solvent.
$\tilde{V}_s$	the partial molar volume of the solvent.
V_T	the observed membrane volume at temperature (T).
$\tilde{V}_w$	the partial molar volume of the solute.
V_w	the solute molar volume.
x	the distance from the membrane layer.
x	the membrane thickness (m).

x_i	the fraction of component (*i*) in the product.
$x_{i,}$	the mole fraction of component (*i*).
x_i	the fraction of component (*i*) in the feed.
x_w	the mole fraction of the solute (*w*).
Δx	the membrane thickness (m).
X_d	the effective membrane charge density (mol/m³).
X_i	the force.
y	the permeate recovery fraction.
Y	a constant.
z_i	the valence of ion (*i*) (dimensionless).

Abbreviations

aq	refers for the aqueous phase.
m	refers for the membrane phase.
m	refers for the membrane.
s	refers for the solvent.
w	for solute.
nstep	the number of steps.
CWFR	the clean water flux recovery.
FR	the flux reduction.
FR_{CWF}	the flux reduction with regards to clean water flux.
FR_{PF}	the flux reduction with regards to permeate flux.
MFI	the modified fouling index (s/l²).
MW	the molecule weight.
WFR	the water flux recovery.

Greek symbols

γ	the liquid surface tension.
γ°_i	the activity of ion (*i*) in the bulk solution.
γ_i	the activity coefficient of ion (*i*) within the pore (dimensionless).
γ`	the exponential constant related to the plasticizing effect of the penetrate on the polymer.
γ	the surface tension (N/m).
γ`	the plasticizing coefficient.
ϕ	the steric partitioning term.
$\varphi_{v,i}$	the volume fraction of the liquid inside the polymer.
$\varphi_{v,j}$	the volume fraction of the polymer.
ϕ	the uncharged solute steric partitioning coefficient (dimensionless) [$\varphi = (1-\lambda)^2$].
ϕ	the pressure ratio.
$\phi\Delta H_v$	the heat flux caused by convective transport through the pores.
$\phi\Delta H_c$	the heat flux caused by convective transport through the pores.
λ	the ratio of ionic or solute radius/pore radius.
λ	the stokes radius of component (*i*) to pore radius ratio.
λ_g	the heat conductivity in the pores.

λ_p	the heat conductivity in the solid part.
λ	the ratio of ionic or solute radius/pore radius.
λ	the mean free path.
λ_m	the overall heat conductivity of the membrane.
ω	the diffusion permeability.
ϖ	the solute permeability coefficient.
α_i	the separation factor.
α_1	the heat coefficients on the warm side of the membrane.
α_2	the heat coefficient on the cold side of the membrane.
α_{ij}	the separation factor of component (*i*) and (*j*).
α	the solute activity
σ	the reflection coefficient of the membrane toward the permeating solute.
σ_d	the Staverman osmotic reflection coefficient for the solute.
σ	the reflection coefficient (dimensionless).
γ_i	the activity coefficient of ion (*i*) in the membrane.
γ_i°	the activity of ion (*i*) in the bulk solution.
$\gamma_i^{`}$	the plasticizing constant for species (*i*).
γ_{SV}	the surface tension of the solid with the liquid vapour.
γ_{LV}	the surface tension of the liquid with the liquid vapour.
γ_{SL}	the tension of solid-liquid interface.
$\gamma^L{}_{i,o}$	the activity coefficient of the feed solution in the liquid phase.
$\gamma_{i,o,(m)}$	the activity coefficient at the feed-membrane interface.
γ_i	the activity coefficient (mol/mol).
θ_i	the tightness of the flows coupling of the solvent and the ions.
θ	the contact angle.
θ	the liquid solid contact angle.
η_T	the water viscosity at temperature (T).
$\eta_{20℃}$	the water viscosity at temperature 20 ℃.
η	the viscosity.
η	the solvent viscosity within pores (N s/m²).
η	the dynamic solvent viscosity.
χ	the interaction parameter.
χ_{ij}	the Flory-Huggins interaction parameter.
τ	the tortuosity.
ρ	the molar density, (mol/cm³).
υ_i	the molar volume of component (*i*).
Γ	the amount of solute absorbed per surface area (ng/cm²).
Γ	the adsorbed quantity of organic material (μg/m²).
Γ_{ij}	the selectivity coefficient.
δ	the boundary layer thickness.
δ	the membrane thickness.
ε	the porosity.
ε	the surface porosity.
ε	the pore volume fraction.
Ψ_c	the fraction of crystalline material present.
Ψ_i^m	the ion (*i*) electrochemical potential in the membrane (J/mol).
Ψ_i	the ion (*i*) electrochemical potential in the solution (J/mol).
Ψ_D	the potential difference (V).
Ψ	the potential within the pore (V).

Ψ_m	the potential in the membrane (V).
Ψ	the electrical potential (V).
$\Delta\Psi_D$	the Donnan potential (V).
$\mu_i^{m,o}$	the ion (*i*) standard reference state of the chemical potential in the membrane (J/mol).
μ°_i	the ion (*i*) standard reference state of the chemical potential in the solution (J/mol).
μ	the uncharged solute chemical potential (J/mol).
μ_i	the chemical potential of component (*i*).
μ_i°	the standard chemical potential and its constant.
$\mu_{i,o}$	the chemical potential in the feed solution.
$\mu_{i,o,(m)}$	the chemical potential in the membrane at the membrane-feed side interface.
μ_i	the electrochemical potential of ion (*i*) (J/mol).
μ_i^o	the chemical potential of pure component (*i*) at reference pressure.
$\Delta\mu_s$	the solvent chemical potential difference.
$\Delta\mu_w$	solute chemical potential difference.
$\beta(T)$	constant characterising the extent to which the penetrate contributes to the free volume.
$\varphi_{polymer,1}$, $\varphi_{polymer,2}$, $\varphi_{polymer,3}$	the volume fractions of membrane polymer components.
φ_i	component (*i*) volume fraction.
φ_p	the volume fraction of penetrate.
φ_1	the volume fraction of non-solvent.
π	the osmotic pressure (N/m^2).
$\Delta\pi_{INORG}$	the osmotic pressure of an inorganic solute.
$\Delta\pi_{ORG}$	the osmotic pressure of an organic solute.
$\Delta\pi$	the osmotic pressure difference across the membrane.
$\Delta\pi_i$	the difference between the osmotic pressures in the external solutions at the membrane for species (*i*).

Abstract

The demand on clean water is increasing, for example because of the increase in the pollutants that are being released to the environment or the lack of natural clean water resources as in the arid areas which is the case in Jordan, which is considered as one of the most scarce water countries in the World. In Jordan, the natural water resources are limited and the country's population is continuing to rise thus increasing the demand on water and the production of wastewater. As a result, a gap between the water supply and the demand on water is increasing because of a high population growth rate and a fast social-economical development. The water problem in Jordan was deepening by the fact that Jordan shares most of its surface water resources with neighbouring countries that control these resources; this partially disallowed Jordan of its fair share of fresh natural water. To overcome the water shortage, water was overdrawn form the highland aquifers, resulting in degradation in water quality. Thus desalinating brackish water using nanofiltration membrane might be a technically and economically practical process to overcome the water scarcity in Jordan. The purpose of this work is to investigate the rejection behaviour of ions from brackish water using nanofiltration membrane.

In this work, both experimental and theoretical work was done in order to try to understand nanofiltration membrane separation behaviour. In the experimental work, two tubular ceramic nanofiltration membranes were used. The used ceramic nanofiltration membranes were made of TiO_2, with 7.00 mm I.D, 10 mm O.D and length of 190 mm, with 0.9 and 1.0 nm mean pore diameter. The zeta-potential for both membranes was measured at a pH range between 3-10, then the iso-electric point (ISP) was found. The ISP was used in determining the membrane charge, were the membrane charge is a major parameter in justifying the ions rejection behaviour. The membrane zeta potential was measured by preparing NaCl at two different concentrations, which were 0.01M and 0.1M. Then the pH of each solution was changed to different values ranging between 3 and 10. For 0.01M concentration solution, the ISP was around 4.6. While for 0.1M concentration solution, the ISP was around 5.0. In addition, it was found that the membrane zeta potential was affected by the salt type. This was investigated by preparing four different salts solutions at three different concentrations (0.01M, 0.1M and 1.0M). The used salts were NaCl, MgCl2, $NaNO_3$ and Na2SO4. The membrane active layer was measured by using SEM-EDXS equipment, and it was found to be around 20.0μm. The membrane active layer was used in the mathematical modelling.

The separation behaviour for 0.9 and 1.0 nm nanofiltration membranes was studied by measuring the rejection of different salts in a single salt solution and tertiary salts solution. The same parameters values such as the feed volumetric flux, the concentration and TMP were used for both membranes. They were used to desalinate water samples containing NaCl, $NaNO_3$, Na_2SO_4, $MgCl_2$, $MgSO_4$ and $CaCl_2$. The salts were divided into two groups, the first group consisted of NaCl, $NaNO_3$, and Na_2SO_4, and the second group consisted of $MgCl_2$, $CaCl_2$ and NaCl. Two different concentration values (0.01M and 0.1M) were used to try to understand the effect of concentration on ions rejection. To study the separation behaviour of the membrane, distilled water was used at first, and then single or tertiary salt solutions. The results of distilled and brackish water were compared to describe the separation behaviour. It was noticed that the permeation of distilled water was higher than the permeation of brackish water - for the different solutions that were used.

In the case of 0.9 nm membrane with 0.1M feed concentration, for $NaNO_3$ solution it was found that the rejection of NO_3^{1-} ions was higher than the rejection of Na^{1+}. The highest rejection for both ions was at the lowest TMP, where the rejection of NO_3^{1-} was about 63% and the rejection of Na^{1+} was about 53%. For Na_2SO_4 solution, the rejection of SO_4^{2-} ions was higher than the rejection of Na^{1+} ions. The highest rejection of SO_4^{2-} was about 31% and the highest rejection of Na^{1+} was about 8%. For NaCl solution, rejection of Cl^{1-} ions was higher than the rejection of Na^{1+} ions. The highest rejection of Cl^{1-} was about 22% and the highest rejection of Na^{1+} was about 8%. For mixed salt solution, the rejection of ions took the following trend: R of SO_4^{2-} > R of NO_3^{1-} > R of Cl^{1-} > R of Na^{1+}. The highest rejection of SO_4^{2-} was 62%, NO_3^{1-} was 51%, Cl^{1-} was 42%, and Na^{1+} was 37%. In the second group, for $MgCl_2$ solution, the rejection of Cl^{1-} ions was higher than the rejection of Mg^{2+} ions. The highest rejection for both ions was at the lowest TMP, where the rejection of Cl^{1-} was about 38.4% and the rejection of Mg^{2+} was about 39%. For $CaCl_2$ solution, the rejection of Ca^{2+} ions was higher than the rejection of Cl^{1-} ions and the highest rejection for Ca^{2+} was about 52% and for Cl^{1-} was about 48%. For a solution containing $MgCl_2$, $CaCl_2$ and NaCl the rejection of ions took the following trend: R of Cl^{1-} > R of Ca^{2+} > R of Mg^{2+} > R of Na^{1+}. The highest rejection of Ca^{2+} was about 57.6%, Mg^{2+} was about 58.3%, Na^{1+} rejection was about 53.9% and Cl^{1-} rejection was about 51%.

In the case of 1.0 nm membrane with 0.1M concentration, the rejection of NO_3^{1-} ions from $NaNO_3$ solution was higher Na^{1+} ions rejection. NO_3^{1-} highest rejection was about 36.0% and

Na^{1+} was about 30.2%. The rejection of SO_4^{2-} ions from Na_2SO_4 solution was higher than Na^{1+} ions rejection. SO_4^{2-} highest rejection was about 33.6% and Na^{1+} was about 20.0%. Cl^{1-} rejection from NaCl solution ions was lower than Na^{1+} rejection. The highest rejection of Cl^{1-} was about 34.7% and Na^{1+} was about 37.3%. For a solution containing Na_2SO_4, $NaNO_3$ and NaCl the rejection of ions took the following trend: R of Na^{1+} > R of NO_3^{1-} > R of Cl^{1-} > R of SO_4^{2-}. The highest SO_4^{2-} rejection was about 53.3%, the highest NO_3^{1-} rejection was about 46.9%, the highest Cl^{1-} rejection was about 43.2% and highest Na^{1+} rejection was about 45.6%, and the highest rejection for all anions was at the lowest TMP. In the second group, the rejection of Cl^{1-} from $MgCl_2$ was higher than the rejection of Mg^{2+}, where the highest rejection of Cl^{1-} was about 48.8% and Mg^{2+} was about 38.6%. The rejection of Ca^{2+} from $CaCl_2$ was lower than the rejection of Cl^{1-}. The highest rejection of Ca^{2+} was about 37.4% and Cl^{1-} was about 40.0%. For a solution containing $MgCl_2$, $CaCl_2$ and NaCl, the rejection of ions took the following trend: R of Cl^{1-} > R of Ca^{2+} > R of Mg^{2+} > R of Na^{1+}. The highest rejection of Ca^{2+} was 43.1%, Mg^{2+} was 42.1%, Na^{1+} was 33.0% and Cl^{1-} was 44.6%.

For 0.01M concentration, $MgCl_2$ and $NaNO_3$ salts were used for both 0.9 and 1.0 nm membranes. In the case of 0.9 nm, the rejection of NO_3^{1-} ions from $NaNO_3$ solution was lower than the rejection of Na^{1+} ions. The highest rejection for both ions was at the lowest TMP, where the rejection of NO_3^{1-} was 46% and the rejection of Na^{1+} was 42%. The rejection of Mg^{2+} from $MgCl_2$ solution was higher than the rejection of Cl^{1-}, where the rejection of Cl^{1-} was 13% and the rejection of Mg^{2+} was 36%. The rejection of ions from $MgCl_2$ and $NaNO_3$ solution took the following trend: R of Mg^{2+} > R of NO_3^{1-} > R of Cl^{1-} > R of Na^{1+}. The highest rejection for all ions was at the lowest TMP, where the rejection of Cl^{1-} was 45.3%, NO_3^{1-} was 55.4%, Na^{1+} was 47.4% and Mg^{2+} about 55.5%. In the case of 1.0 nm, the rejection of NO_3^{1-} from $NaNO_3$ was higher than the rejection of Na^{1+}. The highest rejection for both ions was at the lowest TMP, where the rejection of NO_3^{1-} was 15.3% and Na^{1+} was 11.6%. The rejection of Cl^{1-} ions from $MgCl_2$ was higher than the rejection of Mg^{2+} ions, where the rejection of Cl^{1-} was about 14.4% and the rejection of Mg^{2+} 11%. The rejection of ions from $MgCl_2$ and $NaNO_3$ solution took the following trend: R of Mg^{2+} > R of NO_3^{1-} > R of Cl^{1-} > R of Na^{1+}, where the rejection of Mg^{2+} was 20.0%, NO_3^{1-} was 19.8%, Cl^{1-} was 16.4% and Na^{1+} was 4.8%.

Another parameter that was considered is the pH of the feed solution, to try to understand the pH effect on the rejection. For 1.0 nm membrane pore, a single and a mixed salts solution

were used and their pH was controlled to values of 3, 7 and 10. At pH3, the rejection of Cl^{1-} ions from NaCl solution was lower than the rejection of Na^{1+} ions, where the rejection of Cl^{1-} was about 24.9% and the rejection of Na^{1+} 25.4%. The rejection of SO_4^{2-} from Na_2SO_4 solution was lower than the rejection of Na^{1+}, where the rejection of SO_4^{2-} was 39.6% and the rejection of Na^{1+} was 46.5%. The rejection of SO_4^{2-} ions from mixed salt solution was higher than the rejection of Cl^{1-} ions, where the rejection of SO_4^{2-} was 50.0%, the rejection of Cl^{1-} was 39.0% and the rejection of Na^{1+} was 49.9%. For pH7, the rejection of Cl^{1-} ions from NaCl solution was lower than the rejection of Na^{1+} ions, where the rejecting of Cl^{1-} was about 38.8% and the rejection of Na^{1+} 42.3%. The rejection of SO_4^{2-} ions from Na_2SO_4 solution was higher than the rejection of Na^{1+} ions, where the rejection of SO_4^{2-} was 55.2% and the rejection of Na^{1+} was 48.0%. The ions rejection from mixed salt solution took the following trend: $Na^{1+} > SO_4^{2-} > Cl^{1-}$, where the rejection of SO_4^{2-} was 28.4%, the rejection of Cl^{1-} was 24.1% and the rejection of Na^{1+} was 32.0%. For pH10, the rejection of Cl^{1-} from NaCl was higher than the rejection of Na^{1+}, where the rejection of Cl^{1-} was 27.5% and the rejection of Na^{1+} was 25.5%. The rejection of SO_4^{2-} from Na_2SO_4 was higher than the rejection of Na^{1+}, where the rejection of SO_4^{2-} was 54.6% and the rejection of Na^{1+} was 48.8%. The ions rejection from mixed salt solution took the following trend: $Na^{1+} > SO_4^{2-} > Cl^{1-}$, where the rejection of SO_4^{2-} was 34.1%, the rejection of Cl^{1-} was 28.8% and the rejection of Na^{1+} was 38.5%. The rejection of Na^{1+} and Cl^{1-} from NaCl at pH 3 was lower than the rejection from pH 7 and 10 solutions, but the best rejection was from pH 7 solution. The rejection of Na^{1+} and SO_4^{2-} from Na_2SO_4 at pH 3 was lower than the rejection from pH 7 and 10 solutions. The rejection of Na^{1+}, Cl^{1-} and SO_4^{2-} from mixed salt solution at pH 3 was higher than their rejection from pH 7 and 10 solutions.

Flux-step method was used to measure the rejection of ions at the lowest TMP values for different feed volumetric fluxes. For $MgSO_4$ solution, the rejection of SO_4^{2-} was higher than the rejection of Mg^{2+}. The highest rejection for both ions was at the lowest TMP, where the rejection of SO_4^{2-} was about 72.4% and the rejection of Mg^{2+} was about 72.1%. For $MgCl_2$ solution, the rejection of Cl^{1-} was slightly higher than the rejection of Mg^{2+}. The highest rejection for both ions was at the lowest TMP, where the rejection of Cl^{1-} was about 76.0% and the rejection of Mg^{2+} 76.3%. For mixed salts solution, the rejection of ions took the following trend -except at the lowest TMP-: R of SO_4^{2-} > R of Cl^{1-} > R of Mg^{2+}. The highest rejection for all the ions was at the lowest TMP, where the rejection of Cl^{1-} was about 50.8%, the rejection of SO_4^{2-} was about 57.4%, and the rejection of Mg^{2+} was about 52.3%.

In the theoretical work, Nernst-Planck equation was used to try to understand the separation behaviour of nanofiltration membrane. Nernst-Planck equation was solved by using two mathematical methods, which are Euler and Runge-Kutta methods, and the solution was obtained by using FORTRAN program. The two programs were run for different feed concentration and permeate flux (volume flux based on the membrane area). The model was solved for NaCl solution at two different feed concentrations, which were 0.01 and 0.1 mol/m^3. The membrane active layer thickness was assumed equal to 20.0E-6 m, which was obtained from the experiments. For each concentration value, the model was solved for different volume flux values that ranged between 1.0E-7 to 9.0E-6 $m^3/m^2/s$. These readings were similar to the values used in the exponential part. The change in these parameters values was done to observe their effect on the membrane rejection and if the results obtained from the theory agrees with the results obtained from the experiments. The rejection of Cl^{1-} was higher than the rejection of Na^{1+}. The rejection of Na^{+1} and Cl^{-1} ions increased as the volumetric flux based on membrane area (J_v) increased. Also the concentration of Na^{+1} and Cl^{-1} ions inside the membrane active layer decreased as the volumetric flux based on membrane area (J_v) increased. In addition, the rejection of Na^{+1} and Cl^{-1} ions decreased as the feed concentration increased.

Declaration

No portion of the work referred to in the thesis has been submitted in support of an application for another degree or qualification of this or any other university or other institute of learning.

Rasha Amer Hajarat

Copyright Statement

Acknowledgment

The author wishes to gratefully acknowledge and thank the late Dr. Alec E. James — may his soul rest in peace — for his support, supervision, advice, guidance and patience during the research period and writing process. The author also wishes to gratefully acknowledge and thank Dr. Alastair Martin for his excellent advice and help. The author would like to gratefully acknowledge and thank the internal examiner and advisor Dr. Xue-Feng Yuan for his excellent advice and support.

The author wishes to thank Mr John Riley, Mrs Elizabeth Davenport and Dr. Mustafa Nasser for their valuable help and assistance. The author would also like to thank Mr. Alastair Bewsher and Mr. Paul Lythgoe at the Analytical Geochemistry Unit at the University of Manchester for conducting the analytical analyses for the samples. The author wishes to thank her colleagues Tania Rojas, Amer Al-Naimi, Eddi and Petros for their support.

Dedication

This thesis is dedicated to my family for their support and encouragement, especially my dad who is a big inspiration and great role model to follow up, and my brother Ishaq.

To my dad

You may have thought I didn't see,
Or that I hadn't heard,
Life lessons that you taught to me,
But I got every word.

Perhaps you thought I missed it all,
And that we'd grow apart,
But Dad, I picked up everything,
It's written on my heart.

Without you, Dad, I wouldn't be
The woman I am today;
You built a strong foundation
No one can take away.

I've grown up with your values,
And I'm very glad I did;
So here's to you, dear father,
From your forever grateful kid.

By Joanna Fuchs

Chapter 1 Introduction

The demand on clean water is increasing, for example because of the increase in the pollutants that are being released to the environment or the lack of natural clean water resources as in the arid areas which is the case in Jordan, which is considered as one of the most scarce water countries in the World. Jordan has suffered shortage in water resources since the early 1960s and classified as water scarce. Available water resources in Jordan are limited due to the arid and semi-arid climate. In addition, the economic development and the population growth are increasing the demand on the available water resources, which affect the quantity and the quality of water resources. Furthermore, the water shortage problem faced more complications due to severe drought periods. The major sources of water in Jordan are

- Seawater at the Gulf of Aqaba.
- Brackish water in the South of Ghore.
- Saline water springs.

On the other hand, it is difficult to exploit such resources because of the country's topography, the distance between these scattered resources, the need for special treatment to remove some sorts of chemicals such as manganese. At present, the economy of Jordan cannot support the full implementation of seawater desalination as fresh water source. Thus, a good and cheap method of desalinating brackish water is needed.

Even though efficient conventional desalinating processes are available and commonly used in desalinating brackish water, but by the rise in fuel prices and considering that most of the arid areas or the one which needs clean water resources have limited energy sources, and new types of pollutants are being released to the environment such as heavy metals that conventional desalinating processes do little to remove them, thus alternative processes should be considered for desalinating brackish water such as membrane processes. Nonetheless, conventional processes seem more dependable because the membrane process operating costs are relatively high, compared to the conventional processes, also the low water quality produced by the membranes compared to the conventional processes. However, these obstacles are being overcome by research.

Membrane is a permeable selective barrier that restricts the motion of particles through it, and they differ in their applications and structures; they operate in different ways and their main objective is to separate one component from a mixture by allowing the component to permeate though it, thus preventing the other components from passing through the membrane or vice versa. It has the ability to transport one component more readily than other components because of the differences in physical and/or chemical properties between the membrane and the permeating component. The membrane performance is controlled by two factors: the membrane selectivity of the solute in the solution, and the flux of the solvent through the membrane. To gain the best separation results, the membrane must be thermally stable, have high selectivity toward the solutes, have high permeability and high chemical resistance. Membrane can be homogenous or heterogeneous, symmetric or asymmetric in structure, and may be either neutral or carry positive charge, negative charge or both charges. The separation process can be achieved because of the difference in size, physical and chemical structures between the different components in the solution. Membrane separation process occurs at ambient temperature; as a result, if the solution is insensitive toward temperature, it can be treated without the constituents of being damaged or chemically altered. Membrane separation process is faster, more efficient and more economical than conventional separation techniques. The advantages of membrane separation process are as follows

1. Separation occurs continuously.
2. Energy consumption is low.
3. Membrane process can be combined with other separation processes.
4. Separation can be carried under mild conditions.
5. Separation process can be up-scaled easily.
6. Membranes have different properties and can be adjusted.
7. No additives are required.

On the other hand, it has the following disadvantages

1. Membrane fouling and concentration polarisation.
2. Membrane lifetime is short due to fouling and concentration polarisation.
3. Low selectivity.

The membrane has the property of being selective towards molecules, where the molecules

either can permeate through the membrane or be rejected by the membrane. The membrane selectivity is determined by the flux through the membrane and the membrane itself. Membrane separation technology involves different kinds of processes, which can be divided into the following

1. First generations of membrane processes, which include microfiltration, ultrafiltration, hyper-filtration, nanofiltration, reverse osmosis, electro dialysis and dialysis.
2. The second generation of membrane processes, which include gas separation, pervaporation, membrane distillation and separation by liquid membranes.

An example of a membrane process that would be a good choice to be considered is nanofiltration membrane process, where it can be used in treating water such as removing organic and inorganic compounds, removing hardness, removing viruses and bacteria, removing pesticides and removing taste and odours. Thus, with the ability to do what have been mentioned, gives nanofiltration membrane more favour over conventional desalinating processes because they cannot perform such job in one stage and need additional processes to complete the needed task. In the case of treating brackish water, nanofiltration has the advantages of being selective towards ions types, operates at low applied pressure values and has a high permeate flux. Brackish water is more saline than fresh water but not as saline as seawater, where its salinity ranges between 0.5-30 ppt of salts – salinity is the dissolved salt content of a body of water. Where nanofiltration can remove undesirable materials in one-step, on the other hand conventional processes might need several steps to do so, as a result nanofiltration can be considered more efficient and cheaper. Another competitive process to nanofiltration is reverse osmosis because it has higher rejection rates than nanofiltration. Nonetheless, reverse osmosis requires higher applied pressure than nanofiltration which would result in higher operating costs. In addition, sometimes some minerals have to be added to the treated water by reverse osmosis, which increases the operating cost. On the other hand nanofiltration has lower rejection than reverse osmosis, were some compounds permeates through it and the resulting product would be as desired. Thus to make nanofiltration process more usable and efficient then more research is needed to be done in order to try to understand it’s separation behaviour, so that it could be optimised and made more efficient to be used in real life.

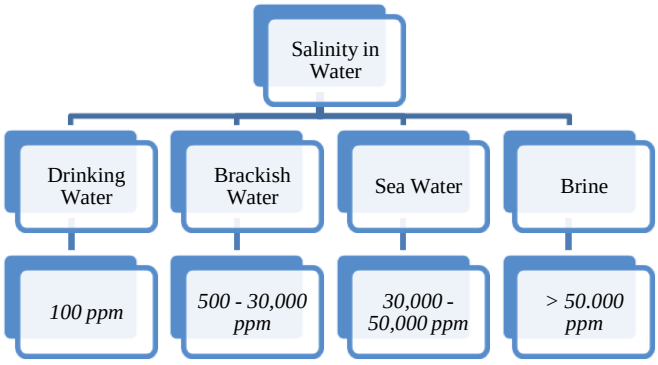

Figure 1-1. Salinity of water.

Membrane process is a new approach that is being considered in treating brackish water such as nanofiltration membrane, because of its capability of being able to reject ions and its selectivity towards ions. Hence, this work would be more concerned with the first generation of membranes especially the nanofiltration membrane process. These different types of membranes would be discussed in more details in the following chapters, such as membrane classifications, membrane characterisation, the different membrane processes, the driving forces through the membranes that would cause the rejection of solutes from solutions and membrane fouling.

Nanofiltration membrane is a pressure-driven membrane with properties that lie between ultrafiltration and reverse osmosis. Nanofiltration membrane is used in different applications such as softening water, removing hardness, natural organic matter, heavy metals, viruses and bacteria, and concentrating organic dyes. Since there are several uses for nanofiltration membrane, there is a need to try to understand its separation behaviour and how to improve its separating mechanism, especially in desalinating brackish water.

1.1 Thesis objective

Since the demand on clean water is increasing then new methods in treating water should be considered such as membrane processes. Nanofiltration process would be a good approach because it has a selective rejection between ions, operates at low pressures and has a high flux. Since nanofiltration is widely used but less knowledge about its separation behaviour is available, as a result lots of work needs to be done in order to try to understand its separation behaviour in-order to increase its separation efficiency. The aim of this work is to try to understand the ions separation behaviour for nanofiltration membrane. In-order to do so theoretical and experimental work was done for different ions that would exist in brackish

water. The main objectives of this work were

1. Try to understand the theory behind nanofiltration process, in-order to obtain the right knowledge required to operate the process theoretically and experimentally. (refs. 7, 66, 170, 219, 257).
2. Try to solve the extended Nernst-Planck equation by using two different mathematical modules. (refs. 7, 13, 97, 290, 325, 326, 327, 339, 344, 348).
3. Run experimental work for two tubular ceramic nanofiltration membrane that are prepared from the same materials but with a different in the pore diameters. Ceramic membranes were chosen because less work have been done using them and in general ceramic membranes have longer life than other types and can be restored to their original conditions by using simple cleaning methods. Different pore diameters were considered in-order to get an idea about how much impact would such property have on the rejection. (refs. 1, 145).
4. Different salts would be used as in single salt and mixed salts solutions for two different concentrations. Where two ions and four ions solutions would be used to try to understand the effect of ions type and valences on the rejection. Most of the available work includes binary or ternary ions; as a result, four different ions were used to try to understand the effect of ions type on their rejection. (refs. 5, 6, 17, 30, 51, 72, 97, 139, 212, 351).
5. Taking into consideration the effect of the solution pH on the rejection of nanofiltration for a single salt and a mixed salts solutions. This would be done to try to understand the effect of pH on the ions rejection along with the existence of different ion types at different concentrations. (refs. 321, 351).
6. Measuring the zeta potential for a powdered membrane, where the membrane powder would be diluted in different salt solutions at different concentrations and pH values. Such procedure would be followed in-order to understand the effect and try to establish a relation between the ion type, the ion concentration and the pH on the zeta potential. Similar approach was followed by Tim Van Gestel et.al (ref. 312) but in this work, the zeta potential would be measured by using a different device, using a different salt types and ions concentration. (refs. 38, 47, 126, 150, 210, 328).
7. Another parameter that would be considered is the TMP because it should have an effect on the ions rejection. Even though TMP had been considered before by many researchers (27, 44, 47, 130, 131), but the aim of this work to use low TMP values – not more than 2

bars – which have not been approached before. Such approach would be considered is to try to link TMP with other parameters such as Donnan effect.

8. Another parameter that would be considered is the feed volumetric flux, where the TMP is at its minimum value for each different feed volumetric flux. This was done to try to find the best conditions for the highest nanofiltration rejection.

1.2 Achievements

Nanofiltration membrane process is a new approach that could be used in desalinating brackish water, and there are several parameters that would affect nanofiltration rejection. The extended Nernst-Planck equation was solved numerically by using the same initial parameters that were used in the experimental part such as the initial ions feed concentration, the membrane thickness, the membrane surface area and the permeate flux (volume flux based on the membrane area). This was done to be able to compare the theoretical with the experimental rejection results, and to be able to have a theoretical understanding about the behaviour of the ions concentration inside the membrane for such parameters. From the theoretical modelling, it was noticed that solving the extended Nernst-Planck equation by using a more accurate mathematical model would give results that would agree with the experimental results except for the ions rejection values. For example the rejection of the ions from the higher initial feed concentration should be less than the rejection of the ions from the lower initial feed concentration, and this was observed from the experimental results and from solving the numerical equations using Runge-Kutta mathematical model, but an opposite results were obtained by using Euler mathematical model. The theoretical modelling was only done for sodium chloride (NaCl) because there were some parameters that it were hard to obtain them from the literature, and they need a set of experiments to be done in-order to obtain their values such as the hindrance factor for convection inside the membrane, the hindered diffusivity and the Donnan potential. Such limitations made it hard to run the programme for the four ions solution that was used in the experiments.

From the pH-controlled experiments, it was found that the ions rejection had better rejections than that obtained from the non-controlled pH experiments. On the other hand, the rejection behaviour differed, where the rejection of ions changed as the membrane charge sign at pH 3 changed, and these results were supported by the obtained zeta potential results. Also at pH 10, the rejection of ions was lower than the rejection from the solutions at pH 3 and 7, which might be due to the increase in the membrane charge, which would have caused

concentration polarisation.

The membrane charge behaviour was obtained from the zeta potential measurements, which supported the rejection results obtained from the controlled and the non-controlled pH experiments. The used approach in measuring the zeta potential would be simpler and somehow gives more accurate results than measuring the zeta potential from the streaming potential (150), because the streaming potential measurements should be instantaneous and this would include human error, which would decrease the readings accuracy.

By comparing the rejection of ions from binary and four ions solutions, the rejection behaviour differed for some ions. This might be due to the higher ions valencies concentration, ions chemical speciation and ions interactions. Nonetheless higher rejections were obtained from mixed salts solutions, this would be more encouraging to use nanofiltration in desalinating brackish water because natural water contains different types of salts. Also since the best rejection values were obtained at the minimum TMP value, this means less operating costs, which could be considered as an advantage.

1.3 Chapters guideline

Chapter 0 Objectives and Summary. This chapter gives a brief justification and a general summary about this work and the used approaches in it.

Chapter 1 Introduction. This chapter gives a brief idea about the membrane processes such as their advantages and disadvantages, the driving forces that cause permeation through the membrane and the membrane efficiency.

Chapter 2 Classification of membranes. This chapter gives a general idea about the membrane categories. Where the membranes are categorised according to the material they are made of into two main groups, which are biological and synthetic membranes. Another approach in classifying the membranes is according to their structure and separating principles, where they are divided into three sub-groups, which are porous, non-porous and liquid membranes. In addition, this chapter gives a general idea about the membrane preparation techniques.

Chapter 3 Membrane characterisation. This chapter discusses the used characterisation techniques that are used in characterising the porous and the non-porous membranes. Where membrane characterisation can relate the membrane structure to the membrane separating properties.

Chapter 4 Types of membranes. In this chapter, the membranes are separated according to their driving forces into four major groups, and these driving forces are the pressure difference, the concentration difference, the temperature difference and the electrical potential difference.

Chapter 5 Separation models. This chapter is concerned with the theory related to the driving forces needed to cause separation between the molecules. In addition, it relates irreversible thermodynamics to the driving forces that causes separation in the membranes.

Chapter 6 Membrane fouling. This chapter is about the major obstacles that limit the use of membranes, which are fouling, concentration polarisation and temperature polarisation. To increase the membrane efficiency, then more knowledge about these barriers is needed to try to decrease their appearance in the membrane processes.

Chapter 7 Nanofiltration membrane. This chapter is related to nanofiltration membrane, which was the used membrane in this work. This chapter goes in details about nanofiltration membrane as in the theory that describes the permeation of charged and uncharged molecules through nanofiltration membrane, factors affecting the retention of molecules through nanofiltration membrane such as the acid-base transformation, and nanofiltration membrane fouling.

Chapter 8 Experiments. This chapter describes and discuses the experimental work that have been done. Where the theory, the used methods, the used experimental procedures and the experimental results have been discussed in details.

Chapter 9 Modelling. This chapter is concerned with the theoretical modelling that has been done. Where Euler and Runge-Kutta numerical methods were used to solve the extended Nernst Planck equation, where it describes the permeation mechanisms of ions through nanofiltration membrane. Where the equations were solved by using Fortran (F77) and the initial conditions used to solve the equations were obtained from the experiments.

Chapter 10 Discussion and conclusion. This chapter includes the discussion of the obtained results from the experimental work, and a comparison between the obtained theoretical and experimental results that have been done.

1.4 Summary

Nanofiltration membrane is becoming a noteworthy process that would be used in treating water as the demand on clean water is increasing and the sources of water with acceptable qualities in the nature are decreasing. Nanofiltration membrane has a selective ability towards

the ions, needs a low TMP to cause ions rejection and low operating costs, which give nanofiltration membrane a good advantages over other membrane processes and conventional desalination processes. Nanofiltration membrane can be used in treating water because it has the ability to remove different types of organic and inorganic materials. Even though the rejection of nanofiltration membrane for some ions such as Na^{1+} and Cl^{1-} is considered low, but since nanofiltration membrane is an adaptable process then the ions rejection can be enhanced by changing the operating conditions. In this work different parameters and conditions such as the ions species, the ions concentration, the TMP and the solution pH, were considered in order to try to understand their effect on nanofiltration membrane rejection and how does the membrane behave under such conditions.

Chapter 2 Classification of membranes

The type of membrane used in a separation process is an important and critical factor. From the membrane classification more information about the membrane and better understanding can be obtained. Where membranes can be classified into two main groups: biological and synthetic membranes. Synthetic membranes can be classified into organic (polymeric) and inorganic membranes. In this work, the used membranes were two different types of synthetic membranes, which were ceramic and polymeric membranes. Another way to classify membranes is to separate the membranes according to their structure and separation principles into porous membranes, nonporous membranes and liquid membranes.

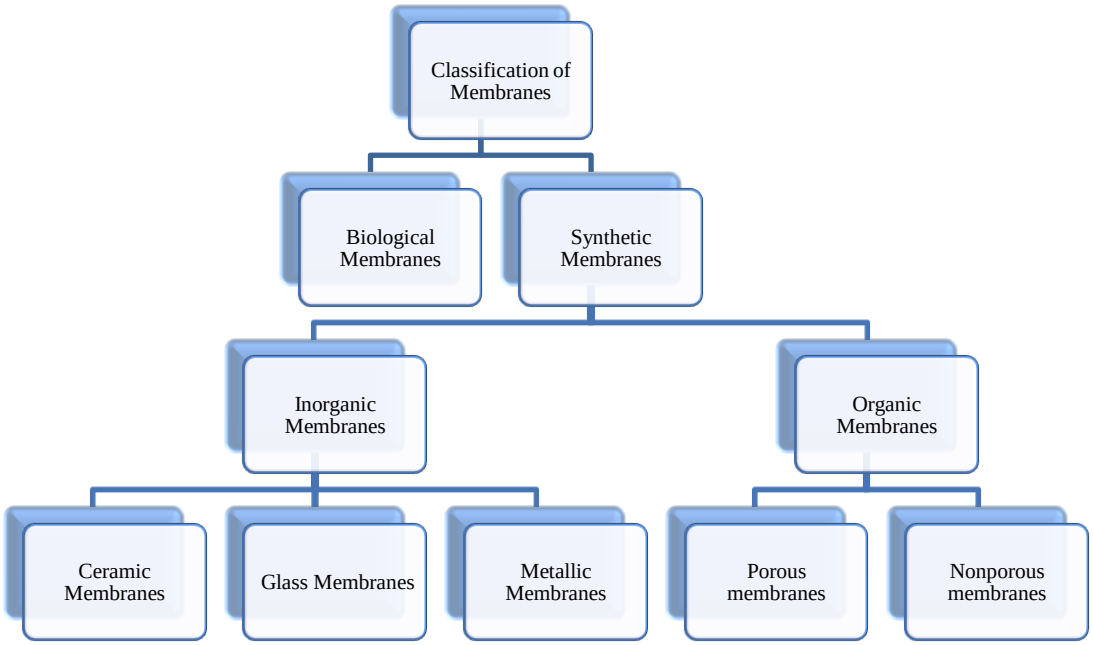

Figure 2-1. Classification of membranes.

2.1 Biological membranes

The biological membranes have very complex structures, while various biological membranes contain a basic lipid bi-layer structure, and each molecule has hydrophobic and hydrophilic parts. The hydrophilic sides are situated toward the solution/membrane interface while the hydrophobic exists between the hydrophilic parts. The biological membranes consist of two main components, which are the lipid bi-layer (the backbone) and the proteins (responsible for the transport function). Two types of transport occur in biological membranes: the passive and active transport. In the active transport, the solute permeates through the membrane against its concentration gradient and is coupled to a chemical

reaction. In the passive transport, the permeation of solute is a result of the concentration gradient across the membrane without the need of chemical energy. There are three different types of passive transport mechanisms:

1. Facilitated diffusion. A carrier (protein) allows the solute to diffuse through the membrane. The transport of the solute is a result of the concentration gradient, where the solute permeates from the higher concentration side to the lower concentration side. The solute can be transported against its concentration gradient (i.e., from low concentration to high concentration) by using a cellular energy.
2. Co-transport. If the solution contains two components A and B, which exists on the same side of the membrane, and the driving force, is the concentration gradient of component A, the two components transport with each other and component B transport against it, which is the concentration gradient.
3. Counter-transport. If two components A and B exist on the opposite sides of the membrane, and the driving force is the concentration gradient of component A, the two components transport in the opposite direction and component B may transport against it, which is the concentration gradient.

2.2 Synthetic membranes

Synthetic membranes are divided into two groups: organic and inorganic membranes. The most important type of membrane materials are organic materials, i.e., polymers.

2.2.1 Organic (polymer) membranes

Polymer membranes are divided into two types, which are open porous and dense non-porous membranes. The reason for this classification is the different requirements of the separation when polymer organics are used.

2.2.1.1 Porous membranes

This type of membrane is used in microfiltration and ultrafiltration membrane processes. For porous membranes, the relation between the pore size and pore size distribution, and the solute molecular size determines the separation process selectivity. The membrane material is an important factor for manufacturing the membrane, and for the chemical and thermal stability of the membrane. The main problem for porous membrane is the flux decline

because of concentration polarisation and fouling. As a result, the choice of the membrane material is very important to prevent fouling and can be cleaned after fouling. In addition, the membrane adsorption of solute must be low because the increase in adsorption increases the resistance of the membrane, which contributes to the flux decline.

2.2.1.2 Nonporous membranes

Nonporous membranes are used in gas separation and pervaporation. The material used in manufacturing nonporous membranes determines the membrane selectivity and the performance of the membrane. The nonporous membranes are used in liquid and gas separation.

2.2.2 Inorganic membranes

The inorganic membranes are made of four different types of materials: ceramic membranes, glass membranes, zeolitic membranes and metallic membranes. Inorganic materials have better chemical and thermal stability compared to organic (polymer) materials; on the other hand, they have weak mechanical stability. For example, polymer membranes can be used in processes with temperatures ranging from 100–300 ℃, while ceramic membranes can be applied in processes with temperatures up to 800 °C. The chemical stability for inorganic membranes is high because

1. They can be applied to any pH and in any organic solvents.
2. In the case of fouling, all kinds of cleaning agents from strong acids to alkaline treatment can be used to clean the inorganic membranes.
3. The lifetime of inorganic membranes is longer than that of organic membranes.
4. The inorganic membranes are very brittle, despite the high tensile modulus.

2.2.3 Synthetic membranes can be classified by another way into the following basic groups

2.2.3.1 Micro-porous media

It consists of a solid matrix with defined pores, which have a diameter ranging between 5nm and 50μm, (refs. 230). Separation is a result of the sieving action, where the separation parameters are the pore diameter and the particle size. The membranes are made of different materials such as ceramics, graphite, metal or metal-oxide and polymers. The different types

of micro-porous media are as follows

1. Sintered membrane. It has a low porosity in the range of 10 to 40%, irregular pore structure and a wide pore size distribution. They are used in the filtration of colloidal solutions and suspensions. If it is prepared from inorganic materials, and it's used for the filtration of corrosive solutions such as acids and baises.
2. Stretched membrane. It's prepared by stretching a homogenous polymer film of a partial crystallinity. The stretched membrane material is first extruded from a powder then stretched perpendicular to the direction of extrusion. This leads to partial fracture of the film and relatively uniform pores with a diameter of 0.1 to 20 μm. Its porosity is high and up to 90%.
3. Capillary pore membrane. It's a micro-porous membrane with a very uniform, almost perfect round cylinder pores, obtained by the track-etching process. It is prepared in two steps: In the first step, a homogenous 10 to 20 μm thick polymer film is exposed to collimated charged particles from a nuclear reactor, where the backbone bonds in the polymer are broken. In the second step, the film is placed in an etching bath, where the damaged material is etched forming uniform cylindrical pores. The pore density is determined by the residence time, and the pore diameter is controlled by the residence time in the etching bath.
4. Micro-porous phase inversion membrane. The membrane is prepared by dissolving the polymer in a solvent and then casted as a 20 to 200 μm thick film. Then a non-solvent in a vapour phase is added to the film, where it precipitates and separates the solution into a solid polymer and a liquid solvent phase.

2.2.3.2 Homogenous membrane

The homogenous membrane consists of a dense film, where a mixture of chemical species is transported through it under the driving force of pressure, concentration, or electrical gradient. Its permeability is low because the mass transport is always restricted by diffusion, (refs. 230, 244). The different types of homogenous membranes are as follows

1. Homogenous polymer membranes, the mass transfer in an amorphous polymer is greater than in highly crystalline or cross-linked polymer.
2. Homogenous metal and glass membranes; important examples for this type of membrane are palladium, palladium-silver or palladium-yttrium. Homogenous glass membrane is

used as pH-electrode.

3. Liquid membranes, which is used in two different configurations; the first is the liquid membrane, which is composed as a thin film stabilised by a surfactant in an emulsion-type mixture. The second is referred to as a supported liquid membrane.
4. Ion exchange membranes, which consist of highly swollen gels carrying fixed positive or negative charges.

2.2.3.3 Asymmetric structure membrane

The two basic properties for any membrane are high mass transport rates for a certain components and a good mechanical strength. The separation characteristics are determined by the nature of the skin polymer and the pore size. The transport rate is characterised by the membrane thickness. The sub-layer is only a support for the thin and fragile skin. Its advantages include a high filtration rate, which acts as a depth filter and retains most particles within their internal structure. The asymmetric membrane consists of a thin skin with a thickness ranging between 0.1 to 0.5μm, which is a very dense layer, which possesses selective property. The sub-layer is a porous layer with a thickness between 0.1 to 0.2 mm; the sub-layer gives a mechanical stability to the membrane. The origin of the asymmetric membrane is the presence of the skin. There are three views on the formation of the skin which are

1. The asymmetry already exists in the cast film of the concentrated polymer solution before precipitation takes place due to surface tension. Further preparation processes, such as coagulation and heat treatment, will only fix the already existing asymmetry.
2. The skin is formed through evaporation from the upper layer of the cast film.
3. The coagulation process is responsible for the formation of the asymmetry. Skin formation and porous sub-layer formation are the result of a complex interplay of phase separation and diffusion processes.

The asymmetric membrane is prepared either by utilisation of phase inversion process or by depositing an extremely thin polymer film on a micro-porous substructure where a composite structure is gained. Asymmetric membranes are divided into two types

1. Integral asymmetric membranes. The top layer and sub-layer consist of the same material. The parameters determining the structure and the properties of the phase inversion

membranes are as follows:

i. The polymer and its concentration in the casting solution.
ii. The solvent or the solvent system.
iii. The precipitant or the precipitant system.
iv. The form of the precipitate (vapour or liquid).
v. The temperature of precipitation.

2. Composite membrane. The top layer and the sub-layer are composed of different materials; as a result, each layer can be optimised separately. This type of membrane is used for reverse osmosis applications. The performance of a composite membrane is determined by the selective film surface, the pore size, the pore distribution and the overall porosity. When preparing this type of membrane, the porous sub-layer is prepared first, then the dense top layer is placed over it by dip-coating, in-situ polymerisation, interfacial polymerisation and plasma polymerisation.

2.2.3.4 Electrically charged barriers

In this method, the separation is influenced by the molecule charge, where the molecule can either pass through a medium because of its charge, or it can be exchanged for anther charged molecule. In general, ion exchangers are composed of cross-linking polymers with functional groups that are electrically active. The ion exchangers can either be a cation exchanger or an anion exchanger, which is determined by the functional group. Ion exchanger efficiency is determined by the ion exchanger affinity toward the ion needed to be separated and the number of active sites available.

2.3 Separation according to the membrane structure

Membranes can be separated according to their structure and separation principles to porous membranes, nonporous membranes and liquid membranes, (refs. 230, 244). The characteristics of these three basic types are as follows

2.3.1 Porous membranes

The selectivity is mainly determined by the pore size in relation to the size of the particles to be separated. The membrane material has a very small effect on the separation process. These

types of membranes are used in microfiltration and ultrafiltration processes.

2.3.2 Nonporous membranes

These types of membranes depend on the difference in solubility and/or diffusivity between the molecules and the membrane material.

2.3.3 Liquid membrane

This membrane is known as liquid membrane or carrier mediated transport membrane. The transport is determined by a very specific carries molecule, thus the selectivity toward a component depends mainly on the specificity of the carrier molecule. Extremely high selectivity can be obtained by the use of specially tailored carriers.

2.4 Preparation of membranes

Several factors affect the membrane performance, (refs. 195, 230, 271). For example, for the porous membrane, the performance is determined by the membrane pore size. The choice of membrane material becomes important with respect to fouling, thermal and chemical stability. For nonporous membranes, the membrane performance is affected by the choice of the polymer. It depends on the type of the polymer because the intrinsic membrane separation properties depend on the chemical structure and hence the choice of the polymer. The concentration of the polymer influences the membrane properties. The process of preparing a membrane depends on the material used as well as the desired membrane structure. The membrane structure depends on the separation process. The choice of the materials used in preparing a membrane limits the employed preparation techniques, the obtained membrane morphology and the allowed separation principles. This means that not every separation problem can be accomplished with every kind of material. As a result, when preparing a membrane, several factors affect its structure that must be considered such as the choice of the polymer, the choice of the solvent and the non-solvent, the composition of the casting solution, the composition of the coagulation bath, the behaviour of the polymer, the location of the liquid-liquid de-mixing gap, the temperature of the casting solution and the coagulation bathe, and the evaporating time. Membranes are prepared using different techniques, the most of which are as follows

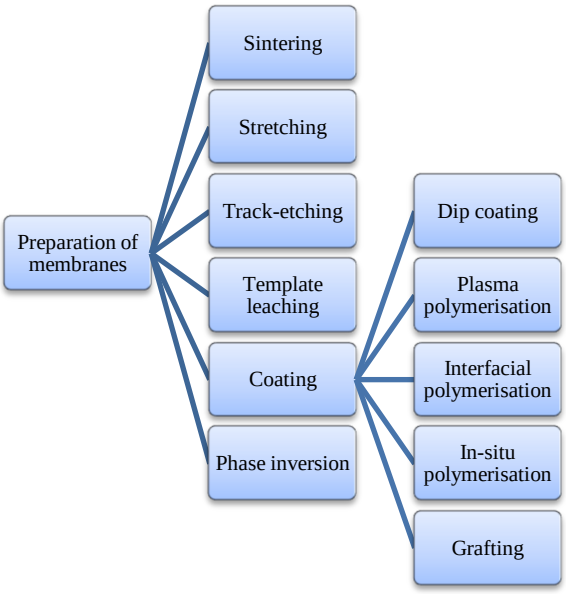

Figure 2-2. Membrane preparation processes.

2.4.1 Sintering

This technique is used to obtain porous membranes from organic and inorganic materials. The method involves pressing powder of particles at a given size and sintering at an elevated temperature, which depends on the used materials. A wide range of different materials can be used such as the powder of the polymers, metals, ceramics, graphite and glass. The pore size of the resulting membrane is determined by the particle size and the particle size distribution in the powder. The narrower the particle size distribution, the narrower the pore size distribution in the resulting membrane. All the materials used as the basic materials for sintering have the common feature of chemical, thermal and mechanical stability. Microfiltration membranes are prepared by sintering. The porosity of the membrane prepared by sintering is generally low.

2.4.2 Stretching

An extruded film or foil is made from a partially crystalline polymeric material, where is stretched perpendicular to the direction of the extrusion; as a result, the crystalline regions are located parallel to the extrusion direction. Ruptures occur and porous structure is obtained because of the applied mechanical stress. The obtained pore size is between 0.1μm and 3μm. The porosity of membranes made by stretching is higher than those made by sintering.

2.4.3 Track-etching

The structure obtained by track-etching is a parallel cylindrical shape pore of uniform dimensions. In the track-etching process, the membrane is prepared by subjecting a film or foil to a high-energy particle radiation, which is applied perpendicularly to the film. The particles damage the polymer matrix and create tracks. Then the film is immersed in an acid or alkaline bath, and the polymeric material is etched away along the tracks to form uniform cylindrical pores with a narrow pore size distribution. The pore size of the membrane ranges between 0.02μm and 10μm, but the membrane surface porosity is low. The materials used in preparing membranes by track-etching process depend on the available film thickness and the energy of the applied particles. When the applied particle energy is increased, the film thickness can also be increased and inorganic materials can be used. The membrane porosity is determined by the radiation time, and the pore diameter is determined by the etching time.

2.4.4 Template leaching

A porous membrane is prepared by leaching out one of the melt components from a film. For example, if a three-component melt is cooled, the melt components will separate into two phases where one phase is soluble and the other is not. The soluble phase will be leached out by an acid or base. The membrane pore diameter will have a minimum value of 0.05μm. Glass membranes are prepared by the template leaching process.

2.4.5 Coating

The effective thickness must be reduced to increase the flux through the membrane. To achieve this, a composite membrane is prepared. The composite membrane consists of two different materials with a very selective membrane material as a thin layer; see Figure 2-3.

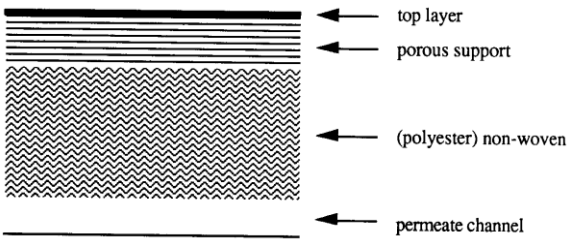

Figure 2-3.The composite membrane layers, (ref. 195).

The actual selectivity is determined by the thin layer, where the porous sub-layers act as a support. These membranes are prepared by coating procedure such as the following

2.4.5.1 Dip coating

Composite membranes with thin and dense top layer prepared by dip coating are used in reverse osmosis, gas separation and pervaporation. The preparation technique starts by immersing the membrane in a coating solution bath containing polymer, pre-polymer or monomer. The membrane is then removed with a thin layer being adhered to it. After removing the film, it is placed in an oven to evaporate the solvent and a cross-linking occurs. The cross-linking causes the thin layer formed to fix to the sub-layer.

2.4.5.2 Plasma polymerisation

Plasma polymerisation is used to prepare the membrane with a thin and dense top layer. The plasma used in this technique is generated by the ionisation of a gas by means of an electrical discharge at high frequency. The gas and the reactants enter the reactor at the same time but separately. As the gas enters the reactor, it will be ionised. Then radicals will be formed through collision with the ionised gas, and the product will precipitate as its molecular weight increases. A thin layer is then formed.

2.4.5.3 Interfacial polymerisation

Interfacial polymerisation is used to deposit a thin layer in a support layer, which is generally an ultrafiltration or microfiltration membrane. The first step is to immerse the support layer in an aqueous solution bath, which contains a reactive monomer. The second step is to immerse the support layer in a second bath, which contains water immiscible solvent and a reactive monomer. Then the two monomers react, forming a dense polymeric top layer.

2.4.5.4 In-situ polymerisation

The in-situ polymerisation includes dispersion and distribution of clay layers in the monomer, which is followed by polymerisation. Where polymerisation is initiated by heat, radiation, diffusion of a suitable initiator, and organic initiator or catalyst. An advantage of in-situ polymerisation is the tethering effect, which enables the nanoclay's surface organic chemical to link with polymer chains during polymerization.

2.4.5.5 Grafting

Another type of coating is when the coating layer plugs the pores in the sub-layer. In this case, the properties of the sub-layer determine the overall properties rather than the coating layer.

2.4.6 Phase inversion

Phase inversion is a process whereby a polymer is transformed in a controlled manner from a liquid to a solid state and the formed membrane is polymeric, (refs. 195, 230). There are different techniques within the phase inversion process, which include the following

1. Precipitation from the vapour phase: the membrane is formed by penetration of a precipitant into the solution film from the vapour phase; the vapour phase is saturated with the used solvent. The produced membrane is porous with an even distribution of the pores and without a skin. The polymer solution is subjected to a non-solvent inflow; the solvent saturated vapour phase prevents the outflow of the solvent. A liquid-liquid phase separation occurs and a micro porous membrane without a skin is formed. The distribution is symmetric. The pore size can be controlled by the preparation variables, where the pore size increases as the temperature increases or as the polymer concentration decreases.
2. Precipitation by controlled evaporating: the polymer is dissolved in a mixture of good and poor solvent (the good solvent is more volatile). When the solvent mixture shifts in composition during evaporation to higher non-solvent content, then the polymer precipitates. The resulted membrane is skinned. If a solution consists of a polymer and a solvent, and the solvent is lost through evaporation, as a result, the polymer concentration increases and gelation takes place. A dense polymer is formed by this process. If gelation occurs through crystallisation, the properties of the film depend on the rate of evaporation and diffusion.
3. Immersion precipitation: the cast polymer film is immersed in a non-solvent bath, and then a polymer precipitates as a result of solvent loss and non-solvent penetration. The determining factor for the skin formation is the local polymer concentration in the top layer in the polymer solution at the moment of precipitation.
4. Thermal precipitation: the polymer solution is mixed with a solvent, and is then brought to separation by a cooling step. In a mixture of a solvent and non-solvent, the polymer is dissolved in the mixture at high temperature. When the temperature is lowered, the solution becomes unstable with respect to liquid-liquid phase separation and a porous

structure is formed.

The phase inversion process is characterised as follows

1. A ternary system, which involves at least one polymer component, one solvent and one non-solvent. The solvent and the non-solvent must be miscible.
2. Mass transfer; the membrane is formed by the transport of the solvent and the non-solvent, where the non-solvent concentration in the film increases. The changes of composition in the film are governed by diffusion.
3. Precipitation; as the non-solvent content increases, the solution becomes unstable thermodynamically. As a result, a phase separation will occur.

2.5 Transport medium

In general, there are four basic types of transport mediums

2.5.1 Permanent pores greater than 5 nm in diameter

Permanent pores greater than 5 nm in diameter, deliberately introduced into the membrane during manufacturing. The molecule transport takes place by convection. An example of membranes with pore diameter greater than 5 nm is macro-porous membrane. The most common way to prepare macro-porous membranes involve a combination of a solvent and a non-solvent polymer, which are used together or in succession. They are used in separation as sieves that retain macromolecules or colloidal particles bigger than the pore size. Small molecules and ions pass through it.

2.5.2 Small pores

Small pores less than 1 nm in diameter. When molecules transport through these pores, they interact with the pore walls and the pore system may not be continuous and interconnecting. Permeation through the membrane has some characteristics of convection and some of diffusion. Micro-porous membrane is an example of a membrane with pore diameter less than 1 nm. As the glass temperature decreases, the pores caused by packing defects increases and their contribution to transport increases. These types of membranes are useful in gas and liquid or vapour separations. Transport takes place by a combination of conviction and diffusion (and perhaps surface diffusion) in the micro-pores with diffusion in the denser

polymer surrounding the pores.

2.5.3 Amorphous polymer.

Permeates can dissolve in an amorphous polymer and travel by diffusion down their concentration gradients motivated by the molecular Brownian motion. An example is the solvent-type membrane. The chain segment of electrometric and flexible polymer above the glass transitions execute motion that is similar to the thermal motions of the molecules in normal liquids. It cannot retain a permanent pore system of near molecular dimensions. The "free volume" is mobile and its distribution is governed by statistical thermodynamic requirements. When a polymer in the form of a membrane separates two reservoirs at different solute activities, the equilibrium concentrations at the membrane faces differ. The solute is then transported down its concentration gradient within the membrane at a rate controlled by the thermal motion in the mixture.

2.5.4 Gel membrane.

The transport of solutes in gels is highly complex, and both diffusion and convective contribute. The gel is formed when the polymer is swollen by imbibing a liquid; the liquid component may move by diffusion and convection. Hindrances exist in the gel and their extent depends upon the degree of swelling of the polymer and the size and nature of solute molecules. Substances dissolved in the liquid can transport through the gel but they interact with it and are hindered by the polymer chain.

2.6 Summary

In this chapter membrane classification and preparation techniques have been explained. Several factors affect the membrane performance such as the membrane pore size, the choice of membrane material and the preparing techniques of a membrane. Such factors either limits or enhance the obtained membrane morphology, the membrane permeability and membrane slectivity. In-order to improve the membrane separation processes and understand them, there are several techniques which are used to characterise the membranes such methods are explained in chapter 3.

Chapter 3 Membrane characterisation

Membrane characterisation can determine structural and morphological properties of a given membrane, where membrane characterisation can relate membrane structural properties to membrane separation properties. Membrane characterisation methods can help to gain the appropriate knowledge about the membrane pore structure such as pore radius, pore density and pore shape. These information's help in choosing the appropriate membrane for a specific application, controlling the membrane quality, understanding the separation behaviour and predicting separation performance for various substances. There are different ways to characterise membranes because of their different properties, which ranges between porous and nonporous membranes. The membrane characterisation becomes more difficult as the pore size decreases. Membranes can be divided according to their characteristics into porous and nonporous membranes. The pore size characterises the membrane, not the membrane material. The pore size mainly determines which particles or molecules will retain and which will pass through the membrane. On the other hand, in dense pervaporation and gas separation membranes, there are no fixed pores present and the membrane material mainly determines the performance. The morphology of the polymer material used in preparing the membrane directly affects the membrane permeability.

3.1 Characterisation of porous membranes

The characterisation methods determine the pore size and pore size distribution. However, in the actual separation processes, the membrane performance is mainly controlled by other factors such as concentration polarisation and fouling. One important factor in the characterisation of porous membranes is the shape of the pore or its geometry. Another factor is the pore size and pore size distribution. For absolute rating, all particles or molecules of pore size at the value of the absolute rate or bigger would retain. For nominal rating, a percentage of the particles or molecules of a pore size at the value of nominal or larger would retain; see Figure 3-1.

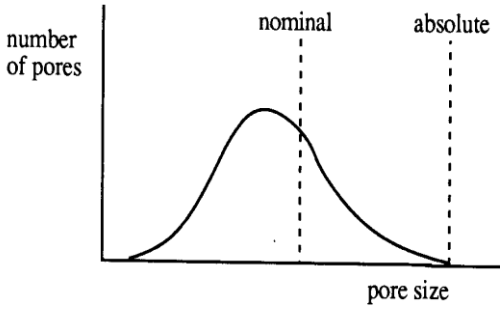

Figure 3-1. Percentage of the particles versus the pore size, (ref. 195).

The surface porosity is another factor in characterising porous membrane. It is an important variable in determining the flux through the membrane in combination with the thickness of the top layer or the length of the pore. There are two methods used to distinguish porous membrane

a. Structure-related parameters; determination of pore size, pore size distribution, top layer thickness and surface porosity.
b. Permeation-related parameter; determination of the actual separation parameters using solutes that are more or less retained by the membrane.

Porous membranes are characterised by different techniques as follows

3.1.1 Electron microscopy

There are two techniques used in electron microscopy, which are the scanning electron microscopy (SEM) and the transmission electron microscopy (TEM). Scanning electron microscopy is a very simple method where a clear and concise picture of the membrane can be obtained for the top layer, cross section and the bottom layer. From the photographs, the pore size, the pore size distribution and the porosity can be estimated. This method was used in the experimental work in-order to have an idea about the used ceramic membrane physical properties and to obtain the thickness of the membrane active layer, where the rejection of ions takes place. Pictures for the membrane surface and for a cross sectional part where obtained by using SEM (FEI Quanta 200, Purge, Czech Republic) and EDXS Machines (EDXS, Amertek Inc, Paoli, PA, USA). For more details about the obtained membrane pictures see section 8.4.

3.1.2 Bubble point method

This method measures the pressure needed to blow air through a liquid-filled membrane. It characterises the membrane's maximum pore size and determines the active pores. It depends on the liquid type, the increase in rate of pressure and the pore length. The pore size distribution can be obtained by a stepwise increase of pressure. This method is independent of the liquid type but different results (radius value for pore size) are obtained with different liquids, (refs. 195).

3.1.3 Mercury intrusion method

This technique is similar to the bubble point method; the difference is that mercury is forced into a dry membrane with the volume of mercury being measured at each pressure. Since the volume of mercury can be determined very accurately, the pore size distribution can be determined by this technique. The disadvantages of this technique are that the apparatus is expensive, and since the small pores need high pressure, this may lead to the damage of the membrane structure. This method measures all the pores present in the structure including dead-end pores.

3.1.4 Permeability method

The pore size can be obtained by measuring the flux through a membrane at constant pressure if capillary pores are assumed present. The minimum pressure needed to measure the flux depends on the type of membrane material present, type of permeate (surface tension) and the pore size. At a certain minimum pressure the large pores will be permeable and small pores will be impermeable. This method can be used for microfiltration and ultrafiltration membranes. Although it is a simple method, the main problem is that it depends on the pore geometry, which is hard to calculate.

3.1.5 Atomic force microscopy

Atomic force microscopy (AFM) is a new method used to characterize the membrane surface, where it can determine the membrane surface structure. Also, atomic force microscopy (AFM) can be used to determine the membrane pore size and porosity by taking a cross-section image.

3.1.6 Bubble point with gas permeation

In this method, the gas is blown through a dry membrane and the applied pressure is measured. Then the membrane is wetted and the gas is blown through it and the gas-applied pressure is measured. At low pressures, the pores stay filled with liquid and gas flow through the membrane is very low and determined by diffusion. There is a certain minimal pressure where the largest membrane pore is empty from liquid and gas flow through these pores will increase by convection.

3.1.7 Gas adsorption-desorption

It is used to determine the pore size and size distribution in porous materials, (refs. 195). The adsorption and desorption of an inert gas is determined as a function of the relative pressure. The relative pressure is equal to the ratio between applied pressure and the saturation pressure. When a gas is passed through a membrane, the gas is absorbed by the membrane; the adsorption isotherm starts at low pressure and small pores start to fill up, and by increasing the pressure, large pores start to fill up. The total pore volume is determined by the quantity of gas adsorbed near the saturation pressure. When the pressure starts to decrease below the saturation pressure, desorption starts to take place. Generally, the desorption curve is not identical to the adsorption curve; the reason is that capillary condensation occurs differently in adsorption and desorption. Its main problem is to relate geometry to a model that allows the pore size and pore size distribution to be determined from the isotherms. Dead-end pores that do not contribute toward transport are measured by this technique. Ceramic membranes give better results because of their structure and it is less susceptible to capillary forces.

3.1.8 Thermoporometry

Thermoporometry is based on the calorimetric measurement of solid-liquid transition in a porous material. The liquid passing through the membrane is cooled until the solution starts to freeze inside the membrane pores. Then the effect of heat transition is measured by using a differential scanning calorimeter (DSC). The liquid then starts to melt and the pore size distribution can be obtained, where a melting curve is measured as a function of under-cooling temperature by using differential scanning calorimeter (DSC). An assumption has to be made about the pore geometry in order to calculate the pore size and the pore size distribution. When all pores are measured including dead-end pores, the pore size distribution can also be determined.

3.1.9 Permporometry

This technique is used to characterise the membrane and information is obtained about the pore size and the pore size distribution of the active pores in the top layer. The top layer of the membrane is dependent on the type of vapour employed. It depends on the blockage of pores by means of a condensable gas, with the simultaneous measurement of gas flux through the membrane. In this method, a condensable gas is used to pass through the membrane. When the relative pressure value is equal to unity, the pores are filled only with liquid. After reducing the relative pressure, the condensed vapour is removed from the largest pores and diffusive gas flow is measured. Then the relative pressure is decreased until it reaches zero value and gas flow through all of the membrane pores. As a result, the pore size distribution can be obtained from the gas flow through the membrane. The principle problem in this technique is the difficulty of maintaining the same vapour pressure on both sides of the membrane.

3.1.10 Solute rejection measurements

The membrane separation can be characterized by the solute rejection, (refs. 195). Where the membrane cut-off is the solute molecular weight, which 90% is rejected by the membrane. The membrane rejection is given as

$$R = 1 - \frac{C_p}{C_f} \qquad (3.1)$$

where R is the membrane rejection, C_p is the solute concentration in permeate and C_f is the solute concentration in the feed. Other important parameters that characterize the membrane separation are the molecular weight of the solute, the shape and the flexibility of the macromolecular solute, the solute interaction with the membrane material and the concentration polarisation phenomena. This approach was followed in-order to try to understand the separation behaviour of the ceramic nanofiltration membrane that was used in this work. The rejection of ions was obtained theoretically by solving numerical equations that describes the separation behaviour of nanofiltration membranes, for more details see chapter 8. In addition, the rejection of different types of ions by nanofiltration membranes were obtained by experimental work to try to understand the separation behaviour of ceramic nanofiltration membrane, for more details go to chapter 8.

3.1.11 Liquid displacement

In this method, two immiscible liquids are used where another liquid displaces a liquid inside the membrane pores. The displacement starts at the largest pores causing a flow that is measured with a mass flow meter. By increasing the pressure, small pores start to be displaced and increase the flux through the membrane. As a result, a relation between the flux and membrane pore radius is obtained. This method is carried either by changing the applied pressure and measuring the flow rate or by changing the flow rate and measuring the pressure. In this method, only active pores are characterized. It is disadvantageous that a membrane swelling may occur because of the liquids that change the pore size.

3.2 Characterisation of nonporous membranes

One of the principles of characterising the nonporous membrane is to determine its permeability toward gases and liquids, (refs. 195). The physical state (rubbery or glassy) is an important factor. Whether a polymer is in a glassy or rubbery state, its state is determined by its glass transition temperature. For glassy polymers, the permeability decreases with increasing pressure due to non-ideal sorption. The glass transition temperature (T_g) and the crystallinity are the structural parameters that affect the membrane permeability. Solution-diffusion mechanism is the driving force in nonporous membranes and separation occurs because of differences in solubility and diffusivity. The physical properties related to the chemical structure are characterized by the following techniques

3.2.1 Permeability method

The permeability method determines the gas and the liquid permeability or permeability coefficient from steady state gas flow in the membranes with known thickness.

3.2.2 Physical methods

Physical methods can determine the different physical properties of membranes such as the glass transition temperature, the crystallinity and density. Physical methods use the following techniques

1. DSC/DTA methods. Differential scanning calorimetry (DSC) and differential thermal analysis (DTA) are used to measure transitions or chemical reactions in polymer.

Differential scanning calorimetry (DSC) determines the energy necessary to counteract any temperature difference between the sample and the reference. Differential thermal analysis (DTA) determines the temperature difference between the sample and the reference upon heating or cooling. The glass transition temperature (T_g) is the point of intersection of the tangents (or the flux point). As degree of crystallinity increases, the density also increases because the density of the crystalline regions is greater than that of amorphous regions.

2. Density gradient columns. Membranes prepared from high-density polymers tend to have lower permeability. Density is related to the glass transition temperature, crystallinity and the free volume. The density is determined by different techniques such as picrometry and dilatometry.
3. Wide-angle X-ray diffraction (WAXS). It is a technique used to collect information about membrane morphology, size and shape of crystallites and degree of crystallinity. In this method, an x-ray beam impinges the membrane or polymer and then the intensity of the scattered x-ray is determined as a function of the diffraction angle, and the shape of peaks results from the relation, where the degree of crystallinity is obtained by calculating the area under the peak.

3.2.3 Plasma etching

Plasma etching measures the thickness of the top layer in asymmetric and composite membranes. In addition, the uniformity of the structure in the top layer, sub-layer and layer just beneath the top layer can be determined. This process involves reaction between the surface of polymeric membrane and plasma produces in a glow discharge. When the gas transport properties are measured as a function of the etching time, information can be obtained about the morphology and thickness of the top layer.

3.2.4 Surface analysis method

When a solid surface is excited by means of radiation, information about the presence of specific groups, atoms or bonds are detected from the emission products. There are different techniques that are used in surface analysis, such as electron spectroscopy for chemical analysis (ESCA), X-ray photoelectron spectroscopy (XPS), secondary ion mass spectrometry (SIMS) and auger electron spectroscopy (AES).

3.3 Summary

The membrane structural properties can be obtained from the membrane characterisation methods, where the membrane characterisation can relate the membrane structural properties to the membrane separation properties. The characterisation methods cannot be applied for each type of membranes because of their different properties, which ranges between porous and nonporous membranes, and membrane characterisation becomes more difficult as the pore size decreases. In this work, two methods were used to characterise ceramic nanofiltration membrane which are the scanning electron microscopy (SEM) and the solute rejection. The membrane effective layer thickness was obtained by using SEM-EDXS equipment; also a general idea about the pores distribution and the supporting layer was achieved. The solute rejection was studied using different types of salts solution, to try to understand the rejection behaviour of ceramic nanofiltration membrane. These characterisation methods would be explained in details in chapter 9.

Chapter 4 Membrane processes

Transport through the membrane takes place because of the driving force acting on the individual components in the feed. Permeation rate (the flux) through the membrane is proportional to the driving force. The relation between the flux and the driving force is a linear phenomenological equation, where the driving force (dX/dx) is expressed as the gradient of (X) (where X can be temperature, concentration and pressure) along the coordinate (x) perpendicular to the transport barrier. The phenomenological equations are Fick's law, Darcy's law, Fourier's law, Newton's law and Ohm's law (refs. 195, 267, 271). When two or more components are permeating through a membrane, coupling phenomena may occur between the fluxes and the driving forces. These couplings can be described using non-equilibrium thermodynamics. An example for the coupling of fluxes is the transport of water with an ion, which is driven across a membrane by an electrical potential gradient. (refs. 230, 244). Mass transport through a membrane may occur as a result of mass diffusion or convection induced by gradients of electrical potential, concentration, pressure or temperature, (refs. 195, 270). The difference in the transport rate of chemical species between the membrane boundaries causes the separation process. The driving force or the forces acting on the individual components and the concentration, as well as the mobility through inter-phases, determine the transport rate. The mobility is determined by the solute's molecular size and the membrane's physical structure. The mobility and concentration of the solute determine how large the flux for a given driving force is. The three basic mass transport forms through a membrane are as follows

1. Passive transport. All the solutes are transported under a driving force of their electro-chemical potential. The gradients of electro-chemical potential in the membrane may be caused by the difference in hydrostatic pressure, concentration, temperature or electrical potential between the two phases separated by the membrane. The solutes are transported from high potential side to low potential side. If no external forces are applied to the system and the difference between potentials is equal to zero, the system will reach equilibrium state.
2. Facilitated transport. The driving force, which transports the solute, is the gradient of its electro-chemical potential across the membrane. Specific solutes are coupled to specific carriers in the membrane phase. The selectivity toward the transported solutes is higher than in other transport forms.

3. Active transport. The solute components are transported against the gradient of the electro-chemical potential. The driving force for transportation is provided by a chemical reaction within the membrane phase. This type of transport is mainly found in the living cell membranes.

The driving forces in the membrane are considered interdependent; for example, the concentration gradient across the membrane may not only cause mass flow but also build-up of a hydrostatic pressure difference, and this phenomenon is known as osmosis. Another example is that the gradient of a hydrostatic pressure may not only cause volume flow but also the formation of a concentration gradient, which is known as reverse osmosis. In the membrane separation process, the important driving forces that lead to a significant flux are as follows

1. A hydrostatic pressure. If the hydrodynamic permeability of the membrane is different for different solutes, the difference in the hydrostatic pressure between the two phases separated by a membrane can lead to a volume flux and separation of solutes.
2. A concentration difference. The difference in concentration between two phases separated by membrane can lead to the transport of solute and the separation of different types of solutes, when the diffusivity and concentration for the different solute types are different.
3. Electrical potential. The difference in electrical potential can cause the transport and separation of solute when the different charged particles show different mobility through the membrane.

The driving force can either be pressure difference, concentration difference, temperature difference or electrical potential difference, where the membrane processes can be separated according to their driving force as follows

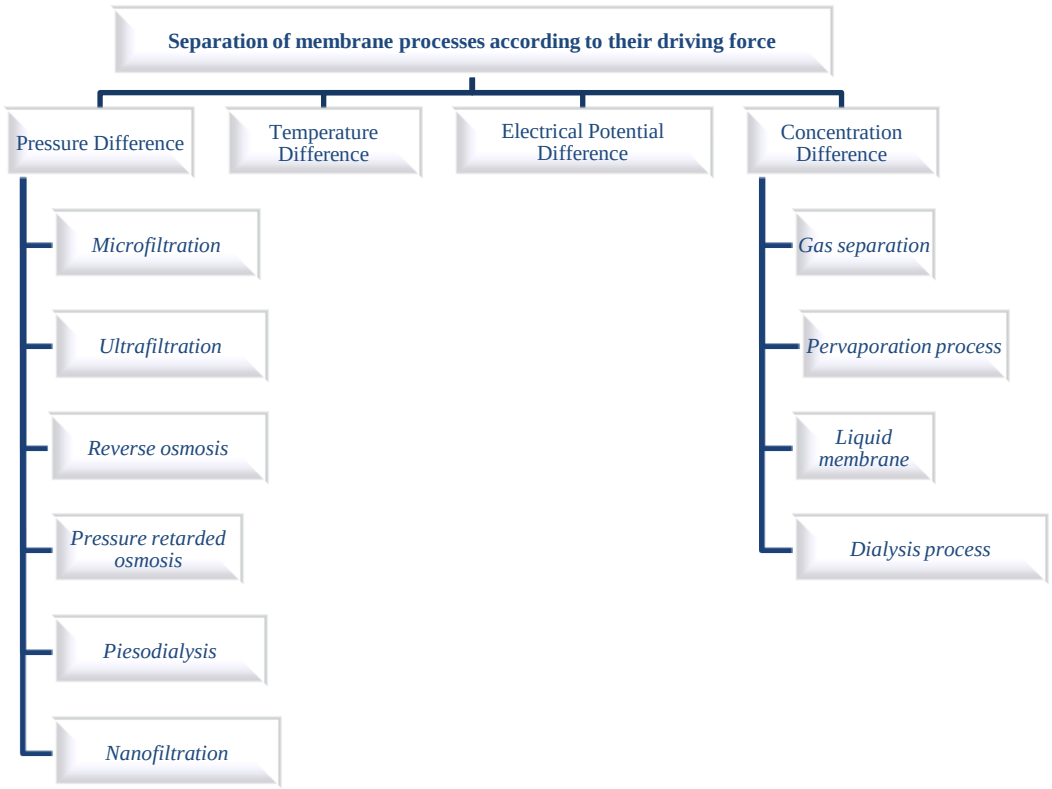

Figure 4-1. Membrane processes.

4.1 Membrane using pressure difference as a driving force

Pressure-driven membranes can be used to concentrate or purify a dilute solution. The membrane pore size and the pore size distribution are determined by the solute properties such as the solute molecule size and the solute chemical properties. The membranes that use the pressure as a driving force include microfiltration, ultrafiltration, nanofiltration and reverse osmosis (hyper filtration). The driving force in the pressure-driven process is the applied pressure, where the solvent permeates through the membrane and the solute in the feed solution is rejected. The difference between microfiltration, ultrafiltration, nanofiltration and reverse osmosis is the separated molecule size and the membrane pore size. The pore size decreases from microfiltration to ultrafiltration to nanofiltration and finally to reverse osmosis, and as a result the applied pressure and the membrane resistance increases, see Figure 4-2. The flux through these processes is inversely proportional to the membrane-effective thickness.

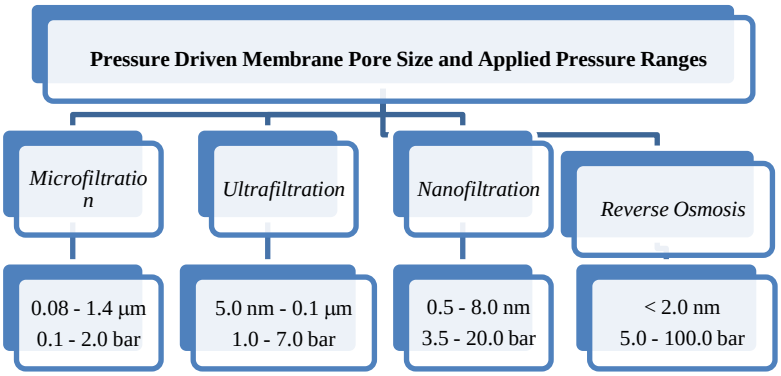

Figure 4-2. Membrane Pore size.

4.1.1 Microfiltration

Microfiltration is used to retain suspensions and emulsions, and it has pores with diameters ranging from 0.05 to 10 µm, (refs. 195, 230, 239). Microfiltration membrane is considered a porous membrane. Separation in microfiltration membrane occurs because of the sieving mechanisms. The volume flow through microfiltration process is described by Darcy's law, (refs. 271, 329) where the flux is given by

$$J = P_{const}\,\Delta p \qquad (4.1)$$

where P_{const} is the permeability constant that contains structural factors such as porosity and pore size. Also the viscosity is inversely proportional to the flux and the structural parameters such as porosity and pore radius are related to the volume flow. To optimise microfiltration membrane, the structural parameters such as porosity must be high while the pore size distribution must be narrow. Microfiltration membrane is prepared from different materials such as organic materials such as polymeric and inorganic materials such as ceramics, metals and glasses. Microfiltration membrane can be classified according to their pore size into tortuous-pore membrane and capillary-pore membrane; see Figure 4-3.

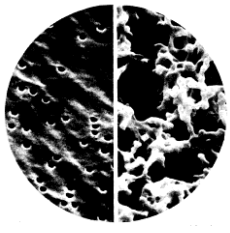

Figure 4-3. On the left-hand side is the capillary-pore membrane and on the right-hand side is the tortuous-pore membrane, (ref. 230).

1. Tortuous-pore membrane is prepared by using the solution-cast process where different types of polymers such as cellulose esters and polyvinyl chloride (PVC) are used. In the solution-cast process, the solvent is evaporated in a humid atmosphere, where it precipitates the polymer around a residual solvent creating the tortuous-pore membrane. The stretching process is also used to manufacture tortuous-pore membranes. It is used in large-scale industries.
2. Capillary-pore membrane. These membranes are prepared by using the track-etch process. The pores in the capillary membrane are straight cylindrical pores and this type of membrane is used in laboratory applications.

Microfiltration can also be separated into screen filter membranes and deep filter membranes. Screen filter membranes have small pores at its surface; as a result, particles with a diameter larger than the pore diameter are separated. Deep filter membranes have a large surface pore diameter, where particles pass through the membrane surface and are then trapped inside the membrane, where the particles are captured by the membrane internal pores or adsorbed by the membrane walls. The pore size in the microfiltration membrane is determined by the bubble point test. Where all the pores in the membrane are wetted, then a pressure is applied to one side of the membrane. The pressure at which the first bubble appears is known as the bubble point pressure; from this pressure, the maximum pore size can be determined. Mercury intrusion porosimeters can be used to determine the pore size distribution where it measures the pits and the pores.

The driving force in the microfiltration membrane is an applied pressure that is less than 2 bar and the principle of separation is the sieving mechanism where molecules are distinguished according to their size and shape where large and wide molecules do not pass through the membrane pores while small and narrow molecules pass. The retention of particles depends on several factors beside the pore size where some particles smaller than the pore size may be absorbed by the membrane and zeta-potential of the membrane medium can affect the retention of opposite-charged particles. When particle size is smaller than the pore size but too large to diffuse with the solvent, it will be captured by the membrane, which is known as inertial-impaction. Small particles are captured by the membrane because the membrane thickness is inversely proportional to the particle size.

Microfiltration membrane is prepared by different ways such as sintering or agglomeration, stretching, track-etching, sol-gel process, thermal phase inversion and chemical phase

inversion. Usually, inorganic materials are used to prepare the microfiltration membrane because of its chemical and thermal resistance, and the pore size can be controlled, thus the pore size distribution is very narrow. Ceramic microfiltration membranes can be prepared by sintering, solution/gel and anodic oxidation processes.

Microfiltration membrane is characterised by scanning electron microscopy (SEM), bubble-point measurements, mercury porometry and permeation measurements methods. Microfiltration membrane disadvantage is the flux decline caused by concentration polarisation and fouling. The membrane fouling is a result of the solute deposition on the membrane pores or at the membrane surface. Fouling occurs during the process where it depends on the process mode. Membranes in the microfiltration process are arranged either as dead-end or cross-flow modes to reduce fouling and concentration polarisation. In dead-end filtration mode, the feed is perpendicular to the membrane surface, and as a result, particles accumulate and form a cake layer at the membrane surface, the permeate decreases with time and the cake layer increases. In cross-flow filtration mode, the feed enters the process along the membrane surface side and thus the retained molecules accumulate and are swept away, which increases the membrane lifetime. Also, fouling depends on the membrane material type where adsorption of materials by the membrane causes fouling. Membrane material is important with respect to membrane stability relative to cleaning. Additionally, to reduce fouling, concentration polarisation and to gain better results of separation, a depth media working as pre-filter is added before the membrane where it removes bulk particles from the solution before it reaches the membrane and as a result, the membrane lifetime increases. Furthermore, the membrane lifetime can be increased by increasing the membrane area and by backwashing the membrane.

Microfiltration membrane is used in laboratories for measuring particulates in water and recovering biomass. In addition, it is used in sterilisation and clarification of all kinds of beverages in food and pharmaceutical industries. In the pharmaceuticals industry, the microfiltration membrane is used to filtrate injectable fluids during manufacturing. In biotechnology, microfiltration is used in cell harvesting and as a part of the membrane bioreactor. Also, microfiltration membranes are used in waste water treatment, continuous fermentation, separation of oil-water emulsions, dehydration of lattices, and filtrating gas and vapour.

4.1.2 Ultrafiltration

Ultrafiltration membrane is prepared from polymeric materials, inorganic (ceramic) materials. Ultrafiltration membrane is prepared from polymeric materials by the phase inversion process. Ultrafiltration membrane separates micro solutes from macro solutes and colloids. Ultrafiltration membranes can be characterised by cut-off measurements, thermoporometry and permporometry techniques, (refs. 239, 271, 329). Permeation through ultrafiltration membrane is affected by the solute molecular weight, the retained molecule shape and the feed solution pH. The performance of ultrafiltration membrane is affected by membrane fouling and concentration polarisation, thus it must be designed in a way that it will reduce fouling. Ultrafiltration membrane process is very good in recovering high-value products, permeate recycling, pollution control and energy saving when permeate can be recycled without the need for heat. The first use for ultrafiltration membrane process was enzyme recovery, protein recovery from cheese whey and electro paint recovery. Ultrafiltration membrane is used for fractionation of macromolecules, where small molecules and solvents pass through the membrane and large molecules are retained. It is used in food and dairy industries, pharmaceutical, textile, chemical, metallurgy, production of pure water, sewage treatment, paper and leather industries.

The pore size of ultrafiltration membranes range between 1 nm to 0.05 μm, and is used to retain macromolecules from a solution. Ultrafiltration is considered a porous membrane, the rejection is determined by the size and the shape of the solute relative to the membrane pore size and if the solvent transport is directly proportional to the applied pressure. Separation not only depends on the pore size and pore size distribution, but also on the chemical affinities of the solute molecules. The separation is considered a sieving separation mechanism. The driving force is an applied pressure on the membrane. The difference between microfiltration and ultrafiltration is that in microfiltration, the membrane resistance is determined by the whole membrane while in ultrafiltration, only a small part of the total membrane thickness, which is the top layer, is used in determining the membrane resistance because of its asymmetric structure. The top layer thickness is less than 1 μm. The flux is directly proportional to the applied pressure; see equation (4.1). The performance of ultrafiltration membrane process is quoted in terms of pure water flux, which is called cut-off. The cut-off technique does not give enough information about the membrane ability to separate solutes from solutions. The ultrafiltration membrane can be characterised in another way by determining the following parameters

1. Permeability

Ultrafiltration membrane permeability is determined by the pore size, the pore density and the thickness of the membrane active layer. The permeability coefficient increases as the solvent volumetric flux through the membrane increases and decreases as the driving force increases, (refs. 195, 230).

2. Pore size distribution

The pore size distribution can be measured by different methods such as high-resolution electron miscopy method and thermoporometry method, (refs. 230). From resolution electron miscopy method, a direct measurement of the membrane surface porosity can be obtained for pores with a diameter lager than 10 nm. Thermoporometry method is a calorimetric technique based on the width of the solidification thermogram of a pure substance held in a porous material that depends on the pore size distribution. The pore size distribution for porous membrane is determined by the calorimetric measurements of transition energy and temperature.

3. Rejection coefficient and cut-off

The cut-off is the upper molecular weight for solute passage. The cut-off is not an intrinsic property because the rejection coefficient depends on the concentration polarisation, the chemical nature of the macromolecules, the solvent used and the conformational changes in the macro-solutes.

Ultrafiltration membrane can be used in three operating processes

1. Enrichment of solution. The aim of this process is to obtain a retentate with macromolecule concentration bigger than in the feed.
2. Purification of solvent. The macromolecule concentration in the permeate is as low as possible.
3. Fractionation of a mixture of solutes, the retentate have a high concentration ratio of macromolecules concentration to small solute concentration.

To obtain the required separation results, several aspects are required such as the following

1. Permeation rate

High permeability rate must be obtained for the long time of the separation period. The difference between the maximum flux and the observed flux is a result of concentration polarisation. Concentration polarisation in the ultrafiltration membrane can be explained either by gel layer theory or by osmotic pressure, (refs. 230).

2. Membrane permeability

The membrane permeability for high permeable membranes is not an important factor in determining the flux in the ultrafiltration membrane process. The advantage of high permeable membrane is that the limiting flux can be obtained at the operating pressure thus saving energy.

3. Flow velocity

The concentration polarisation can be controlled by letting the solution enter parallel to the membrane surface where the tangent ionic velocity is parallel to the membrane surface.

4. Trans-membrane pressure

To maximise the membrane output, the flux must be close to the limiting flux then it will be inefficient to increase the operating pressure because the energy rate would increase and the production rate would not change. Also, the operating pressure should not exceed the limiting point to be able to avoid fouling and flux decline.

5. Temperature

As the temperature increases, the relative velocity deceases and diffusion coefficient of macromolecule increases. The viscosity and diffusion coefficient affects the mass transfer and the flux rate. The permeation rate (flux) increases as the temperature increases.

6. Retentate concentration

When retentate concentration increases, its viscosity increases and polarisation layer thickness increases, thus as a result, the mass transfer decreases.

7. Fouling and flux decline

The membrane fouling takes place in three stages: concentration polarisation, adsorption of macro-solutes and polymerisation of the adsorbed layer. Fouling is considered a problem where the feed solution is of biological origin. In biological solutions, a complex equilibrium is set up and any changes in concentration can destroy this equilibrium. Ultrafiltration membrane can be used to re-concentrate electro-point baths where it can stay working for several months without cleaning and no flux decline occurs. Fouling can be cleaned using several techniques such as using chemical agents and mechanical methods. Mechanical methods include backpressure flushing and sterilisation. Ultrafiltration membrane is cleaned by using chemical and mechanical processes. Chemical cleaning includes treating the membrane with alkaline, enzymatic detergents and acids. Mechanical cleaning includes forcing sponge balls with diameter slightly larger than the membrane pore's diameter. The sponge balls scrape the membrane surface and remove the precipitated layer. Also, mechanical cleaning includes back flushing by applying a pressure on the permeate side, forcing permeate to transport back through the membrane lifting the deposited material from the feed side.

8. Pre-treatment

Membrane fouling can be reduced by the per-treatment of the feed solution. Pre-treatment includes pH adjustment, heat pre-treatment and pre-filtration or centrifugation. Pre-treatment often adds cost to the overall cost treatment. Pre-treatment improves ultrafiltration membrane performance.

4.1.3 Reverse osmosis

If two solutions with two different concentrations are separated by a membrane that is permeable to the solvent and impermeable toward the solute, then the osmotic pressure rises, (refs. 40, 75, 90, 195, 230, 239). If the chemical potential for the solvent in the concentrated solution (phase 1) is given as

$$\mu_{s,1} = \mu_{s,1}^{o} + RT\left(\ln a_{s,1}\right) + V_s p_1 \qquad (4.2\text{-a})$$

and if the chemical potential for the solvent in the dilute solution (phase 2) is given as

$$\mu_{s,2} = \mu^{o}_{s,2} + RT\left(\ln a_{s,2}\right) + V_s p_2 \qquad (4.2\text{-b})$$

The chemical potential for the solvent in the dilute phase is higher than the chemical potential of the solvent in the concentrated phase; as a result, the solvent flows from the dilute phase to the concentrated phase, (refs. 31,37,56, 80, 329, 372). This process continues until the osmotic equilibrium is reached where the chemical potentials are equal as given below

$$\begin{gathered} \mu_{s,1} = \mu_{s,2} \\ RT\left(\ln a_{s,1} - \ln a_{s,2}\right) = V_s\left(p_1 - p_2\right) \end{gathered} \qquad (4.3)$$

The difference in the applied pressure or the hydrodynamic pressure is known as the osmotic pressure

$$\Delta\pi = \left(p_1 - p_2\right) \qquad (4.4)$$

The osmotic pressure depends on the solute concentration. In normal processes, the solvent would move from the dilute concentration phase or the low concentration to the high concentration phase. As a result, to reverse the process and force the solvent to move from the high concentrated phase to the lower concentrated phase, an applied pressure bigger than the osmotic pressure must be applied, which is known as reverse osmosis process. Thus, reverse osmosis can be defined as a process where pressure is used to reverse the normal osmotic flow of solvent across a semi-permeable membrane. The applied pressure is higher than the osmotic pressure. See Figure 4-4.

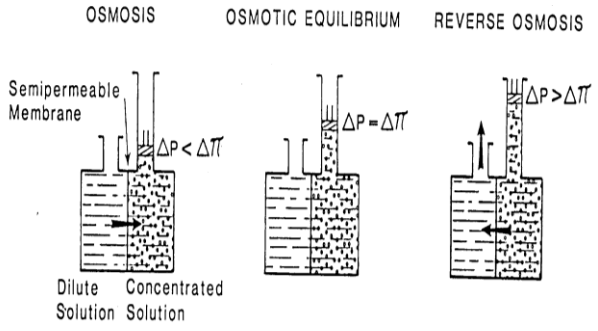

Figure 4-4. The osmotic and reverse osmotic processes, (ref. 230).

Reverse osmosis is used in separating low molecular weight solutes such as inorganic salts or organic molecules. The membrane is dense and its resistance is high. High pressure is applied to force the solvent to flow through the membrane because of high membrane resistance. The

membrane in reverse osmosis is permeable to the solvent and not to the solute, and high pressure is applied to overcome the osmotic pressure. If the applied pressure is less than osmotic pressure, the solvent flows from the dilute solution to the concentrated solution. And if the applied pressure is higher than osmotic pressure, the solvent flows from the concentrated solution to the dilute solution. The reverse-osmosis process takes place at room temperature without phase change; as a result, the energy consumption is low. The energy consumption in the reverse osmosis process is due to the work of pressurising the inlet fluid.

The reverse osmosis process is used with solutions containing low molecular weight solutes and aqueous solutions containing very small amounts of organic solutes. The total flux is the sum of the solute flux J_w and the solvent flux J_s, which is given as follows

$$J_{Total} = J_w + J_S \qquad (4.5)$$

If the membrane is highly selective, the solvent flux is high compared to the solute flux; as a result, the total flux will be equal to the solvent flux, (refs. 195, 230). The solvent flux can be given as

$$J_s = \frac{D_s c_{s,1^m}}{l}\left(\frac{V_s\left[p_1 - p_2 - \Delta\pi\right]}{RT}\right) \qquad (4.6\text{-a})$$

$$J_s = P_s\left(\Delta p - \Delta\pi\right) \qquad (4.6\text{-b})$$

From equations (4.6-*a*) and (4.6-*b*), it can be noticed that if the applied pressure is less than the osmotic pressure, the solvent would flow from the dilute solution side to the high concentrated solution side. If the applied pressure is bigger than the osmotic pressure, the solvent would flow from the high concentrated solution side to the dilute solution side. And if the applied pressure is equal to the osmotic pressure, the process is in equilibrium and no transport occurs, (refs. 195, 230). When no solute permeates through the membrane, the solvent flux is given by equation (4.6-*b*), and if a little amount of the solute passes through the membrane, then equation (4.6-*b*) would be as follows

$$J_s = P_s\left(\Delta p - \sigma\Delta\pi\right) \qquad (4.7)$$

where σ is the reflection coefficient of the membrane toward the permeating solute. The

solvent permeability for a given membrane is considered constant and is given by

$$P_s = \frac{D_s c_s V_s}{RTl} \qquad (4.8)$$

where D_s is the solvent diffusion coefficient and c_s is the solvent concentration. From equation (4.6-*b*), it is noticed that the solvent flux increases linearly when the applied pressure increases. In reverse osmosis, the solute flux is determined only by the concentration difference across the membrane. The membrane selectivity in the reverse-osmosis process is expressed by the rejection coefficient (R).

The applied pressure in reverse osmosis ranges between 20 to 100 bar. The separation principle is the solution-diffusion process. The reverse-osmosis process depends on the choice of membrane materials where it has a high affinity toward the solvent and low affinity toward the solute, while in microfiltration and ultrafiltration processes, the separation depends on the pore size and the chemical resistance. As the solute concentration at the feed side increases, the solvent flux deceases at constant feed pressure. The solute retention increases by decreasing the solute concentration. The solvent flux at osmotic pressure is predicted to be zero, but as the applied pressure increases, the solvent flux increases and the solute rejection increases. The solvent flux through reverse osmosis membrane increases as the temperature increases, but the solute flux decreases as the temperature increases.

Most reverse osmosis membranes have asymmetric structure with a thin top dense layer supported by a porous sub-layer. Reverse osmosis membranes are compact, which means the solvent flux declines even if the membrane is not fouled. The flux through reverse osmosis membrane increases as the temperature increases; also, the solute leakage through the membrane increases as the temperature increases. The solute rejection by reverse osmosis membrane decreases as the temperature increases. On the other hand, the membrane lifetime decreases as the process temperature increases. Rejection in reverse osmosis membrane increases as the applied pressure increases. See Figure 4-5.

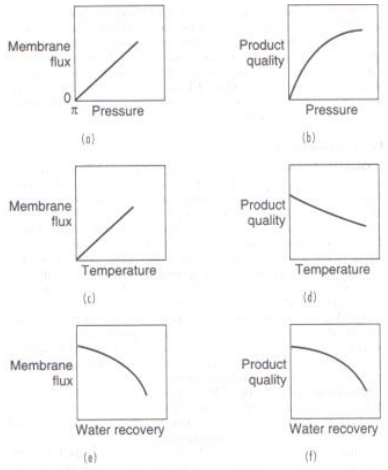

Figure 4-5. Effects of operating variables on reverse osmosis membrane, (ref. 271).

The advantages of reverse osmosis membrane is that it can remove contaminants, viruses, bacteria, and other pathogens, it needs a small area, it can be out near the water source and it can be automated to reduce operating cost. Reverse osmosis membrane disadvantages are the chemical attack, fouling and compaction. Compaction is a result of a creeping and slowing flow of polymer causing a decrease in water permeability through the membrane. The compaction is equal to the slope of the log flux versus the log time. Chemical attack is a result of fouling prevention or cleaning. Fouling in reverse osmosis membrane is caused by scaling, silt, bacteria and organic compounds. To avoid membrane fouling in reverse osmosis process, a high fluid flow parallel to the membrane surface is maintained. The most common salts that cause scale in reverse osmosis membrane are calcium carbonate, calcium sulphate, silica complexes, barium sulphate, strontium sulphate and calcium fluoride. Scale in reverse osmosis membrane is controlled by acidifying the feed solution and anticline chemicals. Silt in reverse osmosis membrane is caused by organic colloids, iron corrosion products, precipitated iron hydroxide, algae and fine particles. Slit is reduced by using a filter before the reverse osmosis membrane. Bio-fouling is caused by bacteria growth on the reverse osmosis membrane surface and is controlled by sterilising such as adding chlorine to the feed solution. Organic materials such as oil and grease cause organic fouling of reverse osmosis membrane. To reduce organic fouling in reverse osmosis, filtration and carbon adsorption is used.

Reverse osmosis membrane separates multivalent ions better than monovalent ions. Dissolved gases permeate very well through reverse osmosis membrane. Acid and base rejection depends on the solution pH, where rejection would be high for ionised acid or base

and would be low for non-ionised acid or base. Neutral organic solute rejection by reverse osmosis membrane increases as the neutral organic solute molecular weight increases. Reverse osmosis membrane process is used in purification of water, mainly in the desalination of brackish water, in the food processing industry, galvanic, dairy, pharmaceutical, chemical and biological industries.

4.1.4 Pressure retarded osmosis

Pressure retarded osmosis is derived from the reverse-osmosis process. Pressure retarded osmosis membrane is either asymmetric or composite membrane with a pore size less than 2 nm. The sub-layer thickness is 150 μm and the top layer thickness is 1 μm. The separation principle is the solution-diffusion method and the driving force is the concentration difference or the osmotic pressure, (refs. 195). When the applied pressure is higher than the osmotic pressure, the solvent flows from the concentrated solution to the diluted solution, and the solvent flow can be used to generate electricity by using a turbine; see Figure 4-6. The power generated by the pressure retarded osmosis increases as the solution concentration increases. The pressure retarded osmosis has several problems, which include the following

1. The concentration of the concentrated solution decreases because of the osmosis pressure process, thus the osmotic pressure decreases.
2. If the membrane is not perfectly semi-permeable, a solute flux will result, causing the solute to flow from the concentrated solution to the dilute solution, thus the osmotic pressure decreases.
3. The formation of concentration polarisation, where the concentration at the membrane surface is different from the bulk solution concentration. In this case, the solute concentration in the sub-layer causes a decrease in the effective osmotic pressure difference.

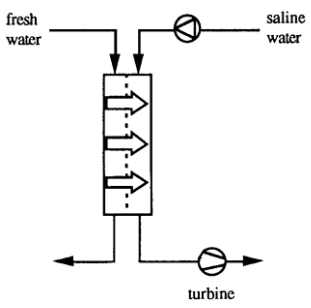

Figure 4-6. Pressure retarded process, (ref. 195).

4.1.5 Piesodialysis

The driving force in the piesodialysis process is pressure and the separation principle is the ion transport. The piesodialysis process separates the ionic solute from the solution where the ionic solute permeates through the membrane rather than the solvent. It consists of cation-exchange and anion-exchange groups. The solute concentration in permeate is higher than that in the feed. The salt flux is increased by increasing the ion-exchange capacity of the membrane and the driving force is the pressure that is equal up to 100 bar. The piesodialysis process is used in salt enrichment.

4.1.6 Nanofiltration

See chapter 7.

4.2 Membrane using concentration difference as a driving force

There are several processes that use concentration difference as the driving force such as gas separation, pervaporation, dialysis, and liquid membrane process, (refs. 195, 230, 244, 267, 271). These processes can be distinguished according to their structure and functionality to synthetic solid membrane as in gas separation, pervaporation and dialysis, and liquid membranes.

4.2.1 Gas separation membrane process

Gas separation membrane is used in separating gases from each other, where the separation depends on the difference between gas solubility and diffusivity in the membrane. The performance of the membrane used in gas separation depends on the membrane selective layer and the membrane support structure, (refs. 195, 267, 271). The membrane selective layer must be thin to minimize the gas flux, and the gas transport through it occurs because of solution-diffusion. The membrane support layer must be mechanically strong and does not contribute any resistance to the gas flow. Gas separation can be carried in porous and non-porous members.

4.2.1.1 Gas separation through porous membranes

Gas transport through membranes depends on the membrane pore diameter. When the

membrane pore diameter ranges between 0.1 to 10 μm, the gas permeation through the membrane occurs due to convection flow where no separation takes place. No separation occurs because of the viscous flow where the mean free path of the gas molecules is small relative to the membrane pore diameter. If the membrane pore diameter is less than 0.1 μm, the gas separation occurs due to diffusion through the membrane. The mean free path of the gas would increase by the decrease in the membrane pore diameter, this is known as Knudsen flow. The flux is inversely proportional to the gas molecular weight. As a result, when separating two gases this means it depends on the square root ratio of their molecular weight, which means in general that the separating factors obtained are low. If the membrane pore diameter ranges between 5 to 20Å, the gas is separated by molecular sieving. See Figure 4-7.

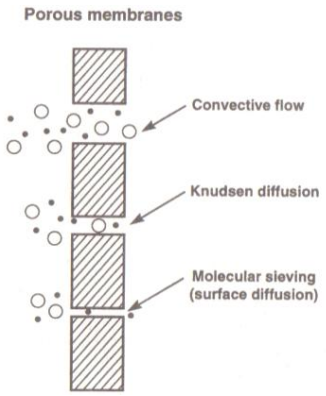

Figure 4-7. Gas permeation mechanisms through porous membranes, (ref. 267).

4.2.1.2 Gas separation through nonporous membranes

Separation of gases in nonporous membranes depends on the gas permeability through the membrane, (refs. 195, 230, 244). Separation of gases occurs due to difference in molecular size and gas solubility in the membrane. Fick's law is the simplest description of gas diffusion through nonporous membrane, where if the gas solubility is proportional to the gas partial pressure and diffusion coefficient is independent of time, position and concentration, then Fick's law can characterise this process. The permeability (refs. 230) is the product of diffusion coefficient (D) and solubility coefficient (s) and is given by

$$P = D\,s \qquad (4.9)$$

The ideal selectivity coefficient for gas separation through nonporous membranes is given by the ratio of the permeability coefficients

$$\Gamma_{ij} = \frac{P_i}{P_j} \qquad (4.10)$$

where Γ_{ij} is the selectivity coefficient, P_i is the permeability of substance (i) and P_j is the permeability of substance (j). The ideal membrane selectivity (Γ_{ij}) is used to measure the membrane ability to separate gas (i) from gas (j). The selectivity coefficient is not equal to the ideal selectivity factor because of plasticisation at high (partial) pressure. Additionally, the selectivity coefficient depends on the permeability ratio across the membrane, where if (P_i / P_j) ratio is high then the selectivity coefficient is high and when (P_i / P_j) $\rightarrow$ 0 then the selectivity coefficient decreases. To establish a driving force, either a high pressure is applied on the feed side or the pressure at the permeate side is reduced. The permeability coefficient (P) depends on the membrane thickness, the membrane area and the driving force. In the case where Henry's law does not apply, the permeability coefficient (P) is not constant and depends on the driving force, i.e., the change in pressure changes the permeability coefficient. The permeability coefficient is affected by the solubility and the diffusion coefficients. The solubility coefficient (s) for gases increases with the increase in the gas molecule size, because as the gas molecule size increases, the gas can condense more readily and then the gas solubility in the membrane increases. Solubility for gases also increases as the gas affinity in the polymer increases. Permeability coefficient is also affected by the gas diffusivity. The diffusivity depends on gas molecular size and the membrane polymer. The diffusion coefficient increases as the molecular size decreases, which causes the permeability coefficient to increase. The diffusion coefficient is inversely proportional to the molecular size; this can be proved by thermodynamic diffusion coefficient. In the gas separation membrane process, the gas permeate through the membrane when the gas partial pressure at the feed side is greater than the partial pressure at the permeate side.

$$n_{io}\, p_o \succ n_{il}\, p_l \qquad (4.11\text{ -a})$$

where p_o is the feed side pressure, p_l is the permeate side feed pressure and n_i is the composition of the gas material (i). By rearranging equation (4.11-a) gives

$$\frac{n_{il}}{n_{io}} \leq \frac{p_o}{p_l} \leq \phi \qquad (4.11\text{-b})$$

where ϕ is the pressure ratio. Equation (4.11-b) expresses the maximum separation that can

be achieved by the membrane. The separation cannot exceed the pressure ratio whatever the membrane selectivity is, (refs. 230, 271, 329).

The two types of membranes suitable for the gas separation process are asymmetric and composite membranes with an electrometric or glassy polymeric top layer. The driving force is the pressure difference. Gas separation using porous membranes is used for hydrogen and helium recovery from purge gas streams in ammonia synthesis, petroleum refineries, methanol synthesis, removal of (H_2S) from natural gas and removal of water, which is known as drying of gases.

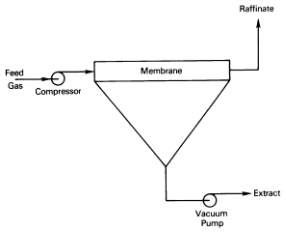

Figure 4-8. Membrane gas separation process, (ref. 230).

4.2.2 Pervaporation process

The pervaporation process is a separation process in which liquid mixtures at the feed side is in direct contact with the membrane, and permeates is removed from the outlet side in a vapour state. Separation depends on the vapour pressure difference between the feed solution and the permeate vapour, where the permeate pressure is lower than the saturation pressure which causes the mass flux, (refs. 195, 230, 271, 329). In pervaporation membrane, the liquid in the feed is maintained at atmospheric pressure and is removed as vapour from the permeate side because of low partial pressure existing in the permeate area. The low partial pressure is achieved by a vacuum pump or by employing a carrier gas; see Figure 4-9.

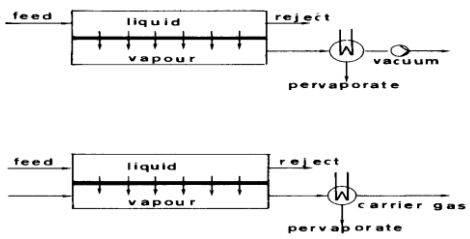

Figure 4-9. Pervaporation process with a vacuum pump and with a carrier gas, (ref. 230).

The pervaporation process involves three sequence steps: the first step is a selective sorption

into the membrane on the feed side; the second step is a selective diffusion through the membrane; and the third step is desorption into a vapour phase on the permeate side. In the pervaporation process, heat and mass transfer occur and separation is based on the differences in solubility and diffusivity. The driving force is the vapour pressure or the activity difference. The separating driving force is influenced by the vapour-liquid equilibrium. The solution-diffusion mechanism causes the transport, and the selectivity is determined by selective sorption and/or selective diffusion. Liquid mixture separation differs from pure liquid separation because of the coupling phenomena and the thermodynamic interactions, (refs. 195, 329). The permeability coefficient for component (*i*) and (*j*) in a mixture of (*i* and *j*) liquids is given by

$$P_i = D_i\, s_i \qquad (4.12\text{-a})$$

$$P_j = D_j\, s_j \qquad (4.12\text{-b})$$

For component (*i*) in liquid mixture, the linear flux-force relation is given as

$$J_i = -L_i \frac{d\mu_i}{dx} \qquad (4.13)$$

where L_i is a proportionality or phenomenological coefficient. Substituting the chemical potential into equation (4.13) gives the following equation

$$J_i = \frac{-L_i RT}{p_{i,v}} \frac{dp_i}{dx} \qquad (4.14)$$

If an ideal transport is assumed in pervaporation of a pure liquid through a nonporous homogeneous polymer membrane, the transport by a solution-diffusion-desorption mechanism occurs. In an ideal system, it is assumed that the membrane thickness is uniform and the diffusion coefficient is independent of the volume fraction of the liquid inside the membrane polymer. The flux is described by integrating equation (4.14), thus the flux will be

$$J_i = \frac{P_i\left(p_{io} - p_{il}\right)}{l} \qquad (4.15)$$

where p_i is the partial pressure of species (*i*). From equation (4.15), it can be noticed that the

flux is proportional to the partial pressure difference across the membrane and inversely proportional to the membrane thickness. If the vapour pressure at the permeate side is low, the concentration varies over the membrane and the driving force is at its maximum. The flux of pure liquid through a membrane and the concentration inside the membrane is the main parameter in determining the flux, as in equation 4.16. As the concentration of component (*i*) in the membrane increases, the flux also increases.

$$J_i = D_{i,c}\left(\exp\left(c_{i,1^m}\right)-1\right) \qquad (4.16)$$

Distinguishing between flow coupling and thermodynamic interaction in a multi-component system must be considered. Flow coupling is described by non-equilibrium thermodynamic (see non-equilibrium section). The thermodynamic interaction is the leading factor in selective transport and is the determining factor in selective transport. In the pervaporation process for a liquid mixture, the flux and the selectivity depend on the composition of the feed. Assume species (A) to be the permeating species; if the concentration decreases, the flux would decrease and the selectivity would increase. Also — but not necessarily true — as downstream pressure increases, the selectivity decreases. The concentration polarization in the pervaporation process at the liquid membrane interface does not affect the overall transfer phenomena. Due to phase change from liquid to vapour, a local temperature drop at the membrane interface occurs, thus the permeation flux is affected.

The membrane used in the pervaporation process must have an open substructure and high surface porosity with narrow pore size distribution. The open substructure is used to avoid capillary resistance and minimize resistance toward vapour transport. Pervaporation is used to separate a small amount of liquid from a liquid mixture, such as removal of water from alcohol or other organic solvent and vice versa. Also, pervaporation is used in chemical processes industries, food and pharmaceutical industrials.

4.2.3 Liquid membrane

Liquid membrane can be used as a separating membrane between two phases; the phases can either be liquid or gas. The component transport between phases occurs because of the driving force applied on liquid or gas feed phase (phase 1). The driving force through liquid membrane in general is the chemical potential gradient. Separation is a result of the difference of the solubility and the diffusivity in the liquid film. Liquid membrane contains

additives to control the stability, the permeability and the selectivity of the membrane. The two basic types of liquid membranes are as follows

1. Immobilised liquid membrane (ILM) or supported liquid membrane (SLM) where the liquid film is immobilised within the pores of a porous membrane where the porous membrane only works as a supporting layer for the liquid film; see Figure 4-10-a, (refs. 159). Immobilised liquid membrane is used for gas separation because the gas diffusion through liquids is of order (10^{-5}-10^{-6}) (cm^2/s). The immobilised liquid membrane selectivity increases by adding selective chemicals toward specific gases where the chemicals absorb the gas. The simplest type of immobilised liquid membrane is a membrane with a saturated wettable micro porous material with liquid. Permeation through the immobilised liquid membrane involves mechanical properties and polymer support. The immobilised liquid membrane can bare pressure up to 20 bars. The membrane choice depends on the gas solubility and the liquid volatility. The membrane micro-porous support should not be reactive with inlet materials, should have high porosity and should have small pore size. The disadvantage of immobilised liquid membrane is that some of the liquid can be lost with gasses diffusion. This disadvantage can be reduced by gelling the liquid by adding a suitable polymer, filling the membrane with a suitable solvent or plasticiser to control the permeation behaviour, or using a barrier film on either side of the membrane, (refs. 195, 230, 267).
2. Emulsion liquid membrane (ELM); see Figure 4-10-b. The emulsion membrane materials are transported from the continuous phase to the fixed phase. The feed material reacts with the emulsion where it is transported to the outlet side of the membrane, where the bond between the permeate material and the emulsion is broken, and the permeate material is released and the emulsion retains back to the feed side of the membrane. The driving force in the emulsion membrane is the concentration difference across the membrane. The membrane selectivity depends on the feed material solubility in the membrane.

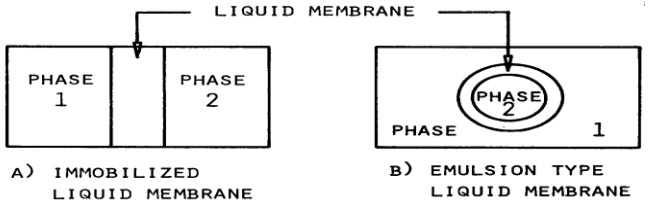

Figure 4-10. 4-10-a is the immobilised liquid membrane and 4-10-b is emulsion liquid membrane, (ref. 230).

The selectivity in the liquid membrane is low, where it depends on the difference in the distribution coefficient of components in the feed phase (phase 1) with the liquid membrane. If the diffusivity of components with comparable sizes in the feed phase (phase 1) are similar, the selectivity will be low. To increase the selectivity, a carrier molecule is added to the liquid membrane, thus the transport of specific components is increased, which is called "carrier-mediated" or "facilitated" transport. The carrier molecule is a reactive material that reacts with one of the feed solution components and transports it to the permeate side. The choice of the carrier molecule depends on the composition of the feed phase, (refs. 159, 230, 270). There are different types of transport through the carrier-facilitated membrane — see Figure 4-11 — which are as follows

1. Passive diffusion

The component diffuses through the membrane due to the concentration gradient. This process is slow and non-selective.

2. Facilitated transport

The membrane contains a carrier that reacts with one of the feed components, then diffuses to the permeate membrane interface. When it reaches the permeate side, the reaction is reversed where the transferred component permeates from the membrane and the carrier is re-formed and diffuses back to the feed side.

3. Couple transport

The membrane contains a carrier that couples with the species in feed and permeate solutions. As a result, one component moves against it, which is the concentration gradient, while the other component moves with it, which is the concentration gradient direction where its concentration gradient value is high, where the carrier couples with component-(1) at the feed side and liberates component-(2) to the feed side. Then component-(1)/carrier diffuses to the permeate side. At the membrane-permeate interface, the reaction is reversed because of the high concentration of component-(2). Component-(1) is released to the permeate and the carrier reacts with component-(2) and diffuses back to the feed side to release component-(2) and react with component-(1).

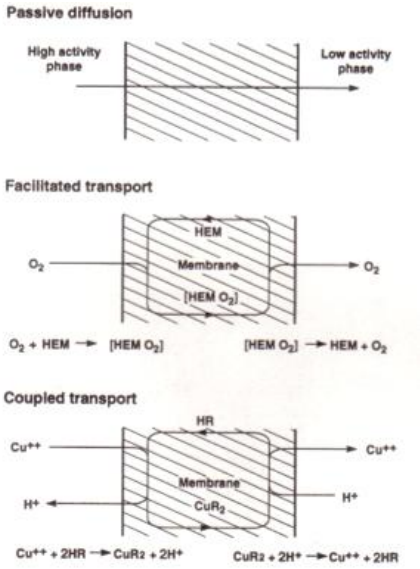

Figure 4-11. Example of passive diffusion, facilitated transport and coupled transport, (ref. 267).

The difference in transport between liquid membrane with carrier-mediated and normal liquid membrane without carrier-mediated can be noticed in Figure 4-12.

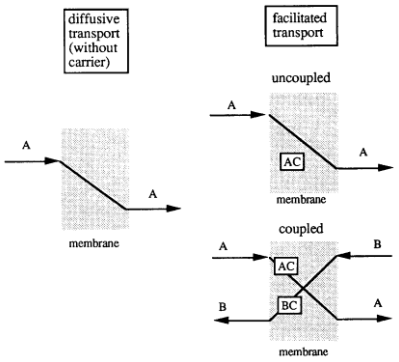

Figure 4-12. The left hand-side is the transport through liquid membrane without carrier-mediated and the right-hand side is the transport through liquid membrane with carrier-mediated, (ref. 195).

In cases where carrier-mediate does not exist, then component (*A*) transports through the liquid membrane by diffusion. In the carrier-mediate case, component (*A*) transports because of its diffusion and the solute-carrier (*AC*) diffusion. If the carrier-mediated liquid membrane is used to separate a component from a liquid mixture, a coupled transport occurs. The basic coupled transport is the co-coupled transport where the two components are moving in the same direction, and the counter-coupled transport where the two components are moving in opposite directions. In the transport mechanism through carrier-mediated (facilitated) liquid membrane, at first a complexation between component (*A*) and carrier at the feed/membrane interface occurs. Then the carrier-solute complex diffuses through the membrane. In the final

step, a decomplexation of the carrier-solute takes place at the membrane/solute (phase 2) interface and free carrier diffuses back to the feed phase (phase 1)/membrane interface. The complexation reaction must be reversible so that the transport of solutes will not stop by using all carriers and forming carrier-solute complex as in the irreversible reaction. The carrier-mediate must be stable in the separation environment; its reaction with the permeating material must be reversible and fast, its mobility through the membrane must be high, and the carrier-solute mobility through the membrane must also be high. Transport of component (*A*) through the carrier-mediated liquid membrane is affected by the rate of complex formation and deformation at the two membrane interfaces and diffusion of the complex through the membrane. The total flux of component (*A*) is the sum of Fickean diffusion and complex carrier-solute diffusion, which is given by the following equation

$$J_A = \frac{D_A}{l}\left(c_{A,0} - c_{iA,l}\right) + \frac{D_{AC}}{l}\left(c_{AC,0} - c_{AC,l}\right) \qquad (4.17)$$

where $c_{A,0}$ is the concentration of (*A*) inside the liquid film at the feed/membrane phase interface, and it is equal to component (*A*) solubility in the liquid when equilibrium thermodynamics occur at the interface, $c_{A,l}$ is component (*A*) concentration at the membrane/permeate phase interface, D_{AC} is the diffusion coefficient of the complex, $c_{AC,0}$ is the complex concentration at the feed/membrane phase interface and $c_{AC,l}$ is the complex concentration at the membrane/permeate phase interface. The first term on the right-hand side in equation (4.17) is the diffusion according to Fick's law, and the second term is the carrier-mediated diffusion where the flux is proportional to the driving force. In equation (4.17), the Fickian diffusion can be the determining transport rate when the concentration of (*AC*) is lower than the concentration of the free component (*A*) ($c_{A,0} \gg c_{AC,0}$), which means that the rate of reaction is lower than the diffusion rate. The complex diffusion can be the determining rate of transport when the rate of reaction is fast and the diffusion rate of the complex is higher than the diffusion rate of un-complex (*A*). Concentration polarization occurs in liquid membranes, which depends on the flow rate through the membrane and mass transfer coefficient of the solutions. Concentration polarisation on the membrane interfaces decreases the solute concentration in the membrane interface and consequently inside the membrane, (refs. 159).

The supported liquid membrane (SLM) consists of the support membrane, organic solvent and carrier. There are several problems encountered by the supported liquid membrane

(SLM), which are explained as follows. The surface and overall porosity of the support membrane must be high to obtain high flux. Also, the membrane support layer must be thin because the permeating rate (flux) is inversely proportional to the membrane thickness. But if the membrane thickness decreases then the rate of reaction will decrease, thus the flux will decrease. If organic solvent is used in the supported liquid membrane (SLM), the organic solvent must be a solvent for the carrier and carrier-solute complex. The viscosity of the organic solvent is important because it is inversely proportional to the diffusion coefficient. The carrier and the carrier-solute concentrations increase the solvent viscosity, which could cause a problem because the increase in carrier concentration increases the flux, but on the other hand, it increases the solution viscosity, hence reducing the diffusion coefficient, which will reduce the flux. Another problem is the instability of the supported liquid membrane (SLM) with time causing loss of the organic phase. The stability of the supported liquid membrane (SLM) can be obtained by gelation of the liquid, which will decrease the diffusion coefficient but the membrane will be more stable. Carrier-mediated liquid membranes are used in the separation of ions (cations and anions), the removal of gases, the separation of organic liquids and the removal of phenol from wastewater.

4.2.4 Dialysis process

The solute diffuses from the feed side to the dialysate or permeate side according to the concentration gradient. The separation is a result of the difference between the diffusion rates of the solutes due to the difference in molecular size. The dialysis membrane is considered a nonporous membrane. Transport occurs because of diffusion; to reduce the resistance toward diffusion, the membrane is swollen, (refs. 230, 270, 271). The diffusion through dialysis process is given by

$$J_s = \frac{D_w k_w \Delta c_w}{l} \qquad (4.18)$$

where D_w is the solute diffusion coefficient, k_w is the solubility or distribution coefficient and Δc_w is the solute concentration difference between the feed and permeate. As the solute diffuses through the dialysis membrane, an osmotic flow due to osmotic pressure difference in the opposite side occurs, which is a counter-current flow. The solute and the solvent flows are coupled when concentration polarisation occurs in the dialysis process, thus the mass transfer resistance is due to the membrane and boundary layers. The dialysis process

efficiency depends on the feed and the dialysis flow rates and on the solute rate constant for transporting between the feed and the dialysate solutions. The efficiency is given as

$$\text{Efficiency} = \frac{\dot{M}}{c_f - c_{f,d}} \qquad (4.19)$$

where $c_{f,d}$ is the solute dialysate inlet concentration and $\dot{M}$ is the mass transfer. Dialysis systems must have a maximum membrane area and a minimum volume. When the liquid phase at both sides of the membrane contain the same solution without any pressure difference and the separation factor is equal to 1, the flux is given as follows

$$J_i = \frac{P_i}{l}\left(c_{i,1^s} - c_{i,2^s}\right) \qquad (4.20)$$

The solute flux in the dialysis process is proportional to the concentration difference and the separation is a result of the difference in permeability coefficient P_i. The dialysis process is used in artificial kidneys and removal of metabolic wastes from the blood, which is called hem filtration. The dialysis process is also used in removal of alcohol from beer and recovery of caustic from hemi-cellulose solution.

4.3 Thermally driven membrane process

Transport of molecules due to temperature difference could occur, (refs. 230). If two phases separated by a membrane have different temperatures, heat will transport from a high temperature phase to a low temperature phase, which is known as heat flux, and when it is occupied with mass flux the process is called thermo-osmosis or thermo-diffusion. In thermo-osmosis (thermo-diffusion) process, porous and non-porous membranes can be used. The membranes act as a barrier and separation is a result of temperature difference where volume flux occurs from high temperature phase to low temperature phase until equilibrium is reached. Distillation is another form of a thermally driven process where two liquid phases are separated by a membrane. The difference between the membrane distillation and the thermo-osmosis that the membrane affects the separation performance in the distillation process, while in thermo-osmosis it is just a barrier, and the selectivity depends on the vapour-liquid equilibrium.

If the two phases have different temperatures, then the vapour pressures of the two phases are

different, causing vapour molecules to transport from the high temperature phase to the low temperature phase. Then the transported molecules will condensate in the low temperature phase. The used membrane must be hydrophobic (not wetted by liquid or solution) to avoid filling the pores with the solution. The membrane only acts as a separating barrier and the selectivity depends on the vapour-liquid equilibrium. The flux is proportional to the temperature difference, which is the driving force. The flux can be written as

$$J_i = B.\Delta p_i \qquad (4.21)$$

where Δp_i is the driving force and depends on the temperature difference and B is the constant related to the minimum local free volume necessary to allow displacement. The proportionality factor (B) depends on the membrane properties such as its thickness, pore structure and porosity. The angle contact between the membrane and the solution determines if the membrane is wetted or not. The membrane wettability depends on the pore size, the liquid surface tension and the contact angle between the liquid and the membrane surface. As the pore size decreases, the pressure difference needed to wet the membrane increases. When the contact angle between the membrane surface and the liquid is bigger than 90°, the liquid will not wet the membrane, and if the contact angle between the membrane surface and the liquid is less than 90°, the liquid will wet the membrane. As the liquid concentration increases, the surface tension decreases and the pressure difference needed to wet the membrane decreases. Then to avoid wetting the membrane, the liquid surface tension must be high, the membrane surface energy low, small pore size and the contact angle (θ) bigger than 90°, and the membrane must be hydrophobic. Since the flux proportionality factor (B) depends on the membrane porosity, where as the porosity increases the flux increases, then the membrane wettability increases, thus the membrane maximum pore size must be near the average size. The thermally driven membrane process is used to produce pure water such as seawater desalination, boiler feed water and concentrating aqueous solutions.

4.4 Electrically driven membrane processes

Electrically driven membrane uses the electrical potential as the driving force, and only the charged molecules are affected by the driving force, and as a result uncharged molecules can be separated from charged ones. Ion-exchange membrane has a charge attached to the polymer backbone of the membrane material. Two types of ion-exchange membranes exist:

the first is cation-exchange membrane, where cations pass through it, and the second is anion-exchange membrane, where only anions pass through it. Membranes used in the ion-exchange process must have low electrical resistance and good ion selectivity. Ion-exchange membrane thickness ranges from 100–500 μm. When the ion-exchange membrane is immersed in aqueous solution, the membrane swells the solvent, causing the membrane to depend on the ionised groups in the matrix concentration and on the hydrophobic-hydrophilic balance of the polymer material. A complete dissolution of the membrane would occur if the density of the ionic group in the solution was large and the membrane was hydrophilic. To avoid membrane dissolution a cross-linking chemical is added to the membrane during manufacturing.

Ion-exchange membranes are either nonporous homogenous or nonporous heterogeneous. The heterogeneous membrane has high electrical resistance and low mechanical strength. The fixed charge of a homogenous membrane is uniformly distributed, while the fixed charge of a heterogeneous membrane is contained in a small domain and distributed through an inert support matrix. Ion-exchange membranes use electrical potential gradients and concentration gradients as the driving forces. In the ion-exchange membrane, it's easier to describe the amount of charge transported by the membrane rather than the amount of transported material. The ion-exchange membrane is used in the separation of amino acids, production of chlorine, caustic soda, sulphuric acid and desalination of water. In neutral membranes, the driving force for ion transport is the concentration difference but in charged membranes or ion-exchange membranes, the driving force is the concentration difference and is affected by the presence of the fixed charge, (refs.).

The fixed charge theory can be used to describe ionic transport through the ion-exchange membrane or charged membrane, (refs. 7, 195, 220, 230, 267). The fixed charge theory is based on two principles: the Nernst-Planck equation and Donnan equilibrium. The fixed charge theory assumes that thermodynamic equilibrium exists across the interface between the solution and the membrane. If the ion-exchange membrane is used to separate ions from ionic solution, the ions in the solution with the same charges of the fixed charge of the membrane cannot pass through the membrane, which is known as the Donnan effect. The Donnan theory shows that the counter-ions of higher valence are more concentrated in the membrane than in the solution and this effect is higher in dilute solutions than in concentrated solutions. In the Donnan theory, equilibrium thermodynamics is used to calculate the

chemical potential of ionic components in the two phases under a conditional state that the ionic solution is in equilibrium with an ionic membrane. Since the Donnan theory occurs under equilibrium thermodynamics, and at equilibrium the electrochemical potentials in both phases are equal, then the Donnan potential can be given as follow

$$E_{don} = \frac{RT}{Z_i F} \ln\left(\frac{a_{i,m}}{a_i}\right) \qquad (4.22)$$

where E_{don} is the Donnan potential. The Donnan potential gives the potential build-up at the membrane-solution interface, (refs. 7, 195). The ionic distribution determines the transport of the charged molecules. For example, if the solution contains anion (-) ions and cation (+) ions and the membrane has a fixed charge, at equilibrium, the following equation will be gained

$$\left[c_{i^+}\right]^m \left[c_{i^-}\right]^m = \left[c_{i^+}\right]\left[c_{i^-}\right] \qquad (4.23)$$

where the left-hand side is the membrane phase and the right-hand side is the solution phase. If electrical neutrality is assumed, then

$$\left[C_{i^+}\right]^m = \left[C_{i^-}\right]^m + \left[C_{R^-}\right]^m$$
$$\left[C_{i^-}\right] = \left[C_{i^+}\right]$$

For an ideal system equation (4.23) becomes as follows

$$\frac{\left[C_{i^-}\right]}{\left[C_{i^-}\right]^m} = \sqrt{\frac{\left[C_{R^-}\right]^m}{\left[C_{i^-}\right]^m} + 1} \qquad (4.\ 24)$$

This is the Donnan equilibrium for the charged solutes and the membrane. But for non-ideal systems, the activity coefficient for cation and anion are added, which gives

$$\frac{\left[C_{i^-}\right]\left[\gamma_{\pm}\right]}{\left[C_{i^-}\right]^m\left[\gamma_{\pm}\right]^m} = \sqrt{\frac{\left[C_{R^-}\right]}{\left[C_{i^-}\right]^m} + 1} \qquad (4.25)$$

If it is assumed that two forces act on the ionic solutes, which are the concentration difference and the electrical potential difference, then the transport of ions is described by Fickian diffusion and ionic conductance, (refs. 7, 230). This is known as the Nernst-Planck equation

$$J_i = -D_i \frac{dc}{dx} - z_i F m_i c_i \frac{dE}{dx} \qquad (4.26)$$

The overall transport rate involves membrane thickness and membrane area, and for this the concentration must be expressed in molar scale. When an electrical current passes through an ion-exchange membrane, a substantial electro-osmotic transfer of the solvent occurs. Coupling occurs between the ions and the solvent flowing through the membrane, and high frictional forces by the ions results because the ions interact with the surrounding solvent molecules; as a result, the solvent motion due to osmosis or electro-osmosis affects the frictional forces.

An example of electrically driven membranes is the electro-dialysis process. In the electro-dialysis process, all ions are separated from uncharged solutes, water and macro-solutes. The electro-dialysis membrane is used in removing salts from brackish water, concentrating seawater and deashing whey. The electro-dialysis membrane is a swollen gel containing polymer with a fixed ionic charge. When the electro-dialysis membrane has a high perm-selectivity, it must have a low electrical resistance, must be physically and chemically stable, must be mechanically strong, should not swell or shrink if the ionic strength changes, and should not deform under thermal stress. The perm-selectivity is the ratio of the transport of electrical charge of a specific ion to the total transport of the electrons through the membrane. The electro-dialysis membrane has cation-exchange and anion-exchange membranes, where the charged membranes of anion-exchange and cation-exchange are placed in an alternating pattern, i.e., one anion-exchange membrane followed by cation-exchange, see Figure 4-13, where each anion-exchange and cation-exchange forms a compartment (cell pair). The basic block for the cation-exchange membrane is the polystyrene copolymerised with divinylbenzene and then suffocated. It is stable and highly ionised over most pH ranges. The major charged group in the anion-exchange membrane is quaternary amines. When the solution passes through electro-dialysis, the anions move toward the anode, and the cations move toward the cathode. The cations pass through the negative charged membrane and the anions pass through positive charged membrane. As a result, one pair cell would be enriched by ions; on the other hand, the adjacent cell would be depleted from ions.

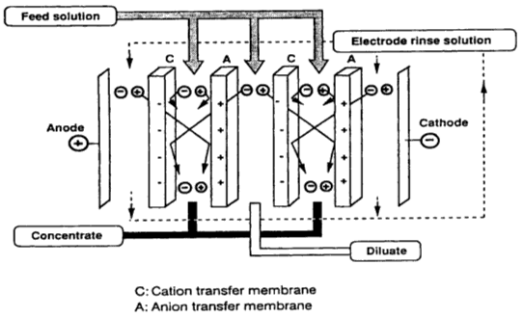

Figure 4-13. Electro-dialysis membrane, (ref. 271).

The electro-dialysis membrane performance is controlled by the ion transport through the diluted cell, where the ion concentration in this cell is low to transport the current; as a result, it limits the current and the ion flux through the membrane. Another factor affecting the membrane performance is the applied voltage across the membrane. As the applied voltage across the membrane increases, the ion flux through the membrane increases, thus the permeating ion concentration near the membrane surface decreases. When the ion concentration at the membrane surface reaches zero, the current through the membrane is called the limiting current density, and the ion transport flux through the boundary layer reaches its maximum value. When the limiting current density is reached, any increase in the applied voltage would not increase the ion transport. The extra applied voltage causes side reaction such as water dissociation.

If a single cationic membrane is considered as in figure 4-14, the ion gradient on the dilute side of the membrane is described by Fick's law, (refs. 7, 230, 267). The diffusion rate of cations to the membrane surface is given by

$$J^+ = D^+ \frac{\left(c_b^+ - c_o^+\right)}{\delta} \qquad (4.27)$$

where D^+ is the diffusion coefficient of the cation in solution, $c_b{}^+$ is the cation concentration in the bulk solution, $c_o{}^+$ is the cation concentration in the dilute solution adjacent to the membrane surface and δ is the boundary layer thickness.

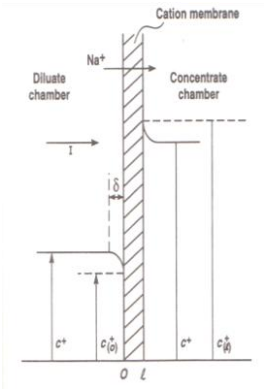

Figure 4-14. Concentration gradient adjacent to cationic membrane in electro-dialysis membrane, (ref. 267).

The total cation flux toward the membrane is the sum of the diffusion rate and electrolyte transport rate, which is given as

$$J^+ = D^+ \frac{\left(c_b^+ - c_o^+\right)}{\delta} + \frac{t^+ I}{F} \qquad (4.28)$$

where t^+ is the cation transport number and I is the current. Transport through the membrane is the sum of the diffusion transport due to the concentration difference on each membrane side and due to the voltage difference, which is given by

$$J^+ = -P^+ \frac{\left(c_b^+ - c_l^+\right)}{l} + \frac{t_m^+ I}{F} \qquad (4.29)$$

where P^+ is the cation permeability through the membrane, $t_m{}^+$ is the membrane transport number for cations, $c_i{}^+$ is the cation concentration in the concentrate solution and l is the membrane thickness. By combining equations (4.28) and (4.29) and assuming that the concentration gradient is small compared to the voltage gradient in equation (4.29) gives

$$D^+ \frac{\left(c_b^+ - c_o^+\right)}{\delta} + \frac{t^+ I}{F} = \frac{t_m^+ I}{F} \qquad (4.30)$$

When the ion concentration at the membrane surface reaches zero, the current is known as the limiting current for cation membrane. The limiting current is the maximum applied current. When the maximum current is exceeded, the undesirable processes occur such as water dissociation and anion transport through the cation membrane. As a result, the membrane efficiency decreases.

There are two types of electro-dialysis, which are unidirectional and reversal electro-dialysis. The unidirectional operation keeps the electrode polarity and ion movement in constant direction. The polarity in the electrodes in the reversal electro-dialysis is reversed, thus the compartments in the membrane are also reversed where dilute compartments become concentrated and vice versa. The reversing electro-dialysis reduces fouling and scaling, the amount of additives in the feed, which are used to reduce fouling and scaling in the feed, and the frequency of cleaning requirements. If no direct current is applied to the membranes, no ion separation occurs and the solution would pass through the membranes without any changes. Also, since a membrane of different charges are arranged to alternate, the concentration of the ions would increase and decrease alternating, thus dilute solution allows ion concentration and concentrated solution (high ion concentration) would vary in alternating. The applied current density has a limit that is equal to the amount of current necessary to transfer all the ions and it must not be exceeded because it could dissociate water. The limiting current density (i) is given by

$$i_{Lim} = \frac{z\Delta F(c_b - c_m)}{\delta(t^m - t^{bL})} \qquad (4.31)$$

where c_b is the bulk concentration and c_m is the concentration at the membrane interface and δ is the membrane thickness. In general, the membranes used in electro-dialysis must have a high selectivity, be a good conductor, and have high mechanical strength, thus a moderate degree of swelling.

4.5 Summary

The membrane processes can be separated into different groups according to their driving force across the effective layer, where the driving force can be pressure difference, concentration difference, temperature difference or electrical potential difference. The pressure-driven membrane uses the applied pressure as a driving force such as microfiltration, ultrafiltration, nanofiltration and reverse osmosis. The difference between microfiltration, ultrafiltration, nanofiltration and reverse osmosis is the separated solute size and the membrane pore size. The membrane processes that use concentration difference as the driving force include gas separation, pervaporation, dialysis, and liquid membrane process. The separation depends on the difference between the solutes solubility and diffusivity in the membrane. Thermally driven membrane processes use the heat flux as the

driving force across the membrane, such as thermo-osmosis process and membrane distillation process. The heat flux across the membrane is coupled with mass flux; as a result, separation occurs. Electrically driven membrane uses the electrical potential as the driving force, and only the charged molecules are affected by the driving force. In this work, nanofiltration membrane was the used which is considered as a pressure driven membrane. On the other hand, the separation process due to the electrical potential should be considered because nanofiltration membrane is considered a charged membrane. Thus, the rejection of the solutes by nanofiltration membrane is due to the pressure force and the electrical potential force. For more details, see chapters 7, 8 and 9.

Chapter 5 Separation models (theoretical analysis of the transport in membranes)

Membrane process is concerned with the exchange of matter or energy between two environments that are separated by the membrane or between the membrane and the environment in which it is immersed, (refs. 120). The separation process does not take place spontaneously and work must be done on the overall system to increase the free energy. The free energy needed to drive the separation process is increased by applying pressure on the feed side and doing mechanical work on the system through the diminishing volume of the feed. The transport of any matter through the membrane is influenced by other substances in the solution and the motion of these substances. A molecule is transported through the membrane because of the force acting on it. The force is determined by the gradient potential across the membrane thickness. In the membrane separation process, there are two important potentials, which are the chemical ($\Delta\mu$) and the electrochemical (ΔF) potentials.

5.1 Driving forces

Transport across a membrane occurs because of driving force acting on the individual components in the system. The driving forces in the membrane are a result of a difference in pressure, concentration, temperature or electrical charges, (refs. 162, 195, 267). These parameters can be divided into two parameters, which are the chemical potential and electrochemical potential. Electrical potential arises when ions are found in the solution and only affects the charged particles or molecules. In the transport between different phases, the flux is carried by a large solute concentration moving under a small thermodynamic force. The driving forces are the chemical and the electrochemical potential gradients, but most of the transport processes occur because of the difference between the chemical potentials. The general chemical and electrochemical potentials of component (i) are given as

$$d\mu_i = RT\left(d\ln c_i\right) + RT\left(d\ln \gamma_i\right) + \tilde{V}_i\left(dp\right) + z_i F\left(d\psi\right) \qquad (5.1)$$

where μ_i is the chemical potential of component (i), c_i is the concentration of component (i), γ_i is the activity coefficient, F is Faraday's number, z_i is the valence of species (i) including the charge, ψ is the electrical potential, $\tilde{V}_i$ is the partial molar volume of species (i), and R is the gas constant. For example, for a steady state process, the flux is constant and the local driving force is the chemical potential gradient for each component that is transported. Then

this method is called the solution-diffusion model, where the membrane is considered to be an active thermodynamic component and is included in Gibbs-Duham equation for the membrane phase, (refs. 195, 220). For the isothermal process, where the temperature is constant and only the pressure and the concentration would affect the chemical potential, and if the concentration is expressed in terms of activity (*a*), the chemical potential equation will be given as follows

$$\mu_i = \mu_i^o + RT\left(\ln a_i\right) + V_i p \qquad (5.2)$$

where a_i is the activities of ionic species (i) in the membrane, V_i is the molar volume of species (i) and μ_i° is the standard chemical potential and it is constant. The concentration in equation (5.2) is given as an activity in order to express the non-ideal saturation vapour pressure. The isothermal gradient of the chemical potential between two phases of single liquid can be created only by a pressure difference. Since the chemical potential is increased by the pressure difference, the pressure at the outlet side can be reduced, thus pressure difference occurs. Also in a membrane, the plasticizing effect of the absorbed liquid on the diffusion must be considered. As mentioned before, the driving force is the potential gradient and the average driving force is the potential difference across the membrane. If the driving force is considered to be the chemical and the electrochemical potential gradients, then the average driving force is as follows

$$F_{ave} = \left(\frac{RT}{l}\frac{\Delta x_i}{x_i}\right) + \left(\frac{z_i F}{l}\Delta E\right) + \left(\frac{V_i}{l}\Delta p\right) \qquad (5.3)$$

where l is the membrane thickness. When comparing the driving forces they must be dimensionless. When comparing the concentration, the electrical and the pressure potentials, it could be concluded that the electrical potential is a very strong driving force in comparison with pressure driving force, (refs. 7, 195, 220, 230). The concentration potential is often equal to unity and the pressure driving force depends on the kind of components involved. Diffusion is the most varied process in the membrane process. The parameters that characterise the membrane transport process, with respect to trans-membrane pressure, convective and diffusion transports of neutral solute and solution, are the hydraulic permeability, the diffusive permeability and the reflection coefficients. The hydraulic permeability is a measure of the ability to transport fluid volume under the action of a

pressure difference across the membrane. The hydraulic permeability (the permeability coefficient) is given by

$$L_p = \frac{J_v}{\Delta p} \qquad (5.4)$$

This definition applies when the solute is absent (but when the solute is present, the membrane is freely permeable to the solute). When there is a difference in the solute composition at both sides of the membrane and the membrane is not freely permeable to the solute, the flux is affected by the osmotic pressure difference across the membrane. Then the volumetric flux is given by

$$J_v = L_p\left(\Delta p - \left[\sigma_d \Delta \pi_i\right]\right) \qquad (5.5)$$

where J_v is the volumetric flux, σ_d is the Staverman osmotic reflection coefficient for the solute, and $\Delta \pi_i$ is the difference between the osmotic pressures in the external solutions at the membrane for species (*i*). The diffusion permeability characterises the transmissibility of the membrane for the solute when the volumetric flux is equal to zero. When the volumetric flux is equal to zero, this means that the pressure difference on the membrane boundaries and the Staverman osmotic reflection coefficient for the solute are equal to zero, and the membrane is freely permeable to the solute.

5.2 Permeation through membrane

Permeation through the membrane is described by two models, which are the solution-diffusion model and the pore flow model. The solution diffusion model is when a solute dissolves in the membrane then diffuses through the membrane down the concentration gradient. As a result, the separation of a solute depends on the solute solubility in the membrane and the solute diffusion rate through the membrane. In the pore model, the solute is transported through the membrane by a pressure-driven convective flow where part of the solute passes through the membrane pores while others do not, (refs. 27, 220, 267).

In the solution diffusion model, diffusion is defined as the transport of a solute because of its concentration gradient. For example, if a solution is separated by a membrane and the solute concentration at each side of the membrane is different, then the solute would move from the

high concentration side to the low concentration side of the membrane. This is described by Fick's law of diffusion

$$J_i = -D_i \frac{dc}{dx} \qquad (5.6)$$

where J_i is the mass flux of component (*i*), dc_i/dx is the concentration gradient of component (*i*) and D_i is the diffusion coefficient of component (*i*). In the pore flow model, the solute flow is described by the pressure-driven convective flow. This can be described by Darcy's law

$$J_i = K' c_i \frac{dp}{dx} \qquad (5.7)$$

where dp/dx is the pressure gradient in the porous medium, c_i is the concentration of component (*i*) in the membrane and K' is the coefficient reflecting the membrane nature.

5.2.1 Solution-diffusion model

Solution-diffusion occurs in nanofiltration, reverse osmosis, pervaporation, and gas permeation membranes. Temperature, pressure and fluid composition on the membrane-feed interface determines the concentration of the diffusing components through the membrane surface, (refs. 27). From thermodynamics, the overall driving force that permeates the solute through the membrane is the chemical potential gradient. The flux of component (*i*) is given as follows

$$J_i = -L_i \frac{d\mu_i}{dx} \qquad (5.8)$$

where L_i is the proportionality coefficient of component (*i*) and μ_i is the chemical potential gradient of component (*i*). The chemical potential gradient is used as the general driving force because there are different kinds of driving forces. Driving forces can be concentration gradient, pressure gradient, temperature gradient and electrical gradients, (refs. 220, 258, 267). For example, the reverse-osmosis process involves pressure and concentration gradients as the driving forces. The chemical potential for reverse osmosis is written as

$$d\mu_i = RT\left(d\ln\left(\gamma_i n_i\right)\right) + \upsilon_i\left(dp\right) \qquad (5.9)$$

where n_i is the molar fraction of component (i) (mol/mol), γ_i is the activity coefficient (mol/mol), p is the pressure and υ_i is the molar volume of component (i). Integrating equation (5.9) for incompressible phase, where the volume does not change with pressure, with respect to concentration and pressure become as follows

$$\mu_i = \mu_i^o + RT\ln\left(\gamma_i n_i\right) + \upsilon_i\left(p - p_i^o\right) \qquad (5.10)$$

where μ_i^o is the chemical potential of pure component (i) at reference pressure and p_i^o is the reference pressure of component (i). Integrating equation (5.9) for compressible phase such as gases, it becomes

$$\mu_i = \mu_i^o + RT\ln\left(\gamma_i n_i\right) + RT\ln\left(\frac{p}{p_i^o}\right) \qquad (5.11)$$

Solutes at each side of the membrane are in equilibrium with the solutes at the interface, which is the general assumption in the solution-diffusion model. As a result of the general assumption, the chemical potential through the membrane is continuous. Another assumption is that the pressure is uniform in the membrane and the chemical potential gradient across the membrane is expressed as the concentration gradient. If the pressure within the membrane is assumed to be constant and has a high value, then by combing equations (5.8) and (5.9) at a constant activity coefficient (γ_i), and sbstituting concentration terms instead of the mole fraction term, gives the following equation

$$J_i = -\frac{RT\,L_i}{c_i}\frac{dc_i}{dx} \qquad (5.12)$$

From Fick's law (equation (5.6)), the diffusion coefficient is given as

$$D_i = \frac{RT\,L_i}{c_i} \qquad (5.13)$$

Integrating Fick's law over the membrane thickness gives

$$J_i = \frac{D_i\left(c_{i,o,(m)} - c_{i,p,(m)}\right)}{l} \qquad (5.14)$$

where $c_{i,o,(m)}$ is the concentration of component (i) at the membrane-feed interface and $c_{i,p,(m)}$ is the concentration of component (i) at the membrane-permeate interface. When there is no pressure gradient in the membrane, even though concentration and pressure values at both sides of the membrane are different, the process can be expressed by Fick's law. Examples of membrane processes where the solution-diffusion model is applied are as follows

5.2.1.1 Dialysis membrane

The solution-diffusion model applies for the dialysis membrane. The only driving force is the concentration gradient. By assuming that the solutes in the feed and the permeate are in equilibrium with the solutes at the membrane adjacent surface, then the chemical potential at the feed-membrane interface is assumed to be equal. Applying the above condition on equation (5.10) and replacing the reference pressure (p_i^o) with the vapour saturation pressure ($p_{i,sat}$) gives the following

$$\mu_i^o + RT\ln\left(\gamma_{i,o}^L n_{i,o}\right) + \upsilon_i\left(p_o - p_{i,sat}\right) = \mu_i^o + RT\ln\left(\gamma_{i,o,(m)} n_{i,o,(m)}\right) + \upsilon_i\left(p_o - p_{i,sat}\right) \qquad (5.15)$$

where $n_{i,o}$ is the molar fraction of component (i) in the feed solution, $n_{i,o,(m)}$ is the molar fraction of component (i) at the feed-membrane interface, $\gamma^L{}_{i,o}$ is the activity coefficient of the feed solution in the liquid phase, $\gamma_{i,o,(m)}$ is the activity coefficient at the feed-membrane interface, p_o is the pressure at the feed solution side and $p_{i,sat}$ is the saturation pressure of component (i). Rearranging equation (5.15) and substituting the concentration terms instead of the mole fraction term, gives

$$c_{i,o,(m)} = \frac{\gamma_{i,o}^L\ \rho_m}{\gamma_{i,o(m)}\ \rho_o} c_{i,o} = K_i^L c_{i,o} \qquad (5.16)$$

where $c_{i,o}$ is the concentration of component (i) in the feed solution, $c_{i,o,(m)}$ is the concentration of component (i) at the membrane-feed solution and $K^L{}_i$ is the sorption coefficient of component (i) in the liquid phase. The same procedure is applied for the permeate-membrane side, which gives the following

$$c_{i,p,(m)} = K_i^L c_{i,p} \qquad (5.17)$$

where $c_{i,p}$ is the concentration of component (i) in the permeate solution and $c_{i,p,(m)}$ is the concentration of component (i) at the permeate-feed solution. Substituting equations (5.16) and (5.17) into equation (5.6) gives the following

$$J_i = \frac{D_i K_i^L}{l}\left(c_{i,o} - c_{i,p}\right) = \frac{P_i^L}{l}\left(c_{i,o} - c_{i,p}\right) \qquad (5.18)$$

where P^L_i is the permeability coefficient in the liquid phase and l is the membrane thickness.

5.2.1.2 Reverse osmosis membrane

If a solution is separated from a pure solvent by a membrane, then the pure solvent would move from the pure solvent region to the solution region, which is known as the normal osmosis process. When a pressure is applied at the solution region then the pure solvent flow would decrease, and the pure solvent flow would stop when the applied pressure reaches the osmotic pressure. If the applied pressure is higher than the osmotic pressure, then the pure solvent flow direction would change. The solvent would move from the high concentrated solution side to the pure solvent side. This is known as the reverse-osmosis process, (refs. 195, 220, 230, 267, 271). At the feed-membrane interface, the chemical potential and the pressure are equal. Following the same procedure as in the dialysis process results in

$$c_{i,o,(m)} = K_i^L c_{i,o} \qquad (5.19)$$

At the membrane-permeate interface, the chemical potentials are equal and by substituting equation (5.10) into this condition and replacing the reference pressure (p_i°) with the vapour saturation pressure ($p_{i,sat}$) and rearrange it gives the following

$$\ln\left(\gamma_i^L n_{i,l}\right) = \ln\left(\gamma_i^L n_{i,l,(m)}\right) + \frac{\upsilon_i\left(p_o - p_l\right)}{RT} \qquad (5.20)$$

where p_o is the pressure at the feed solution side and p_l is the pressure at the permeate side. Substituting the concentration terms instead of the mole fraction term into equation (5.20) gives

$$c_{i,p,(m)} = K_i^L c_{i,p} \exp\left(-\frac{\upsilon_i (p_o - p_l)}{RT}\right) \qquad (5.21)$$

Substituting equations (5.19) and (5.20) into Fick's law gives the following equation

$$J_i = \frac{D_i K_i^L}{l}\left(c_{i,o} - c_{i,p} \exp\left(-\frac{\upsilon_i (p_o - p_l)}{RT}\right)\right) \qquad (5.22)$$

For a solute, equation (5.22) can be written as follows

$$J_j = \frac{D_j K_j^L}{l}\left(c_{j,o} - c_{j,p} \exp\left(-\frac{\upsilon_j (p_o - p_l)}{RT}\right)\right) \qquad (5.23)$$

When the term ($-\upsilon_j(p_o-p_l)/RT$) is small, then the exponential term is equal to 1; as a result, equation (5.23) become as

$$J_j = \frac{D_j K_j^L}{l}\left(c_{j,o} - c_{j,p}\right) \qquad (5.24)$$

The solute concentration flux is independent on the pressure as indicated in equation (5.24). But for the solvent, the flux remains small when the applied pressure is smaller than the osmotic pressure. And when the applied pressure is higher than the osmotic pressure, the solvent flux increases as the applied pressure increases. The rejection coefficient (R) for the membrane is given as

$$R = \left(1 - \frac{c_{j,p}}{c_{j,o}}\right) \times 100\% \qquad (5.25)$$

where $c_{j,o}$ is the solute concentration in the feed solution and $c_{j,p}$ is the solute concentration in permeate.

5.2.1.3 Gas separation membrane

In the gas-separation process, (refs. 159, 195, 230, 267, 271), the applied pressure at the feed side (p_o) is higher than the pressure at the permeate pressure side (p_l). At the feed-membrane interface, assuming that the solutes in the feed are in equilibrium with the solutes at the

membrane adjacent surface, then the chemical potential at the feed-membrane interface is assumed to be equal, and replacing the reference pressure (p_i^o) with the vapour saturation pressure ($p_{i,sat}$) gives the following

$$n_{i,o,(m)} = \frac{\gamma_{i,o}^{G}}{\gamma_{i,o,(m)}} \frac{p_o}{p_{i,sat}} n_{i,o} \exp\left(- \frac{\upsilon_i \left(p_o - p_{i,sat} \right)}{RT} \right) \qquad (5.26)$$

The exponential part is considered to be equal to 1 even at high pressures, and substituting the concentration terms instead of the mole fraction term, gives

$$c_{i,o,(m)} = m_i \rho_m \frac{\gamma_{i,o}^{G}}{\gamma_{i,o,(m)}} \frac{p_{i,o}}{p_{i,sat}} \qquad (5.27)$$

Equation (5.27) can be rewritten by introducing the gas phase sorption coefficient (K^G_i), then it becomes as follows

$$c_{i,o,(m)} = K_i^G p_{i,o} \qquad (5.28)$$

The same procedure is followed for the membrane-permeate interface, which gives the following equation

$$c_{i,p,(m)} = K_i^G p_{i,l} \qquad (5.29)$$

Substituting equations (5.28) and (5.29) into the integrated Fick's law gives the following

$$J_i = \frac{D_i K_i^G}{l} \left(p_{i,o} - p_{i,l} \right) \qquad (5.30)$$

5.2.1.4 Pervaporation membrane

The pervaporation membrane is used to separate multi-component liquids, where the permeating components are removed as a vapour on the permeate side, (refs. 267, 271). The vapour pressure at the permeate side is kept lower than the feed side of the membrane. At the feed-membrane interface, the chemical potentials are assumed to be equal at the same pressure, and by applying such condition it gives

$$c_{i,o,(m)} = \frac{\gamma^{L}_{i,o}\ \rho_m}{\gamma_{i,o(m)}\ \rho_o} c_{i,o} = K^{L}_{i} c_{i,o} \qquad (5.31)$$

where K^{L}_{i} is the liquid-phase sorption coefficient. At the membrane-permeate gas interface, the chemical potentials are in equilibrium, and by applying this condition it gives

$$n_{i,l,(m)} = \frac{\gamma^{G}_{i,l}}{\gamma_{i,l,(m)}} \frac{p_l}{p_{i,sat}} n_{i,l} \exp\left(- \frac{\upsilon_i \left(p_o - p_{i,sat} \right)}{RT} \right) \qquad (5.32)$$

The exponential term in equation (5.32) is assumed to be equal to 1, substituting the concentration terms instead of the mole fraction term and replacing the ($n_{i,l}\, p_l$) term with the partial pressure ($p_{i,l}$), gives

$$c_{i,p,(m)} = m_i\ \rho_m \frac{\gamma^{G}_{i,l}\ p_{i,l}}{\gamma_{i,l,(m)}\ p_{i,sat}} = K^{G}_{i}\, p_{i,l} \qquad (5.33)$$

Integrating Fick's law and substitute equations (5.31) and (5.33) into it, gives the following equation

$$J_i = \frac{D_i \left(K^{L}_{i} c_{i,o} - K^{G}_{i}\, p_{i,l} \right)}{l} \qquad (5.34)$$

If it assumed that the permeate vapour is in equilibrium with the feed solution, then the liquid phase sorption coefficient (K^{L}_{i}) and the gas phase sorption coefficient (K^{G}_{i}) have the same relationship toward each other, and by applying the vapour-liquid equilibrium and substituting the concentration terms instead of the mole fraction term, gives

$$c^{L}_{i} = m_i\ \rho \frac{\gamma^{G}_{i}\ p_i}{\gamma^{L}_{i}\ p_{i,sat}} = \frac{K^{G}_{i}}{K^{L}_{i}}\, p_i \qquad (5.35)$$

Substituting equation (5.35) into equation (5.34) gives the following equation

$$J_i = \frac{D_i K^{G}_{i} \left(p_{i,o} - p_{i,l} \right)}{l} \qquad (5.36)$$

where p_i is the partial vapour pressure.

5.2.2 Pore flow membrane model

Separation mechanisms include molecular sieving, adsorption of particles by the membrane interior and by using both molecular sieving and adsorption. Membrane using pore-flow as a separation mechanism can be characterised by the membrane porosity (ε), the membrane tortuosity (τ) and the membrane pore diameter (d) , (refs. 267). The membrane porosity (ε) is defined as the fraction of the total porous membrane volume. The membrane porosity (ε) can be measured by weighing the membrane before and after filling the membrane pores with liquid. The membrane tortuosity (τ) is defined as the average pore compared to the membrane thickness; see Figure 5-1. The pore flow model describes the transport of the permeating solute in a micro-porous membrane such as microfiltration and ultrafiltration membranes.

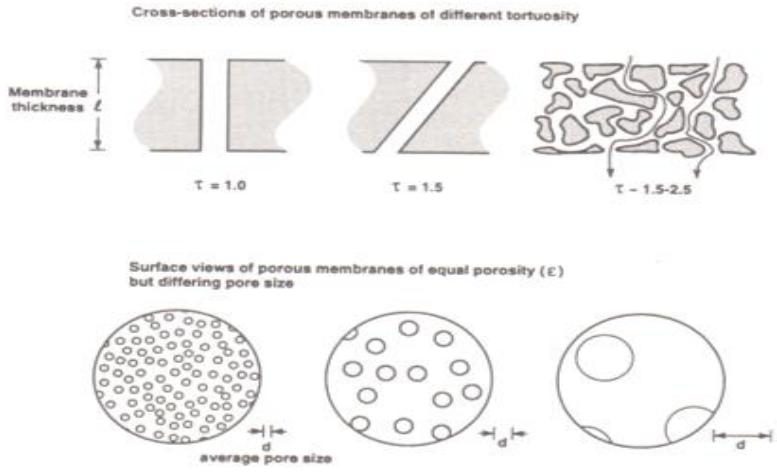

Figure 5-1. The membrane is characterised by the membrane porosity (ε), the membrane tortuosity (τ) and the membrane pore diameter (d), (ref. 267).

Separation in the micro-porous membrane takes place either at the surface of the membrane or inside the membrane. The membrane surface pore diameter is smaller than the solute diameter, thus the solute is captured at the membrane surface. On the other hand, when very small solutes pass through the membrane surface and are not captured by the interior of the membrane, this is known as the screen filter method. This kind of membrane structure consists of micro-porous thin surface layer supported by open micro-porous media. Inside the membrane, the average pore diameter is often ten times larger than the smallest permeating solutes, which prevent the solutes from permeating through the membrane, which is known as the depth filter method. See Figure 5-2.

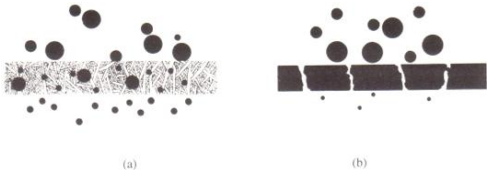

Figure 5-2. a. Depth filter, b. Screen filter, (ref. 162).

5.2.2.1 Screen filter

The membrane pores are assumed to be equal to circular capillaries with a large radius, which allows the solvent to pass through it, (refs. 267). If the parabolic velocity profile of the fluid passing through the membrane pore is included, then the effective fractional pore for the solute is given as

$$\left(\frac{A}{A_o}\right)' = 2\left(1-\frac{a}{r}\right)^2 - \left(1-\frac{a}{r}\right)^4 \qquad (5.37)$$

where A is the membrane pore area which allows the solute to permeate through it, A_o is the pore area where the solvent passes through it, a is the solute radius and r is the pore radius. Where the ratio between the membrane pore area (A), which allows the solute to permeate through it, to the pore area (A_o), which allows the solvent to pass through it, is given as

$$\left(\frac{A}{A_o}\right)' = \left(\frac{c_p}{c_f}\right) \qquad (5.38)$$

where c_p is the solute concentration in the permeate and c_f is the solute concentration in the feed. Then the membrane rejection can be written as

$$R = 1-\frac{c_p}{c_f} = 1-2\left(1-\frac{a}{r}\right)^2 + \left(1-\frac{a}{r}\right)^4 \qquad (5.39)$$

5.2.2.2 Depth filter

The solutes are separated by sieving mechanisms and adsorption on the membrane interior surface. The adsorption mechanism consists of inertial capture, Brownian diffusion and electrostatic adsorption. The inertial capture occurs for large diameter solutes where the solutes are captured when they impact the membrane pore wall. The Brownian diffusion

occurs for small solutes, (refs. 267). Small solutes are subjected to Brownian motion because of their small size; therefore, the solutes are absorbed by the membrane surface. The electrostatic adsorption causes the charged solutes to be absorbed by the membrane surface charged group. See Figure 5-3.

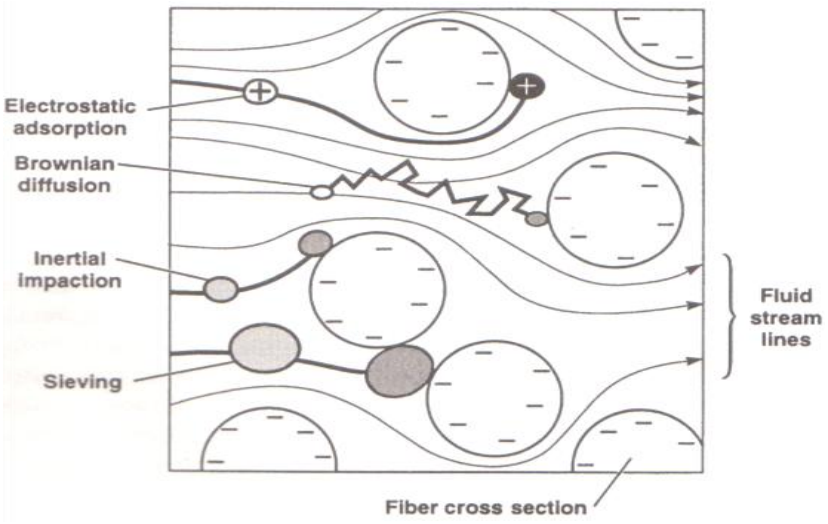

Figure 5-3. Depth filtration mechanism for separating particles, (ref. 267).

5.3 Membranes thermodynamics

Equilibrium thermodynamics cannot be used to describe transport though the membrane thus non-equilibrium thermodynamics is used, (refs. 195). When irreversible thermodynamics is used, the membrane is considered a black box and no information is required about the membrane structure. Coupling of forces and/or fluxes can be described by irreversible thermodynamics. In an irreversible process, entropy is produced when a constant driving force is maintained and free energy is provided. Entropy in the irreversible process can be given by the dissipation function (ϕ) as follows

$$\phi = T\frac{dS}{dt} = \sum J_i X_i \qquad (5.40)$$

where S is the entropy, T is the temperature and X_i is the force. Equation (5.40) shows the transport of mass, heat and electrical current through the membrane. If one component (1) exists where the driving force is the chemical potential gradient then the phenomenological equation can be written as

$$J_1 = L_1 X_1 = -L_1 \frac{d\mu_1}{dx} \qquad (5.41)$$

And if two components (1 and 2) exist and the driving force is the chemical potential gradient, the phenomenological equation for both components 1 and 2 can be written as

$$J_1 = -L_{11} \frac{d\mu_1}{dx} - L_{12} \frac{d\mu_2}{dx} \qquad (5.42\text{-a})$$

$$J_2 = -L_{21} \frac{d\mu_1}{dx} - L_{22} \frac{d\mu_2}{dx} \qquad (5.42\text{-b})$$

The first term on the right-hand side of equation (5.42-*a*) is the flux of component (1) under its gradient and the second term on the right-hand side is the flux of component (1) under component (2) gradient. The first term on the right-hand side of equation (5.42-*b*) is the flux of component (2) under component (1) gradient and the second term on the right-hand side is the flux of component (2) under its gradient. If the flux of component (1) increases the flux of component (2), a net positive flux results and thus the selectivity decreases.

A system composed of a solvent and a solute can be characterised by the solvent permeability (P_s) and the solute permeability (P_w) and the reflection coefficient (σ). If the dissipation function in a dilute system is the sum of the solute and the solvent flow multiplied by their driving forces, the dissipation function would be given as follows

$$\phi = J_w \Delta\mu_w + J_s \Delta\mu_s \qquad (5.43)$$

where $\Delta\mu_s$ is the solvent chemical potential difference, and $\Delta\mu_w$ is the solute chemical potential difference. The solvent chemical potential difference ($\Delta\mu_s$) between phase (2) (the permeate side) and phase (1) (the feed side) is given as follows

$$\Delta\mu_s = V_s(\Delta p - \Delta\pi) \qquad (5.44)$$

where V_s is the solvent molar volume and Δp is the pressure difference. The chemical potential difference for the solute ($\Delta\mu_w$) is given as follows

$$\Delta\mu_w = V_w \Delta p + \frac{\Delta\pi}{\bar{c}_w} \qquad (5.45)$$

where V_w is the solute molar volume and $\bar{c}_w$ is the mean logarithmic concentration. Substituting equations (5.44) and (5.45) into equation (5.43), the dissipation function would be written as

$$\phi = \Delta p\left(J_w V_w + J_s V_s\right) + \Delta\pi\left(\frac{J_w}{\bar{c}_w} - J_s V_s\right) \qquad (5.46)$$

The first term on the right-hand side is the total volume flux (J_v), and the second term on the right-hand side is the flux difference (J_d). The phenomenological equations (5.42-*a*) and (5.42-*b*) for the total volume flux (J_v) and the flux difference (J_d) for the solute and the solvent can be given as follows

$$J_v = L_{11}\Delta p + L_{12}\Delta\pi \qquad (5.47\text{-a})$$

$$J_d = L_{21}\Delta p + L_{22}\Delta\pi \qquad (5.47\text{-b})$$

If the pressure difference is equal to zero, there is still a volume flux according to equation (5.51-*a*). And even if the solute concentration at both sides of the membrane are equal, there is still a flux but only if the pressure is not equal to zero according to equation (5.47-*b*). When the osmotic pressure difference is equal to zero, then equation (5.47-*a*) becomes

$$J_v = L_{11}\Delta p \Rightarrow L_{11} = \frac{J_v}{\Delta p} = L_p \qquad (5.48)$$

where L_{11} is the hydrodynamic permeability or the solvent permeability coefficient, and is referred to as L_p. And when the pressure difference is equal to zero, equation (5.47-*b*) becomes

$$J_d = L_{22}\Delta\pi \Rightarrow L_{22} = \frac{J_d}{\Delta\pi} = \varpi \qquad (5.49)$$

where L_{22} is the osmotic permeability or the solute permeability coefficient and is referred to as ϖ. If the total volumetric flux (J_v) does not exist or is equal to zero, then equation (5.47-*a*)

becomes as follows

$$\Delta p = -\frac{L_{12}}{L_{11}}\Delta\pi \qquad (5.50)$$

If the hydrodynamic pressure difference (Δp) is equal to the osmotic pressure difference ($\Delta\pi$), then (L_{11}) is equal to (L_{12}), which means that the solute is not permeating across the membrane and is considered semi-permeable, but since the membrane is not semi-permeable then the ratio of (L_{12}) to (L_{11}) is given as

$$\sigma = \frac{L_{12}}{L_{11}} \qquad (5.51)$$

where σ is the reflection coefficient and it is less than unity. The reflection coefficient is a measure of the membrane selectivity and its values range between 0 and 1. If the reflection coefficient value is equal to zero, the membrane is not selective, and as a result, both the solute and the solvent pass through the membrane. And if the reflection coefficient is equal to 1, the membrane is ideal and no solute permeates through the membrane. And if the reflection coefficient value is less than 1, the membrane is semi-permeable and some of the solute permeates through it. Substitute equations (5.48), (5.49) and (5.51) into equations (5.47-*a*) and (5.47-*b*) gives

$$J_v = L_p\left(\Delta p \quad - \quad \sigma \quad \Delta\pi\right) \qquad (5.52\text{-a})$$

$$J_w = \bar{c}_w\left(1-\sigma\right)J_v + \varpi \quad \Delta\pi \qquad (5.52\text{-b})$$

Equations (5.52-*a*) and (5.52-*b*) indicates that the characterising parameters of the membrane properties with respect to convective and diffusive transport of neutral solute and solvent are the solvent permeability coefficient (L_p), the solute permeability (ϖ) and the reflection coefficient (σ). From equations (5.52-*a*) and (5.52-*b*), it can be noticed that if the solute is not completely retained, the reflection coefficient is less than 1 and the osmotic pressure is equal to ($\sigma * \Delta\pi$). And if the membrane is permeable, where the solute and the solvent permeate through the membrane, then the reflection coefficient is equal to zero and no osmotic pressure exists. The solvent permeability coefficient can be obtained by using it as a pure solvent because the osmotic pressure difference for pure solvents is equal to zero and the

linear relation between the volumetric flux (J_v) and the pressure difference (Δp) can be obtained. The solvent permeability coefficient can be obtained from the slope of the flux-pressure curve; see Figure 5-4.

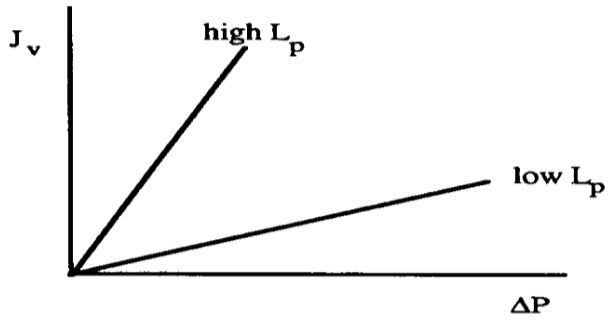

Figure 5-4. The flux-pressure curve, (ref. 195).

The solute permeability coefficient (ϖ) and the reflection coefficient (σ) can be obtained experimentally at various solute concentrations and by re-arranging equation (5.52-*b*) into

$$\frac{J_w}{\Delta c} = \frac{\bar{c}(1-\sigma)J_v}{\Delta c} + \varpi \qquad (5.53)$$

where Δc is the concentration difference between the feed and the permeate and $\bar{c}$ is the mean logarithmic concentration. The mean logarithmic concentration is given as follows

$$\bar{c} = \frac{c_f - c_p}{\ln\left(\frac{c_f}{c_p}\right)} \qquad (5.54)$$

By plotting ($J_w/\Delta c$) versus ($\bar{c}J_v/\Delta c$), then the solute permeability coefficient value would be equal to the line intercept and the ($1-\sigma$) value will be equal to the slope; see Figure 5-5.

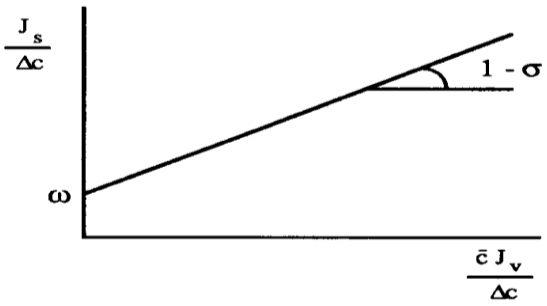

Figure 5-5. The ($J_w/\Delta c$) versus ($\bar{c}J_v/\Delta c$) plot, (ref. 195).

The non-equilibrium thermodynamics and phenomenological equations can be used to describe the coupling between the solvent and the solute transport such as water and salt. The retention of a given solute depends on the relation between the molecular size and the membrane pore size; the interaction between solute molecules is less important. For small particles, the Stokes-Einstein equation can be used to find the solute size. Where the molecule radius is given as

$$r = \frac{kT}{6\pi\eta D} \qquad (5.55)$$

where r is the molecule radius and k is the mass transfer coefficient. From equation (5.55), it can be noticed that the molecular size is inversely dependant on the diffusion coefficient (D). In addition, the coupling between heat and mass transfer can be described using the non-equilibrium thermodynamics and the phenomenological equations, where the temperature difference across the membrane causes heat and mass transfer. Also, coupling between the electrical potential difference and the hydrostatic pressure in electro-osmosis process, where the solvent is transported across the membrane by the electrical potential difference with absence of the hydrostatic pressure, can be described by using non-equilibrium thermodynamics and phenomenological equations. If two salt solutions exist, the separation occurs because of an electrical potential difference or because of a pressure difference. For a system where electrical and hydrostatic pressure are applied, the dissipation function can be written as the sum of fluxes and forces in the system as follows

$$\phi = T\frac{dS}{dt} = \sum J_i X_i = J\Delta p + I\Delta E \qquad (5.56)$$

where ΔE is the electrical potential difference and I is the electrical current. And the corresponding phenomenological equations can be written as

$$I = L_{11}\Delta E + L_{12}\Delta p \qquad (5.57\text{-a})$$

$$J = L_{21}\Delta E + L_{22}\Delta p \qquad (5.57\text{-b})$$

If L_{11} and L_{12} are the coupling coefficients, then different conditions can be distinguished

1. Even if the electrical current is absent, an electrical potential still exists because of the

pressure difference, which is called streaming potential.

2. If the pressure difference is equal to zero, the solvent transport is a result of the electrical current, which is known as the electro-osmosis transport.

3. If the flux is equal to zero, the pressure builds up because of an electrical potential difference.

4. If the electrical potential difference is equal to zero, the electrical current is generated because of the flux across the membrane.

5.4 Transport through porous and nonporous membranes

Transport through membrane is considered to occur by diffusion (ν_D) and convective flow (u_c). The flux for component (i) through a membrane can be written as

$$J_i = c_i\left(v_{D,i} + u_{c,i}\right) \qquad (5.58)$$

For porous membrane, the convective flow is the main term for transport through it, while in the nonporous membrane, only diffusion flow contributes to the transport through it. In general, the solution-diffusion model is used for each component dissolved in the solution and diffuses through the membrane, then for various processes, a simple flux equation can be obtained, (refs. 195, 230, 244). In the case where no convective flow exists, the flux can be described in terms of concentration and diffusion flow velocity as follows

$$J_i = c_i v_{D,i} \qquad (5.\ 59)$$

The mean diffusion velocity is determined by the driving force acting on component (i) and the frictional resistance exerted by the membrane as follows

$$v_{D,i} = \frac{X_i}{f_{r,i}} \qquad (5.60)$$

where $f_{r,i}$ is the frictional resistance for component (i). The frictional coefficient is given as

$$f_{r,i} = \frac{RT}{D_i} \qquad (5.61)$$

where D_i is the diffusion coefficient for component (*i*). By substituting the driving force in equation (5.60) by the chemical potential gradient and then substitute equations (5.60) and (5.61) into equation (5.59), the following equation is obtained

$$J_i = \frac{c_i D_i}{RT} \frac{d\mu_i}{dx} \qquad (5.62)$$

And substituting the chemical potential in equation (5.1) into equation (5.62) , then the flux for component (*i*) is given as follows

$$J_i = \frac{c_i D_i}{RT} \left(RT \frac{d \ln a_i}{dx} + V_i \frac{dp}{dx} \right) \qquad (5.63)$$

5.4.1 Transport through porous membranes

Porous membranes consist of a polymeric matrix in which the pore ranges between 2nm to 10μm. The pores and the membrane geometry vary; for example, in the microfiltration membrane, the same structure exists over the whole membrane thus the membrane resistance is determined by the total thickness, while the ultrafiltration membrane has an asymmetric structure and its resistance is determined by the top layer, (refs. 195, 230, 244). See Figure 5-6, which shows the different types of pore geometry in membranes.

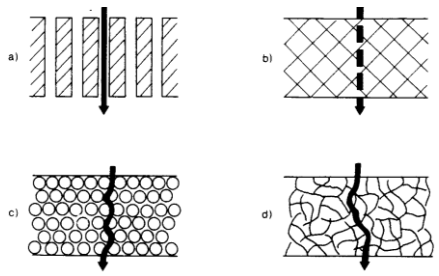

Figure 5-6. Different membrane structures where 5-6a is a porous membrane structure, 5-6b is nonporous membrane structure, 5-6c is nodular membrane structure and 5-6d is sponge membrane structure, (ref. 230).

Because of the different pore geometries, there are different models that describe the transportation process through the membranes. Thus, from the different models the structural parameters of the membrane can be determined and the membrane performance can be improved. One model considers the membrane pores to be parallel cylinders and perpendicular to the membrane surface; see Figure 5-6a. The pore length is equal or almost equal to the membrane thickness. The volume flux can be described by using Hagen-

Poiseuille equation and assuming that the membrane pore diameters are equal as follows

$$J_v = \frac{\varepsilon \quad r^2}{8\eta\tau}\frac{\Delta p}{l} \qquad (5.64)$$

where τ is the tortuosity, η is the viscosity and ε is the surface porosity. The surface porosity is given as follows

$$\varepsilon = \frac{n_p \pi r_p^2}{A_m} \qquad (5.65)$$

where n_p is the number of pores, π is a constant. Equation (5.64) gives a good description of transport through the membrane consisting of parallel pores. Other models suggest that the membrane consists of closed packed spheres; see Figure 5-6c. Such structure is found in organic and inorganic sintered membranes, and in phase inversion membranes with a modular top structure. The volumetric flux through this type of membrane can be calculated by using the Kozeny-Carman equation

$$J_v = \frac{\varepsilon^3}{K\eta A_{\text{int}}^2 (1-\varepsilon)^2}\frac{\Delta p}{l} \qquad (5.66)$$

where K is Kozeny-Carman constant, ε is the pore volume fraction and A_{int} is the internal surface area. Kozeny-Carman constant depends on the pore's shape and tortuosity.

Another approach that is used to describe transport through porous membranes is the friction model, (refs. 27, 195). The friction model suggests that transport through membrane occurs because of viscous flow and diffusion. The friction model implies that the pore size is very small; therefore, the solute cannot pass freely through the pores and friction results between the solute and the pore wall, between the solvent and the pore wall, and between the solvent and the solute. The friction force is related to the velocity difference or the relative velocity linearly. If the process is assumed to be thermodynamically irreversible, (refs. 195, 230, 244), isothermal and no friction exists, the driving force can be described as the gradient of the chemical potential as follows

$$X_i = -\frac{\partial \mu_i}{\partial x} \qquad (5.67)$$

But if friction exists and the separation process is non-ideal, then the upper equation becomes

$$X_i = -\frac{\partial \mu_i}{\partial x} + F_i^{`} \qquad (5.68)$$

The solute flux is given as

$$J_w = m_{sw} c_{wm} \left(-\frac{\partial \mu_w}{\partial x} + F_{wm}^{`} \right) \qquad (5.69)$$

The solute flux in the membrane is described as a combination of diffusion flow ($\partial \mu_w / \partial x$) and viscous flow ($F'_{wm}$). If the solution is ideal, the chemical potential gradient for the solute is given as follows

$$\left(\frac{\partial \mu_w}{\partial x} \right)_{P,T} = \frac{\partial \mu_w}{\partial c_{wm}} \left(\frac{\partial c_{wm}}{\partial x} \right) \qquad (5.70)$$

And if the solution is dilute, the chemical potential gradient for the solute is given as

$$\left(\frac{\partial \mu_w}{\partial x} \right)_{P,T} = \frac{RT}{c_{wm}} \qquad (5.71)$$

The friction coefficient of the solute and the membrane (f_{wm}) is related to the friction coefficient of the solute and the solvent (f_{ws}) as follows

$$b = \frac{f_{ws} + f_{wm}}{f_{ws}} = 1 + \frac{f_{wm}}{f_{ws}} \qquad (5.72)$$

where b is the friction factor. Then equation (5.72) for the solute flux can be written as follows

$$J_w = -\frac{RT}{f_{ws} b} \frac{dc_{wm}}{dx} + \frac{c_{wm} v_w}{b} \qquad (5.73)$$

Also, the distribution of the solute in the membrane is given by the following equation

$$c_{wm} = K^{`} c \qquad (5.74)$$

where $K`$ is the uptake of the solute by the membrane from the feed. The frictional coefficient between the solute and the solvent is related to the diffusion of the solute into the solvent coefficient as follows

$$D_{ws} = \frac{RT}{f_{ws}} \qquad (5.75)$$

If the following assumptions were made

$$J_v = \varepsilon v$$
$$J_i = J_w \varepsilon$$
$$\xi = x\tau$$

and substituted into equation (5.52-b), the flux would become

$$J_i = -\frac{K` D_{ws}}{b\tau}\frac{dc}{dx} + \frac{cK` Jv}{b} \qquad (5.76)$$

Integrating the above equation by using the following boundaries

$$x = 0 \Rightarrow c_{1,w,m} = K` c_f$$
$$x = l \Rightarrow c_{2,w,m} = K` c_p$$

gives

$$\frac{c_f}{c_p} = \frac{b}{K`} + \left[\left(1 - \frac{b}{K`}\right)\exp\left(-\frac{lJ_v\tau}{\varepsilon D_{ws}}\right)\right] \qquad (5.77)$$

If the left-hand side (c_f / c_p) is plotted versus ($lJ_v\tau/\varepsilon D_{ws}$), the following graph results; see Figure 5-7.

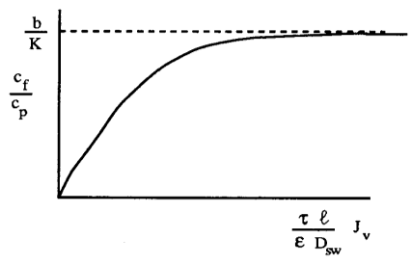

Figure 5-7. (c_f/c_p) versus ($lJ_v\tau/\varepsilon D_{ws}$) plot, (ref. 195).

The maximum value of (*b/K`*) is obtained when (*b*) value is the maximum and (*K`*) is the minimum. The solute rejection by the membrane is given as follows

$$R = \frac{c_f - c_p}{c_f} = 1 - \frac{c_p}{c_f} \qquad (5.78)$$

5.4.2 Transport through nonporous membranes

In nonporous membranes, prose exists on the molecular level in order to allow transport in such membranes. The transport of gases and liquids through the membrane are somehow similar but there is still a difference such as the affinity between the liquids and the polymers is much greater than that between the gases and the polymers. Another difference is that a mixture of gas components flow independently through a dense membrane, but the liquid mixture component's flow is influenced by the flow coupling and the thermodynamic interaction. The mass transport through the nonporous membrane occurs either by ionic conduction or by dissolving through the membrane then diffusing as a result of a chemical potential gradient. The chemical potential gradient may be a change in concentration, vapour pressure or electrical potential, (refs. 195, 230, 244). The transport of molecules through dense nonporous membrane is described by the solution-diffusion mechanism, where the permeability is given below as

$$\textit{Permeability (P) = Solubility (s) * Diffusivity (D)} \qquad (5.79)$$

Solubility is defined as the measure of penetrate adsorbed by the membrane under equilibrium conditions. Diffusivity depends on the penetrate geometry; as the molecular size increases the diffusion coefficient decreases. The diffusion coefficient also depends on the penetrate molecule's concentration, where diffusivity increases as the penetrate or the solute concentration increases. Therefore, two cases must be considered; the first is an ideal system where the diffusivity and solubility are constant and the second case is a concentration-dependant system where the solubility and diffusivity are functions of the concentration, (refs. 195, 230, 244). The simplest way to describe the transport of molecules through a membrane is by using Fick's law as follows

$$J_i = -D_i \frac{dc_i}{dx} \qquad (5.80)$$

The flux is proportional with the concentration gradient and the proportionality constant is the diffusion coefficient. Mass flux occurs because of concentration difference if part of membrane is taken as in Figure 5-8.

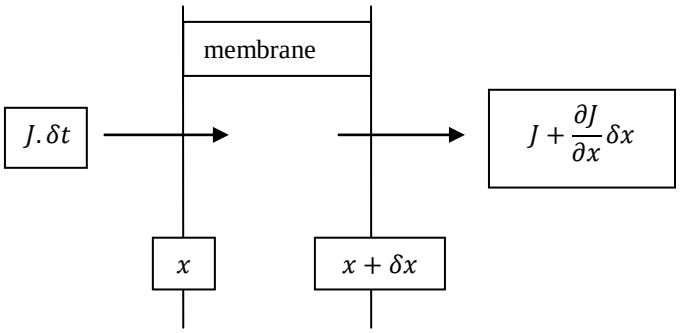

Figure 5-8. Flow through part of the membrane, (ref. 195).

Then the change in concentration (*dc*) in the volume between (*x*) and ($x+\delta x$) is given as

$$dc = \frac{\left[J\delta t - \left(J + \frac{\partial J}{\partial x}\delta x \right)\delta t \right]}{\delta t} \Rightarrow dc = -\frac{\partial J}{\partial x} t\delta \qquad (5.81)$$

If the transport process occurs at infinite small periods of time where ($\delta x \Rightarrow 0$ and $\delta t \Rightarrow 0$), equation (5.83) becomes as follows

$$\frac{\partial c}{\partial t} = -\frac{\partial J}{\partial x} \qquad (5.82)$$

Substituting Fick's law into equation (5.82) gives

$$\frac{\partial c}{\partial t} = -\frac{\partial}{\partial t}\left(D\frac{\partial c}{\partial x} \right) \qquad (5.83)$$

And if the diffusion coefficient (*D*) is assumed to be constant, equation (5.83) becomes

$$\frac{\partial c}{\partial t} = -D\frac{\partial^2 c}{\partial x^2} \qquad (5.84)$$

This is known as Fick's second law, where the concentration is a function of time and distance. The diffusion coefficient depends on the size of diffusing particles and on the nature

of the membrane material. The diffusion coefficient decreases as the particle size increases. Diffusion can be described in terms of friction where molecules move through the membrane with velocity (*v*). The velocity (*v*) is a result of the chemical potential gradient acting on the molecules. The force is important to maintain the velocity against the membrane resistance. The amount of molecules permeating through the membrane per unit time (mass flow) is given by

$$J = vc = -\frac{D_T}{RT} c\left(\frac{\partial \ln a}{\partial x}\right) = -D_T\left(\frac{\partial \ln a}{\partial \ln c}\right)\left(\frac{\partial c}{\partial x}\right) \qquad (5.85)$$

where D_T is the thermodynamic diffusion coefficient.

5.4.2.1 Ideal system

In an ideal system, it is assumed that ideal sorption and diffusion occur, (refs. 27, 195, 230, 244). If the solute solubility in the membrane obeys Henry's law, the solute flux can be given as follows

$$J = \frac{P}{l}\left(p_1 - p_2\right) \qquad (5.86)$$

It can be noticed from equation (5.86) that the flux of a solute passing through a membrane is proportional to the pressure difference and inversely proportional to the membrane thickness. The diffusion coefficient decreases as the molecule size increases, while the solubility increases when the molecular size increases. Small molecules have high permeability because of their high diffusivity, while large molecules have high permeability because of their high solubility.

In ideal systems, the diffusion coefficient is constant and can be determined by using the permeation method. If the penetrate amount passing through the membrane at time (*t*) is assumed to be given as

$$\frac{Q_t}{lc_{f,i}} = \frac{Dt}{l^2} - \frac{1}{6} - \frac{2}{\pi}\sum\left[\frac{(-1)^{n`}}{n`^2}\exp\left(\frac{-Dn`^2\pi^2 t}{l^2}\right)\right] \qquad (5.87)$$

where $c_{f,i}$ is component (*i*) concentration in the feed, $n`$ is an integer and Q_t is the volumetric

flow rate of penetrate. If the time approaches infinity ($t \Rightarrow \infty$) then equation (5.87) becomes

$$Q_t = \frac{Dc_{f,i}}{l}\left(t - \frac{l^2}{6D}\right) \qquad (5.88)$$

If the left hand-side of equation (5.87), ($Q_t/lc_{f,i}$) is plotted versus time (t), then the following graph is obtained; see Figure 5-9.

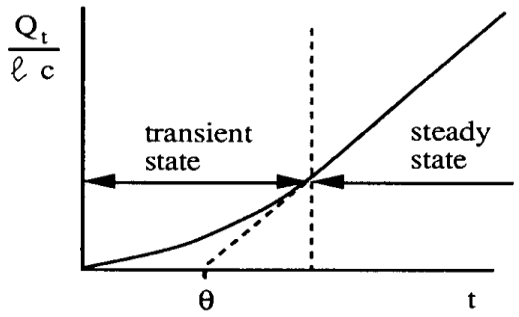

Figure 5-9. ($Q_t/lc_{f,i}$) versus time (t) plot, (ref. 195).

From the graph (figure 5-9), the time lag (θ_{lag}) can be obtained and it is noticed that the separation process needs time to change from a transient state to a steady state.

5.4.2.2 Concentration dependant system

The solubility coefficient (s) is a function of concentration because the process is not ideal, (refs. 195, 230, 244). High solubility increases segmental motion, thus the free volume is increased. Additionally, diffusion depends on the concentration where the diffusion increases as the penetrate concentration increases. The difference between the ideal and the non-ideal processes is that in the non-ideal process, the diffusion coefficient is not constant and the solubility is not described by Henry's law. The solubility of organic vapours and liquids in a non-ideal process is described by Flory-Huggin's thermodynamics. The penetrate activity in membranes is given by

$$\ln a_i = \ln\left(\frac{p_i}{p^o}\right) = \ln \varphi_1 + \left(1 - \frac{V_i}{V_p}\right)\varphi_p + \chi_p^2 \qquad (5.89)$$

where χ is the interaction parameter, φ_p is the volume fraction of penetrate, φ_1 is the volume

fraction of non-solvent, V is the molar volume. If the interaction parameter value ranges between ($0.5<\chi<2.0$), the interaction between the membrane and penetrate is strong and the permeability is high. Diffusion coefficient depends on the concentration but no specific relation describes the dependence because the diffusion coefficient varies from one membrane material to another (from polymer to another); in general, the following experimental relation is used

$$D = D_o \exp\left(\gamma` \varphi_p\right) \qquad (5.90)$$

where D_o is the diffusion at zero concentration where it is small for small molecules and large for large molecules, and $\gamma`$ is the exponential constant related to the plasticizing effect of the penetrate on the polymer. Diffusivity is influenced by the volume fraction of the penetrate ($\varphi_p$) and the exponential constant ($\gamma`$). The exponential constant ($\gamma`$) can be considered a plasticizing constant, which indicates the plasticizing action of penetrate on segmental motion. The free volume theory can be used to describe the dependence of the diffusion coefficient on concentration. The free volume theory assumes that the introduction of a penetrate increases the free volume of the membrane (polymer). The free volume in the membrane is the volume generated by thermal expansion of initially closed-packed molecules at zero temperature; the free volume is given as

$$V_f = V_T - V_o \qquad (5.91)$$

where V_f is the free volume in the membrane, V_T is the observed membrane volume at temperature (T) and V_o is the membrane volume occupied by molecules at zero temperature. The observed volume can be obtained from the membrane polymer density, and the occupied membrane volume at zero temperature can be estimated from the group contribution. The fractional free volume increases linearly with temperature above the glass transition temperature (T_g). The free volume theory is useful in describing the transport of small molecules through membranes where a molecule can only diffuse from one free volume to another if there is sufficient free volume within the membrane. The free volume increases as the penetrate size increases. The mobility of penetrate depends on finding free volume with sufficient size that allows displacement. If the membrane and penetrate were non-interacting and the membrane polymer morphology is not influenced by the presence of penetrate, then there is no extra contribution toward the free volume. On the other hand, if the membrane and

the penetrate were interacting, the free volume is a function of temperature and penetrates concentration. Also clustering of molecules affect the permeation of molecules through the membrane, (refs. 195). Where the clustering of diffusing penetrate molecules as di-meric or tri-meric form - not as single molecule - causes deviation; as a result, the diffusing component size increases and the diffusion coefficient decreases. The extent of clusters depends on the type of the membrane polymer and other existing solutes. The amount of solution inside the membrane and the solution composition are very important factors, (refs. 30). If a solution feed mixture phase is in equilibrium with a polymeric membrane phase, see Figure 5-10.

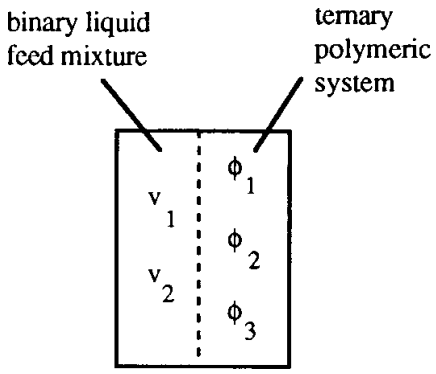

Figure 5-10. Feed liquid in equilibrium with the membrane, (ref. 195).

Then the concentration of component (*i*) in the solution and in the polymeric phase is given by

$$c_i = \frac{\varphi_i}{\varphi_{polymer,1} + \varphi_{polymer,2}} = \frac{\varphi_i}{1 - \varphi_{polymer,3}} \qquad (5.92)$$

where $\phi_{polymer,1}$, $\phi_{polymer,2}$ and $\phi_{polymer,3}$ are the volume fractions of membrane polymer components, ϕ_i is component (*i*) volume fraction. The preferential sorption is given by

$$\varepsilon_{sorption} = c_i - v_i \qquad (5.93)$$

where ν_i is the partial specific volume of component (*i*). The equilibrium condition is given by equality of the chemical potential in two phases. Then the chemical potential for two the phases of the feed (*f*) and the membrane (*m*) are related to each other as follows

$$\Delta\mu_{f,1} = \Delta\mu_{m,1} + \pi V_1 \qquad (5.94\text{-a})$$

$$\Delta\mu_{f,2} = \Delta\mu_{m,2} + \pi V_2 \qquad (5.94\text{-b})$$

By using Flory-Huggins concentration independent interaction parameter and eliminating the osmotic pressure (π) under the following conditions

$$\frac{V_1}{V_3} \approx \frac{V_2}{V_3} \approx 0 \quad and \quad \frac{V_1}{V_2} \approx \vartheta$$

gives

$$\ln\left(\frac{\varphi_1}{\varphi_2}\right) - \ln\left(\frac{v_1}{v_2}\right) = \left[(\vartheta - 1)\ln\left(\frac{\varphi_2}{v_2}\right)\right] - \left[\chi_{12}(\varphi_2 - \varphi_1)\right] - \left[\chi_{12}(v_1 - v_2)\right] - \left[\varphi_3(\chi_{13} - \vartheta\chi_{23})\right] \quad (5.95)$$

where (1) is for non-solvent and (2) is for solvent. When equation (5.95) is solved numerically, the composition of the solution inside the membrane can be gained. From equation (5.95), several factors can be understood

1. The difference in molar volume. If only entropy effects are considered, the molecule with a smaller molar volume would be absorbed by the membrane. As the molecule concentration in the membrane increases, the difference in molar volume increases.
2. The affinity toward the polymer. If the enthalpy of mixing is considered, the component with highest affinity to the membrane polymer will make a positive contribution toward sorption. If sorption is assumed to be ideal, the affinity toward the membrane polymer influences the solubility.
3. Mutual interaction. The influence of mutual interaction on preferential sorption depends on concentration and on the value of Flory-Huggins interaction parameter for non-solvent and solvent (χ_{12}).

Transport of a solution through a membrane can be described by using Fick's law, and for a concentration dependant system by using the diffusion coefficient. The diffusion coefficient is given by the following equation

$$D_i = D_{o,i} \exp\left(\gamma_i c_i\right) \qquad (5.96)$$

where D_i is the diffusion coefficient of species (i) at concentration (c), $D_{o,i}$ is the diffusion coefficient of species (i) when its concentration is equal to zero and $\gamma`_i$ is the plasticizing constant for species (i). In equation (5.96), the plasticizing constant is used to express the influence of the plasticizing action of the solution on the segmental motion. Substituting equation (5.96) into Fick's law and integrating it over the following boundaries

$$c_i = c_{i,1} \quad at \quad x = 0$$
$$c_i = 0 \quad at \quad x = l$$

gives

$$J_i = \frac{D_{o,i}}{\gamma` l} \exp\left(\gamma` c_{i,1^m} - 1\right) \qquad (5.97)$$

where $c_{i,1}{}^m$ is the concentration of solute in the membrane and (1) is for solvent, $D_{o,i}$ is the diffusion coefficient of species (i) when its concentration is equal to zero, l is the membrane thickness and $\gamma`$ is the plasticizing coefficient. Equation (5.97) represents the flux solution in the membrane, and the flux is determined by the concentration of the solute in the membrane. The permeation rate for a solute is determined by the interaction between the membrane and the penetrates. If the affinity between the penetrate and the membrane increases, the flux through the membrane increases. For a solution transporting through a membrane, the flux can be described by solubility and diffusivity. For a solution, two phenomena must be distinguished, which are flow coupling and thermodynamic interaction. For a binary system, the coupling may be described by non-equilibrium thermodynamics as follows

$$-J_i = L_{ii} \frac{d\mu_i}{dx} - L_{ij} \frac{d\mu_j}{dx} \qquad (5.98\text{-a})$$

$$-J_j = L_{ji} \frac{d\mu_i}{dx} - L_{jj} \frac{d\mu_j}{dx} \qquad (5.98\text{-b})$$

In equation (5.98-*a*), the first term on the right-hand side describes the flux of component (i) due to its chemical potential gradient. The second term on the right-hand side describes the flux of component (i) due to the chemical potential gradient of component (j), while in equation (5.98-*a*), the first term on the right-hand side describes the flux of component (j) due to component (i) chemical potential gradient. The second term on the right-hand side

describes the flux of component (*j*) due to its chemical potential gradient. The two equations (5.98-*a*) and (5.98-*b*) represent the coupling of fluxes; if coupling does not occur, ($L_{ij} = L_{ji} = 0$) and the two components (*i*) and (*j*) permeate through the membrane independently from each other.

5.5 Transport through homogeneous membrane

A homogeneous membrane consists of a single substance or stable mixture of substances not separated by internal interfaces and constrained within the membrane boundaries. This membrane is uniform in any lateral direction but may be non-uniform in the flux direction, provided the gradients of composition between its faces are continuous everywhere, (refs. 230, 244). Substance can enter a homogeneous membrane from an external phase by dissolving in the membrane material to form a thermodynamically stable mixture. A continuous membrane is defined as a phase or group of phases containing all the resistances to flow, thus it is implied that some information is available on the location of the resistances and on the structure of the membrane. Part of the resistance may be due to mass transfer limitations in the adjacent bulk phases. Discontinuous membrane is when the structural information on the membrane is not available; it may be treated as a region of discontinuity between the two uniform phases.

5.5.1 Fickian diffusion

The simplest membrane transport process is the permeation of a single substance or the only permeating component of a solution, from one reservoir at concentration (c_1°) to another at concentration (c_2°). For ideal conditions, the flux is given by

$$J = L_p^{'}\left(c_1^o - c_2^o\right)\ l \qquad (5.99)$$

where c_1° is the concentration of a single substance, a gas or the only permeating component of a solution in the first reservoir and c_2° is the concentration of a single substance, a gas or the only permeating component of a solution in the second reservoir. The total flux through the membrane is obtained by multiplying the flux density (*J*) by the area (*A*). The upper equation goes under the following conditions:

1. Concentrations in the external phases must be uniform up to the membrane faces.

2. The permeate partition equilibrium must be maintained at the membrane faces.
3. The permeate partition coefficient (k`) between the membrane and the adjacent phases must be independent of solute concentration in reservoirs ($c°$).
4. The permeate diffusion coefficient (D) must be independent of its concentration (c) in the membrane.

5.5.2 Diffusion coefficient and mobility

When the diffusing solution through the membrane is dilute, the swelling may be neglected and the encounters between the diffusing solutes are rare, thus the molecular diffusion confirms to the Brownian motion theory, (refs. 230, 244). The diffusion coefficient is expressed by the following equation

$$D = uRT \qquad (5.100)$$

The temperature (T) is the absolute temperature.

5.5.3 The chemical potential gradient as a driving force

In a non-ideal system, the diffusion coefficient (D) is determined from the flux (J) by using Fick's law, where the diffusion coefficient (D) varies with concentration (c).

5.5.4 Flow under pressure

If the chemical potential gradient is the driving force in transport processes, any factor that influences the chemical potential must also influence the transport. A pressure contribution to the permeation flux by a linear gradient can be tested by studying the flow of a pure liquid under pressure through a membrane. Then the flux density is given by

$$J = \frac{L_p c^o \overline{V}\left(p_1 - p_2\right)}{RT} \qquad (5.101)$$

where c° is the concentration of pure liquid in the reservoir and L_p is the permeability coefficient.

5.5.5 Charged gel membrane

The uptake of ions from the solution by the membrane may be dealt by the Donnan theory since the surface of the membrane may be regarded as an interface that prevents the fixed charges from entering the solution, (refs. 244). The ion activity is given by

$$a_i = a_i^o \exp\left(\frac{-z_i F \psi_D}{RT}\right) \qquad (5.102)$$

where a_i° is the activities of ionic species (i) in the solution, a_i is the activities of ionic species (i) in the membrane, z_i is the valence of species (i) including the charge, Ψ_D is the potential difference and F is the Faraday's number.

5.6 Transport through heterogeneous membranes

A heterogeneous membrane consists of a random or ordered array of discrete volume elements with different chemical or physical properties, (refs. 244).

5.6.1 Parallel arrays of elements

An example of heterogeneous membrane is a set of transport pathways arranged in parallel. The permeability of the whole membrane is the sum of the permeability of its parts, which is given as follows

$$\bar{P} = \sum_m \frac{P_m \overline{a_m}}{\tau_m^2} \qquad (5.103)$$

where $\bar{P}$ is the whole membrane permeability and P_m is the permeability of membrane parts.

5.6.2 Porous membranes

Beside the bulk flow phenomena in the pores, the surface flow phenomena may be highly significant when the surface of the capillaries is large. One of the porous polymer models is random mesh of non-circular, tortuous and interconnecting pores. Carman has shown the flow properties of such a system in terms of an effective pore diameter (d) given by

$$d = \sqrt{\left(\frac{80 J_v \eta l}{\varepsilon [p_1 - p_2]}\right)} \qquad (5.104)$$

where ε is the porosity.

5.6.3 Series arrays of layers

Another type of heterogeneous membrane is a set of plane layers with different properties arranged in series at right angle to the net flow. The flux for a steady state is characterised by Henry's law coefficient ($k_{d,a}$ and $k_{d,b}$) and Fickian diffusion (D_a and D_b), the flux is given as follows

$$J = \frac{D_a k_{d,a}\left(c_1^{'} - c_2^{'}\right)}{l_a} = \frac{D_b k_{d,b}\left(c_1^{'} - c_2^{'}\right)}{l_b} \qquad (5.105)$$

where c'_i is the concentration of a hypothetical bulk phase in equilibrium with the interfacial concentrations inside the membrane at the boundary between two layers.

5.6.4 Stagnant boundary layers

When a substance is transported between two supposedly uniform reservoirs (the gradient of the chemical potential is zero), a problem arises of conveying the transported substances up to the accepting face of the membrane dissipating it at the delivery face. If the permeation process is sufficiently rapid and the potential gradients in the reservoir cannot be zero, then the bulk phase transport processes may limit the total flux.

5.7 Summary

The separation models were discussed in this chapter. The transport of solute and solvent across a membrane occurs because of driving forces which are a result of a difference in pressure, concentration, temperature or electrical charges. The driving forces are divided into chemical potential and electrochemical potential. Permeation through the membrane is described by two models, which are the solution-diffusion model and the pore flow model. The solution diffusion model is when a solute dissolves in the membrane then diffuses through the membrane down the concentration gradient. In the pore model, the solute is transported through the membrane by a pressure-driven convective flow where part of the solute passes through the membrane pores while others do not. Also, the non-equilibrium thermodynamics can be used to describe the coupling between the solvent and the solute transport such as water and salt through a membrane. The retention of a given solute depends

on the relation between the molecular size and the membrane pore size. From the separation models, the theory that describes the separation behaviour of ions by nanofiltration membrane can be understood, which would be discussed in more details in chapter 7.

Chapter 6 Membrane fouling

The membrane permeate flux depends on time, where it decreases with time because of concentration polarisation, fouling, adsorption of molecules by the membrane material which plugs the membrane pores and temperature polarisation, (refs. 9, 60, 89, 176, 195). Concentration polarisation, fouling, temperature polarisation and molecule adsorption by the membrane increases the resistance through the membrane, hence the permeate flux declines and the membrane rejection decreases. The decrease in the permeate flux depends on the membrane and the feed phase characteristics. In an ideal process, the total resistance affecting the permeate flux is the membrane resistance. The membrane resistance (R_m) is due to its ability to transport one type of molecule more than the other types or retain molecules. From the membrane resistance property, another type of resistance appears, which is the concentration polarisation resistance (R_{cp}) and is due to the molecule or particle layer formed because they cannot permeate through the membrane. If this layer concentration increases to a degree where it changes to a gel layer, a gel layer resistance (R_g) appears. If some solute particles penetrate through the membrane pores and block the membrane, a pore-blocking resistance (R_p) appears. If the membrane adsorbs the solute, this causes adsorption resistance (R_a). Beside concentration polarisation, a temperature polarisation occurs in a heat flux-driven processes. Transport through the membrane is affected by temperature polarisation, concentration polarisation and fouling. Consequently to avoid the decrease in the permeate flux and the rejection of a solute, then fouling, concentration polarisation and temperature polarisation behaviour should be understood in-order to avoided such phenomenon's. Thus fouling, concentration polarisation and temperature polarisation would be discussed in this chapter.

6.1 Concentration polarization

The solute concentration in permeate is less than the solute concentration in the feed bulk, which is due to the membrane where it retains the solute and allows the solvent to permeate through it. The retained molecule's concentration increases with time at the membrane surface and become more concentrated than its concentration in the bulk solution; this effect is known as the concentration polarisation. Concentration polarisation occurs because of the difference in the permeating rate for different components in the feed, which causes concentration gradient at both sides of the membrane. In addition, the retained molecules will diffuse back to the feed bulk. When a steady state is reached, the solute convective flow

toward the membrane surface will be balanced by the solute flux through the membrane and the diffusing flux of solutes back to the feed bulk away from the membrane surface. See Figure 6-1. One approach to describe concentration polarisation is by using the boundary layer thin film model, where a thin layer of unmixed fluid is assumed between the membrane and the well-mixed bulk solution. The solute concentration in the feed bulk is equal to (c_b) at distance (d) and at the membrane surface the concentration increases and reaches the maximum value (c_m). When a steady state condition is reached, the flux at any point in the membrane is equal to the permeate flux, which is equal to the convective flux toward the membrane in the boundary layer minus the diffusion flux away from the membrane in the boundary layer. Then the convective transport of the solute toward the membrane is given by

$$J_v c_i = J_v c_{ip} + D_i \frac{dc_i}{dx} \qquad (6.1)$$

where J_v is the volumetric flux in the boundary layer, c_{ip} is the concentration of ion (i) in the permeate and D_i is the diffusion coefficient of ion (i) , (refs. 195, 267).

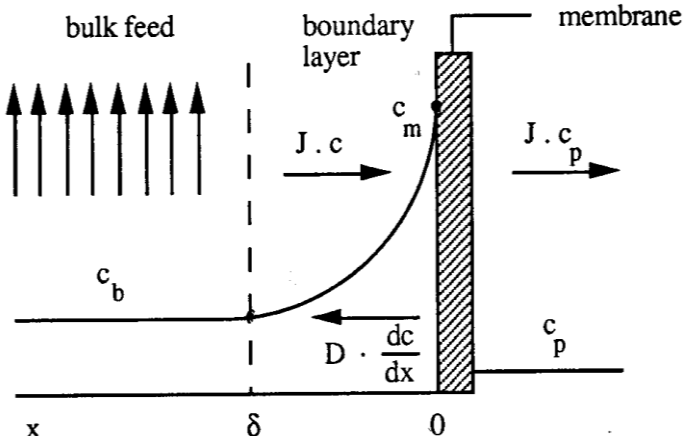

Figure 6-1. Concentration profile, (ref. 195).

Integrating equation (6.1) by using the following boundary conditions

$$x = 0 \Rightarrow c = c_m$$
$$\delta_o x = \delta \Rightarrow c = c_b$$

Then equation (6.1) becomes

$$\frac{c_{im} - c_{ip}}{c_{ib} - c_{ip}} = \exp\left[\frac{J_v \delta}{D_i}\right] \qquad (6.2)$$

where c_{im} is the concentration of component (i) at the feed-membrane interface and c_{ib} is the concentration of component (i) in the bulk-feed solution. The intrinsic retention is given by

$$R_{\text{int}} = 1 - \frac{c_{ip}}{c_{im}} \qquad (6.3)$$

where R_{int} is the intrinsic retention. Concentration polarisation is determined from the increase or decrease in the ratio between the solute concentration at the membrane surface and the solute concentration in the bulk solution. This is known as the concentration polarisation modulus and can be obtained by substituting equation (6.3) into (6.2), which gives

$$\frac{c_{im}}{c_{ib}} = \frac{\exp\left(\frac{J_v}{k}\right)}{R_{\text{int}} + (1 - R_{\text{int}})\exp\left(\frac{J_v}{k}\right)} \qquad (6.4)$$

where c_{im}/c_{ib} is the concentration polarisation module and k is the mass transfer coefficient. The concentration polarisation modulus depends on the boundary layer thickness (δ), the intrinsic retention (R_{int}), the volumetric flux through the membrane (J_v) and the diffusion coefficient in the boundary layer. The boundary layer and the diffusion coefficient appear in the mass transfer coefficient. The concentration polarisation modulus (c_{im}/c_{ib}) increases as the flux and the intrinsic retention increases, while the mass transfer coefficient decreases. As the boundary layer decreases, the concentration polarisation modulus becomes small. Concentration polarisation increases exponentially as the total volume flow flux increases. The relation between convective and diffusion transport in the membrane is described by Peclet number ($J_v\delta/D_i$). If Peclet number is large, the convective transport is balanced easily by the diffusion transport and the concentration polarisation modulus would be large. But if the Peclet number is small, the convection transport is balanced by diffusion transport and as a result, the concentration polarisation is near to unity.

Concentration polarisation can be described by treating the membrane resistance and the fluid

layers adjacent to the membrane as resistances in series, (refs. 267). The flux across the membrane and the fluid layers adjacent to the membrane boundary layer is given as

$$J_i = k_{ov}\left(c_{ib} - c_{ip}\right) \qquad (6.5)$$

where k_{ov} is the overall mass transfer coefficient and c_{ib} is the concentration of component (i) in the bulk-feed solution. If the concentration polarisation is assumed to occur at the feed side, (refs. 267), the flux is given as

$$J_i = k_{bl}\left(c_{ib} - c_{im}\right) \qquad (6.6)$$

where k_{bl} is the fluid boundary layer mass transfer coefficient. And if the concentration polarisation is assumed to occur in the membrane, the flux is given as

$$J_i = k_m\left(c_{im} - c_{ip}\right) \qquad (6.7)$$

where k_m is the membrane mass transfer coefficient. The overall mass transfer coefficient is given as follows

$$\frac{1}{k_{ov}} = \frac{1}{k_m} + \frac{1}{k_{bl}} \qquad (6.8)$$

When the fluid boundary layer mass transfer coefficient (k_{bl}) is large, the fluid boundary layer resistance is small; as a result, the total resistance is determined by the membrane. And if the fluid boundary layer mass transfer coefficient (k_{bl}) is small, the fluid boundary layer increases and the overall resistance becomes the net of the membrane resistance and the fluid boundary layer resistance. Then the overall mass transfer coefficient (k_{ov}) decreases and the flux also decreases.

Concentration polarisation is high in microfiltration and ultrafiltration relative to nanofiltration and reverse osmosis because the flux is high and the diffusion coefficient and the retained particles are small. Concentration polarisation could be reduced by controlling the flux and the mass transfer coefficient. The mass transfer can be increased by increasing the velocity along the membrane, breaking the boundary layer, using turbulences promoter and increasing the temperature, thus causing concentration polarisation to decrease. Temperature also has an effect on the flux; as the temperature increases the mass transfer

coefficient increases, hence the flux increases. The flux increases opposite to the mass transfer coefficient increase goal, which is to reduce the polarisation coefficient. The concentration polarisation is high in ultrafiltration and microfiltration because of the high flux and the low mass transfer coefficient. In nanofiltration and reverse osmosis, the concentration polarisation is low because of the low flux and the low mass transfer coefficient for low molecular weight molecules. In electro-dialysis, the concentration polarisation is high as in microfiltration and ultrafiltration. For pressure-driven membranes, the flux through the membrane is given as

$$J = \frac{\Delta P}{\eta R_m} \qquad (6.9)$$

where R_m is the hydrodynamic membrane resistance where it is constant and does not depend on the applied pressure or the feed composition and concentration. The flux through the membrane has a limiting value where it would not increase even if the applied pressure increases and it is called the limiting flux (J_∞). The limiting flux is given by

$$J_\infty = k \ln\left(\frac{c_m}{c_b}\right) \qquad (6.10)$$

When the flux is high, the macromolecules diffusion is low and the retention is high, thus the solute concentration at the membrane surface is very high. When the solute concentration at the membrane surface increases, a thin layer starts to form on the membrane surface. As the retained solute concentration increases and reaches the maximum value, a gel layer starts to form. The gel layer concentration (c_g) depends on the chemical structure, the size and the shape of solute and on the degree of solvation. The gel concentration does not depend on the solute concentration in the bulk solution; this is described by the gel model. As the gel layer thickness increases, the flux decreases to maintain a balance between the rate of the solute brought to the membrane and the rate of the solute diffusion back to the bulk-feed solution. The flux through the membrane increases as the applied pressure increases, but when it reaches the limiting flux value, no effect would occur as the applied pressure is increased. When the limiting flux is reached, the gel layer thickness increases as the applied pressure is increased and the flux remains constant. The limiting flux decreases as the feed concentration increases. See Figure 6-2.

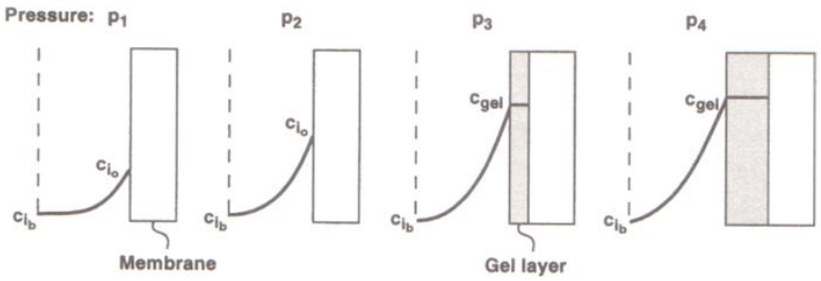

Figure 6-2. Pressure effect on the gel layer formation, where the gel layer thickness increases as the pressure increases, (ref. 267).

The gel layer adds a resistance to the membrane resistance and the gel layer resistance becomes the limiting factor toward the flux, (refs. 195). The limiting flux in this case is given as

$$J_{\infty} = \frac{\Delta p}{\eta\left(R_m + R_g\right)} = k \ln\left(\frac{c_g}{c_b}\right) \qquad (6.11)$$

where c_g is the gel concentration. In the osmotic pressure model where an osmotic pressure exists because of the retained low molecular weight molecules, equation number (6.9) would not be accurate and it becomes

$$J = \frac{\Delta p - \Delta \pi}{\eta R_m} \qquad (6.12)$$

This is known as the osmotic pressure model. For macromolecules, the osmotic pressure is given as

$$\Delta \pi = a.c^n \qquad (6.13)$$

where a is a constant and n is an exponential, which is greater than (1). If the solute is 100% rejected by the membrane then its concentration in the permeate would be $c_p = 0$ thus in equation (6.4) the rejection would be equal to 1 ($R_{int} = 1$) and by substituting equations (6.4) and (6.13) into equation (6.12) gives the following

$$J = \frac{\Delta p - a c_b^n \exp\left(\frac{nJ}{k}\right)}{\eta R_m} \qquad (6.14)$$

Deriving equation (6.14) gives the following equation

$$\frac{\partial J}{\partial \Delta p} = \left(\eta R_m + \frac{n}{k} \Delta \pi \right)^{-1} \qquad (6.15)$$

From equation (6.15), it can be seen that the flux does not increase linearly as the pressure difference increases. The increase in the membrane resistance is attributable to the osmotic pressure. The gel layer and the osmotic pressure models give similar results. For the gel layer model, if the flux in equation (6.11) is plotted versus (ln c_b), the slope will be (-k) and the x-intercept is (ln c_g); see Figure 6-3.

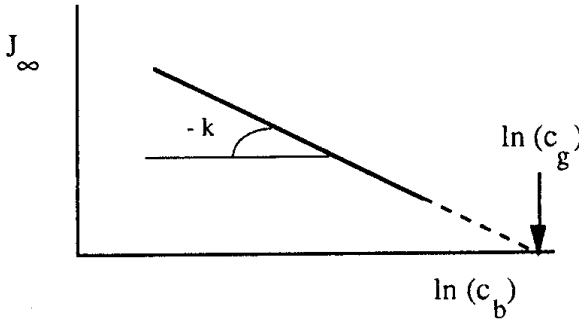

Figure 6-3. (J_∞) is plotted as a function of (ln c_b), (ref. 195).

In the osmotic pressure model, equation (6.14) is derived as follows

$$\frac{\partial J}{\partial \ln(c_b)} = -K\left(1 + \frac{R_m k \eta}{\Delta \pi_n} \right)^{-1} \qquad (6.16)$$

Where the following graph is obtained by plotting (J_∞) versus (ln c_b); see figure 6-4. If the membrane resistance (R_m) is small and is neglected, the slope would be equal to (-k) and the x-intercept of the slope is ($\Delta \pi = \Delta p$).

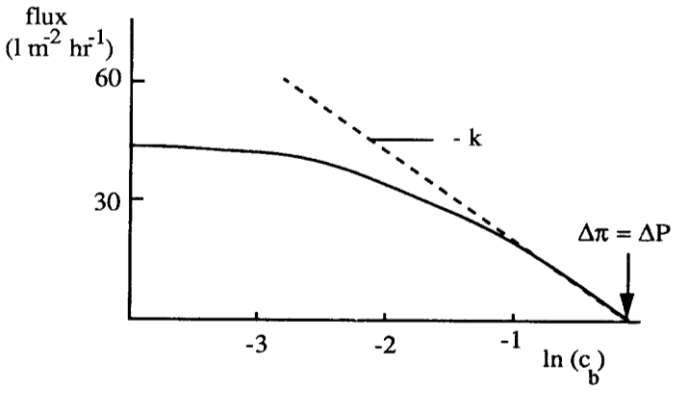

Figure 6-4. (J_∞) is plotted as a function of bulk concentration, (ref. 195).

If the solute rejection by the membrane is 100% and a steady state is reached, the convective flow of the molecules toward the membrane would be equal to the diffusion flow of the molecules toward the bulk, (refs. 195). Since the molecule concentration increases and if it is assumed that no gel layer is forming and a hydrodynamic resistance occurs at the boundary layer, then equation (6.9) becomes

$$J_v = \frac{\Delta p}{\eta\left(R_m + R_{bl}\right)} \qquad (6.17)$$

where R_{bl} is the boundary layer resistance. The boundary layer resistance depends on the molecule's molecular weight and the solute concentration. If the boundary layer resistance (R_{bl}) is integrated over the boundary layers (x=0) and (x=δ) as follows

$$R_{bl} = \int_0^{\delta} P x^{-1}.dx \qquad (6.18)$$

where P is the permeability. Then the flux through the boundary layer's resistance can be given as follows

$$J_v = \frac{-\Delta\pi_{bl}}{\eta R_{bl}} \qquad (6.19)$$

6.2 Temperature polarisation

In processes where heat is used to transport or retain molecules or solvent through a membrane such as distillation and thermo-osmosis, heat and mass polarisation occur, (refs. 195, 230). Since the solvent in the feed side has a higher temperature than the permeate side, the solvent would evaporate and the solvent vapour pressure would increase, thus the solvent vapour would transport to the permeate side of the membrane and condensate. The heat required to increase the temperature and vaporise the solvent is supplied by the bulk solution; on the other hand, some of the heat is lost by conducting through the membrane and the membrane pores to the other side (colder side). A steady state is reached when the heat supplied by the bulk solution is equal to the heat lost by the membrane. The temperature polarisation is the temperature difference between the bulk solution and the membrane surface temperature. The heat balance for a steady state is given by

$$\phi = \alpha_1(T_\infty - T_{m1}) - \phi\Delta H_v = \frac{\lambda m}{l}(T_{m1} - T_{m2}) = \alpha_2(T_{m2} - T_{b2}) + \phi\Delta Hc \qquad (6.20)$$

where α_1 is the heat coefficients on the warm side of the membrane, α_2 is the heat coefficient on the cold side of the membrane, $\phi\Delta H_v$ is the heat flux caused by convective transport through the pores, $\phi\Delta H_c$ is the heat flux caused by convective transport through the pores and λ_m is the overall heat conductivity of the membrane. The following boundaries were considered

$$\begin{aligned} T_{b1} - T_{m1} &= T_{m2} - T_{b2} = \Delta T_{bl} && \text{Boundary layer} \\ T_{m1} - T_{m2} &= \Delta T_m && \text{Across the membrane} \\ T_{b1} - T_{b2} &= \Delta T_{bl} && \text{Bulk feed and permeate} \end{aligned}$$

In addition, if the heat coefficients were assumed to be equal ($\alpha_1 = \alpha_2 = \alpha$), equation (6.20) becomes

$$\Delta T_m = \frac{\Delta T_b - (\frac{2\phi\Delta H_c}{\alpha})}{\left[1 + \left(\frac{2\lambda m}{l\alpha}\right)\right]} \qquad (6.21)$$

The overall heat conductivity (λ_m) is equal to the sum of the heat conductivity in the pores (λ_g) and the heat conductivity in the solid part (λ_p). The overall heat conductivity is given by

$$\lambda_m = \varepsilon\lambda g + (1 - \varepsilon)\lambda p \qquad (6.22)$$

Equation (6.22) is for cylindrical pores with surface porosity (ε). If the ($\phi\Delta H_c = \rho\Delta H_v J$) and by substituting it into equation (6.21) gives

$$\Delta T_m = \frac{\Delta T_b - (\frac{2J\rho\Delta H_v}{\alpha})}{\left[1 + \left(\frac{2\lambda m}{l\alpha}\right)\right]} \qquad (6.23)$$

The temperature polarisation (ΔT_m) increases when the volumetric flux and the heat conductivity by the solid part of the membrane increase, and the temperature polarisation (ΔT_m) decreases when the heat transfer coefficient and the membrane thickness increases. In

thermo-osmosis, the heat transfer is a result of conduction through the membrane. For the thermo-osmosis process, equation (6.21) becomes

$$\Delta T_m = \frac{\Delta T_b}{\left[1+\left(\frac{2\lambda m}{l\alpha}\right)\right]} \qquad (6.24)$$

The overall heat conductivity of the membrane in thermo-osmosis is high, thus the polarisation temperature in distillation is greater than in thermo-osmosis because the convective term depends on the volumetric flux.

6.3 Membrane fouling

Membrane fouling is an irreversible process where particles are retained on the membrane surface, and the flux keeps decreasing and does not become steady with time as in concentration polarisation. Fouling occurrence depends on the separation process and the membrane that is used; for example, fouling exists in microfiltration, ultrafiltration, nanofiltration and reverse osmosis but nearly does not appear in pervaporation and gas separation. Fouling depends on the solution's physical and chemical parameters such as concentration, pH, temperature and ionic strength. Fouling can be reduced by using several methods such as

1. Pre-treatment of the feed solution, which includes pre-microfiltration, pre-filtration, pH adjustment, heat treatment and addition of complexing agents.
2. Changing membrane properties.
3. Changing the process conditions; for example, fouling decreases as the concentration polarisation decreases, hence concentration polarisation can be reduced by increasing the mass transfer coefficient and reducing the membrane flux.
4. Cleaning; there are three types of cleaning: hydraulic cleaning, mechanical cleaning and chemical cleaning. Cleaning methods depend on the membrane chemical resistance, module configuration and foulants type.

6.4 Summary

This chapter discusses concentration polarisation, fouling, and temperature polarisation. and molecule adsorption by the membrane increases the resistance through the membrane. The

permeate flux through the membrane decreases with time because of concentration polarisation, fouling, adsorption of ions by the membrane material and temperature polarisation, consequently the rejection of ions decreases. Since fouling and concentration polarisation would occur when ions permeate through nanofiltration membrane, thus fouling and concentration polarisation should be investigated in-order to understand their effect on ions rejection. In this work, concentration polarisation and fouling is investigated for two different membranes with different pore size for different types of ions and concentration. Because the permeate flux and the ions rejection is effected by the membrane pore size and the feed solution characteristics. This is discussed in more details in chapter 8.

Chapter 7 Nanofiltration membrane

Nanofiltration membrane is a pressure-driven membrane with properties lying between ultrafiltration and reverse-osmosis membranes. Nanofiltration membrane permeate flux is higher than reverse osmosis permeate flux but the rejection is lower. The separation mechanism involves steric (sieving), electrostatic (Donnan) effects, convection and diffusion, (refs. 7, 25, 145, 207). The rejection of mono-valent ions and non-ionised organics with molecular weight less than 150 by nanofiltration membrane is low while the rejection of multi-valent ions and organics with molecular weight higher than 300 is high. Most nanofiltration membranes are either positively charged or negatively charged. The advantages of nanofiltration membrane are that it operates at lower pressure than reverse osmosis membrane, has selective rejection between mono-valent and multi-valent ions and has high permeate flux. The disadvantage of nanofiltration membrane (and membranes in general) is fouling, which is caused by adsorbing foulants on the pore walls, pore blockage and surface fouling such as cake and gel layer formation. Nanofiltration membrane is used for softening water, removing hardness, natural organic matter, heavy metals, viruses and bacteria, and concentrating organic dyes. Nanofiltration membranes can be classified into two major groups, which are polymeric and ceramic membranes, where ceramic nanofiltration membrane was considered in this work. Even though polymeric nanofiltration membranes have been widely used because they can be easily prepared and cheaply produced at a large scales, but they have disadvantages, which are low chemical stability, low thermal stability and low mechanical stability. Even though ceramic nanofiltration membranes are more expensive and complex to produce but they can tolerate high temperatures, tolerate extreme pH values, resist being swelled by solvents and have longer lifetime. In addition, ceramic nanofiltration membranes can be easily cleaned and restored to their original conditions, unlike polymeric nanofiltration membranes. There are several models used to describe the transport mechanism through nanofiltration membrane, (refs. 7, 25, 145, 207, 219, 220, 257, 289, 290, 314, 321, 324, 325, 326, 328, 342, 343, 344), such as the following

1. Solute rejection based on continuum hydrodynamic model.
2. Irreversible thermodynamics, which considers the membrane as a black box ignoring the membrane structure and any transport mechanism, (refs. 7, 83, 195).
3. Electro-kinetic space-charge model, (refs. 343).
4. Donnan-Steric-Pore model (DSPM), which includes the hindrance effects for diffusion

and convection. Membrane characterisation depends on the pore radius (r_p), the effective ratio of membrane thickness to porosity ($\Delta x/A_k$) and the effective membrane charge density (X_d), (refs. 25, 290, 314).

5. Extended Nernst-Planck equation is used to describe ion transport through the membrane with the Poisson-Boltzmann equation, which is used to describe the radial distribution across the pore. Membrane characterisation depends on the effective ratio of membrane thickness to porosity ($\Delta x/A_k$) and the effective membrane charge density (X_d) , (refs. 7, 314).
6. The electrostatic and the steric-hindrance model, where the transport of charged solutes through nanofiltration membrane depends on the membrane charged pore structure, (refs. 342, 344).
7. The Spiegler-Kedem model, where nanofiltration membrane is characterised in terms of the solute permeability and the reflection coefficient, (refs. 300).

7.1 Characterisation of nanofiltration membrane

Nanofiltration membranes are generally made of polymeric or inorganic (ceramic) materials. Inorganic nanofiltration membranes have pore diameters ranging between 0.5–2 nm and they do not swell in water. The polymeric nanofiltration membranes are either non-porous cross-linked structures with anionic group, which swells in water, or meso-porous with a top layer and porous support. The separation performance of meso-porous and non-porous membranes is the same but the separation mechanism is different; see Figure 7-1.

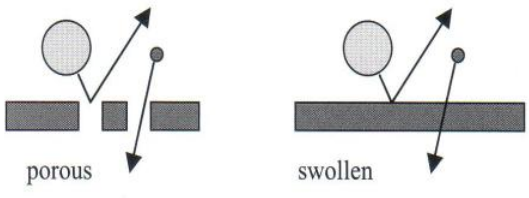

Figure 7-1. Separation of uncharged molecule by porous and nonporous nanofiltration membrane, (ref. 7).

The sieving mechanism is used in the porous nanofiltration membrane and the solution diffusion mechanism is used in the swollen membranes. If the feed solution contains ions, the main separation mechanism for both porous and swollen membranes is the Donnan exclusion. Different parameters can be used to characterise nanofiltration membranes, such as

7.1.1 Performance parameters

The membrane performance can be characterised by the retention of charged and uncharged solutes, (refs. 7, 30, 38, 125), as well as the solvent permeability.

7.1.1.1 Charged molecules retention

If the membrane were charged, then the Donnan effect would contribute to the separation performance. Charged membrane would repel ions with the same charge as the fixed membrane charge; as a result, the ion's concentration in the membrane and the transport rate are low. If a charged membrane is at equilibrium condition, then the chemical potentials (μ) for different ions at the membrane interface between the solution and the membrane are equal, which is given as

$$\mu_i = \mu_i^m \qquad (7.1)$$

The ion electrochemical potential (Ψ) in the solution is given as

$$\psi_i = \mu_i^o + RT \ln a_i + zFE \qquad (7.2)$$

Moreover, the ion electrochemical potential (Ψ) in the membrane is given as

$$\psi_i^m = \mu_i^{m,o} + RT \ln a_i^m + zFE^m \qquad (7.3)$$

where Ψ_i is the ion (i) electrochemical potential in the solution (J/mol), μ°_i is the ion (i) standard reference state of the chemical potential in the solution (J/mol), a_i is the ion (i) activity in the solution (dimensionless), E is the measured potential in the solution (V), Ψ_i^m is the ion (i) electrochemical potential in the membrane (J/mol), $\mu_i^{m,o}$ is the ion (i) standard reference state of the chemical potential in the membrane (J/mol), a_i^m is the ion (i) activity in the membrane (dimensionless) and E^m is the measured potential in the membrane (V). At the membrane-feed solution interface, an electrical potential would develop because of the difference in the ionic concentration between the membrane phase and the solution phase, this is known as the Donnan potential. The Donnan potential is given as

$$E_{don} = E^m - E = \frac{RT}{z_i F} \ln \frac{a_i}{a_i^m} \qquad (7.4)$$

The membrane rejection can be predicted from the ion distribution at the solution-membrane

interface. At the solution-membrane interface for a dilute mono-valent solution (such as NaCl) and a negatively charged membrane, the concentration is given as

$$c_+ \times c_- = c_+^m \times c_-^m \qquad (7.5)$$

where c_+ is the concentration of positively charged ions in the solution, c_- is the concentration of negatively charged ions in the solution, $c^m{}_+$ is the concentration of positively charged ions in the membrane, and $c^m{}_-$ is the concentration of negatively charged ions in the membrane. If electro-neutrality condition is maintained as follows

$$\sum z_i c_i = 0 \qquad (7.6)$$

then applying the electro-neutrality condition for the solution phase and the membrane phase results in

$$c_+ = c_- \qquad (7.7\text{-a})$$

$$c_+^m = c_-^m + c_{X-}^m \qquad (7.7\text{-b})$$

where $c^m{}_{X-}$ is the concentration of membrane fixed charge. Substituting equations (7.7-a) and (7.7-b) into equation (7.5) gives

$$\frac{c_-^m}{c_-} = \frac{c_-}{\left(c_-^m + c_{X-}^m\right)} \qquad (7.8)$$

Equation (7.8) can be written for 2-1 salt such as ($CaCl_2$) and 1-2 salt such as (Na_2SO_4) as follows

$$\frac{c_-^m}{c_-} = \left(\frac{2c_-}{\left(2c_-^m + c_{X-}^m\right)}\right)^2 \qquad (2-1\ salt) \qquad (7.9)$$

$$\frac{c_-^m}{c_-} = \sqrt{\frac{c_-}{\left(c_-^m + c_{X-}^m\right)}} \qquad (1-2\ salt) \qquad (7.10)$$

From equations (7.8), (7.9), and (7.10), the ion distribution at the solution-membrane interface can be indicated and the membrane rejection can be predicted. For a negatively

charged membrane, a high rejection is expected for (1-2 salt) type and the concentration of ions in the membrane is low. While for (2-1 salt) type, the concentration in the membrane would be high and as a result, the rejection is low.

7.1.1.2 Retention of uncharged solutes

For porous nanofiltration membrane, separation is due to the sieving mechanism, and for non-porous nanofiltration membrane, the separation is due to the solution-diffusion mechanism. Molecular weight cut-off (MWCO) is used to characterise nanofiltration membrane where it is defined as the molecular weight of 90% of retained particles by the membrane. Since molecular weight cut-off (MWCO) is affected by adsorption, concentration polarisation, pressure, and feed concentration, then it cannot be used as the absolute characterisation parameter. Separation for swollen (non-porous) nanofiltration membrane is characterised by the solubility and the molecular size; as a result, the molecular weight cut-off is considered a bad characterising parameter and is insufficient to characterise swollen and polymeric nanofiltration membranes. The rejection of solute by nanofiltration membrane increases as the solute molecular weight cut-off (MWCO) and solute molecule size increase. Rejection (retention) depends on the flux and pressure across the membrane, (refs. 7). From irreversible thermodynamics, the solute flux (J_s) is given as

$$J_s = -L_s \frac{dc_s}{dx} + (1-\sigma) J_v c_s \qquad (7.11)$$

In addition, the solvent flux (J_v) is given as

$$J_v = -L_p \left(\frac{dP}{dx} - \sigma \frac{d\pi}{dx} \right) \qquad (7.12)$$

where L_p is the solvent permeability coefficient (m³/m².s.bar), L_s is the local solute permeability ($L_s = L_s' \Delta x$), P is the pressure (bar), σ is the reflection coefficient (dimensionless), π is the osmotic pressure (N/m²), Δx is the membrane thickness (m) and L_s' is the solute permeability (m/s). The retention (R) is given as

$$R = \frac{c_f - c_p}{c_f} \qquad (7.13)$$

where c_f is the feed concentration (mol/l) and c_p is the permeate concentration (mol/l). Integrating equation (7.11) and considering ($c_p=J_s/J_v$) then substituting it into equation (7.13) gives the following

$$R = \frac{\sigma\left(1 - e^{Pe}\right)}{1 - \sigma\, e^{Pe}} \qquad (7.14)$$

where (Pe) is the Peclet number, which is given as

$$Pe = -J_v \frac{(1-\sigma)\Delta x}{L_s} \qquad (7.15)$$

It can be noticed that the retention increases as the solvent flux increases. When the solvent flux is very big ($J_v \to \infty$), the retention (R) would be equal to the reflection coefficient (σ).

7.1.2 Morphology parameters

Nanofiltration membrane performance can be determined by the membrane morphology parameters such as the membrane surface roughness, the membrane hydrophobicity, and the membrane chemical structure, (refs. 1, 7). Membrane porosity can be measured using different methods such as gas adsorption-desorption, permporometry, microscopy and surface force-pore flow. The gas adsorption-desorption method is used to measure the pore size of a porous inorganic membrane such as ceramic membranes. The gas adsorption-desorption method depends on the vapour pressure difference between the curved and flat surfaces. The adsorbed gas volume is measured by adsorption and desorption of the gas at different vapour pressures. When the relative vapour pressure (P_{rel}) is equal to zero, all the membrane pores will be open. By increasing the relative vapour pressure, the gas adsorption starts to occur at the pore wall, and a further increase in the relative vapour pressure causes condensation. An increase in the relative vapour pressure will start to fill the membrane pores, and all the membrane pores will be filled with vapour when the relative vapour pressure reaches unity (P_{rel} = 1). The relative vapour pressure where adsorptions take place is related to the membrane pore size as follows

$$\ln \frac{P}{P^o} = \frac{2\gamma V_{mol}}{RT\, r_k} \cos\theta \qquad (7.16)$$

where γ is the surface tension (N/m), V_{mol} is the molar volume (mol/m³), r_k is the Kelvin radius (m), (θ) is the contact angle, P is the pressure (bar) and P° is the vapour pressure (bar).

Permporometry is another method used to measure the pore size and the pore size distribution for porous membranes for pore diameter larger than 2nm. Permporometry depends on condensation on the pore walls and the gas diffusion through them. Firstly, the pores are filled with condensable vapour, and when the relative pressure is equal to unity, the pores are filled and no gas permeation occurs. Secondly, the relative pressure is reduced and as a result, condensed vapour is removed and gas diffuses through the membrane. Finally, the gas diffusion flow is measured.

Pore size and pore size distribution are determined by the surface force-pore flow method. The solute and the solvent are assumed to be able to permeate through the membrane pores perpendicular to the membrane surface under the surface force influence. As the pores in the membrane upper layer increase, the flux increases and the retention also increases.

The membrane hydrophobicity is used to characterise the membrane because it causes the solute to deposit on the membrane surface causing fouling. Hydrophobicity is expressed in terms of contact angle (θ) where the edge of the two boundary phases ends a third phase. The contact angle (θ) is the membrane wettability, which is the amount of adsorbed water. The contact angle (θ) is given as

$$\cos\theta = \frac{\gamma_{SV}\gamma_{SL}}{\gamma_{LV}} \qquad (7.17)$$

where θ is the contact angle, γ_{SV} is the surface tension of the solid with the liquid vapour, γ_{LV} is the surface tension of the liquid with the liquid vapour and γ_{SL} is the tension of the solid-liquid interface.

7.1.3 Charge parameters

Nanofiltration membrane charge affects the membrane retention and fouling. The charge of nanofiltration membrane is a result of dissociating functional groups, adsorption of ions from the solution, adsorption of polyelectrolyte's, adsorption of ionic surfactants, and adsorption of

charged macromolecules. The membrane surface (negatively and positively) fixed charges can be measured by titration. The membrane ion conductivity is measured using impedance spectroscopy. In this work, nanofiltration membrane charge is considered an important parameter that would affect the membrane rejection behaviour. Consequently, the effect of ions concentration and pH on the membrane charge sign was investigated (see chapter 9).

7.2 Chemical interaction affect on nanofiltration membrane rejection

The retention of nanofiltration membrane is affected by acid-base transformation, complexation, precipitation, oxidation-reduction and adsorption, (refs. 7, 68, 131, 248). These chemical reactions were considered in this work in-order to try to understand and justify the rejection behaviour for nanofiltration membrane (see chapter 9).

7.2.1 Acid-base transformation

The acid-base behaviour of a solute may influence nanofiltration membrane retention, where the gain and loss of protons may form different forms (speciation) of species. The different new species formed may have different properties than the original solute such as being more or less charged, which as a result would have an influence on retention.

7.2.2 Complexation

When solutes are dissolved in a solution, cations and anions are formed. The interaction between cations and anions results in different types of complexes. Since the actual solute distribution depends on the solution conditions such as pH, concentration and temperature, the retention of the solute is affected. For example, the retention of nanofiltration membrane would change by the change of species in the solution from highly negatively charged at high pH to divalent cations in an acidic solution. The retention of negatively charged solute at high pH solution is higher that the retention for positively or non-charged solutes.

7.2.3 Precipitation

When precipitates are formed, they will be retained by nanofiltration membrane except for dissolved complexes. Complexes are expected to pass through nanofiltration membrane unless they are retained because of size exclusion, Donnan exclusion or adsorption effect. Precipitation of solutes at nanofiltration membrane surface is related to concentration

polarisation; as the solute's precipitated amount increases, the concentration polarisation increases thus retention also increases.

7.2.4 Oxidation-reduction

The oxidation-reduction transformation may cause change in the solute form such as the solute charge or being dissolved or precipitated, and this would affect the separation process by nanofiltration membrane. The oxidation-reduction reaction causes a change and a formation of new species that differs from the original species. The behaviour of the original solutes and the new formed materials in nanofiltration membrane are different, thus the retention behaviour would differ.

7.2.5 Adsorption

Retention is affected by the adsorption of particles by the nanofiltration membrane or adsorption by the accumulated layer on the membrane surface. Adsorption is affected by several elements such as the solute concentration, the solution pH and the particle size.

7.3 Nanofiltration membrane theory

Nanofiltration can separate charged and uncharged solutes from the solution, (refs. 7, 14, 30, 47, 350). The uncharged molecule's separation is a result of the size exclusion or the difference between the diffusion rates. The charged solute's (ions) separation is a result of the interaction between the membrane surface charge and the solute charge. Also, charged molecules separation depends on their size; if the molecule size is bigger than the membrane pore then it will be retained by the membrane. Solute permeates through nanofiltration membrane by two mechanisms: convection and diffusion. Convection transfer is affected by the physical parameters such as pressure and conversion rate, while diffusion transfer is affected by the chemical parameters such as concentration and pH. As a result, convection is more effective at high pressure than low pressure and larger ions are better retained by the membrane because convection depends on the physical parameters. Since diffusion depends on the chemical parameters, the chemical selectivity is more important than the physical selectivity in nanofiltration membrane; as a result, the selectivity is much higher at low pressure. Nanofiltration membrane selectivity is high at low pressure because of diffusion and its retention is high at high pressure because of convection. One of the aims of this work

is to study the effect of ion type and ion concentration on nanofiltration membrane selectivity and rejection at low applied pressure values, see chapter 9 for more details.

7.3.1 Rejection of uncharged solutes

The uncharged solute flux is given as a combination between hindered convection and diffusion as follows

$$j_s = K_c c V - \frac{c D_p}{RT} \frac{d\mu}{dx} \qquad (7.18)$$

where j_s is the uncharged solute flux (mol/m².s), K_c is the uncharged solute hindrance factor for convection (dimensionless), c is the uncharged solute concentration within the pore (mol/m), V is the solvent velocity (m/s), D_p is the uncharged solute pore diffusion coefficient (m²/s), R is the gas constant (8.314 J/mol.K), T is the absolute temperature (K), μ is the uncharged solute chemical potential (J/mol), and x is the membrane thickness (m). If the chemical potential (μ) for uncharged solute is given as

$$\mu = RT \ln a + V_s P + \text{constant} \qquad (7.19)$$

where a is the uncharged solute activity (mol/m³), and V_s is the uncharged solute partial molar volume (m³/mol). For a dilute solution, which is assumed to behave ideally, and differentiating equation (7.19) and substituting it in equation (7.18) gives

$$j_s = K_c c V - D_p \frac{dc}{dx} - \frac{c D_p}{RT} V_s \frac{dP}{dx} \qquad (7.20)$$

In addition, the solute flux is given as

$$j_s = C_p V \qquad (7.21)$$

where C_p is the uncharged solute bulk permeate concentration (mol/m³). For porous nanofiltration membrane, the solvent velocity is given by the Hagen-Poiseuille equation as follows

$$V = \frac{r_p^2 \Delta P_e}{8\eta \Delta x} \tag{7.22}$$

where r_p is the effective pore radius (m), ΔP_e is the effective pressure driving force (N/m), η is the solvent viscosity within pores (N s/m²), and Δx is the membrane thickness (m). By rearranging equation (7.22) and assuming that the pressure gradient is constant, the pressure gradient can be given as

$$\frac{dP}{dx} = \frac{\Delta P_e}{\Delta x} = \frac{8\eta V}{r_p^2} \tag{7.23}$$

Substituting equations (7.21) and (7.23) into equation (7.20) gives

$$\frac{dc}{dx} = \frac{V}{D_p}\left[\left(K_c - \frac{8D_p V_s \eta}{RTr_p^2}\right)c - C_p\right] \tag{7.24}$$

Assuming that the uncharged solute pore diffusion coefficient (D_p) and the uncharged solute partial molar volume (V_s) to be independent of concentration and by assuming the dimensionless group (Y) is given as

$$Y = \frac{8D_p V_s \eta}{RTr_p^2} \tag{7.25}$$

Then equation (7.24) becomes

$$\frac{dc}{dx} = \frac{V}{D_p}\left[(K_c - Y)c - C_p\right] \tag{7.26}$$

Moreover, by integrating equation (7.26) over the following boundaries

$$at \quad x = 0 \longrightarrow c = \phi\, C_f$$
$$at \quad x = \Delta x \longrightarrow c = \phi\, C_p$$

where ϕ is the uncharged solute steric partitioning coefficient (dimensionless) [$\varphi = (1-\lambda)^2$], and C_f is the uncharged solute bulk feed concentration (mol/m³), gives the following:

$$\frac{C_p}{C_f} = \frac{[(K_c - Y)\phi]\exp Pe'}{[(K_c - Y)\phi] - 1 + \exp Pe'} \qquad (7.27)$$

The Peclet number (*Pe'*) is given as

$$Pe' = \frac{(K_c - Y)V\Delta x}{D_p} = \frac{(K_c - Y)r_p^2 \Delta Pe}{8\eta D_p} \qquad (7.28)$$

Then the rejection (*R*) for the nanofiltration membrane can be given as

$$R = 1 - \frac{C_p}{C_f} = 1 - \frac{[(K_c - Y)\phi]\exp Pe'}{1 - ([1 - (K_c - Y)\phi]\exp Pe')} \qquad (7.29)$$

From equations (7.28) and (7.29), it can be noticed that the rejection (*R*) of uncharged solute is independent on the membrane thickness (Δx). Also from the Peclet number, it can be noticed that the uncharged solute rejection depends on the porous radius.

7.3.2 Rejection of salts

For charged solute, the ionic flux of component (*i*) is given as

$$j_i = K_{i,c} c_i V - \frac{c_i D_{i,p}}{RT} \frac{d\mu_i}{dx} \qquad (7.\ 30)$$

where j_i is the ionic flux of ion (*i*) (mol/m².s), $K_{i,c}$ is the hindrance factor for convection of ion (*i*) (dimensionless), c_i is the concentration of ion (*i*) within the pore (mol/m³), $D_{i,p}$ is the pore diffusion coefficient of ion (*i*) (m²/s), and μ_i is the electrochemical potential of ion (*i*) (J/mol). The ion flux equation is the same as the uncharged solute flux equation, (refs. 4, 5, 6, 7, 27, 351), but the difference is that the electrochemical potential for ion (*i*) is given as

$$\mu_i = RT \ln a_i + V_i P + z_i F \psi + \text{constant} \qquad (7.31)$$

where a_i is the activity of ion (*i*) (mol/m³), V_i is the partial molar volume of ion (*i*) (m³/mol), z_i is the valence of ion (*i*) (dimensionless), *F* is the Faraday constant (96487 C/mol), and Ψ is the potential within the pore (V). The activity of ion (*i*) is given as

$$a_i = \gamma_i c_i \qquad (7.32)$$

where γ_i is the activity coefficient of ion (i) within the pore (dimensionless). Differentiating equation (7.31) and substituting it into equation (7.30) and rearranging the equation results in

$$j_i = K_{i,c} c_i V - c_i D_{i,p} \frac{d \ln \gamma_i}{dx} - \frac{c_i D_{i,p}}{RT} V_i \frac{dP}{dx} - D_{i,p} \frac{dc_i}{dx} - \frac{z_i c_i D_{i,p}}{RT} F \frac{d\Psi}{dx} \qquad (7.33)$$

The ion flux can be written as

$$j_i = C_{i,p} V \qquad (7.34)$$

where $C_{i,p}$ is the solute concentration for component (i) in bulk solution (mol/m^3). The dimensionless group (Y) used for uncharged solute can be written for ion (i) as follows

$$Y_i = \frac{8 D_{i,p} V_i \eta}{R T r_p^2} \qquad (7.35)$$

Assuming that the concentration in the pore is small, the activity coefficient (γ_i) gradient in equation (7.33) can be neglected. By substituting equations (7.34) and (7.35) into equation (7.33) and rearranging the equation gives the concentration gradient as follows

$$\frac{dc_i}{dx} = \frac{V}{D_{i,p}} \left[\left(K_{i,c} - Y_i \right) c_i - C_{i,p} \right] - \frac{z_i c_i}{RT} F \frac{d\Psi}{dx} \qquad (7.36)$$

Assuming the electro-neutrality condition in the membrane pore to be as follows

$$\sum_{i=1}^{n} z_i c_i = -X_d \qquad (7.37\text{-a})$$

where X_d is the effective membrane charge density (mol/m³), and the electro-neutrality condition in the bulk solution is given as

$$\sum_{i=1}^{n} z_i C_i = 0 \qquad (7.37\text{-b})$$

where C_i is the concentration in the bulk concentration (mol/m³). Integrating the electro-

neutrality condition (equation (7.37-a)) over the membrane thickness is the same as multiplying equation (7.36) by (z_i) and summation for all the ions in the solution where the summation is equal to zero according to equation (7.37-b). Therefore, rearranging the equation gives the potential gradient as follows

$$\frac{d\Psi}{dx} = \frac{\sum_{i=1}^{n} \frac{z_i V}{D_{i,p}} \left[\left(K_{i,c} - Y_i \right) c_i - C_{i,p} \right]}{\frac{F}{RT} \sum_{i=1}^{n} z_i^2 c_i} \qquad (7.38)$$

In salt separation, the Donnan effect causes ion rejection as a result of the ion and the membrane charge. The Donnan-steric partitioning is given as

$$\left(\frac{\gamma_i c_i}{\gamma_i^o C_i} \right) = \phi \exp\left(- \frac{z_i F}{RT} \Delta\Psi_D \right) \qquad (7.39)$$

where c_i is the concentration in the membrane (mol/m³), C_i is the concentration in the bulk concentration (mol/m³), γ_i is the activity coefficient of ion (i) in the membrane, γ°_i is the activity of ion (i) in the bulk solution, ϕ is the steric partitioning term and $\Delta\Psi_D$ is the Donnan potential (V). The concentration of ions with the same charge as the membrane charge (co-ions) is higher inside the membrane than that in the solution, while the concentration of ions with opposite charge of the membrane charge (counter-ions) is smaller inside the membrane than that in the solution. Because of the concentration difference at the membrane/solution interface, a potential difference is generated. The potential is known as the Donnan potential. The Donnan potential is given as

$$\Delta\psi_D = \psi_m - \psi = \frac{RT}{z_i F} \ln \frac{a_i}{a_{i,m}} \qquad (7.40)$$

where Ψ_m is the potential in the membrane (V), Ψ is the potential in the solution (V), a_i is the activity of ion (i) in the solution (dimensionless) and $a_{i,m}$ is the activity of ion (i) in the membrane (dimensionless).

7.4 Nanofiltration membrane fouling

Fouling decreases the membrane performance and causes a flux decline. Fouling is an

irreversible process and need to be cleaned, where the cleaning process includes chemical and physical cleaning. Fouling may be caused by precipitation of a solute at the membrane surface where the solute solubility is exceeded, deposition of colloidal matters on the membrane, solutes reacting at the membrane surface, solutes reacting with the membrane material, adsorption of molecules by the membrane, formation of irreversible gel layer and colonisation of bacteria. There are several types of fouling such as organic, inorganic, particulate and biological fouling. Fouling can be reduced and the membrane life can be increased by feed pre-treatment, selecting the appropriate membrane material and module design, and the cleaning process, (refs. 7, 8).

7.4.1 Fouling characterisation

The clean water flux is used to characterise fouling. The clean water flux is given as

$$J_O = \frac{\eta_T}{\eta_{20°C}} \frac{Q}{A\Delta P} \qquad (7.41)$$

where J_O is the initial water flux, η_T is the water viscosity at temperature (T), $\eta_{20°C}$ is the water viscosity at temperature 20 ℃, Q is the volume flow rate, A is the membrane surface area, and ΔP is the trans-membrane pressure. Equation (7.41) is valid for dilute solution. The flux reduction (FR) is determined as follows

$$FR_{CWF} = \frac{J_{Ob} - J_{Oa}}{J_{Ob}} \times 100\% \qquad (7.42)$$

where FR_{CWF} is the flux reduction with regards to clean water flux, J_{Oa} is the clean water flux after feed filtration, and J_{Ob} is the clean water flux before feed filtration. Flux reduction can also be determined as follows

$$FR_{PF} = \frac{J_{Ob} - J}{J_{Ob}} \times 100\% \qquad (7.43)$$

where J is the water flux, and FR_{PF} is the flux reduction with regards to permeate flux. Before using nanofiltration membrane and measuring the water flux, the membrane is compacted at high pressure to avoid membrane compaction during the filtration process. Compaction is not considered a form of fouling and is found in nanofiltration membranes. Compaction is due to

the applied pressure during the filtration process. Compaction affects the membrane active layer and the membrane support layer, and may change these layers' properties. To overcome compaction, the membrane is compacted at high pressure (the applied pressure is higher than the operating pressure) before being used to make sure of flux stability during filtration and before measuring clean water flux. The modified fouling index (*MFI*) is used to achieve a linear relationship between concentration and flux decline. The modified fouling index (*MFI*) is given as

$$MFI = \frac{\eta_{20^{\circ}C}}{\eta_T}\frac{\Delta P}{210}\tan\alpha \qquad (7.44)$$

where α is the solute activity, and *MFI* is the modified fouling index (s/l²).

7.4.2 Fouling mechanisms

When foulant permeates through the membrane, fouling potential increases. Additionally, fouling increases if the interaction between the foulants and the membrane overcome the electrostatic repulsion between the membrane and the foulants. For laminar conditions, the pure water flux for tortuous porous membrane is given as

$$J = \frac{\Delta P}{\eta R_M} \qquad (7.45)$$

where η is the dynamic solvent viscosity, ΔP is the trans-membrane pressure difference, and R_M is the clean membrane resistance. A fouled membrane resistance consists of several types of resistances such as (R_{cp}), which is the concentration polarisation resistance, (R_A), which is the resistance due to adsorption, (R_G), which is the gel layer resistance, (R_p), which is the internal pore fouling resistance and (R_c), which is the cake formation resistance. Then the flux for a fouled membrane is given as

$$J = \frac{\Delta P}{\eta\left(R_M + R_{cp} + R_A + R_G + R_p + R_c\right)} \qquad (7.46)$$

When small molecules exist in the solution, they can develop osmotic pressure at the boundary layer. Then the flux is written as

$$J = \frac{\Delta P - \Delta \pi}{\eta R_M} \qquad (7.47)$$

where $\Delta\pi$ is the osmotic pressure difference across the membrane.

7.4.2.1 Concentration polarisation

Concentration polarisation is defined as the accumulation of the solute in the boundary layer; as a result, the solute concentration in the boundary layer is higher than its concentration in the bulk solution. The solute is transported into the boundary layer by convection and back to the bulk solution by diffusion. The flux in nanofiltration membrane decreases because of concentration polarisation, where concentration polarisation increases osmotic pressure and causes gel layer to form because of retained particles. See Figure 7-2.

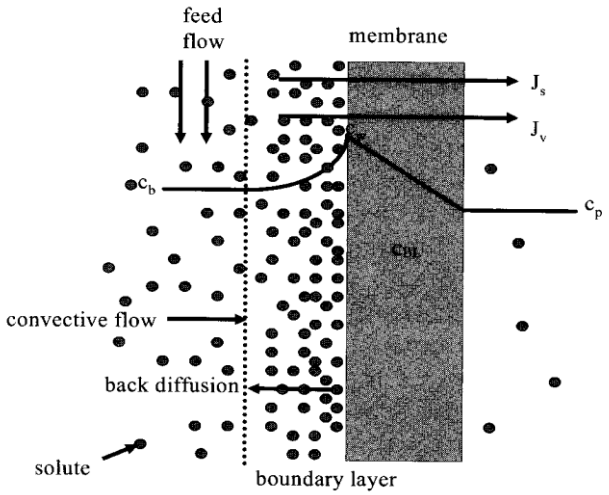

Figure 7-2. Concentration polarisation, (ref. 7).

The mass conservation for the boundary layer at the membrane surface is given as

$$-Jc_p + Jc_f + D_s \frac{dc_{BL}}{dx} = 0 \qquad (7.48)$$

where c_f is the solute concentration in the feed, D_s is the solute diffusivity, c_{BL} is the solute concentration in the boundary layer, x is the distance from the membrane layer, and c_p is the solute concentration in permeate. Integrating equation (7.48) over the following boundary

$$c = c_W \rightarrow x = 0$$
$$c = c_b \rightarrow x = \delta$$

where c_w is the solute concentration at the membrane/water (solvent) interface, c_b is the solute concentration in the bulk concentration and δ is the boundary layer thickness, gives

$$J = k_s \ln \frac{(c_W - c_p)}{(c_b - c_p)} \qquad (7.49\text{-a})$$

where k_s is the solute mass transfer coefficient, and it is given as follows

$$k_s = \frac{D_s}{\delta} \qquad (7.49\text{-b})$$

Concentration polarisation can be decreased by increasing the turbulence at the feed side; for example, by using cross-flow. When concentration polarisation occurs, it affects the membrane performance and the observed retention (R_{OBS}) is given as follows

$$R_{OBS} = \left(1 - \frac{c_p}{c_b}\right) \times 100\% \qquad (7.50)$$

The observed retention does not give the exact membrane characteristics because the real retention is higher due to the increased wall concentration (c_W) at the membrane surface. The real retention (R_O) is given as

$$R_O = \left(1 - \frac{c_p}{c_W}\right) \times 100\% \qquad (7.51)$$

The relation between the real and the observed retention is given as

$$\ln\left(\frac{1 - R_{OBS}}{R_{OBS}}\right) = \ln\left(\frac{1 - R_O}{R_O}\right) + \frac{J}{k_W} \qquad (7.52)$$

where J is the water flux (solvent), and k_W is the solvent mass transfer coefficient that depends on Reynolds number. Concentration polarisation is a reversible process and contributes to other fouling problems such as solute adsorption, solute precipitation and gel layer formation. Concentration polarisation is controlled by increasing cross-flow velocity,

permeate pulsing, ultrasound or electric field. The osmotic pressure is affected by concentration polarisation, where the increase in organic and inorganic solutes concentration at the membrane surface increases osmotic pressure and as a result, the effective pressure decreases and the solvent flux decreases. The osmotic pressure of an inorganic solute ($\Delta \pi_{INORG}$) is given as

$$\Delta\pi_{INORG} = \sum j_i \frac{n_i}{V_i} RT \qquad (7.53)$$

where j_i is the factor mole increase due to dissociation for solute (i), n is the number of moles, R is the ideal gas constant and T is the absolute temperature. The osmotic pressure of an organic solute ($\Delta \pi_{ORG}$) is given as follows

$$\Delta\pi_{ORG} = A_1 c + A_2 c^2 + A_2 c^3 \qquad (7.54\text{-a})$$

$$A_1 = \frac{RT}{M} \qquad (7.54\text{-b})$$

where A_i is the viral coefficient and M is the average molar mass of organic/polymer. Concentration polarisation degree can be expressed by the polarisation modulus (M) as follows

$$M = \frac{c_w}{c_b} = \exp\left(\frac{J}{k}\right) \qquad (7.55)$$

where J is the flux and k is the mass transfer coefficient. The concentration polarisation modulus is the relation between the increase in the membrane surface concentration relative to the bulk solution. Fouling increases as the concentration polarisation modulus increases.

7.4.2.2 Adsorption

Adsorption occurs at the membrane surface and in the membrane pores. The partitioning coefficient (K) between the membrane and the bulk solution is used to measure the adsorption, thus the partitioning coefficient is given as

$$K = \frac{\Gamma}{Mc} \qquad (7.56)$$

where Γ is the adsorbed quantity of organic material (μg/m²), M is the molar mass of the adsorbing compound (g/mol) and c is the equilibrium concentration of the solute in the solution (mmol/l). The mass balance can be used to measure the adsorbed amount by the membrane as follows

$$c_f V_f = A\Gamma + V_p \sum_1^n c_{pi} + c_c V_c \qquad (7.57)$$

where A is the membrane area (cm²), Γ is the amount of solute adsorbed per surface area (ng/cm²), n is the number of permeate samples, c_f is the feed solute concentration, c_p is the solute concentration in the permeate, c_c is the concentrate solute concentration, V_f is the feed volume, V_p is the permeate volume and V_c is the concentrate volume.

7.4.2.3 Gel layer

As the concentration at the membrane wall increases and exceeds the organic solute solubility, the organic solute precipitates on the membrane surface and forms a gel layer. When a steady state flux reaches the limiting value, where the flux does not increase as the pressure increases, the solute solubility limit is reached and a gel layer is formed. The limiting flux is given as

$$J_{\lim} = k_s \ln \frac{c_G}{c_b} \qquad (7.58)$$

where c_G is the gel layer concentration. The concentration in the boundary layer cannot increase beyond the gel layer concentration (c_G).

7.4.2.4 Cake formation

Cake formation depends on the membrane pore to the particle size ratio. If the solute diameter is less than the pore diameter, the solute deposits on the pore walls, thus the flux decreases, (refs. 73). If the solute diameter is nearly similar to the membrane pore diameter, the solute blocks the membrane pore; as a result, the membrane porosity and the flux decreases. If the solute diameter is bigger than the membrane pore diameter, the solute retains because of the sieving mechanism, and a cake forms on the membrane surface.

7.4.2.5 Critical flux and operating conditions

The critical flux is the limiting flux, where below its value the flux does not decline with time. The critical flux is divided into weak and strong critical fluxes. The strong critical flux is the point where the actual flux deviates from the clean water flux. The weak critical flux is the point where the flux increase with pressure is not linear. The critical flux increases with cross-flow velocity. The increase in the solute concentration decreases the critical flux. In this work, the critical flux was considered as an important parameter. Where the critical flux was used as an indicator to know if fouling took place during the experimental procedure, this would be discussed in more details in chapter 9 about the different experimental procedures that can be used - and the used one - to try to find the critical flux.

7.4.3 Organic fouling

Organic fouling causes irreversible flux decline because of adsorption and desorption of organic material on the membrane. Organic fouling occurs in different shapes such as adsorption of molecules, adsorption as a mono-layer, gel formation on the membrane surface, cake formation by organic colloids, deposition of organic colloids on the membrane and pore blocking. Organic fouling depends on the organic material type and its chemical characteristics. Organic materials may cause fouling in different ways such as depositing on the membrane or being absorbed by the membrane, thus causing change in the flux and the fouling behaviour. The organic materials that cause organic fouling can be a nutrient source for microorganisms causing bio-fouling. In addition, organic materials can be absorbed into the colloidal, causing them to stabilise and become harder to be removed by the pre-treatment process. Adsorption of organic materials can cause fouling or be a reason for another type of fouling. Adsorption of organic materials affects the membrane surface characteristics, thus result changes the flux through the membrane. Adsorption depends on the membrane pore size, the molecular size and shape, and the solution chemistry. Organic materials cause pore blocking, which depends on the molecular and pore size. Small molecules that pass through the membrane pores and adsorbed by the membrane pore walls causes pore narrowing. As a result, the flux declines due to pore blocking and narrowing by organic materials. If the solution contains organic materials with salt (especially cations), it causes fouling because the organic materials and the cations forms complexes that coagulate or precipitate forming a gel layer. Moreover, cations cause intermolecular bridging between the organic materials and the membrane.

7.4.4 Scaling

Scaling occurs when the solute concentration exceeds its solubility limit; as a result, the solute precipitate on the membrane in a form of a hard scale. Scaling decreases the flux and reduces the membrane lifetime. Scaling in nanofiltration membrane depends on the salt concentration in the concentrate, pH, temperature, velocity, time, ionic strength, super-saturation ratio, membrane surface roughness, substrate material, membrane material and membrane module type. Scaling in nanofiltration mostly occurs at the concentrate stream because of the high solute concentration, (refs. 7, 116). As the solution permeates through nanofiltration membrane, the concentration of rejected solutes at the boundary layer increases more than in the bulk solution, thus super-saturation increases in the boundary layer and scaling risk increases. Scaling increases as the permeate flux increases and the flow velocity decreases. The concentration polarisation factor in the boundary layer is given as

$$CPF = \exp\left(K_i y\right) \qquad (7.59)$$

where K is the semi-empirical constant that depends on the permeate flux and ion diffusivity, and y is the permeate recovery fraction. The common scalants that cause scaling in nanofiltration membrane are calcium sulphate ($CaSO_4$), which precipitate as gypsum ($CaSO_4.2H_2O$), calcium carbonate ($CaCO_3$), which forms dense and extremely adherent deposits (it cause a major problem in nanofiltration membrane), barium sulphate ($BaSO_4$), strontium sulphate ($SrSO_4$), silica, which is a big problem for nanofiltration membrane because its scaling cleaning is expensive, and calcium phosphate.

7.4.5 Colloidal and particle fouling

Flux and permeate retention decreases because of accumulated and retained colloidal and particulates on the membrane surface. Colloidal particles are suspended particles of the size ranging between few nanometers to few micrometers. Colloidal foulants include inorganic materials such as silica, organic materials such as synthetic organics, and biological materials such as bacteria maters. Nanofiltration membrane properties contribute to the colloidal fouling, where nanofiltration membrane with high hydraulic resistance enables a colloidal cake layer to form before fouling is detected.

7.4.6 Bio-fouling

Bio-fouling is caused by microbial organisms where they grow and form microbial bio-films

at the membrane surface. Bio-fouling causes blockage of pores, modules collapse and cause the biodegradation of nanofiltration membrane, (refs. 49, 113). Microbes are transported toward the membrane by passive diffusion, gravitational settling or active movement. Bio-fouling starts by the adhesion of organisms to the membrane surface; the rate of microbial deposition on the membrane depends on the fluid theological properties. When microorganisms are attached to the membrane surface, they start to grow. Microorganisms keep growing and building more bio-films, forming microclines where a cohesive layer of glycocalyx holds microorganisms together. Bio-film in membranes can be detected by comparing the cell counts in the inlet and outlet streams. Furthermore, when comparing the feed solution and the retentate solution samples for cluster of microorganisms sloughed, if the cluster of microorganisms sloughed was found in the retentate and none was found in the feed, this means there is bio-film formed inside the membrane or on the membrane surface. In addition, scanning electron microscopy can be used to detect bio films by analysing the membrane space surfaces. Flux declines strongly when colonisation and bio film starts, but after a period of time, flux decline becomes slower because of the equilibrium between bio-film growth and removal.

7.4.7 Fouling prevention and cleaning

Fouling can be reduced in nanofiltration membrane by using pre-treatment processes such as settling the matter until a free particle feed is achieved. Biocides and chlorine pre-treatment are used to avoid bio-fouling. Microfiltration and ultrafiltration membranes can be used as a pre-treatment process for nanofiltration membrane. Nanofiltration membrane can be modified to avoid fouling such as producing a more resistant membrane, more hydrophilic or a membrane with a higher fixed charge. The disadvantage of membrane modification is that the modifying materials take space inside the membrane, thus the membrane flux decreases. Fouling in nanofiltration membrane can be removed by physical and chemical cleaning methods. Physical cleaning includes back flush, forward flush, reverse flush, scrubbing, air sparge, carbon dioxide (CO_2) back permeation, vibrations and sonication. In chemical cleaning, bonds and adhesion forces between nanofiltration membrane and foulants are broken down by a chemical reaction. Cleaning depends on the membrane and foulants. Alkaline cleaning is used to remove organic foulants from membrane surface and pores. Acid cleaning is used to remove scaling (precipitated salts) from the membrane surface and pores. Enzymatic cleaning is used to clean bio-fouling and polysaccharides foulants. Enzymes are

used when the pH is neutral, and care must be taken to prevent the enzyme from attacking the membrane. Cleaning processes depend on the foulant type and the membrane tolerance toward the cleaning method. The cleaning process recovery can be determined by measuring the flux for clean water before and after filtration, and after the cleaning process. The flux is measured to find if it is recovered and returned to its original value. The water flux recovery (*WFR*) is given as follows

$$WFR = \frac{J_c}{J_o} \tag{7.60}$$

where J_c is the flux after cleaning and J_o is the original flux of the unfouled membrane. The clean water flux recovery (*CWFR*) through the membrane is given as follows

$$CWFR = \frac{J_o}{J_c} \tag{7.61}$$

Cleaning effectiveness can be determined by investigating the cleaning solution by measuring its pH, turbidity, colour, total solids (TS) and cations amount. Comparing the amount of particles removed by the cleaning solution to the amount remaining in the membrane gives information about the cleaning process efficiency and foulants reversibility. Cleaning process efficiency increases by increasing the temperature but it's restricted to the membrane tolerance toward the heat. Nanofiltration membranes can be cleaned at temperatures equal to 50 ℃, if it can tolerate it. High temperature is good to enhance foulants as the heat removes sensitive microbes. During the cleaning process, high pressure is not used because it causes foulants to move deeper inside the membrane and compact at the membrane walls, which is true for open nanofiltration membrane.

7.5 Summary

In this chapter, nanofiltration membrane was discussed in more detail such as the effect of the membrane charge on ions rejection, the effect of the solute interaction with the membrane material and with other solutes on their rejection, fouling mechanisms and the effect of membrane type on ions rejection. Nanofiltration membranes were divided into polymeric and ceramic membranes. Ceramic nanofiltration membrane was used in this work because it has more advantages over polymeric membranes. In addition, characterisation methods that are

used in characterising nanofiltration membrane and the chemical reactions that affect the rejection were discussed. The chemical reactions were considered in this work in-order to try to understand and justify the rejection behaviour of nanofiltration membrane (see chapter 8). In addition, the separation theory for charged and uncharged molecules was discussed, which would be explained in more detail for charged solutes in chapter 9.

Chapter 8 Experiments

Nanofiltration membranes can be classified into two major groups, which are polymeric and ceramic nanofiltration membranes**.** Ceramic nanofiltration membrane was used in this work because it has more advantages over the polymeric nanofiltration membranes. At the begging of this work, polymeric flat sheet nanofiltration membranes were used, but there were several difficulties and disadvantages in using them related to the membrane and the membrane rig, which resulted in switching over to ceramic nanofiltration membranes. For example, in some cases distilled water did not permeate through the polymeric nanofiltration membrane under several TMP values. In addition, the membrane rig used to bend as the TMP was increased which was a disadvantage; because high TMP values were needed to obtain solution permeation through the membrane and cause ions rejection. In this chapter several methods where used to characterise the ceramic nanofiltration membrane such as determining the membrane critical flux, the membrane ions rejection, the membrane fixed charge and the membrane active layer physical properties. The used methods in characterising nanofiltration membrane such as the critical flux methods, the types of ceramic nanofiltration membranes, which were used in the experiments, and the results obtained by using them are discussed in details through this chapter.

8.1 Methods

One way of characterising nanofiltration membrane is by determining its critical flux. The critical flux is the flux where below it no decrease in the flux with time occurs, and above it fouling can be observed. There are two forms of the critical flux: the strong critical flux and the weak critical flux. The strong critical flux is the flux where TMP starts to deviate from the distilled water flux, and the membrane resistance for the solution and distilled water is the same. The weak critical flux is the flux where all of its values are lower than that of the distilled water flux, where the membrane resistance for the solution is different from that of the distilled water, and the membrane resistance changes with the increasing flux after the critical flux is reached. See Figure 8-1. When distilled water permeates through the membrane, the permeate flux is linearly proportional to the trans-membrane pressure (TMP). On the other hand, when a solution permeates through the membrane, the relation between the permeate flux and the TMP is not linearly proportional. As a result, the critical flux is the flux where the TMP deviates from the distilled water flux or it is the flux at which irreversible fouling occurs. The critical flux overcomes the particle’s repulsion and causes the

particles to coagulate on the membrane surface. (refs. 17, 24, 25, 30, 47, 60, 66, 72, 86, 94, 96, 97, 121, 130, 131, 187, 198, 210, 212, 248, 256, 257, 289, 339).

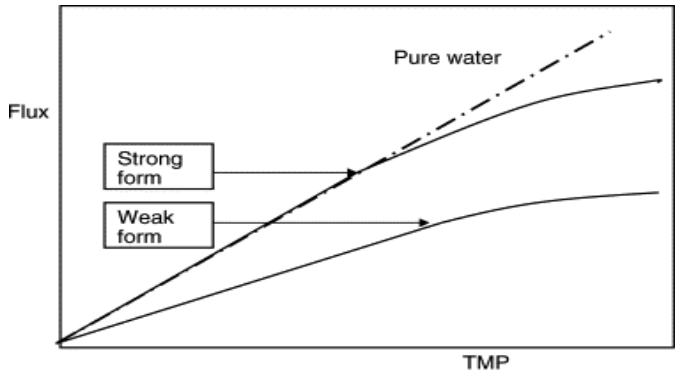

Figure 8-1. The strong and the weak critical flux, (ref. 3).

Critical flux should be differentiated from the limiting flux. The limiting flux is known as the maximum flux that can be reached by increasing the TMP. As a result, the flux value would not increase by increasing the TMP above the limiting value. In addition, the limiting flux is also known as the maximum flux were no fouling occurs. The critical flux increases with the increase in particle size and cross flow velocity, and decreases with the increase in concentration. The critical flux is measured in different ways, which are as follows

8.1.1 Flux-pressure observation

Flux and pressure can be used to measure the critical flux either by keeping the flux constant and changing the pressure, or by keeping the pressure constant and changing the flux. If the constant pressure method was used, the process does not depend on time and fouling is reduced because of the steady state flux. Using the constant pressure method gives an idea about the sustainability of the process. When the constant flux method is used, the fouling rate can be determined. In this method, fouling increases because of the increase in pressure with time. In the constant flux method, the pressure is changed for a specified pressure interval. Moreover, in the constant pressure method, the flux is changed for a specified flux interval. For the constant flux mode, the TMP should stay constant for each different flux and any increase in the TMP indicates that fouling has occurred. In the constant pressure mode, fouling is indicated by the flux decrease. For both methods, the critical flux is determined by plotting the flux versus TMP. The relation between the flux and the TMP is linear for distilled water; as a result, any deviation from the line means that fouling occurred and the relation becomes nonlinear. The point at which the behaviour becomes nonlinear is the

critical flux point. However, if the relation between the flux and the TMP is linear and the slope gradient is less than that of the distilled water, the critical flux is of the weak type.

In the pressure-step method, the flux is increased in step form and then decreased. The first step is to set the flux to be equal to J_1 and leave the process to reach the steady state condition; the TMP is then recorded and set to be equal to TMP_1. The second step is to increase the flux to be equal to J_2 until it reaches the steady state condition. The flux is then decreased to its initial value J_1, and the TMP value is recorded as $TMP`_1$. The difference between $TMP_1$ and $TMP`_1$ is called the deviation. If the deviation is equal to zero, fouling did not occur. Then the flux is increased to J_2, and left to reach a steady state condition, thus the TMP is recorded as TMP_2. After this, the flux is increased to J_3 and left to reach the steady state condition, and then decreased to J_2. After the flux is decreased to J_2 value, the TMP is recorded as $TMP`_2$. If the difference between $TMP_2$ and $TMP`_2$ was equal to zero, fouling did not take place. The above procedure is followed until a deviation is reached and the critical flux point is determined. Irreversible fouling can be determined by the pressure-step method. For example, if the flux is increased by two steps and decreased by one step (as mentioned earlier) and measuring the TMP at each step, if the flux does not return back to its original value after increasing and decreasing the flux, this means that irreversible fouling occurred. See Figure 8-2.

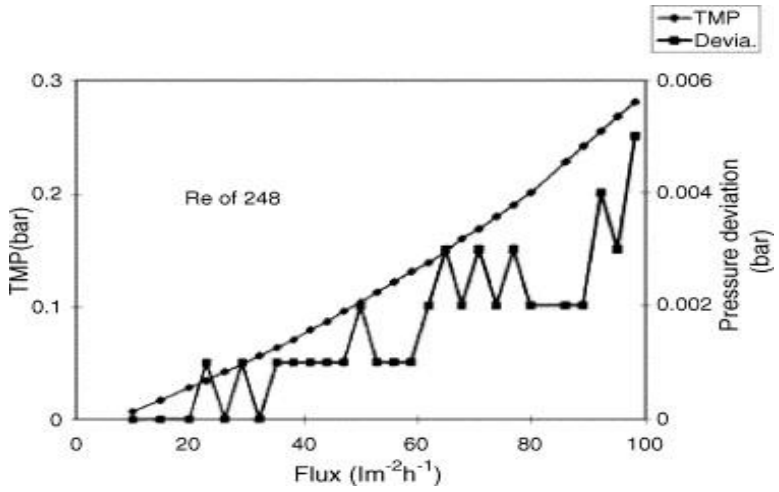

Figure 8-2. Critical flux determination by the pressure-step method, (ref. 3).

In the flux-step method, the change of TMP at constant fluxes is measured. In the first step, the process is run at constant flux J_1 for period of time t. For each step, both the initial and final TMP is recorded as TMP^1_i and TMP^1_f. In the second step, the flux value is increased to

J_2 and run for period of time t, and the initial and final TMP is recorded as TMP^2_i and TMP^2_f. See Figure 8-3. The previous procedure is repeated over different values of fluxes. The initial increase in TMP is given as

$$\Delta P_0 = TMP_i^{n+!} - TMP_f^n \qquad (8.1)$$

Moreover, the rate of increase in TMP is given as

$$\frac{dP}{dt} = \left(TMP_f^n - TMP_i^n\right)/\left(t_f^n - t_i^n\right) \qquad (8.2)$$

In addition, the average TMP is given as

$$P_{ave} = \left(TMP_f^n + TMP_i^n\right)/2 \qquad (8.3)$$

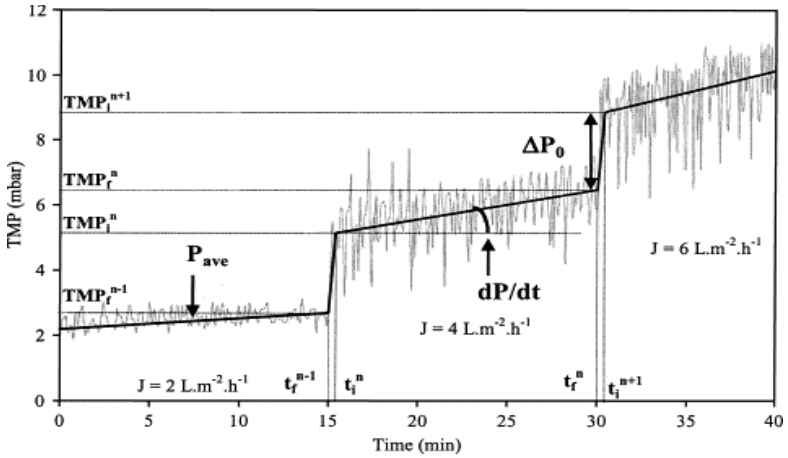

Figure 8-3. Critical flux determination by the flux-step method, (ref. 12).

Another method to measure the critical flux value is by comparing the pure distilled water permeate flux behavior to that of the solution permeate flux behavior. In this method, the inlet flux is kept constant for all of the different TMP. And the permeate flux is measured for distilled water and solution at each different TMP for a specific period of time. Then the permeate flux is plotted versus TMP and from the line deviation between the pure distilled water and the solution, the critical flux can be determined. This procedure was used as the main method in this work. In some experiments, the flux-step method was also used in order to compare the results with the method mentioned above and to see if there would be a difference between the two methods and if they had different impacts on salt separation. The pressure-step method was not used because it was hard to keep the TMP constant while

changing the flux. In order to keep the TMP constant, the permeate pressure had to be controlled but in this case was hard because the permeate volume was very small; as a result, it was hard to control the pressure by using a pump.

8.1.2 Mass balance

The critical flux can be determined by measuring the solute concentration in the inlet, outlet and permeate, where the rate of solute deposition on the membrane surface can be calculated from the permeate flux and concentration. The first step is to measure the adsorption rate of solute particles by the membrane, where the experiment is run at permeate flux equal to zero. The second step is to calculate the deposition rate at different permeate fluxes. The deposition rate can be calculated from the concentration logarithmic rate and adsorption rate (at permeate flux equal to zero). Where the deposition rate is given as

$$\textit{Deposition rate} = \textit{concentration logarithmic rate} - \textit{adsorption rate} \qquad (8.4)$$

The concentration logarithmic rate is given as the gradient A in the following equation:

$$Ln\left(\frac{C_t}{C_0}\right) = -At \qquad (8.5)$$

where C_O is the feed concentration at time 0, C_t is the feed concentration at time t, and t is the time. The third step is to plot the permeate flux versus deposition rate and from the graph the critical flux is determined. The critical flux is considered the flux at which deposition rate is equal to zero.

8.1.3 Membrane rejection

This work is concerned with the separation of ions from solution by using ceramic nanofiltration membrane. The rejection (R) of ion (i) is given as

$$R = 1 - \frac{C_{i,p}}{C_{i,f}} \qquad (8.6)$$

where $C_{i,p}$ is the concentration of ion (i) in the permeate (mol/m^3) and $C_{i,f}$ is the concentration of ion (i) in the feed (mol/m^3). The TMP was calculated as follows

$$TMP = \left(\frac{P_{inlet} + P_{outlet}}{2}\right) - P_{permeate} \quad (8.7)$$

Where the pressure at the permeate side was assumed to be equal to zero, and as a result the TMP would be as follows

$$TMP = \left(\frac{P_{inlet} + P_{outlet}}{2}\right) \quad (8.8)$$

8.2 Experimental selection

In the beginning of this work, polymer flat sheet nanofiltration membranes were used to try to understand the separation behaviour of ions from brackish water by using nanofiltration membrane. However, many obstacles were encountered during the experiments and the obtained results were not satisfactory. An example of the encountered obstacles was the bending of the membrane rig as the TMP pressure was increased even though the used TMP values were low and did not exceed 1.2 bar. In addition, the distilled water permeation through the membrane samples was not consistence. Thus, the membranes were changed to tubular ceramic nanofiltration membrane. The chosen membranes were TiO_2 ceramic nanofiltration membranes with 0.9 and 1.0 nm mean pore radius. To try to understand the separation behaviour of the ceramic nanofiltration membrane and the parameters that would affect the membrane rejection, thus several approaches and parameters were taken into consideration such as the ions valences, the ions type, the ions feed concentration, TMP values, the feed volumetric flux, the feed solution pH value and the membrane pore radius. At the beginning of this work, for both ceramic nanofiltration membranes with 0.9 and 1.0 nm mean pore radius and for different TMP values, the ions feed concentration, the ions types and the ions valencies were considered and their effect on the ions rejection were observed. Then for ceramic nanofiltration, membrane with 1.0 nm mean pore radius the effect of the feed solution pH on the ions rejection was studied. In addition, the effect of the feed solution volumetric flux at the lowest TMP value on the rejection of ions was studied. This approach was considered to try to find out what role would the electrical potential (in Nernst-Planck equation) play in the rejection of ions by ceramic nanofiltration. The pH parameter is known to have an effect on the membrane charge and consequently affects the ions rejection for that it was taken into consideration. The zeta potential for both membranes was measured in-order to find the membrane charge and under what conditions it would change because it is a very important parameter that would explain the ions rejection behaviour by ceramic nanofiltration

membrane. In addition, the membranes cross sectional pictures were taken to find the thickness of the membrane active layer. These variables are discussed in more details in the following sections. See figure 8-4.

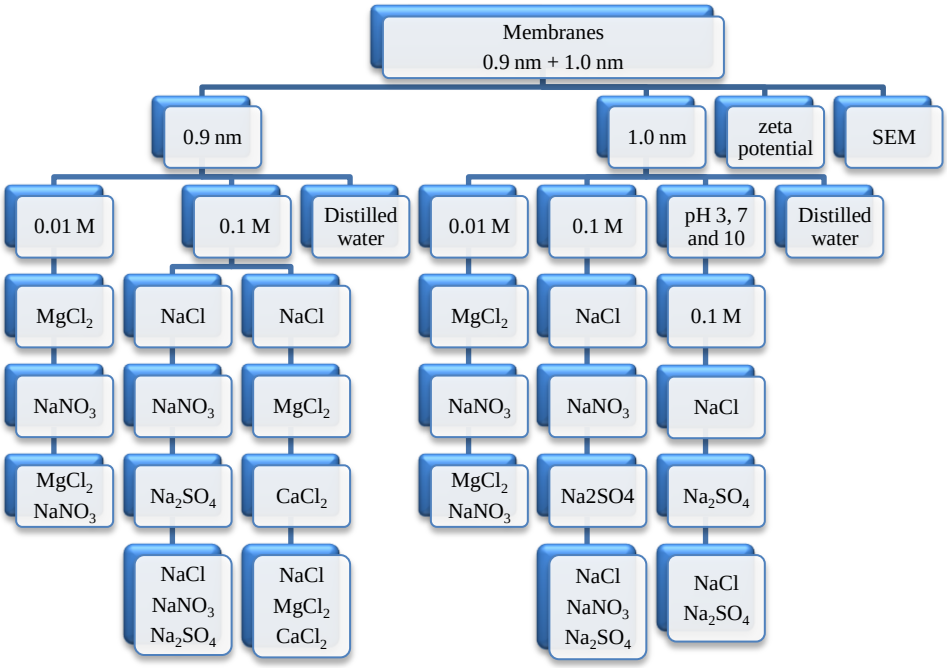

Figure 8-4. The experiments that were done during this work.

8.3 Zeta potential measurements

Two different procedures were used to measure the membrane zeta potential to find what factors affect the membrane zeta potential. In the first procedure, one salt was used to prepare two solutions with different concentrations. For each solution the pH was changed from 3 to 10 values. This was done in order to study the effect of pH and concentration on the membrane zeta potential. In the second procedure, four salts were used, where three different concentration solutions for each salt were prepared. This was done in order to study the effect of salt type and concentration on the membrane zeta potential.

8.3.1 Different pH values

In order to measure the membrane zeta potential, sodium chloride (NaCl) salt was used. Two solutions were prepared using NaCl at two different concentrations; the concentrations that were used were 0.01M and 0.1M. Then the pH of each solution was changed to different values ranging between 3 and 10. The pH of these two solutions was changed using 0.1M HCl solution and 0.1M NaOH solution. This was done in order to study the effect of pH and

concentration on membrane zeta potential. After preparing the solution, the crushed membrane was added to these solutions. For 0.01M concentration solution, the zeta potential decreased as the pH increased. See Figure 8-5. While for 0.1M concentration solution, the zeta potential did not have a specific trend but in general, but in general, the membrane zeta potential decreased as the pH increased. See Figure 8-6. From 0.01M solution, it was found that the membrane had an ISP around 9.3. From 0.1M solution, it was found that the membrane had three ISPs, which were 4.8, 5.5 and 8.2. These results were not accurate, which might be due to the impurities within the membrane that were not removed by cleaning the membrane only with distilled water. Thus to obtain more accurate results the crushed membrane was soaked in HCl solution to remove any type of impurities that would affect the ISP.

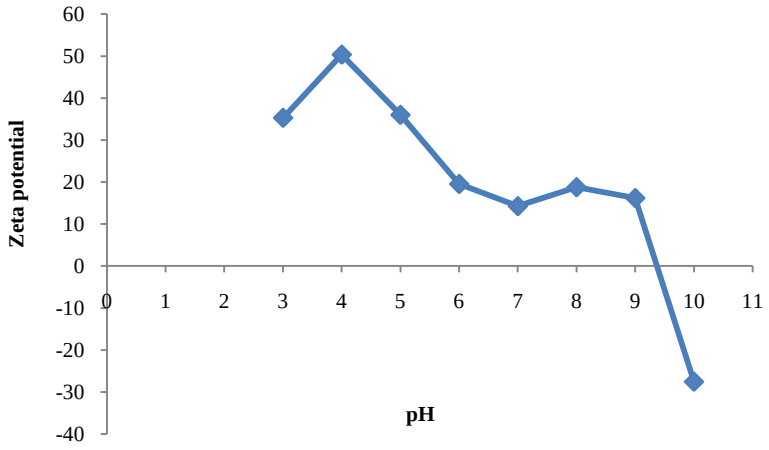

Figure 8-5. Zeta potential at 0.01M concentration.

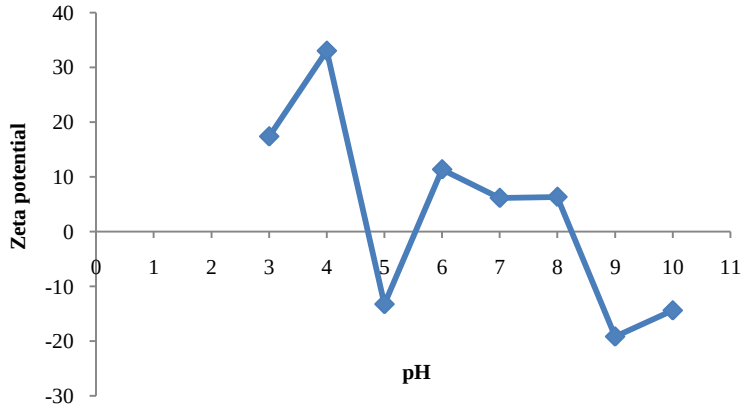

Figure 8-6. Zeta potential at 0.1M concentration.

The same procedure was followed, but before adding the membrane powder to the solutions mentioned above, the membrane powder was soaked in 0.1M HCl solution for 24 hours;

afterwards, the membrane powder was washed with distilled water until it had a neutral pH value. Then the membrane was added to 0.01M and 0.1M NaCl solutions. For 0.01M concentration solution, the zeta potential decreased as the pH increased, where the ISP was at pH 5. See Figure 8-7. While for 0.1M concentration solution, the membrane zeta potential decreased as the pH increased, and the ISP was at pH 4.6. See Figure 8-8. The higher the pH, the more negative the membrane zeta potential was. As the concentration increased, the ISP decreased. In addition, the zeta potential values were higher for 0.01M NaCl solution than 0.1M NaCl solution.

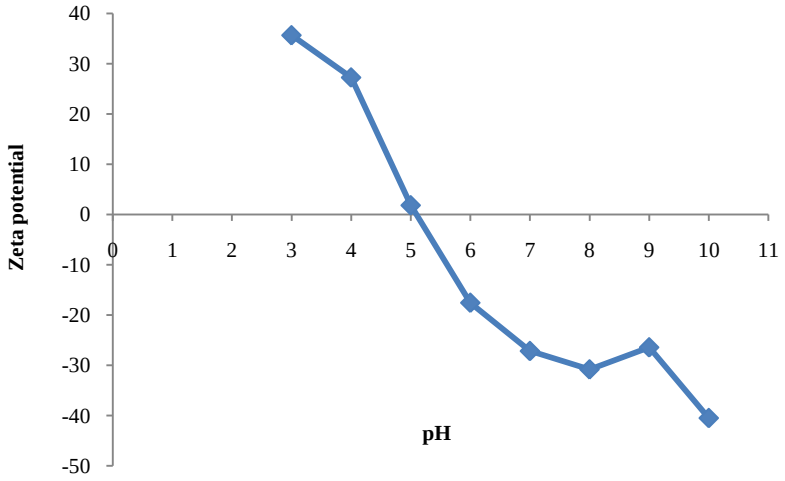

Figure 8-7. Zeta potential at 0.01M concentration.

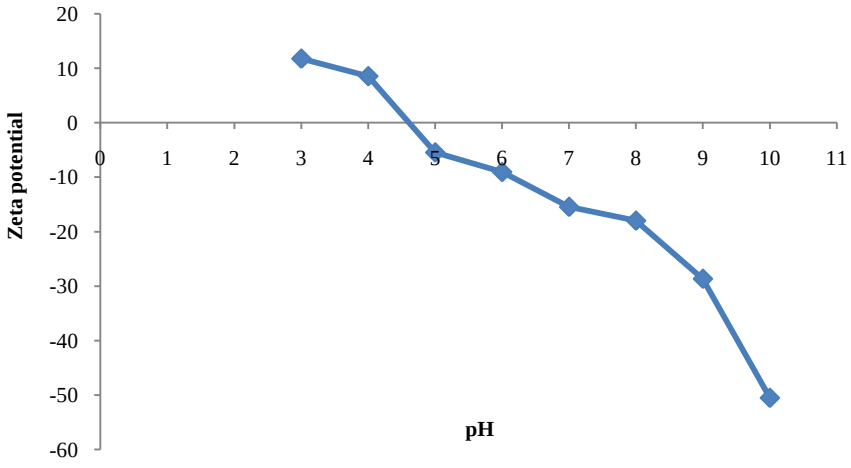

Figure 8-8. Zeta potential at 0.1M concentration.

8.3.2 Different salts at different concentration values

In order to measure the membrane zeta potential, four different salts were used in preparing

different solutions at three different concentrations. The salts that were used were sodium chloride (NaCl), magnesium chloride ($MgCl_2$), sodium nitrate ($NaNO_3$) and sodium sulphate (Na_2SO_4). Three different solutions of each salt were prepared at three different concentrations. The concentrations that were used are 0.01M, 0.1M and 1.0M. After preparing the solutions, the membrane was washed with distilled water then left to dry; afterwards, the membrane was crushed into a powder using crushing crucible. After crushing the membrane, the membrane powder was soaked in 0.1M HCl solution for 24 hours; afterwards, the membrane powder was washed with distilled water until it had a neutral pH value. Then the membrane powder was added to the prepared solutions and was left to settle down and the top layer of the solution was taken to measure its zeta potential. The membrane zeta potential was measured using a zeta-sizer device. The membrane had positive zeta potential values when $MgCl_2$ and NaNO3 solutions were used and negative values when Na_2SO_4 was used. However, when NaCl solution was used, the membrane had a negative zeta potential value for the 0.01M concentration solution, but positive zeta potential values for 0.1M and 1.0M solutions. See Figure 8-9. It was noticed that the membrane zeta potential is affected by salt type and the salt concentration.

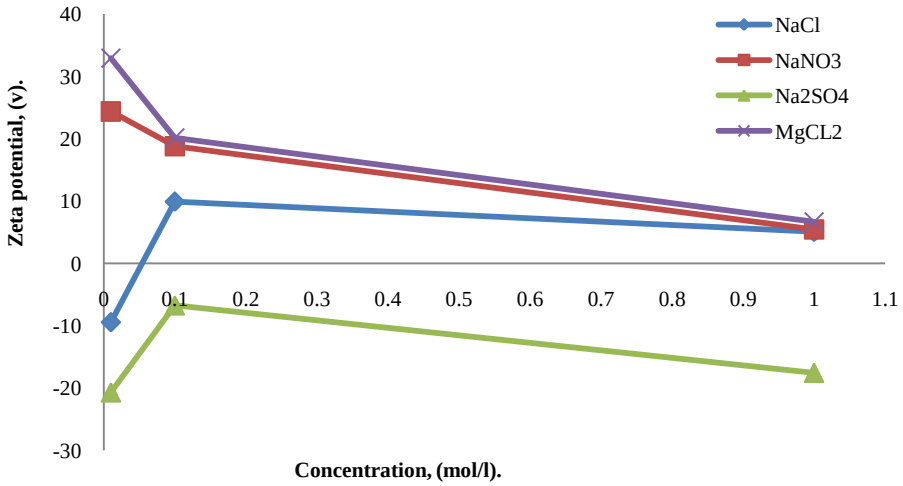

Figure 8-9. Zeta potential versus concentration for four different salts solutions.

8.4 SEM- EDXS pictures

Pictures for the membrane active layer and the membrane support layer for both the 0.9 and 1.0 nm nanofiltration membranes were taken. The device that was used to obtain these photos was SEM (FEI Quanta 200, Purge, Czech Republic) and EDXS equipment (EDXS, Amertek

Inc, Paoli, PA, USA). The pictures for the membrane active layer were taken at different scales. From these pictures, the membrane active layer thickness was measured which was used in the modelling of the Nernst-Planck equation, see chapter 9.

8.4.1 0.9nm membrane active layer and its supporting layer

The membrane active layer and the membrane support layer are shown in figure 8-10. The membrane support layer is identified in figure 8-11. See appendix 5.

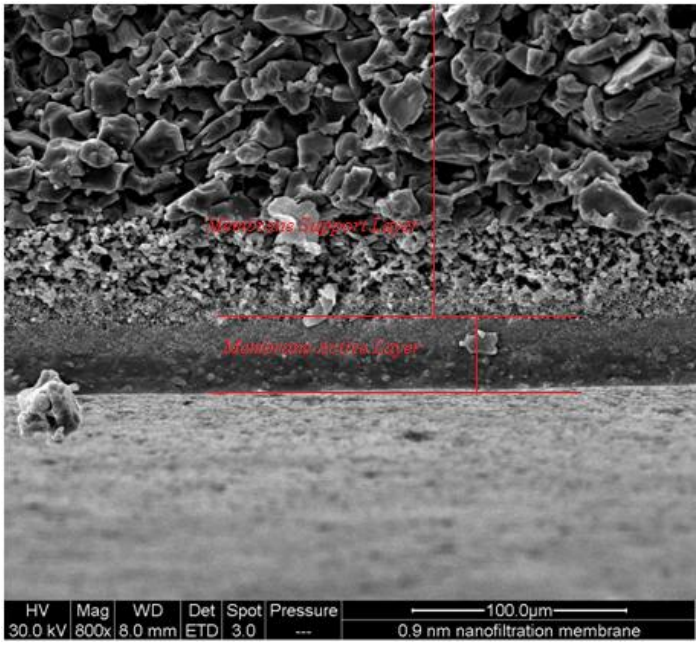

Figure 8-10. 0.9nm membrane at 100.0µm.

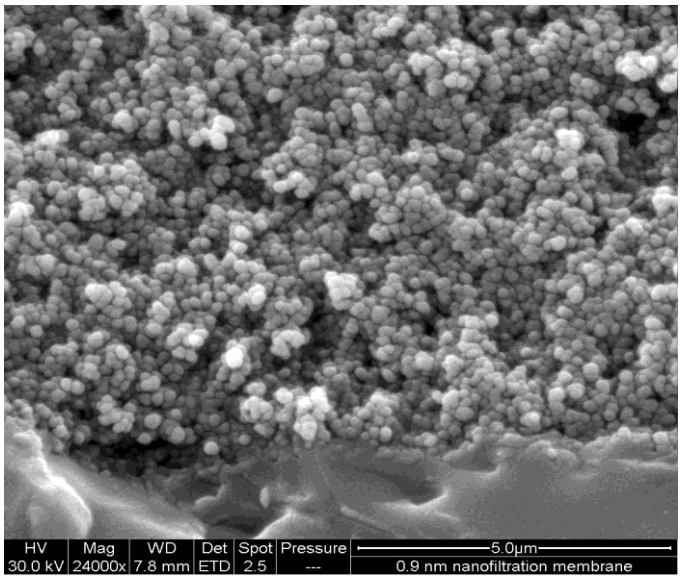

Figure 8-11. 0.9nm membrane at 5.0µm.

8.4.2 1.0nm membrane active layer and its supporting layer

The whole membrane, including the membrane active layer and the membrane support layer, is shown in figure 8-12. The membrane active layer appears more clearly, at two different scales, in figures 8-13 and 8-14. See appendix 6.

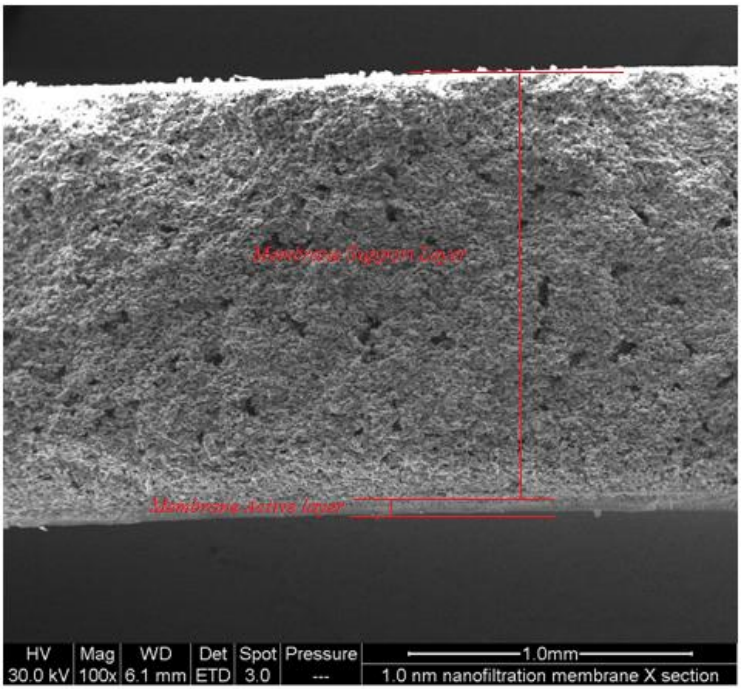

Figure 8-12. 1.0nm membrane at 1.0mm.

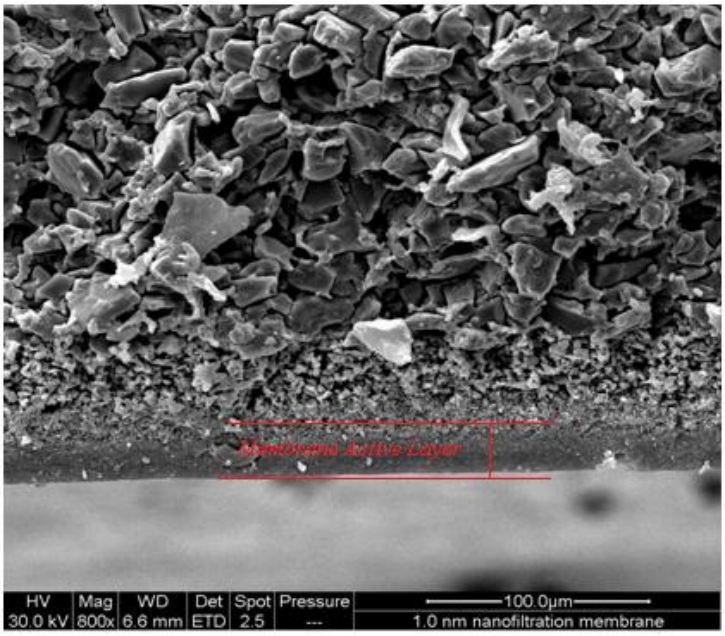

Figure 8-13. 1.0nm membrane at 100.0µm.

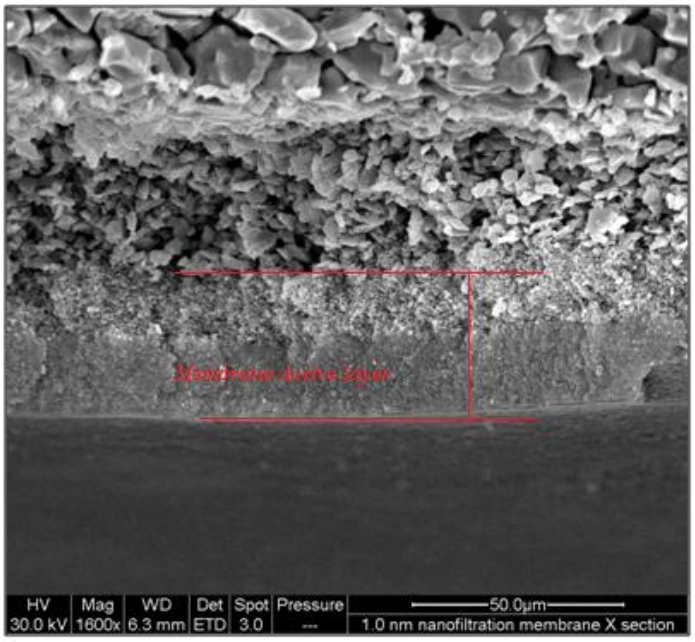

Figure 8-14. 1.0nm membrane at 50.0µm.

8.5 Ceramic membrane experiments

In this work, a tubular ceramic nanofiltration membrane was used (the membrane made of TiO_2, with 7.0 mm I.D, 10.0 mm O.D and length of 190 mm, with 0.9 and 1.0 nm mean pore radius, from inopor company); see Figure 8-15. It was used to desalinate water samples containing sodium chloride, sodium nitrate, sodium sulphate, magnesium chloride, and calcium chloride. The salt concentration value that was used is 0.1 M. To study the separation behaviour of the membrane, distilled water was used at first, and then distilled water with single or tertiary salt solution. The results of distilled and brackish water were compared to describe the separation behaviour and to find out if fouling took place. (refs. 44, 54, 97, 98, 104, 107, 125, 139, 154, 201, 240, 306, 312, 351).

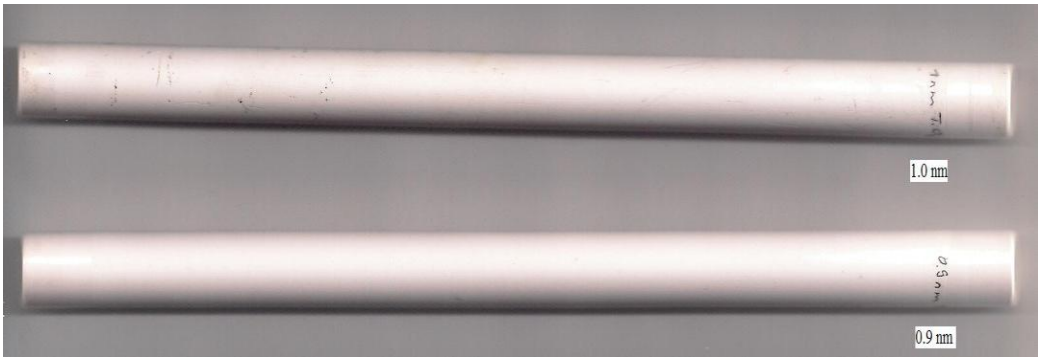

Figure 8-15. TiO_2 nanofiltration membrane with two different pore diameters.

The bench scale membrane rig is shown in Figure 8-16. The main components are a variable speed pristatic pump (type 603S, Watson-Marlow, UK), magnetic stirrer (RW20, IKAMAG, UK), glass container (10 l), tubular membrane module, pressure-relief valve, PVC-reinforced flexible piping, marprene flexible piping for the pump (Watson-Marlow, UK), flow-meter (Gemü Gebr Müller, Germany), pH/ORP controller (Oakton), Accumet pH/Ion/Conductivity Meter (Fisher Scientific, Model 50), balance and stop watch. The membrane module, which was used during the experiments, is shown in Figure 8-18. This module was constructed by Toshio Baldeón (ref. 313).

Figure 8-16. Bench scale of the NF membrane rig.

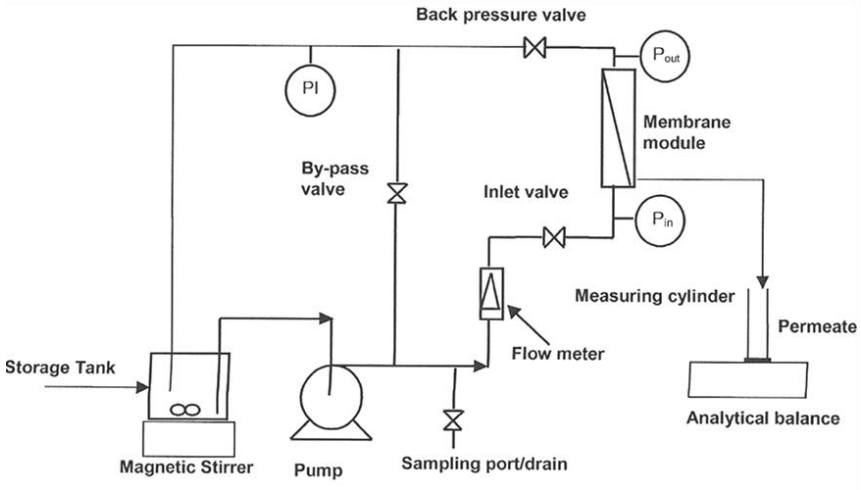

Figure 8-17. Schematic diagram of the tubular NF membrane rig, (ref. 242).

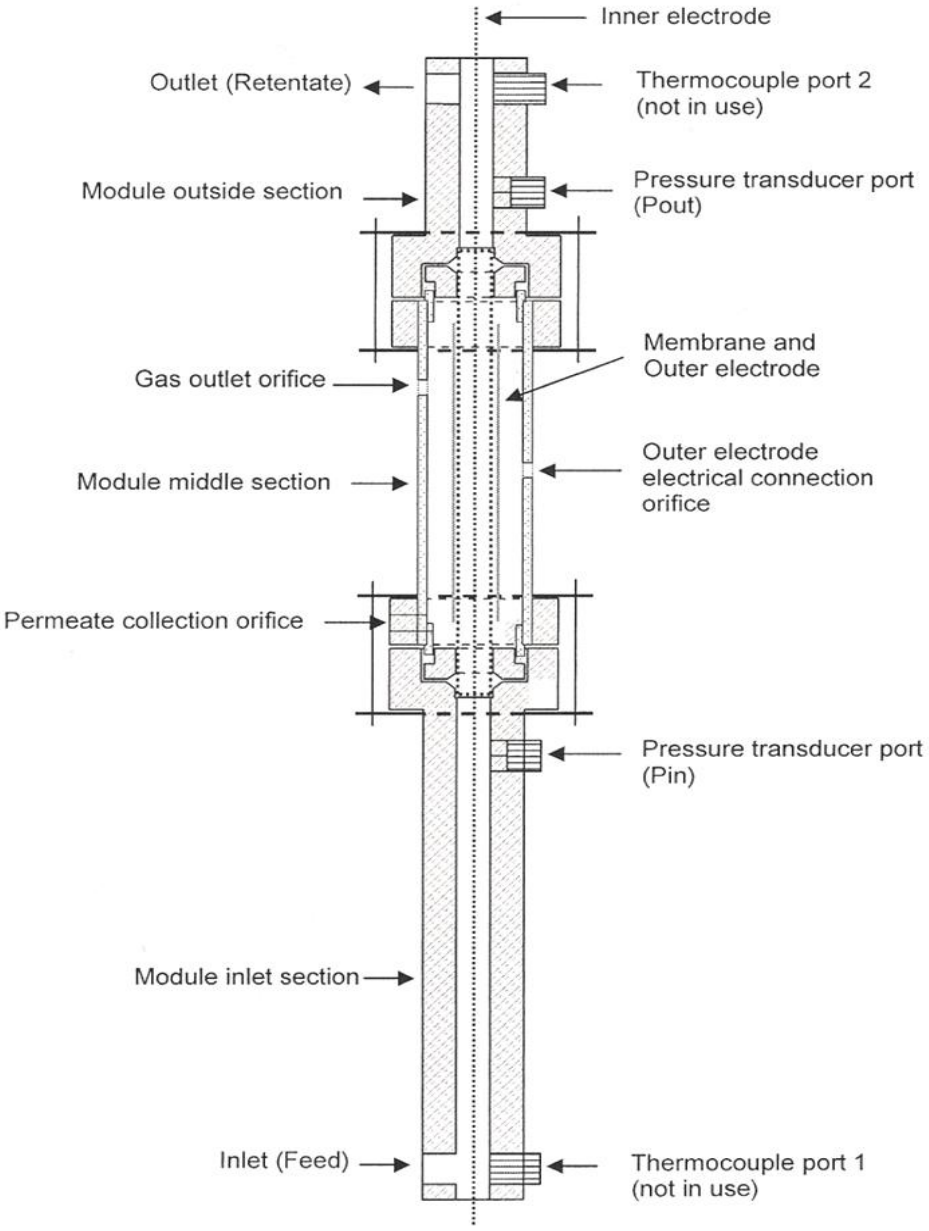

Figure 8-18. Schematic of tubular membrane module that was used in the experiments (refs. 242, 313).

8.5.1 Materials

The salts that were used in the experiments were sodium chloride (NaCl), sodium nitrate ($NaNO_3$), sodium sulphate (Na_2SO_4), magnesium chloride ($MgCl_2$) and calcium chloride ($CaCl_2$). All of these salts were obtained from Sigma-Aldrich. The chosen salts were with high purities as follows, NaNO3 ≥ 99%, NaCl ≥ 99.5%, Na_2SO_4 ≥ 99.99%, $MgCl_2$ ≥ 99.99% and $CaCl_2$ ≥ 99.99%. The solution pH was controlled using sodium hydroxide (NaOH ≥ 99.99%) and hydrochloric acid (HCl 5.0M), in addition NaOH was used in cleaning the membrane.

8.5.2 Experimental procedure

The same experimental procedure was followed for the two different sets of solutions for both 0.9 and 1.0nm membranes. At first, distilled water was used to permeate through 0.9 nm and 1.0 nm membranes at constant inlet volumetric flow rate equal to 3.056E-5 m^3/s (110 l/h), where the inlet pressure was increased from 0.3 bar to 2.0 bar, which gives TMP values between 0.2 bar to 1.9 bar. The pressure was increased at 0.2 intervals each 30 minutes. Permeates for both membranes were collected for 25 minutes. The pH and conductivity for each sample were measured to make sure that the process was stable and there was nothing affecting the process. The same procedure was followed for the brackish except that the inlet pressure was increased each 90 minutes for 0.9 nm membranes and 60 minutes for 1.0 nm membrane. For 0.9 nm membrane, the permeate sample was taken each 85 minutes and for 1.0 nm each permeate sample was taken each 55 minutes. After each experiment the membrane was cleaned as follows; at first the membrane was washed with distilled water several times to make sure that the ions from the solution were removed from the process, the checking was done by measuring the water conductivity from the outlet side and the permeate side. After that, the membrane was cleaned with 0.1M NaOH solution for 1 hour, and then the membrane was washed with distilled water several times until the ions were removed from the process. The final step was cleaning the membrane continuously for at least 18 hours with distilled water, and the process was checked to be cleaned and the ions were removed by measuring the water conductivity from the outlet side and the permeate side. After cleaning the membrane, a run for distilled water was done in-order to compare the permeation of the distilled water through the membrane before and after the permeation of a solution through the membrane. Such procedure can help in determining the type of permeate flux and if fouling took place during the experiment or not.

The ion concentration was measured by using ion chromatography and ICP-AES. The ion chromatography measured the anion's concentration and ICP-AES measured the cation concentration. Ion chromatography equipment is a Dionex DX600 Ion Chromatograph. The column is a Dionex AS4A-SC. The detector is a conductivity cell and the mobile phase is a mixture of $Na_2CO_3/NaHCO_3$. The ICP-AES samples are diluted and then acidified with nitric acid to approximately 3%HNO_3. The concentration of cations and anions were measured using the above equipments because the permeate sample volumes were too small for any alternative method such as titration.

8.5.3 First experimental set (first concentration)

Two different sets of solutions were used, where either the cation or the anion was the common ion. The salts that were used were sodium chloride (NaCl), sodium nitrate ($NaNO_3$), sodium sulphate (Na_2SO_4), magnesium chloride ($MgCl_2$), and calcium chloride ($CaCl_2$). The first set consisted of sodium chloride (NaCl), sodium nitrate ($NaNO_3$) and sodium sulphate (Na_2SO_4), while the second set consisted of sodium chloride (NaCl), magnesium chloride ($MgCl_2$), and calcium chloride ($CaCl_2$). At first, a single solution of each salt was prepared with 0.1M concentration. Then a mixed solution of the three salts was prepared at 0.1M concentration for each salt. Single and tertiary salt solutions were used to compare the effect of ion type and ion charge on separation.

8.5.3.1 0.9 nm membrane

8.5.3.1.1 Common cation

Sodium nitrate ($NaNO_3$) diluted in distilled water was the first solution to be used. $NaNO_3$ permeate flux (volume flux based on the membrane area) through the membrane increased from 6.5E-08 to 4.0E-07 $m^3/m^2/s$ as the TMP increased. It was found that the rejection of nitrate ions was slightly higher than the rejection of sodium ions. The highest rejection for both ions was at the lowest TMP, where the rejection of NO_3^{1-} was about 63% and the rejection of Na^{1+} was about 53%. When excluding the minimum TMP value, in general it can be noticed that the rejection of NO_3^{1-} remained almost constant as the TMP increased, while the rejection of Na^{1+} slightly increased as the TMP increased. In addition, the rejection for both ions had more negative values, which means that no rejection was taking place and the ions were passing through the membrane. See Figure 8-19. In addition, when comparing the permeation of distilled water through the membrane, before and after $NaNO_3$ solution permeation through the membrane, it was found that distilled water permeation was higher than $NaNO_3$ solution. This means that fouling did not occur or it was weak and did not have an effect on separation. The pH and conductivity of the inlet and retentate were measured. The conductivity of both solutions remained almost constant as the TMP increased, while the pH increased as the TMP increased. See Figures 8-20 and 8-21. The pH and the conductivity of the permeate were not measured because the permeate volume produced by the membrane was not enough to get a reading.

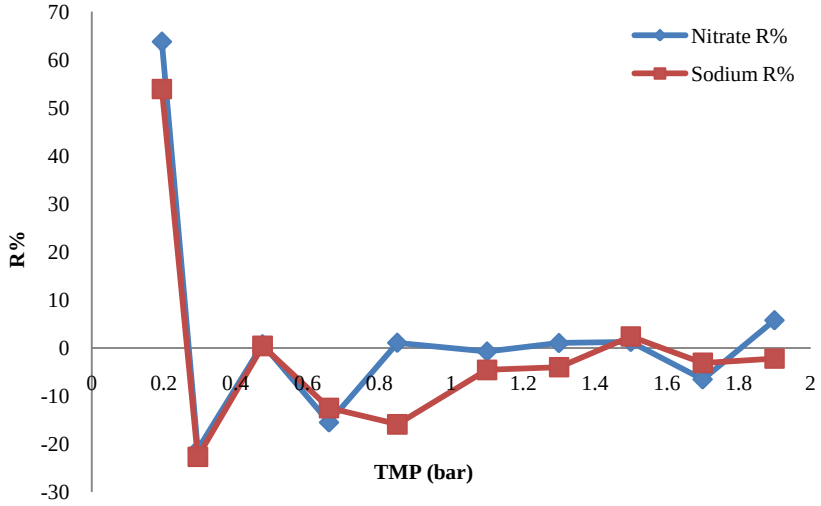

Figure 8-19. Sodium nitrate rejection versus TMP.

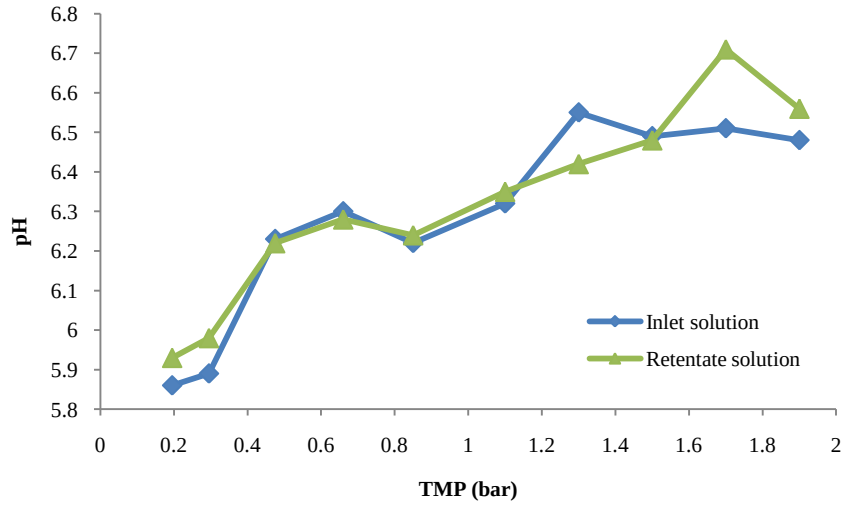

Figure 8-20. pH of sodium nitrate solution versus TMP.

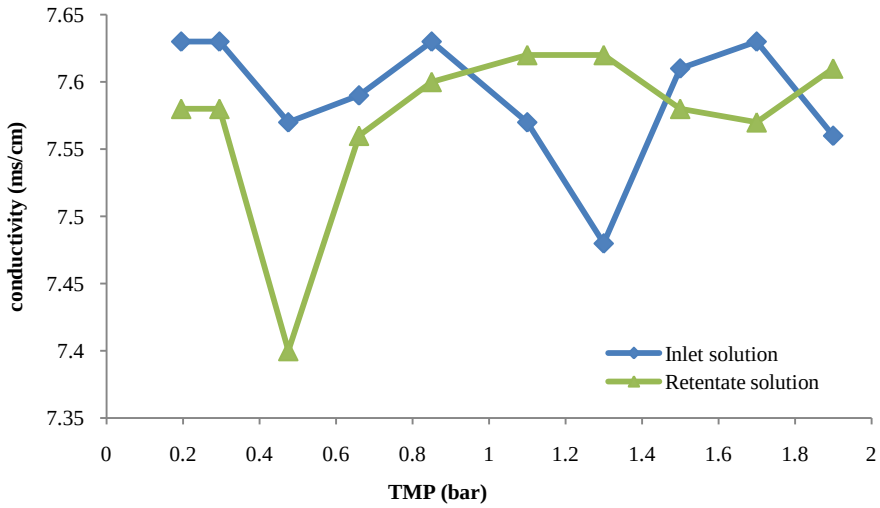

Figure 8-21. Conductivity of sodium nitrate solution versus TMP.

The second solution was prepared by diluting sodium sulphate (Na_2SO_4) in distilled water. Na_2SO_4 permeate flux (volume flux based on the membrane area) through the membrane increased from 2.8E-08 to 5.0E-07 $m^3/m^2/s$ as the TMP increased. It was found that the rejection of sulphate (SO_4^{2-}) ions was higher than the rejection of sodium (Na^{1+}) ions. Where the rejection of SO_4^{2-} ions almost remained constant at lower TMP, the SO_4^{2-} rejection started to increase as the TMP increased. See Figure 8-22. The highest rejection of SO_4^{2-} was about 31% at a TMP value equal to 1.9 bar. On the other hand, the Na^{1+} rejection did not have a specific trend. However, as the TMP reached 1.1 bar, the Na^{1+} rejection started to increase and almost stayed constant as the TMP passed 1.5 bar value. Na^{1+} had some negative rejection values, which means it passed freely through the membrane. The highest rejection of Na^{1+} was about 8% at a TMP value equal to 1.5 bar. When comparing the permeation of distilled water through the membrane, before and after the sodium sulphate (Na_2SO_4) solution permeation through the membrane, it was found that distilled water permeation was higher than the permeation of sodium sulphate (Na_2SO_4) solution. This means that fouling did not occur or was weak and did not have an effect on separation. The pH and conductivity of the inlet and retentate were measured. The pH of both solutions increased as the TMP increased. See Figure 8-23. The conductivity of both solutions was almost constant as TMP increased; then the conductivity increased when the TMP reached 0.9 bar and almost remained constant, and then decreased when TMP reached 1.5 bar and almost remained constant. See Figure 8-24. The pH and the conductivity of permeate were not measured because the permeate volume produced by the membrane were not enough to get a reading.

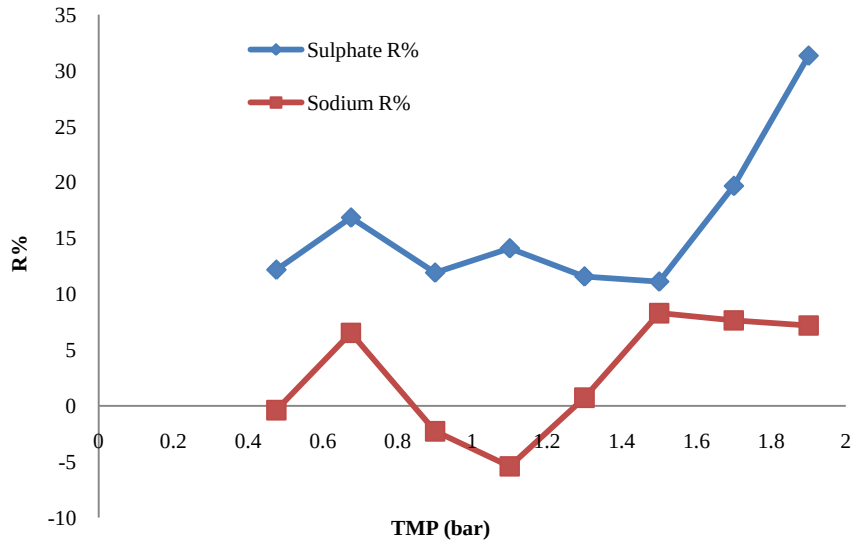

Figure 8-22. Sodium sulphate rejection versus TMP.

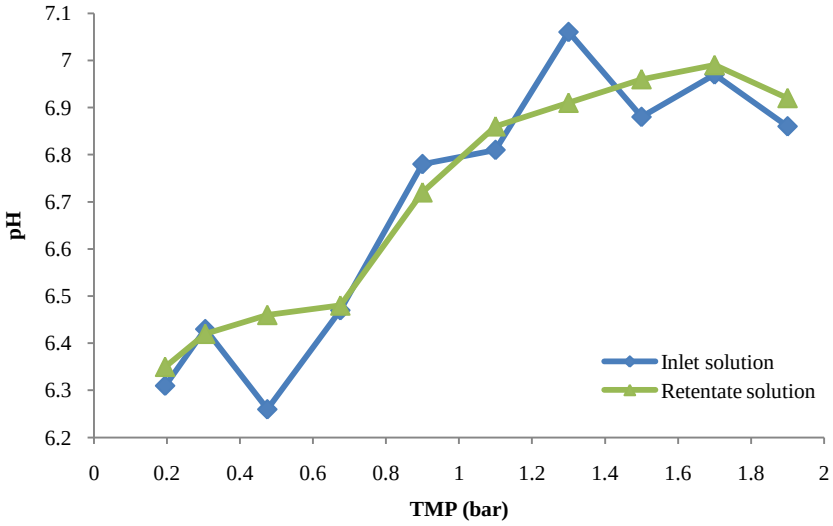

Figure 8-23. pH of sodium sulphate solution versus TMP.

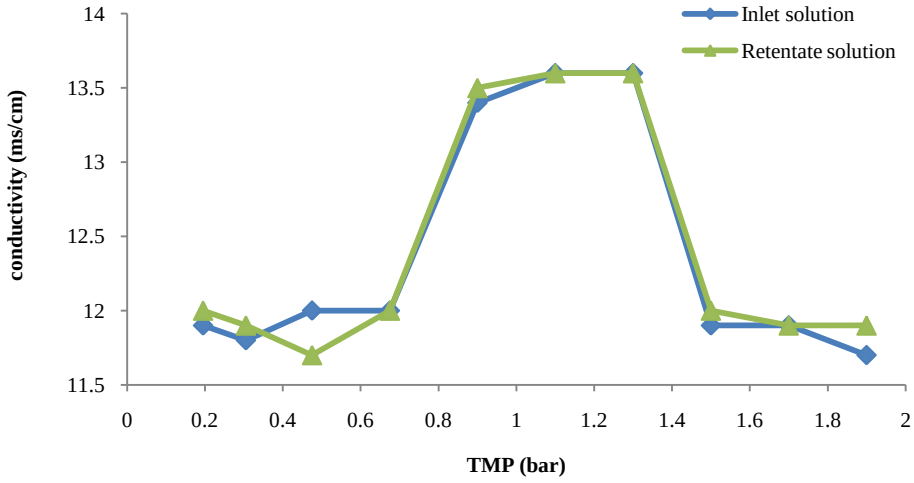

Figure 8-24. Conductivity of sodium sulphate solution versus TMP.

The third solution was prepared by diluting sodium chloride (NaCl) in distilled water. NaCl permeate flux (volume flux based on the membrane area) through the membrane increased from 1.6E-08 to 9.7E-07 $m^3/m^2/s$ as the TMP increased. It was found that the rejection of chloride (Cl^{1-}) ions was higher than the rejection of sodium (Na^{1+}) ions, where the rejection of Cl^{1-} ions increased as the TMP increased. See Figure 8-25. The highest rejection of Cl^{1-} was about 22% at a TMP value equal to 1.9 bar. On the other hand, the Na^{1+} rejection increased as TMP increased, but decreased as TMP reached 1.5bar. In general, Na^{1+} had negative rejection values, which means it passed freely through the membrane. The highest rejection of Na^{1+} was about 8% at a TMP value equal to 1.5 bar. When comparing the permeation of distilled water through the membrane, before and after the sodium chloride

(NaCl) solution permeation through the membrane, it was found that distilled water permeation was higher than that of the sodium chloride (NaCl) solution. This means that fouling did not occur or was weak and did not have an effect on separation. The pH and conductivity of the inlet and retentate solutions were measured. The pH of both solutions increased as the TMP increased. See Figure 8-26. The conductivity of the inlet solution was almost constant as TMP increased, while the conductivity of retentate solution remained constant until TMP reached 0.675 bar where it decreased, but increased when the TMP reached 1.5 bar; thus after this point, the conductivity decreased. See Figure 8-27. The pH and conductivity of permeate were not measured because the permeate volume produced by the membrane were not enough to get a reading.

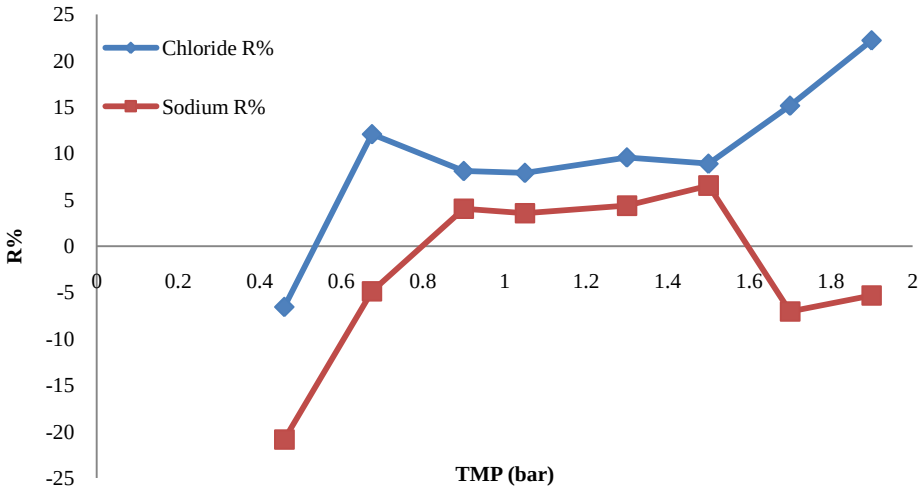

Figure 8-25. Sodium chloride rejection versus TMP.

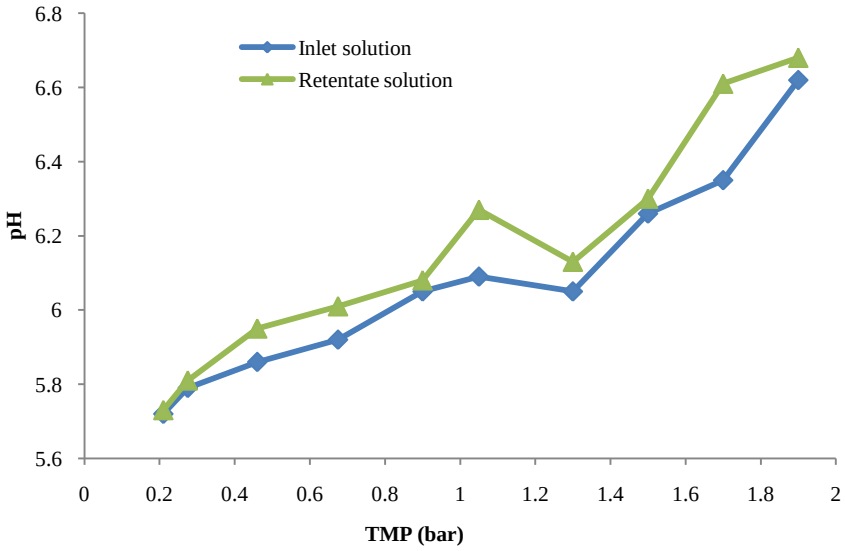

Figure 8-26. pH of sodium chloride solution versus TMP.

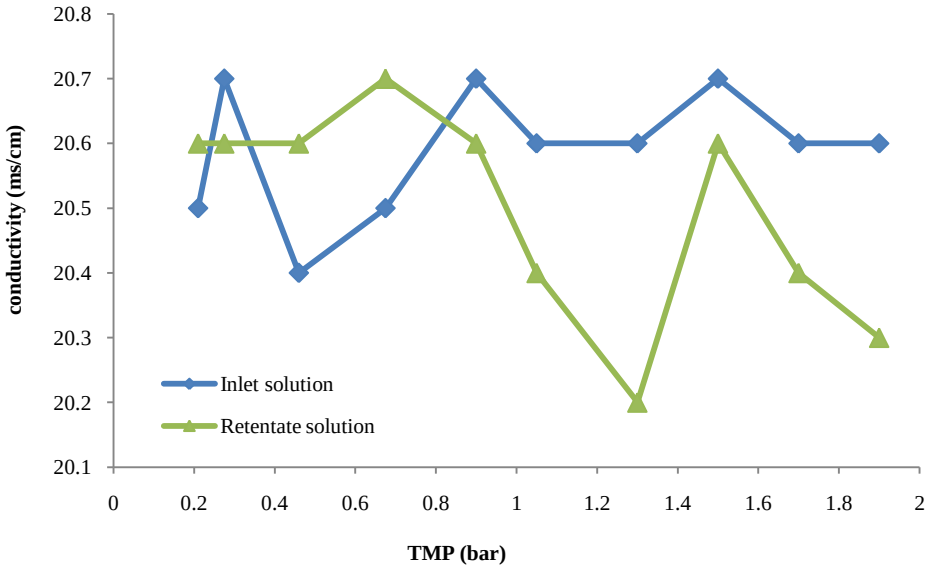

Figure 8-27. Conductivity of sodium chloride solution versus TMP.

The forth solution that was used was prepared by diluting sodium sulphate (Na_2SO_4), sodium nitrate ($NaNO_3$) and sodium chloride (NaCl) in distilled water. See Figure 8-28. The mixed salt solution permeates flux (volume flux based on the membrane area) through the membrane increased from 4.7E-09 to 5.0E-07 $m^3/m^2/s$ as the TMP increased. It was found that the rejection of ions took the following trend: R of sulphate (SO_4^{2-}) > R of nitrate (NO_3^{1-}) > R of chloride (Cl^{1-}) > R of sodium (Na^{1+}). The rejection of all anions decreased after the first TMP and remained almost constant as the TMP increased. The highest rejection for all anions was at the lowest TMP. The highest SO_4^{2-} rejection was about 62%, the highest NO_3^{1-} rejection was about 51%, and the highest Cl^{1-} rejection was about 42%. The rejection of cation Na^{1+} decreased after the first TMP and almost stayed constant as the TMP increased. The highest Na^{1+} rejection was about 37%. In general, cation Na^{1+} had negative rejection values, which means that it passed freely through the membrane. When comparing the permeation of distilled water through the membrane, before and after the mixed solution permeation through the membrane, it was found that distilled water permeation was higher than that of the mixed solution. This means that fouling did not occur or it was weak and did not have an effect on separation. The pH and conductivity of the inlet and retentate were measured. The pH of both solutions increased as the TMP increased. See Figure 8-29. The conductivity of the inlet and retentate solutions did not have a specific trend but in general, it decreased as TMP increased. See Figure 8-30. The pH and conductivity of permeate were not measured because the permeate volume produced by the membrane was not enough to get a reading.

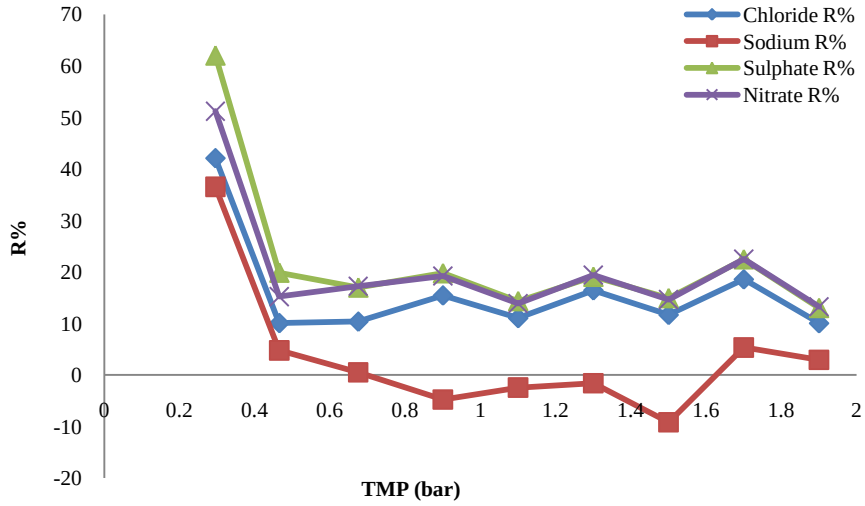

Figure 8-28**. Mixed salt rejection versus TMP.**

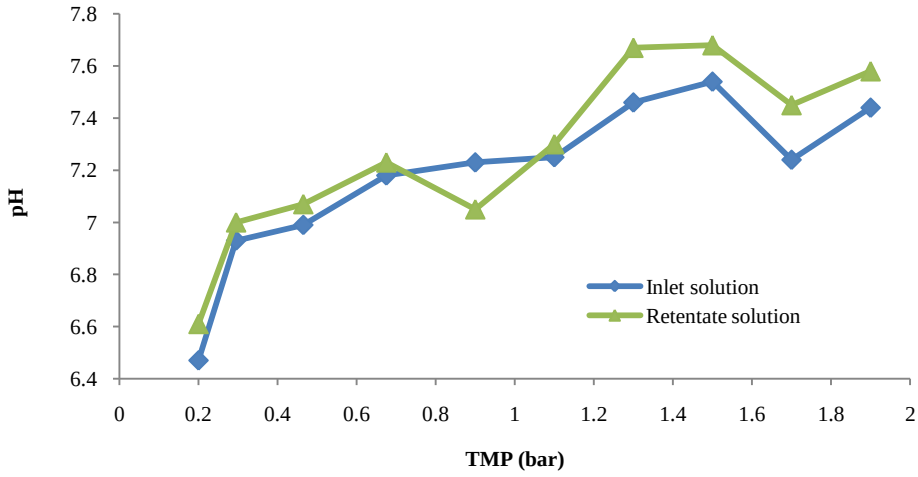

Figure 8-29. pH of mixed salt solution versus TMP.

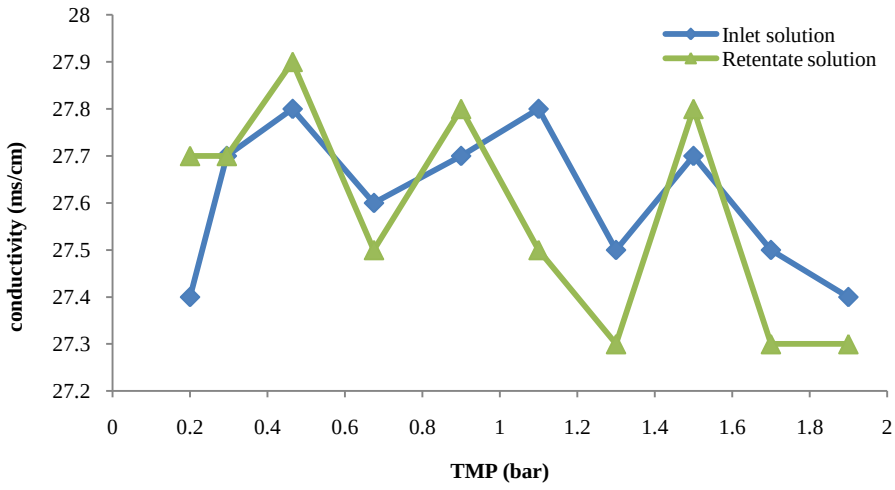

Figure 8-30. Conductivity of mixed salt solution versus TMP.

Several factors affect ion rejection, such as ion charge density, ion concentration and membrane charge. Therefore, rejection of ions would differ, where the rejection of divalent ions should be higher than mono-valent ions. The co-ions (have the same charge as the membrane charge) with higher valences would have a higher rejection because the repulsion interaction with the membrane charge would be more effective. The counter-ions (have an opposite charge of the membrane charge) with small ion valences would have higher rejection because the membrane charge shielding would be weak. Higher concentration would cause counter-ions to shield the membrane charge, thus decreasing rejection. Rejection of co-ions because of repulsion interaction with the membrane charge is known as the Donnan effect. Donnan exclusion has less of an effect on mono-valent ions when compared to divalent ions. Because of the Donnan exclusion effect, the membrane would reject counter-ions to maintain electro-neutrality condition in the solution.

In addition, different species of the same element (ion) may exist in a solution, with different concentrations of the various species. This depends on the solution conditions such as pH, pressure, temperature, total component concentration and component ionic strength. The different species of a specific component are a result of transformation processes, which are acid-base transformation, oxidation-reduction reaction, complexation, precipitation and adsorption. These transformation processes have an effect on species distribution and consequently affect ion retention behaviour.

Acid-base transformation affects the membrane rejection, where membrane rejection is influenced by the gain and loss of protons that is associated by the solute acid-base behaviour. Acid-base behaviour is a result of the change in ion speciation, where speciation is the existence of ions in various forms as the solution pH changes. Ion speciation may include formation of different types of species with more or less charge and may include change in dominance from dissolved to solid states. In this case, the species concentration is a function of pH. Acid-base formation at different pH values affects ion rejection, where co-ions are rejected by the membrane because of the repulsion interaction with the membrane charge; hence, counter-ion concentration increases in order to keep the electro-neutrality condition. As ion concentration increases, the membrane charge would be shielded, causing rejection to decrease.

Complexation is the interaction between cationic and anionic species in the aqueous solution, which would result in the formation of a variety of soluble species alongside the actual

species. Complexation depends on pH, reactant concentration and temperature. The formed complex's rejection is affected by its size and charge.

Precipitation has an effect on ion rejection. If solid species precipitate, its retention would increase, but this would be accompanied by concentration polarisation. The accumulation of solutes in the concentration polarisation layer adjacent to the membrane may lead to a more rapid exceedance of the solute solubility constraints than in the homogenous solution, causing it to be rejected by the membrane. Nanofiltration membrane rejects precipitates, where precipitate rejection depends on size exclusion, the Donnan exclusion and adsorption effect. The Donnan exclusion is a result of the interaction between the membrane charge and the solute (precipitate) charge, where the Donnan exclusion effect decreases as the counter-ion concentration increases because the counter-ion would shield the membrane charge. In addition, the Donnan exclusion decreases as the solute concentration increases.

The oxidation-reduction transformation has an effect on nanofiltration membrane rejection, where the oxidation-reduction transformation may cause changes in the element's form such as dissolved/precipitated and charged/uncharged. The redox transformation would have dramatic changes on the retention of the element of interest if the product is in solid form and the reactant is in dissolved form or vise versa. However, if the redox transformation results in a product of different charges to the initial species, it would have significant changes on retention but less dramatic than the above case.

In addition, adsorption of solutes by the membrane would alter the membrane rejection behaviour. Adsorption takes place at the membrane surface or in the membrane pores. Additionally, adsorption of solutes by the membrane increases as the solute concentration increases. Membrane rejection decreases as adsorption of solutes increases, causing membrane fouling.

When comparing the experiment results, it was found that the ion charge and size had an effect on the rejection of ions. Furthermore, the electrostatic interaction between the membrane charge (where the membrane charge is negative for the conditions used during these experiments, see section 8.3) and the ion charge plays a significant role, if it is not overcome by another factor. In the case of sodium nitrate ($NaNO_3$), the rejections of cations and anions were negative (except at the lowest TMP value). This means that the electrostatic interaction between the membrane and ion charges was not strong enough to overcome the

effect of TMP on rejection. At the lowest TMP, the rejection of anion NO_3^{1-} was slightly higher than the rejection of cation Na^{1+}. In this case, the ion size did play role on the rejection of NO_3^{1-}. Since both ions have the same charge strength and electrostatic interaction with the membrane charge would be at the same magnitude, and because of the neutrality condition at both sides of the membrane, the anion rejection was higher because of its bigger ion size. Additionally, the ion charge did play a role in the rejection because NO_3^{1-} had the same charge as the membrane, which caused its repulsion away from the membrane, thus causing its rejection. While for Na^{1+}, it had an opposite sign of the membrane charge, which increased the permeate of Na^{1+} through the membrane. These are known as the surface forces, where they do not depend on the TMP and stay constant as the TMP increases. Convection transport (depends on pressure gradient) did not cause any kind of rejection of anion NO_3^{1-}, where the ions passed freely through the membrane as the TMP increased. In the case of the cation Na^{1+}, convection transport can be considered to play a positive role because the rejection of Na^{1+} increased from negative rejection to zero rejection. Diffusion transport, which is caused by the concentration gradient across the membrane, did not have an effect on the rejection of anion NO_3^{1-} because there was no rejection of NO_3^{1-}. While the rejection of cation Na^{1+} can be considered to increase as the TMP increased, but still in the negative value, this means that Na^{1+} permeating though the membrane decreased as the TMP increased.

In the case of sodium sulphate ($Na_2SO_4^{2-}$), the rejection of anion SO_4^{2-} was higher than the rejection of cation Na^{1+}, which may be due to the Donnan exclusion and ion size. The electrostatic interaction (Donnan exclusion) between the membrane charge (which is negative in this case) and SO_4^{2-} charge causes repulsion between the membrane charge and SO_4^{2-} charge, which results in the rejection of the SO_4^{2-} ion. On the other hand, the cation Na^{1+} is attracted by the membrane charge, thus it passes freely through the membrane. SO_4^{2-} rejection was higher than Na^{1+} rejection due to its higher ion charge (which is the same as the membrane charge) and its bigger ion size. The higher rejection of SO_4^{2-} than that of Na^{1+} rejection can also be related to the neutrality condition at both sides of the membrane. Where SO_4^{2-} had to diffuse through the membrane to neutralize the charge on the permeate side, because it has double the charge of that of Na^{1+}, it means that a lower amount of SO_4^{2-} is needed to diffuse through the membrane to cause charge neutrality. This reason explains the low rejection of both ions. For SO_4^{2-} ion, convective transport decreased as the TMP increased. While for Na^{1+}, convective transport increased as the TMP increased then decreased as the TMP increased. Besides this, SO_4^{2-} rejection would be higher than Na^{1+}

rejection due to ion complexation where more anions were formed such as HSO_4^{1-} (the pH of inlet solution increased as the TMP increased). Since the membrane charge is negative, repulsion between HSO_4^{1-} and the membrane charge would occur and as a result, SO_4^{2-} rejection increased. While Na^{1+} rejection by the membrane decreased because of the ion complexation, Na^{1+} ions had to pass through the membrane to keep the electro-neutrality condition because H^{1+} ions were interacting with SO_4^{2-} thus forming HSO_4^{1-}.

In the case of sodium chloride (NaCl), the rejection of anion Cl^{1-} was higher than the rejection of cation Na^{1+}. This may be due to electrostatic interaction between the membrane charge (which is negative in this case) and the ion charge. The rejection of Cl^{1-} is a result of the repulsion between the membrane charge and Cl^{1-} charge. On the other hand, the cation Na^{1+} is attracted by the membrane charge and passes freely through the membrane. Cl^{1-} rejection was higher than Na^{1+} rejection because it has same charge as the membrane charge and bigger ion size. The low rejection of both ions can be explained by the electro-neutrality condition at both sides of the membrane. Where Cl^{1-} and Na^{1+} had to diffuse through the membrane to neutralize the charge on the permeate side, this condition reduced ion rejection. However, for Cl^{1-} this effect is lower because it has bigger ion size and the same charge as the membrane. For Cl^{1-} ion, convective transport decreased as the TMP increased. While for Na^{1+}, convective transport decreased as the TMP increased then decreased as the TMP increased.

In the case of mixed salt solution, the rejection of ions took the following trend: R of sulphate (SO_4^{2-}) > R of nitrate (NO_3^{1-}) > R of chloride (Cl^{1-}) > R of sodium (Na^{1+}). When excluding the lowest TMP pressure, it was noticed that for all the ions the rejection stayed almost constant as the TMP increased. Na^{1+} had the lowest rejection values and negative rejection values. The rejection of ions can be explained by the Donnan exclusion, electro-neutrality condition at both sides of the membrane and ion size. Since the anions had the same charge as the membrane, this would cause repulsion of the anions away from the membrane and back to the solution. Since the cation Na^{1+} had an opposite charge of the membrane charge, this caused the cation to pass through the membrane and decrease its rejection rate. The ion size had an influence on rejection where rejection increased as the ion size increased; as a result, the rejection of ions had the following trend: R of sulphate (SO_4^{2-}) > R of nitrate (NO_3^{1-}) > R of chloride (Cl^{1-}) > R of sodium (Na^{1+}). Since SO_4^{2-} has the biggest ion size, it had the highest rejection, which was about 62%, followed by NO_3^{1-} where its rejection was about 51%,

followed by Cl^{1-} with a rejection value about 42% and Na^{1+} with a rejection value of 36%. Furthermore, electro-neutrality played an important role in the rejection of ions. To maintain the electro-neutrality condition at both sides of the membrane, ions had to pass through the membrane, which explains the low rejection values for both the cation and the anions. Especially for Na^{1+}, since it is the only cation in the solution, this might explain the lowest rejection rate of all the ions. If H^{1+} and OH^{1-} (come from H_2O) were included in the separation process, the H^{1+} ion would react with SO_4^{2-} forming HSO_4^{1-}. As a result, more Na^{1+} has to pass through the membrane to maintain the electro-neutrality condition, and this explains the low rejection of Na^{1+} ion. In addition, the pH of the inlet and retentate solutions increased as the TMP increased, which supports this explanation. For higher TMP values, the mentioned conditions above would be considered negligible when comparing them to the pressure force. This might explain the decrease in rejection rate as the TMP increased. Moreover, since it is the main driving force, this would explain why the ion rejections remained constant as the TMP increased.

When comparing the separation of ions from single salt solution and mixed salt solution, it was noticed that the rejection of cation Na^{1+} from single salt solution or mixed salt solution did not differ. This means that Na^{1+} was not affected by the anion type or concentration of cation or anions. The same was noticed for SO_4^{2-} and Cl^{1-} anions, where their rejections from single salt solution and mixed salt solution were almost similar. This means that their rejections were not affected by the existence of other types of anions. On the other hand, this did not imply for NO_3^{1-} anion, where its rejection from mixed salt solution was higher than its rejection from the single salt solution.

8.5.3.1.2 Common anion

The first solution was prepared by diluting magnesium chloride ($MgCl_2$) in distilled water. $MgCl_2$ solution permeates flux (volume flux based on the membrane area) through the membrane increased from 8.1E-08 to 2.30E-06 $m^3/m^2/s$ as the TMP increased. It was found that the rejection of chloride ions was slightly higher than the rejection of magnesium ions. The highest rejection for both ions was at the lowest TMP, where the rejection of Cl^{1-} was about 38.4% and the rejection of Mg^{2+} was about 39%. When excluding the minimum TMP value, in general, it was noticed that the rejection of Cl^{1-} and Mg^{2+} remained almost constant as the TMP increased, where the rejection of Cl^{1-} ions was more stable, and the rejection of Mg^{2+} had more negative values, which means that no rejection took place and the Mg^{2+} ions

were passing freely through the membrane. See Figure 8-31. Also, when comparing the permeation of distilled water through the membrane, before and after $MgCl_2$ solution permeation through the membrane, it was found that the distilled water permeation was higher than $MgCl_2$ solution. This means that fouling did not occur or it was weak and did not have an effect on the separation process. The pH and conductivity of the inlet, retentate and permeate solutions were measured. The pH of the inlet and retentate solutions decreased as the TMP increased, but after TMP reached 1.1 bar, the pH remained constant. The permeate pH remained constant as the TMP increased. See Figure 8-32. The conductivity of the inlet increased as the TMP increased, but after the TMP reached 0.74 bar value, the conductivity decreased and remained constant. The conductivity of the retentate almost remained constant as the TMP increased. The permeate conductivity increased as the TMP increased. See Figure 8-33.

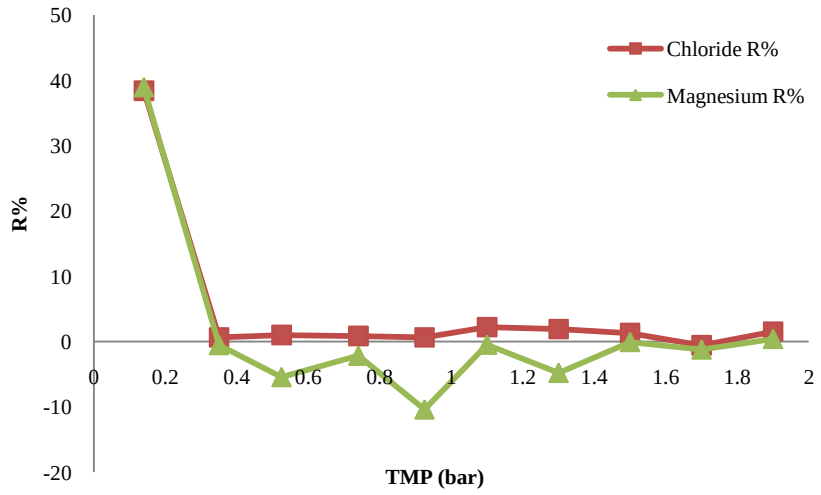

Figure 8-31. Magnesium chloride rejection versus TMP.

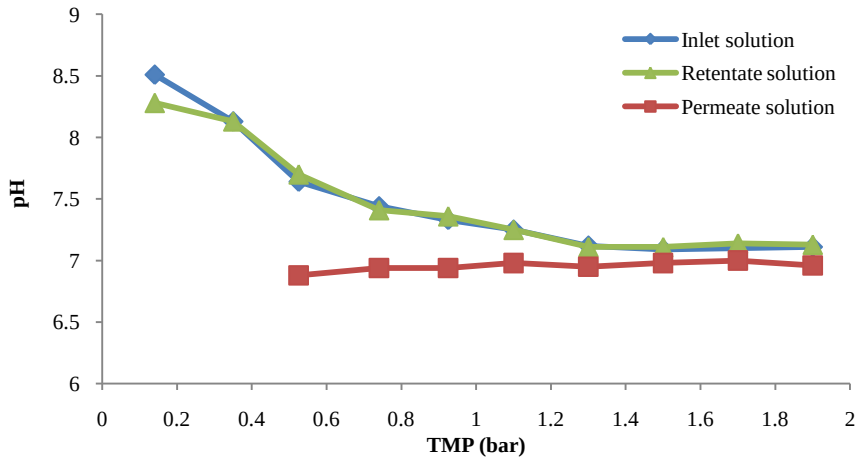

Figure 8-32. pH of magnesium chloride solution versus TMP.

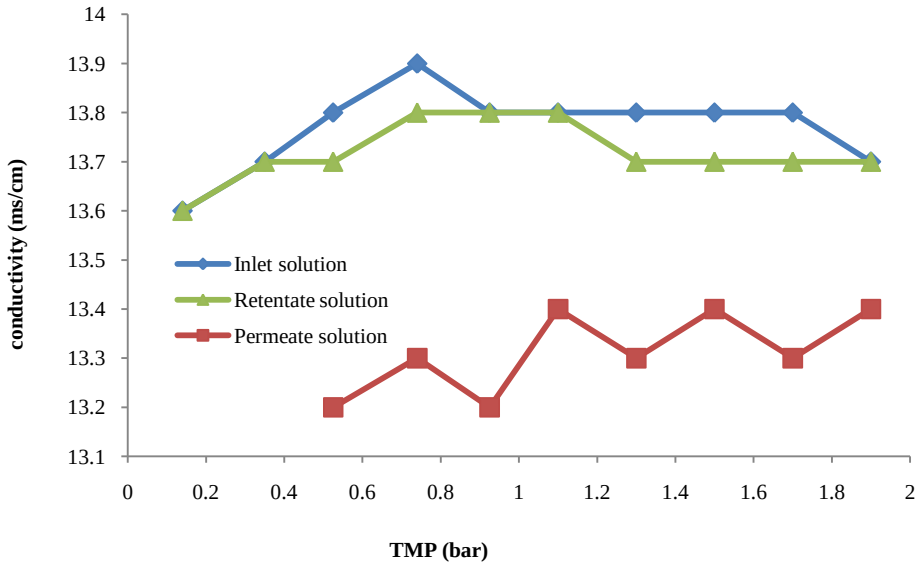

Figure 8-33. Conductivity of magnesium chloride solution versus TMP.

The second solution was prepared by diluting calcium chloride ($CaCl_2$) in distilled water. $CaCl_2$ permeate flux (volume flux based on the membrane area) through the membrane increased from 7.6E-08 to 2.0E-06 $m^3/m^2/s$ as the TMP increased. It was found that the rejection of calcium (Ca^{2+}) ions was slightly higher than the rejection of chloride (Cl^{1-}) ions. When excluding the lowest TMP value, it was found that the rejection of both ions remained constant as the TMP increased. The highest rejection of both ions was at the lowest TMP, where the rejection of Ca^{2+} was about 52% and the rejection of Cl^{1-} was about 48%. See Figure 8-34. When comparing the permeation of distilled water through the membrane, before and after calcium chloride ($CaCl_2$) solution permeation through the membrane, it was found that distilled water permeation was higher than the permeation of calcium chloride ($CaCl_2$) solution. This means that fouling did not occur or was weak and did not have an effect on separation. The pH and conductivity of the inlet, retentate and permeate were measured. The pH of the inlet and retentate decreased as the TMP increased. The permeate pH remained constant as the TMP increased. See Figure 8-35. The conductivity of the inlet and the retentate remained constant as the TMP increased. The permeate conductivity increased as the TMP increased, but after the TMP reached 1.3 bar, the conductivity remained constant as the TMP increased. See Figure 8-36.

The third solution was prepared by diluting sodium chloride (NaCl) in distilled water. See section 8.5.3.1.1 (the previous section).

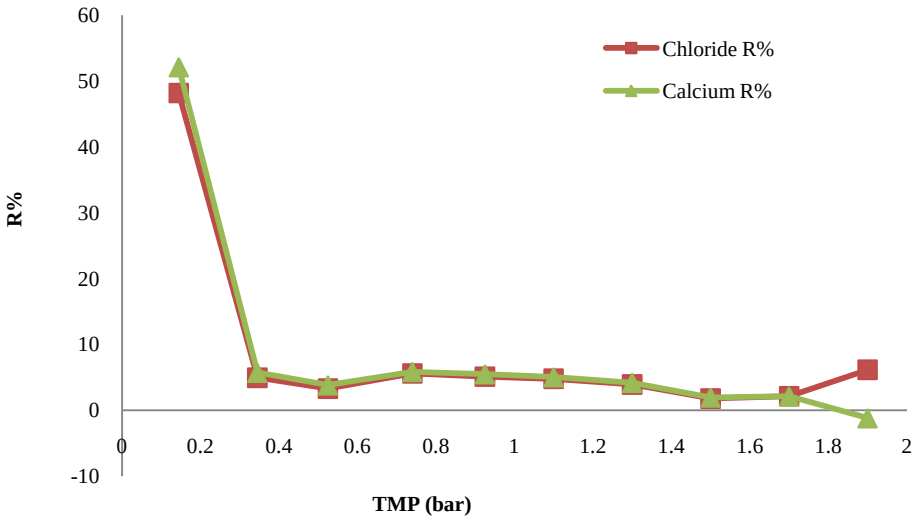

Figure 8-34. Calcium chloride rejection versus TMP.

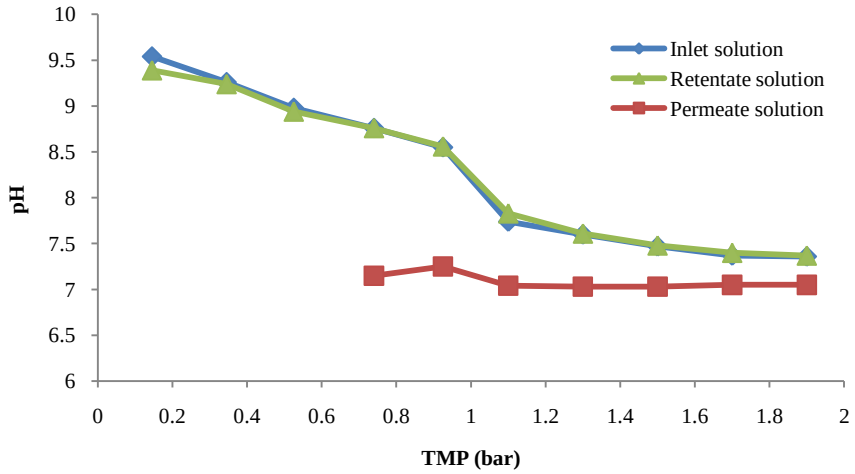

Figure 8-35. pH of calcium chloride solution versus TMP.

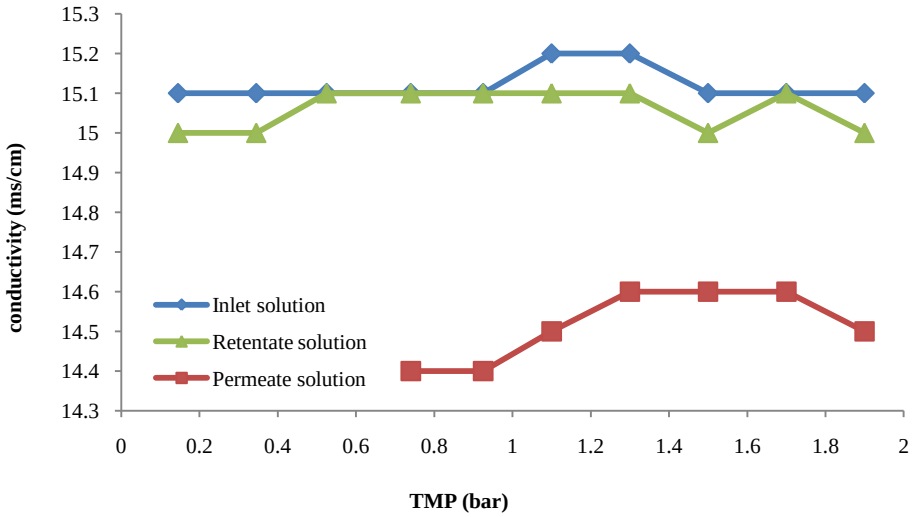

Figure 8-36. Conductivity of calcium chloride solution versus TMP.

The forth solution that was used was prepared by diluting sodium chloride (NaCl), magnesium chloride ($MgCl_2$) and calcium chloride ($CaCl_2$) in distilled water. See Figure 8-37. The mixed salt solution permeates flux (volume flux based on the membrane area) through the membrane increased from 6.0E-08 to 1.70E-06 $m^3/m^2/s$ as the TMP increased. It was found that the rejection of ions took the following trend: R of chloride (Cl^{1-}) > R of calcium (Ca^{2+}) > R of magnesium (Mg^{2+}) > R of sodium (Na^{1+}). The rejection of all cations decreased after the first TMP and remained almost constant as the TMP increased. In addition, the highest rejection for all cations was at the lowest TMP. The highest Ca^{2+} rejection was about 57.6%, the highest Mg^{2+} rejection was about 58.3%, and the highest Na^{1+} rejection was about 53.9%. In general, cation Na^{1+} had negative rejection values, which means that it passed freely through the membrane. The rejection of cation Cl^{1-} decreased after the first TMP and almost stayed constant as the TMP increased. The highest Cl^{1-} rejection was about 51%. When comparing the permeation of distilled water through the membrane, before and after the mixed solution permeation through the membrane, it was found that distilled water permeation was higher than that of the mixed solution. This means fouling did not occur or it was weak and did not have an effect on separation. The pH and conductivity of the inlet, retentate and permeate were measured. The pH of the inlet, retentate and permeate decreased as the TMP increased. See Figure 8-38. The conductivity of the inlet and the retentate remained constant as the TMP increased. The permeate conductivity increased as the TMP increased. See Figure 8-39.

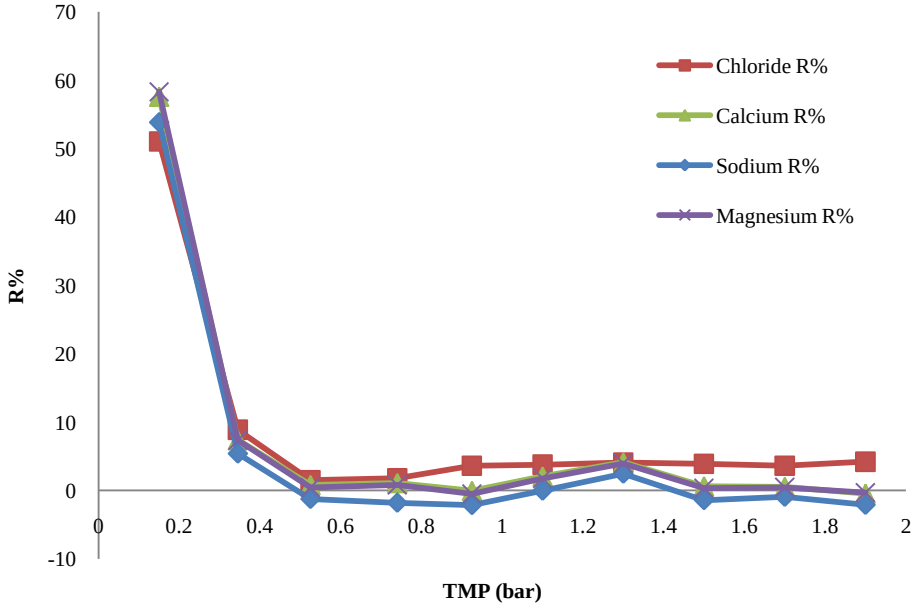

Figure 8-37. Mixed salt rejection versus TMP.

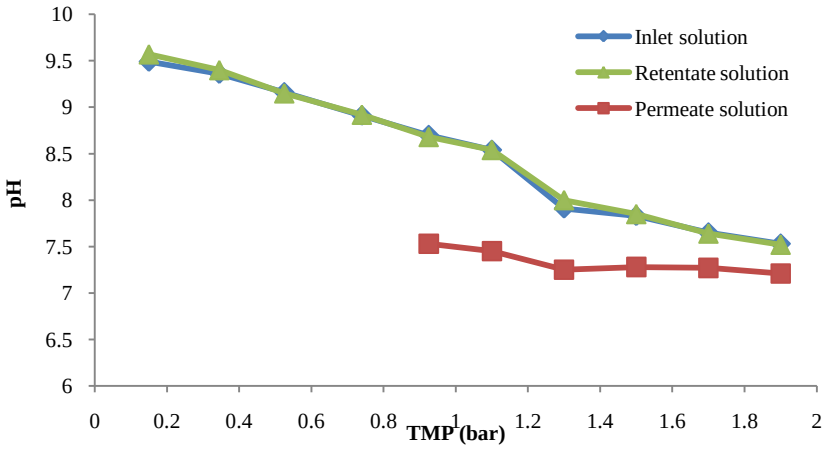

Figure 8-38. pH of mixed salt solution versus TMP.

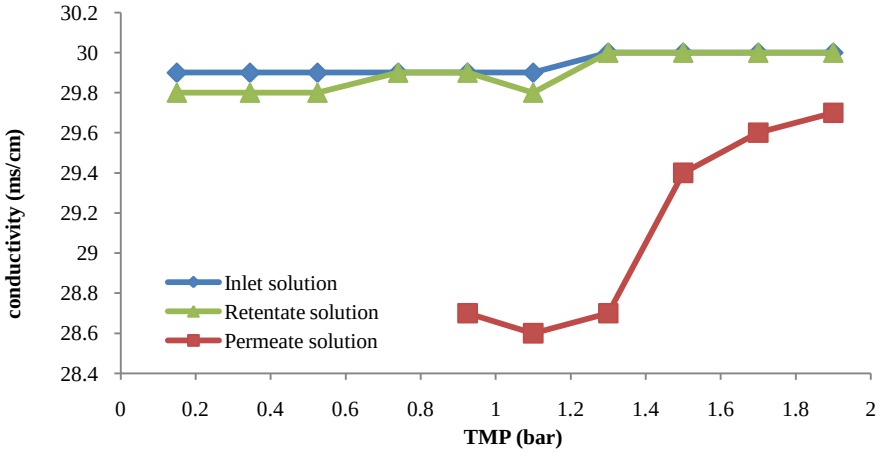

Figure 8-39. Conductivity of mixed salt solution versus TMP.

When comparing the experimental results, it was found that several factors affect the rejection of ions such as the ion size, the electrostatic interaction between the membrane and ion charge, the electro-neutrality condition, the convection force and diffusion force. In the case of magnesium chloride ($MgCl_2$), the rejection of Cl^{1-} was higher than the rejection of Mg^{2+} (except at the lowest TMP value). This might be explained by the electrostatic interaction between the membrane charge and ion charge, which is known as the Donnan exclusion, where the membrane charge is negative and Mg^{2+} charge is positive, which causes attraction between them, as a result Mg^{2+} passes more freely through the membrane than Cl^{1-}. On the other hand, Cl^{1-} has a negative charge, which is the same as the membrane charge, and would cause repulsion between the membrane and Cl^{1-}, thus rejecting Cl^{1-} by the membrane and back to the solution. In addition, ion size played a role in rejection, where Cl^{1-} ion size is bigger than Mg^{2+} ion size, which would cause Mg^{2+} to pass more freely through the

membrane pores than Cl^{1-}. Everything mentioned above is true except at the lowest TMP, where the rejection of Cl^{1-} is lower than the rejection of Mg^{2+}, which might be explained by the electro-neutrality condition. In order to reach charge equilibrium at both sides of the membrane, some ions have to pass through the membrane. Because Mg^{2+} has a higher ion charge than Cl^{1-}, this means that less amount of Mg^{2+} has to permeate through the membrane to cause electro-neutrality. This might explain the higher rejection of Mg^{2+} at the lowest TMP value. The small values of rejection are due to TMP, where it overcomes the Donnan exclusion effect between the ion charge and the membrane charge, thus forcing the ions to pass through the membrane. Convection transport, which depends on the pressure gradient, did not have any effect on the rejections of Cl^{1-} and Mg^{2+}, where the ions passed freely through the membrane as the TMP increased. The electro-neutrality condition might explain the reason for low rejection values as the TMP increases, where the ions diffuse from high concentration to lower concentration until equilibrium is reached, and in this case, until charge equilibrium is reached. Since the TMP force has more effect than any other force that would cause ion rejection, this would cause the ions to pass more freely through the membrane, resulting in low rejection values. In the case of sodium chloride (NaCl), see the previous section 8.5.3.1.1

In the case of calcium chloride, the rejection of anion Ca^{2+} was higher than the rejection of cation Cl^{1-}. This cannot be explained by the electrostatic interaction (Donnan exclusion) between the membrane charge (which is negative) and the ion charge, where Cl^{1-} rejection should be higher than the rejection of Ca^{2+}. Because Ca^{2+} has an opposite sign from that of the membrane, which causes attraction between the membrane and Ca^{2+}, this should cause Ca^{2+} to pass more freely through the membrane. Even this cannot be explained by the ion size, where Ca^{2+} has a smaller ion size than Cl^{1-}, where theoretically Cl^{1-} ions should have higher rejection than Ca^{2+} ions, but in this case, Ca^{2+} ions had higher rejection than Cl^{1-}. Cl^{1-} ion rejection is a result of its repulsion away from the membrane because Cl^{1-} has the same charge as the membrane.

As the TMP increased, the rejection of both ions (Ca^{2+} and Cl^{1-}) decreased and almost stayed constant. This may be due to the electro-neutrality condition at both sides of the membrane, where both ions (Ca^{2+} and Cl^{1-}) have to pass through the membrane to the permeate side to reach an electro-neutrality condition. In addition, the higher rejection of Ca^{2+} ions may be related to electro-neutrality condition, where Ca^{2+} has higher charge value than Cl^{1-}; as a

result, less amount of Ca^{2+} ions have to permeate through the membrane to cause the electro-neutrality condition. Therefore, Ca^{2+} ions would have higher rejection than Cl^{1-} ions. Because of the electro-neutrality condition, the concentration of Ca^{2+} at the inlet side would increase, which might have shielded the membrane charge. As a result, the membrane charge effect on rejection would decrease, which might explain the higher rejection of Ca^{2+} than Cl^{1-} rejection. For both ions (Ca^{2+} and Cl^{1-}), convective transport increased as the TMP increased.

In the case of mixed salt solution, the rejection of ions took the following trend: R of chloride (Cl^{1-}) > R of calcium (Ca^{2+}) > R of magnesium (Mg^{2+}) > R of sodium (Na^{1+}). This is true except at the lowest TMP value. When excluding the lowest TMP pressure, it has been noticed that for all the ions, the rejection stayed almost constant as the TMP increased. Na^{1+} had the lowest rejection values and negative rejection values. The rejection values of these ions can be explained by the ion charge, where Cl^{1-} has a negative charge the same as the membrane charge, which causes repulsion between the membrane and Cl^{1-} ions; as a result, Cl^{1-} ion would have a higher rejection than the other ions, while the cations Ca^{2+}, Mg^{2+} and Na^{1+} have the opposite charge sign of that of the membrane charge sign, which causes attraction by the membrane and they pass more freely through the membrane. Furthermore, ion size plays a part in the rejection results, where the ion size of the cations and anion used took the following trend: (Cl^{1-}) ion size > calcium (Ca^{2+}) ion size > sodium (Na^{1+}) ion size > magnesium (Mg^{2+}) ion size. Since Cl^{1-} ion has the biggest ion size, as a result the Cl^{1-} ion had the highest rejection. Then the Ca^{2+} ion had the second-highest rejection. Nevertheless, this cannot explain why Mg^{2+} had a higher rejection than Na^{1+}, even though the Na^{1+} ion has a bigger ion size than the Mg^{2+} ion.

In general, the low rejection values of the three cations and one anion may be due to the electro-neutrality condition at both sides of the membrane, where ions permeate from the feed side (high concentration) to the permeate side (lower concentration) to fulfil the charge equilibrium condition. Another reason behind the low rejection may be due to membrane charge shielding by the cations Ca^{2+}, Mg^{2+} and Na^{1+}. As a result, the Donnan exclusion effect would be weak, thus membrane rejection would decrease. In addition, low rejection values may be due to higher TMP values, where it became stronger than the other factors causing lower ion rejection.

The rejection of ions at the lowest TMP took the following trend: R of magnesium (Mg^{2+}) > R of calcium (Ca^{2+}) > R of sodium (Na^{1+}) > R of chloride (Cl^{1-}). This cannot be explained by

the ion size because Cl^{1-} has the biggest ion size, and in this case, it had the lowest rejection. Besides, the Mg^{2+} ion has the smallest ion size and had the highest rejection. In addition, the ion charge cannot explain it because the three cations (Ca^{2+}, Na^{1+} and Mg^{2+}) had an opposite charge sign from that of the membrane charge and still had higher rejection than the rejection of the anion (Cl^{1-}). This result might be due to membrane charge shielding by the cations Ca^{2+}, Mg^{2+} and Na^{1+}. Where the net charge in the membrane pores would be positive, as a result increasing the rejection of the cations Ca^{2+}, Mg^{2+} and Na^{1+} because of repulsion. Moreover, Cl^{1-} rejection decreases because of the attraction by the positive charge, where it would pass freely through the membrane.

When comparing separation of ions from the single salt and mixed salt solutions, it was noticed that the rejection of cation Mg^{2+} from the mixed salt solution was higher than its rejection from the single salt solution. For the Ca^{2+} ion case, its rejection from the single salt solution was higher than its rejection from the mixed salt solution. For the Na^{1+} case, there was not a difference between its rejection from the single salt solution and that of a mixed salt solution. This means that Na^{1+} ion rejection was not affected by the existence of another type of cation. The same goes for Cl^{1-} ion, where its rejections from single salt and mixed salt solutions were almost similar, which implies that its rejection did not depend on other ion types or its concentration in the solution. Concentration of Cl^{1-} did not have an effect on its rejection because it had a similar rejection trend from either single salt or mixed salt solutions.

8.5.3.2 1.0 nm membrane

8.5.3.2.1 Common cation

The first solution that was used was prepared by diluting sodium sulphate (Na_2SO_4) in distilled water. Na_2SO_4 permeate flux (volume flux based on the membrane area) through the membrane increased from 5.4E-07 to 1.0E-05 $m^3/m^2/s$ as the TMP increased. It was found that the rejection of sulphate (SO_4^{2-}) ions was higher than the rejection of sodium (Na^{1+}) ions. When excluding the lowest TMP value, the rejection of SO_4^{2-} ions almost remained constant as the TMP increased. See Figure 8-40. The highest rejection of SO_4^{2-} was about 33.6% at the lowest TMP value, which was equal to 0.195 bar. On the other hand, the Na^{1+} rejection decreased as the TMP increased, and as the TMP reached 1.5 bar, the rejection of Na^{1+} started to increase. Na^{1+} had some negative rejection values, which means it passed freely through the membrane. The highest rejection of Na^{1+} was about 20.0% at the lowest TMP.

When comparing the permeation of distilled water through the membrane, before and after sodium sulphate (Na_2SO_4) solution permeation through the membrane, it was found that distilled water permeation was higher than the permeation of sodium sulphate (Na_2SO_4) solution. This means that fouling did not occur or was weak and did not have an effect on separation. The pH and conductivity of the inlet, retentate and permeate solutions were measured. The pH of the inlet and retentate increased as the TMP increased, while the permeate pH almost remained constant as the TMP increased. See Figure 8-41. The conductivity of the inlet and the retentate almost remained constant as the TMP increased. The permeate conductivity did not have a specific trend, but it can be considered almost constant as the TMP increased. The permeate conductivity was higher than the inlet and the retentate conductivity. See Figure 8-42.

In the case of sodium sulphate, the rejection of anion SO_4^{2-} was higher than the rejection of cation Na^{1+}. This may be due to electrostatic interaction between the membrane charge (which is negative) and the ion charge, which is known as the Donnan exclusion. The rejection of SO_4^{2-} is a result of the repulsion between the membrane charge and SO_4^{2-} charge. On the other hand, the cation Na^{1+} is attracted by the membrane charge where it passes freely through the membrane, and this might explain the negative rejection values. Also, higher rejection of SO_4^{2-} than Na^{1+} might be due to its higher ion charge (which is the same as the membrane charge) and bigger ion size, where Na^{1+} has a small ion size, thus it can pass more freely through the membrane pores. In addition, the higher rejection of SO_4^{2-} than that of Na^{1+} rejection can also be related to the electro-neutrality condition at both sides of the membrane. Were SO_4^{2-} had to diffuse through the membrane to neutralize the charge on the permeate side, since it has double the charge of that of Na^{1+}, this means that a lower amount of SO_4^{2-} is needed to diffuse through the membrane to cause electro-neutrality. This reason explains the low rejection of both ions. For the SO_4^{2-} ion, convective transport almost stayed constant as the TMP increased. While for Na^{1+}, convective transport increased as the TMP increased then decreased as the TMP increased. In addition, the lower rejection of Na^{1+} than that of SO_4^{2-} may be related to the solute acid-base behaviour, where the acid-base behaviour is a result of speciation, where the solute exists in various forms. The main solute ions were Na^{1+} and SO_4^{2-}, and because of speciation, several ions would form such as HSO_4^{1-}.

$$Na_2SO_4 + H_2O \rightarrow Na^{1+} + SO_4^{2-} + H^{1+} + OH^{1-}$$

As a result, the rejection of SO_4^{2-} and HSO_4^{1-} would be higher than the rejection of OH^{1-}

because they had higher ion size. Moreover, OH^{1-} would pass through the membrane to maintain electro-neutrality condition at both sides of the membrane. This could be supported by the increase in pH of the inlet and retentate solutions. See Figure 8-41.

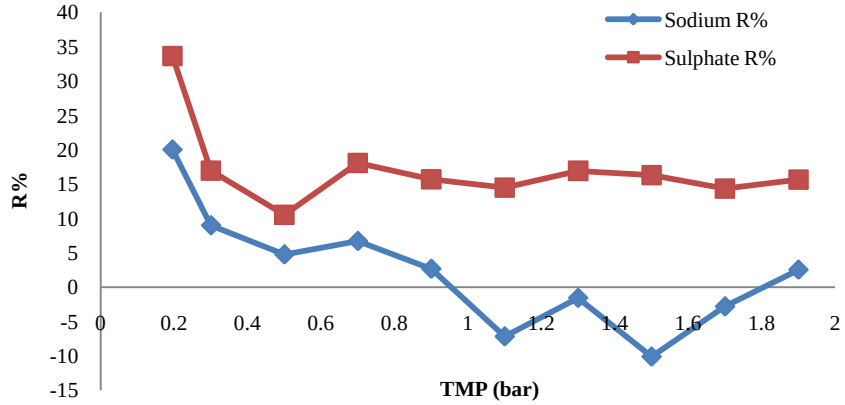

Figure 8-40. Sodium sulphate rejection versus TMP.

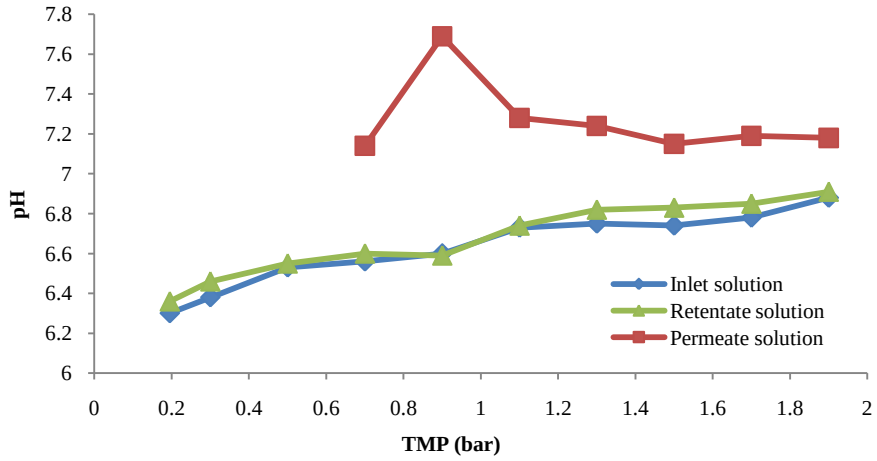

Figure 8-41. pH of sodium sulphate solution versus TMP.

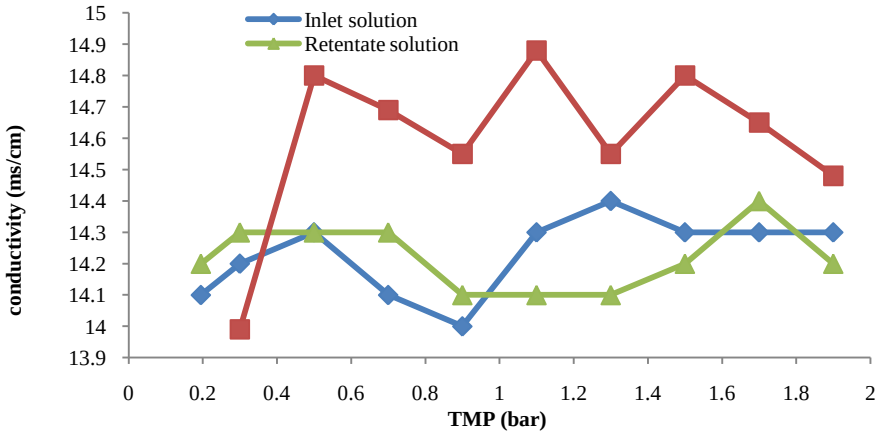

Figure 8-42. Conductivity of sodium sulphate solution versus TMP.

The second solution that was used was prepared by diluting sodium nitrate ($NaNO_3$) in distilled water. $NaNO_3$ permeate flux (volume flux based on the membrane area) through the membrane increased from 5.3E-07 to 9.0E-06 $m^3/m^2/s$ as the TMP increased. It was found that the rejection of nitrate (NO_3^{1-}) ions was higher than the rejection of sodium (Na^{1+}) ions. The highest rejection for both ions was at the lowest TMP, where the rejection of NO_3^{1-} was about 36.0% and the rejection of Na^{1+} was about 30.2%. When excluding the minimum TMP value, the rejection of NO_3^{1-} and Na^{1+} almost remained constant as the TMP increased. See Figure 8-43. In addition, when comparing the permeation of distilled water through the membrane — before and after $NaNO_3$ solution permeation through the membrane — it was found that the distilled water permeation was higher than the $NaNO_3$ solution. This means fouling did not occur or was weak and did not have an effect on separation. The pH and conductivity of the inlet, retentate and permeate were measured. The pH of the inlet and retentate increased as the TMP increased, while the permeate pH slightly decreased as the TMP increased. See Figure 8-44. The conductivity of the inlet, the retentate and the permeate almost remained constant as the TMP increased. The permeate conductivity was higher than the inlet and the retentate solution's conductivity. See Figure 8-45.

The rejections of NO_3^{1-} and Na^{1+} were low, which means that the electrostatic interaction between the membrane charge and ion charge was not strong enough to overcome the effect of TMP on rejection. The higher rejection of NO_3^{1-} than Na^{1+} can be explained by the ion charge and size. Where the NO_3^{1-} ion has the same charge sign as the membrane, this would cause repulsion between the membrane and NO_3^{1-} ion, and as a result, the NO_3^{1-} ion would move away from the membrane back to the solution causing its rejection. While the Na^{1+} ion has an opposite charge sign from that of the membrane that would cause attraction between them, thus the Na^{1+} ion would pass more freely through the membrane. Furthermore, the NO_3^{1-} ion has a bigger ion size than the Na^{1+} ion, which would be harder for the NO_3^{1-} ion to pass through the membrane pores than the Na^{1+} ion; as a result, the NO_3^{1-} had higher rejection than Na^{1+}. These are known as the surface forces, where they do not depend on the TMP and stay constant as the TMP increases. When excluding the lowest TMP, convection transport (which depends on the pressure gradient) was almost constant as the TMP increased. This means that it did not have an effect on the rejection of both ions NO_3^{1-} and Na^{1+}. Low rejection values of both ions may be due to electro-neutrality conditions, where ions would pass through the membrane until electro-neutrality condition is reached at both sides of the membrane.

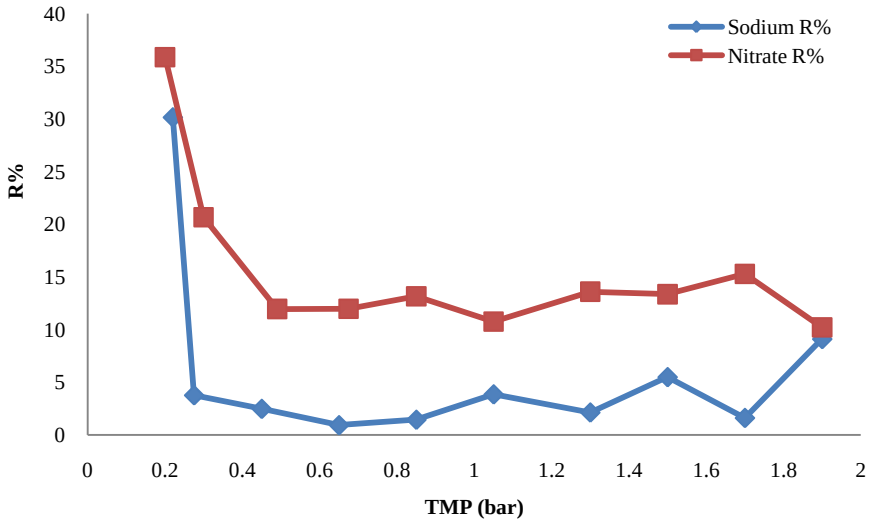

Figure 8-43. Sodium nitrate rejection versus TMP.

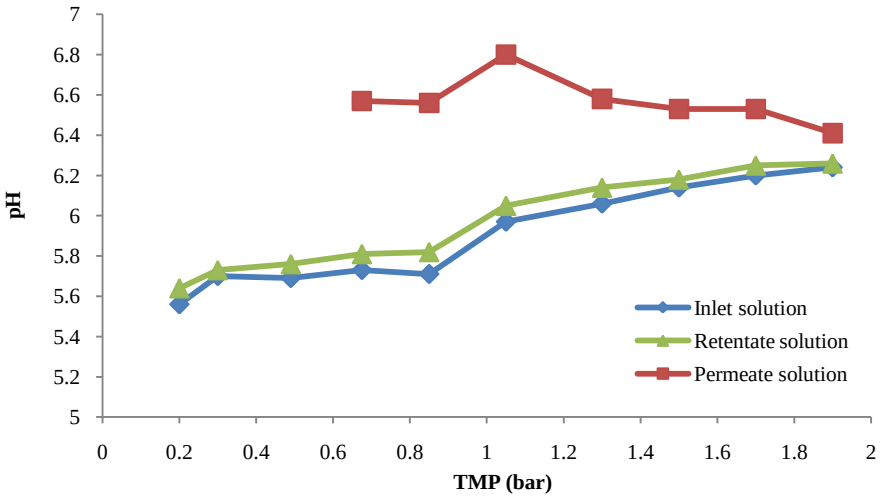

Figure 8-44. pH of sodium nitrate solution versus TMP.

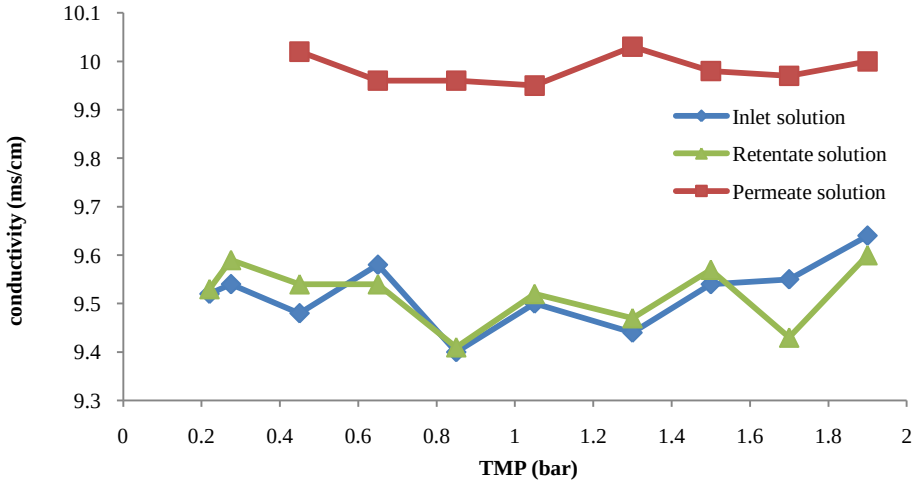

Figure 8-45. Conductivity of sodium nitrate solution versus TMP.

The third solution that was used was prepared by diluting sodium chloride (NaCl) in distilled water. NaCl permeate flux (volume flux based on the membrane area) through the membrane increased from 2.3E-07 to 3.9E-05 $m^3/m^2/s$ as the TMP increased. It was found that the rejection of chloride (Cl^{1-}) ions was lower than the rejection of sodium (Na^{1+}) ions, where the rejection of Cl^{1-} ions had more values that are negative. See Figure 8-46. The highest rejection of both ions was at the lowest TMP, where the rejection of Cl^{1-} was about 34.7% and the rejection of Na^{1+} was about 37.3%. When comparing the permeation of distilled water through the membrane, before and after sodium chloride (NaCl) solution permeation through the membrane, it was found that distilled water permeation was higher than that of the sodium chloride (NaCl) solution. This means that fouling did not occur or was weak and did not have an effect on separation. The pH and conductivity of the inlet, retentate and permeate solutions were measured. The pH of the inlet and retentate increased as the TMP increased, while the pH of the permeate increased after TMP reached the value of 0.9 bar, and then remained almost constant as the TMP increased. See Figure 8-47. The conductivity of the inlet and retentate increased as the TMP increased, while the permeate conductivity decreased as the TMP increased. The permeate conductivity was higher than the inlet and the retentate solution's conductivity. See Figure 8-48.

In the case of sodium chloride (NaCl), the rejection of anion Na^{1+} was higher than the rejection of cation Cl^{1-}. This cannot be explained by the ion size and ion charge because Cl^{1-} has a bigger ion size than Na^{1+}, and as a result, Cl^{1-} should have a higher rejection than Na^{1+}. Moreover, these results cannot be explained by the ion charge, because Cl^{1-} has the same charge sign as that of the membrane, thus repulsion occurs, causing the Cl^{1-} ion to diffuse back to the solution, resulting in higher Cl^{1-} rejection. In addition, convective transport cannot explain these results because convective transport stayed constant as the TMP increased. These results might be explained by ion diffusivity through the membrane material. If Cl^{1-} has a higher diffusivity coefficient through the membrane material than Na^{1+}, it would pass more easily through the membrane, thus resulting in lower rejection than Na^{1+}. Another approach in explaining these results is through the solution pH and the existing ions. Where the pH of the inlet and retentate solutions increased as the TMP increased, which means it became more basic, where the exciting solute and solvent ions,

$$NaCl + H_2O \rightarrow Na^{1+} + Cl^{1-} + H^{1+} + OH^{1-}$$

Since Na^{1+} rejection is higher than Cl^{1-}, the solution pH is increasing by the increase in TMP

and to maintain the electro-neutrality at both sides of the membrane, as a result, the membrane rejected OH^{1-} and H^{1+} passed freely through the membrane. The electro-neutrality condition can explain the low rejection values for Na^{1+} and Cl^{1-}, where the ions had to move from a higher charged concentration area to a lower charge concentration area until the electro-neutrality condition is reached at both sides of the membrane. In addition, membrane charge shielding by the ions would cause lower rejection by the membrane.

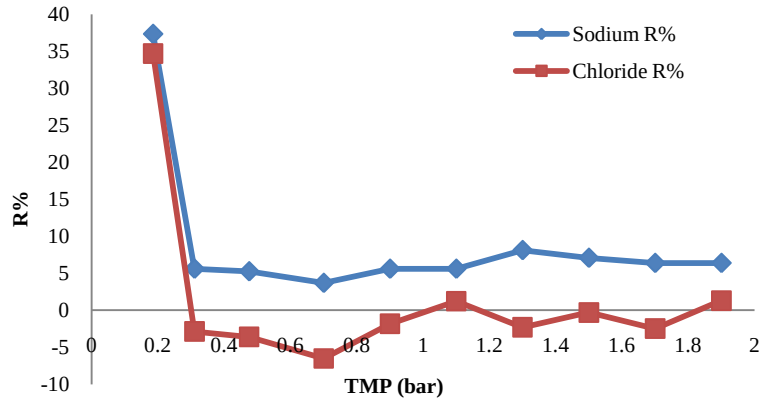

Figure 8-46. Sodium chloride rejection versus TMP.

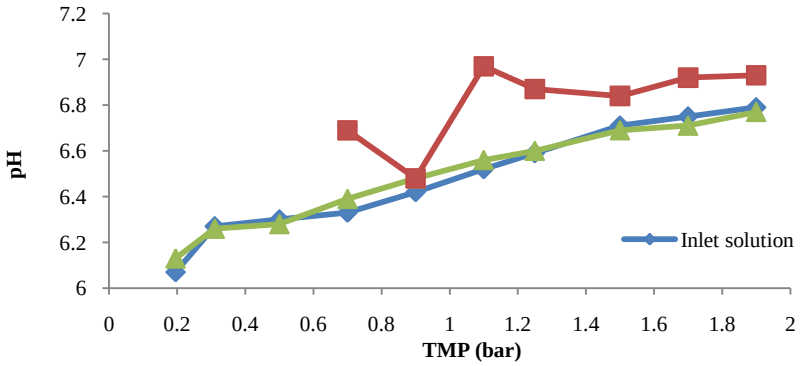

Figure 8-47. pH of sodium chloride solution versus TMP.

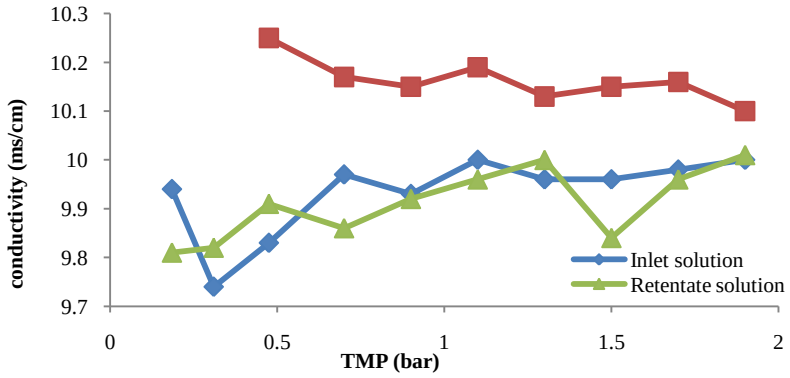

Figure 8-48. Conductivity of sodium chloride solution versus TMP.

The fourth solution that was used was prepared by diluting sodium sulphate (Na_2SO_4), sodium nitrate ($NaNO_3$) and sodium chloride (NaCl) in distilled water. See Figure 8-49. The mixed salt solution permeates flux (volume flux based on the membrane area) through the membrane increased from 2.4E-07 to 3.3E-05 $m^3/m^2/s$ as the TMP increased. When excluding the minimum TMP, it was found that the rejection of ions took the following trend: R of sodium (Na^{1+}) > R of nitrate (NO_3^{1-}) > R of chloride (Cl^{1-}) > R of sulphate (SO_4^{2-}). The rejection of all anions decreased after the first TMP and stayed almost constant as the TMP increased. The highest rejection for all anions was at the lowest TMP, and it took the following trend: R of sulphate (SO_4^{2-}) > R of nitrate (NO_3^{1-}) > R of sodium (Na^{1+}) > R of chloride (Cl^{1-}). The highest SO_4^{2-} rejection was about 53.3%, the highest NO_3^{1-} rejection was about 46.9%, the highest Cl^{1-} rejection was about 43.2% and highest Na^{1+} rejection was about 45.6%. In general, the anions NO_3^{1-}, Cl^{1-} and SO_4^{2-} had negative rejection values, which mean that at some point they passed freely through the membrane. When comparing the permeation of distilled water through the membrane, before and after the mixed solution permeation through the membrane, it was found that distilled water permeation was higher than that of the mixed solution. This means that fouling did not occur or it was weak and did not have an effect on separation. The pH and conductivity of the inlet, retentate and permeate were measured. The pH of the inlet and retentate increased as the TMP increased, while the pH of permeate decreased as the TMP increased. See Figure 8-50. The conductivity of the inlet, the retentate and permeate almost remained constant as the TMP increased. The permeate conductivity was lower than the inlet and the retentate conductivity. See Figure 8-51.

The charge effects and the ion size can explain the higher rejection of $NO3^{1-}$ and SO_4^{2-} ions Cl^{1-} and Na^{1+} ions at the lowest TMP. Since NO_3^{1-} and SO_4^{2-} anions have the same charge as the membrane charge, this would cause repulsion of the anions away from the membrane and back to the solution. In addition, NO_3^{1-} and SO_4^{2-} ions have a bigger ion size than Cl^{1-} and Na^{1+} ions, which means their permeation through the membrane would be more difficult than Cl^{1-} and Na^{1+} ions, causing them to be rejected by the membrane. On the other hand, Na^{1+} lower rejection may be due to the opposite charge of that the membrane charge, which caused the cation to pass through the membrane, thus decreasing its rejection rate, while Cl^{1-} lower rejection cannot be explained either by its ion size or ion charge, since it had the same charge of the membrane then it should have had a higher rejection than Na^{1+}; also, it has a bigger ion size than Na^{1+}, but still had a lower rejection. If acid-base transformation is considered to

play a role, lower rejection of Cl^{1-} than Na^{1+} might be affected by it. Where acid-base transformation includes loss and gain of protons, as a result, different types of species would have formed such as HSO_4^{1-}. To obtain the electro-neutrality at both sides of the membrane, Cl^{1-}, Na^{1+} and H^{1+} ions would permeate through the membrane decreasing Cl^{1-} and Na^{1+} rejections. The increase in the pH of the inlet and retentate as the TMP increased supports this assumption. The permeate pH decreased as the TMP increased because more H^{1+} ions were permeating through the membrane to obtain the electro-neutrality condition at both sides of the membrane. Also, this might be explained by its diffusivity through the membrane, if Cl^{1-} had higher diffusivity ability through the membrane material then it would have lower rejection, and this might be the case.

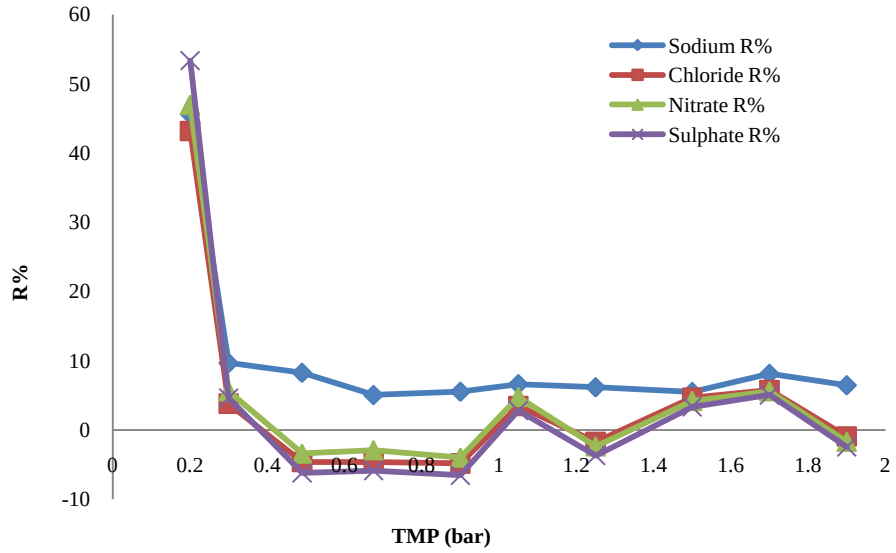

Figure 8-49. Mixed salt rejection versus TMP.

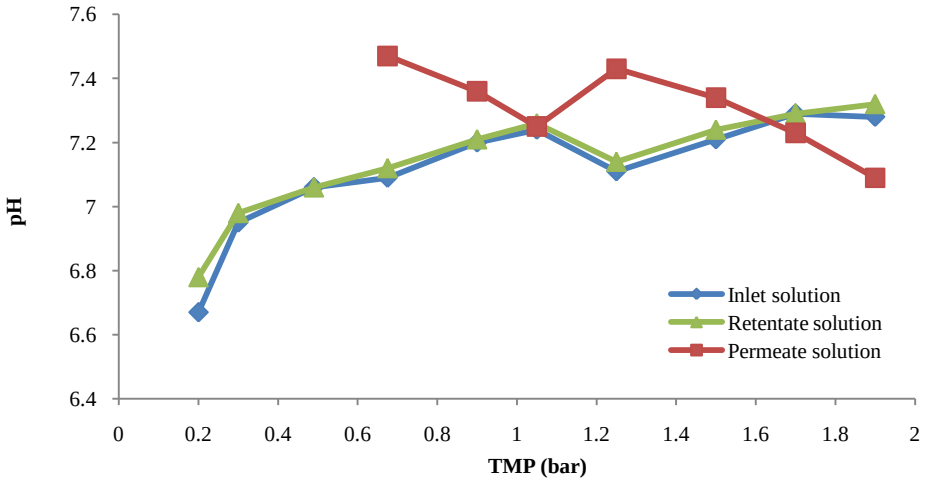

Figure 8-50. pH of mixed salt solution versus TMP.

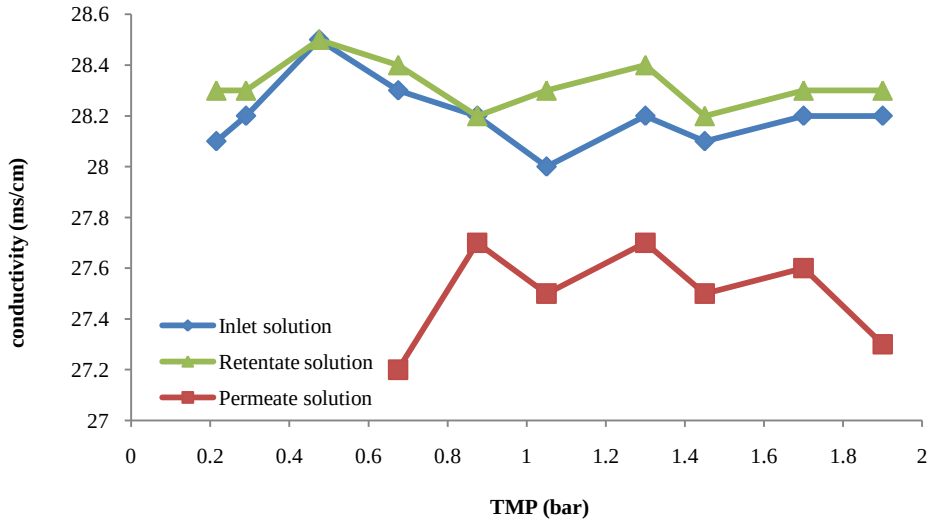

Figure 8-51. Conductivity of mixed salt solution versus TMP.

The low rejection values might be due to electro-neutrality condition and TMP, where to maintain the electro-neutrality conditions at both sides of the membrane, ions had to permeate through the membrane from a high concentration area to a low concentration area, resulting in low rejection values. Furthermore, the TMP effect would overcome the ion size and ion charge effects where they can be considered negligible when compared to the pressure force; as a result, the rejection rate would decrease as the TMP increased. In addition, since it is the main driving force, this would explain why the ion rejections remained constant as the TMP increased.

When comparing separation of ions from a single salt solution and from a mixed salt solution, it was noticed that the rejection of cation Na^{1+} from single salt solution or a mixed salt solution did not differ. This means that Na^{1+} was not affected by the anion type or concentration. The same was noticed for Cl^{1-} where its rejection from a single salt solution and a mixed salt solution was almost similar. This means that their rejections were not affected by the existence of another type of anion. On the other hand, this did not imply for NO_3^{1-} and SO_4^{2-} anion, where their rejection from a mixed salt solution was lower than their rejection from a single salt solution. This means their rejection was affected by the existence of another type of anion.

8.5.3.2.2 Common anion

The first solution was prepared by diluting magnesium chloride ($MgCl_2$) in distilled water. $MgCl_2$ permeate flux (volume flux based on the membrane area) through the membrane

increased from 2.7E-07 to 4.2E-06 $m^3/m^2/s$ as the TMP increased. The rejection of chloride ions was slightly higher than the rejection of magnesium ions. The highest rejection for both ions was at the lowest TMP, where the rejection of Cl^{1-} was about 48.8% and the rejection of Mg^{2+} was about 38.6%. When excluding the minimum TMP value, in general the rejection of Cl^{1-} and Mg^{2+} remained almost constant as the TMP increased. The rejection of Mg^{2+} had negative values, which means that Mg^{2+} ions were permeating freely through the membrane. See Figure 8-52. In addition, when comparing the permeation of distilled water through the membrane, before and after $MgCl_2$ solution permeation through the membrane, it was found that distilled water permeation was higher than the $MgCl_2$ solution. This means that fouling did not occur or it was weak and did not have an effect on separation. The pH and conductivity of the inlet, retentate and permeate were measured. The pH of the inlet and retentate decreased as the TMP increased, while the pH of permeate almost remained constant as the TMP increased. See figure 8-53. The conductivity of the inlet and retentate almost remained constant as the TMP increased, while permeate conductivity decreased as the TMP increased. The permeate conductivity was higher than the inlet and the retentate conductivity. See Figure 8-54.

Several factors affect the rejection of ions such as the ion size, the electrostatic interaction between the membrane and the ion charge, the electro-neutrality condition, the convection force and the diffusion force. In the case of magnesium chloride ($MgCl_2$), the rejection of Cl^{1-} was higher than the rejection of Mg^{2+}. This might be explained by the electrostatic interaction between the membrane charge and ion charge, which is known as Donnan exclusion, where the membrane charge is negative and Mg^{2+} charge is positive, which causes attraction between them; as a result, Mg^{2+} passes more freely through the membrane than Cl^{1-}. On the other hand, Cl^{1-} has a negative charge, which is the same as the membrane charge. This would cause repulsion between the membrane and Cl^{1-} and rejecting Cl^{1-} pass through the membrane and back to the solution. In addition, ion size played role in rejection, where Cl^{1-} ion size was bigger than Mg^{2+} ion size, which would cause Mg^{2+} to pass more freely through the membrane pores than Cl^{1-}. The small values of rejection might be due to TMP, where it overcomes the charge force between the ion charge and the membrane charge, and forcing the ions to pass through the membrane. If H^{1+} and OH^{1-} were considered to be affected by the membrane separation, then these ions might explain the lower rejection of Mg^{2+} than Cl^{1-}. As mentioned above, electro-neutrality condition is obtained at both sides of the membrane by Mg^{2+}, Cl^{1-}, H^{1+} and OH^{1-} ions passing through the membrane. pH of inlet and retentate

solutions decreased as the TMP — see Figure 8-53 — which suggests that OH^{1-} is permeating through the membrane and H^{1+} is rejected. An increase of OH^{1-} passing through the membrane would increase the rejection of Cl^{1-}, which would explain the higher rejection of Cl^{1-} than Mg^{2+}. Convection transport (which depends on the pressure gradient) did not have any effect on the rejections of Cl^{1-} and Mg^{2+}, where the ions passed freely through the membrane as the TMP increased. In addition, the electro-neutrality condition might explain the low rejection values. According to electro-neutrality condition, the ions permeate from the higher concentration side of the membrane to the lower concentration side; as a result, the ions would permeate through the membrane to the permeate side until equilibrium is reached. Since TMP force has more effect than any other force that would cause ion rejection, this would cause the ions to permeate more freely through the membrane, resulting in low rejection values.

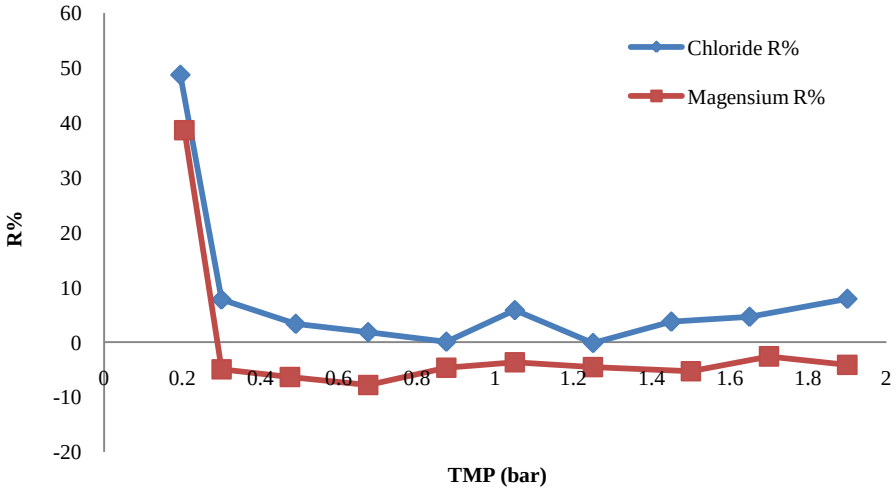

Figure 8-52. Magnesium chloride rejection versus TMP.

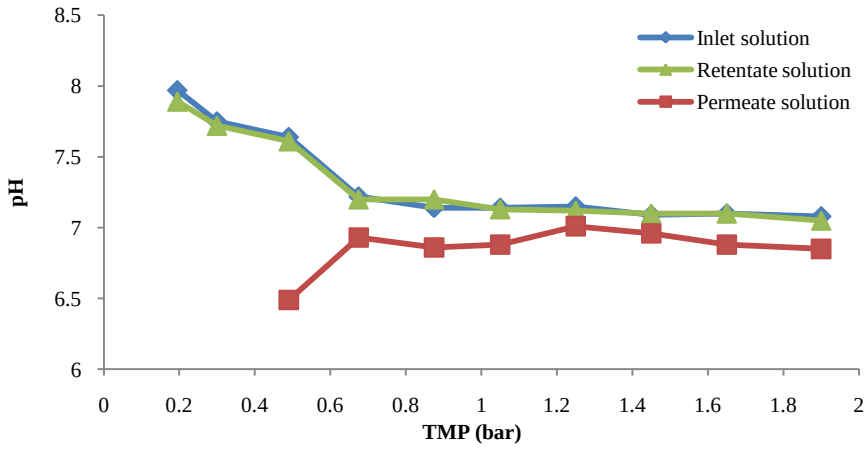

Figure 8-53. pH of magnesium chloride solution versus TMP.

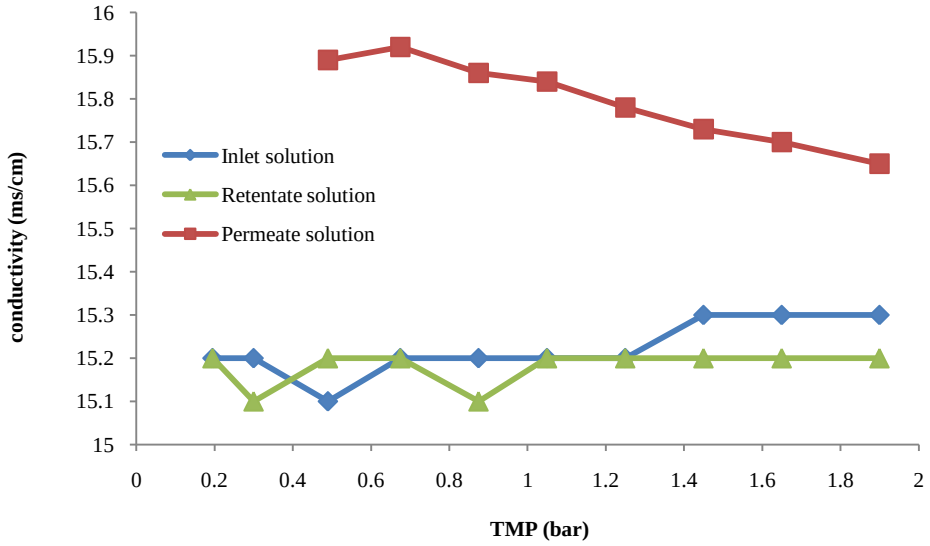

Figure 8-54. Conductivity of magnesium chloride solution versus TMP.

The second solution was prepared by diluting calcium chloride ($CaCl_2$) in distilled water. $CaCl_2$ permeate flux (volume flux based on the membrane area) through the membrane increased from 3.8E-07 to 6.6E-06 $m^3/m^2/s$ as the TMP increased. The rejection of calcium (Ca^{2+}) ions was lower than the rejection of chloride (Cl^{1-}) ions. When excluding the lowest TMP value, the rejection of both ions remained constant as the TMP increased. The highest rejection of both ions was at the lowest TMP, where the rejection of Ca^{2+} was about 37.4% and rejection of Cl^{1-} was about 40.0%. See Figure 8-55. When comparing the permeation of distilled water through the membrane, before and after calcium chloride ($CaCl_2$) solution permeation through the membrane, it was found that distilled water permeation was higher than the permeation of the calcium chloride ($CaCl_2$) solution. This means that fouling did not occur or was weak and did not have an effect on separation. The pH and conductivity of the inlet, retentate and permeate were measured. The pH of the inlet and the retentate decreased as the TMP increased, while the pH of permeate increased as the TMP increased. See Figure 8-56. The conductivity of the inlet, retentate and permeate almost remained constant as the TMP increased. This is true for permeate conductivity when excluding it at the lowest TMP value. The permeate conductivity was higher than the inlet and the retentate conductivity. See Figure 8-57.

The lower rejection of Ca^{2+} than that of Cl^{1-} maybe due to the electrostatic interaction between the membrane charge (which is negative) and the ion charge. Since Ca^{2+} has an opposite sign from that of the membrane, it would cause attraction between the membrane and Ca^{2+}, thus Ca^{2+} would permeate more freely through the membrane. Since Ca^{2+} has a

smaller ion size than Cl^{1-}, as a result the Cl^{1-} ion has a higher rejection than the Ca^{2+} ion. Cl^{1-} ion rejection was due to their repulsion away from the membrane because they have the same charge as the membrane. As the TMP increased, the rejection of both ions (Ca^{2+} and Cl^{1-}) decreased and almost stayed constant. This may be due to the electro-neutrality condition at both sides of the membrane, where both ions (Ca^{2+} and Cl^{1-}) have to pass through the membrane to the permeate side to reach an electro-neutrality condition. In this case Ca^{2+} rejection should be higher than Cl^{1-} rejection because less amount of Ca^{2+} than Cl^{1-} should permeate through the membrane to obtain electro-neutrality condition, since Ca^{2+} have bigger valence than Cl^{1-}, but in this case Cl^{1-} rejection was higher. However, if OH^{1-} and H^{1+} ions are included, these rejection results can be explained. The pH of the inlet and retentate decreased as the TMP increased, which means that the membrane rejected H^{1+} ions. On the other hand, pH of permeate increased as TMP increased, which means that OH^{1-} ions permeated through the membrane easily. See Figure 8-56. As more OH^{1-} ions permeate though the membrane, fewer amounts of Cl^{1-} ions need to permeate through the membrane to obtain an electro-neutral condition at both sides of the membrane. As a result, the rejection of Cl^{1-} ions would be higher than the rejection of Ca^{2+} ions. Also, low rejection might be due to membrane charge shielding by Ca^{2+}, where the Donnan exclusion effect would decrease and as a result, rejection of ions decrease.

The third solution that was used was prepared by diluting sodium chloride (NaCl) in distilled water. See section 8.5.3.2.1 (previous section).

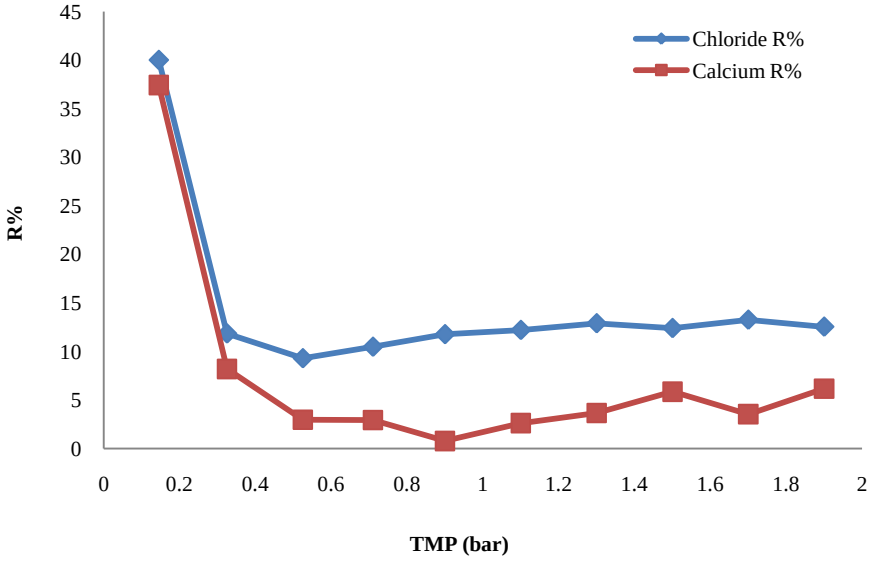

Figure 8-55. Calcium chloride rejection versus TMP.

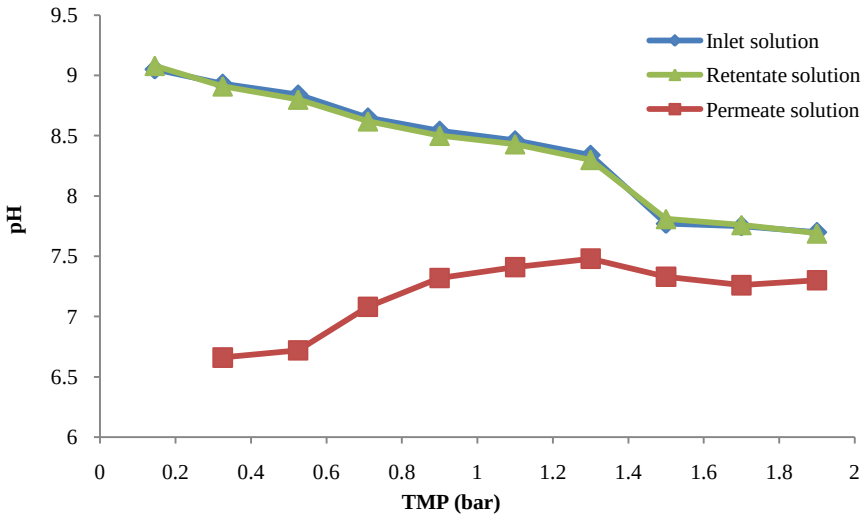

Figure 8-56. pH of calcium chloride solution versus TMP.

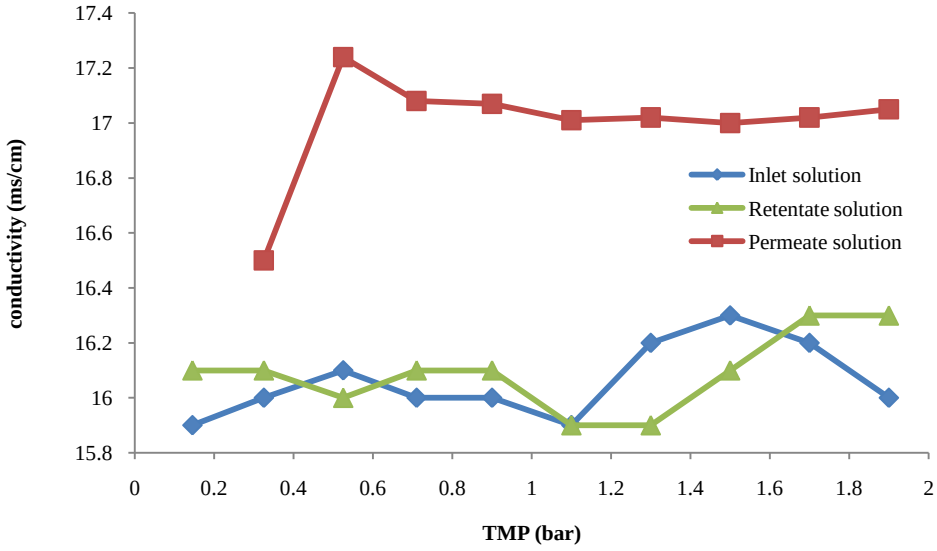

Figure 8-57. Conductivity of calcium chloride solution versus TMP.

The fourth solution was prepared by diluting sodium chloride (NaCl), magnesium chloride ($MgCl_2$) and calcium chloride ($CaCl_2$) in distilled water. See Figure 8-58. The mixed salt solution permeates flux (volume flux based on the membrane area) through the membrane increased from 2.7E-07 to 4.6E-05 $m^3/m^2/s$ as the TMP increased. It was found that the rejection of ions took the following trend: R of chloride (Cl^{1-}) > R of calcium (Ca^{2+}) > R of magnesium (Mg^{2+}) > R of sodium (Na^{1+}). The rejection of all cations decreased after the first TMP and then remained almost constant as the TMP increased. The highest rejection for all cations was at the lowest TMP. The highest Ca^{2+} rejection was about 43.1%, the highest Mg^{2+} rejection 42.1%, and the highest Na^{1+} rejection was about 33.0%. In general, cation Na^{1+} had

negative rejection values, which means that it permeated freely through the membrane. The rejection of cation Cl^{1-} decreased after the first TMP and almost stayed constant as the TMP increased. The highest Cl^{1-} rejection was about 44.6%. When comparing the permeation of distilled water through the membrane, before and after the mixed solution permeation through the membrane, it was found that distilled water permeation was higher than that of the mixed solution. This means that fouling did not occur or was weak and did not have an effect on separation. The pH and conductivity of the inlet, retentate and permeate were measured. The pH of the inlet, retentate and permeate decreased as the TMP increased. See Figure 8-59. The conductivity of the inlet, retentate and permeate almost remained constant as the TMP increased. The permeate conductivity was higher than the inlet and the retentate conductivity. See Figure 8-60.

The rejection of ions took the following trend: R of chloride (Cl^{1-}) > R of calcium (Ca^{2+}) > R of magnesium (Mg^{2+}) > R of sodium (Na^{1+}). When excluding the lowest TMP pressure, the rejection of ions almost remained constant as the TMP increased. Na^{1+} had the lowest rejection with negative values. The rejection values of these ions can be explained by the ion charge, where Cl^{1-} has a negative charge the same as the membrane charge, which caused repulsion between the membrane and Cl^{1-} ion; as a result, Cl^{1-} ion rejection was higher than the other ion rejections, while the cations Ca^{2+}, Mg^{2+} and Na^{1+} had the opposite charge sign of that of the membrane, which caused attraction between the cations and the membrane, thus they permeated more freely through the membrane. Also, ion size plays part in the rejection results, where the ion size of the cations and anion used took the following trend: (Cl^{1-}) ion size > calcium (Ca^{2+}) ion size > sodium (Na^{1+}) ion size > magnesium (Mg^{2+}) ion size. Since Cl^{1-} ion has the biggest ion size, as a result Cl^{1-} ion had the highest rejection. Then Ca^{2+} ion had the second-highest rejection. However, this cannot explain why Mg^{2+} had a higher rejection than Na^{1+}, even though the Na^{1+} ion has a bigger ion size than the Mg^{2+} ion. In general, the low rejection values of the three cations and one anion might be due to the electro-neutrality condition at both sides of the membrane, where ions permeate from the feed side (high concentration) to the permeate side (lower concentration) to fulfil the charge equilibrium condition. In addition, low rejection values may be due to higher TMP values, where it became stronger than the other factors causing lower ion rejection. Beside this, if membrane charge shielding by the cations took place, ions would permeate through the membrane and rejection decreases.

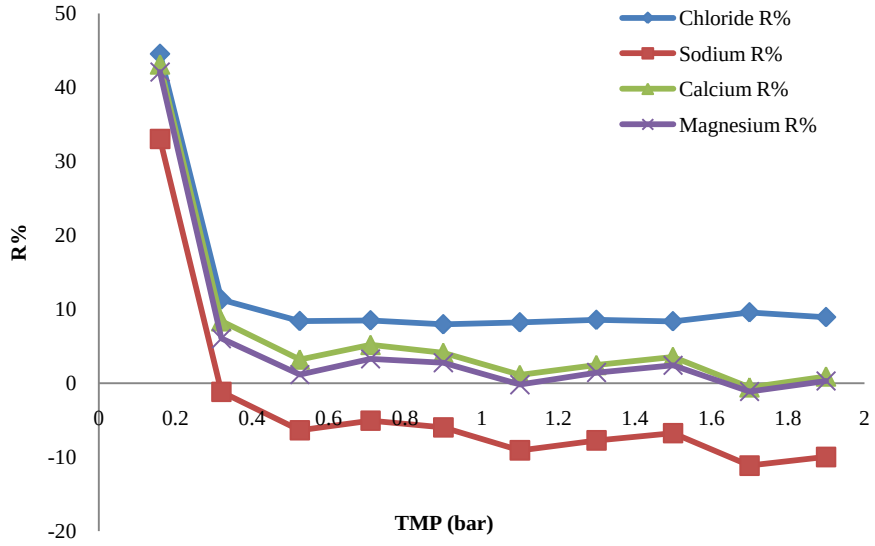

Figure 8-58. Mixed salts rejection versus TMP.

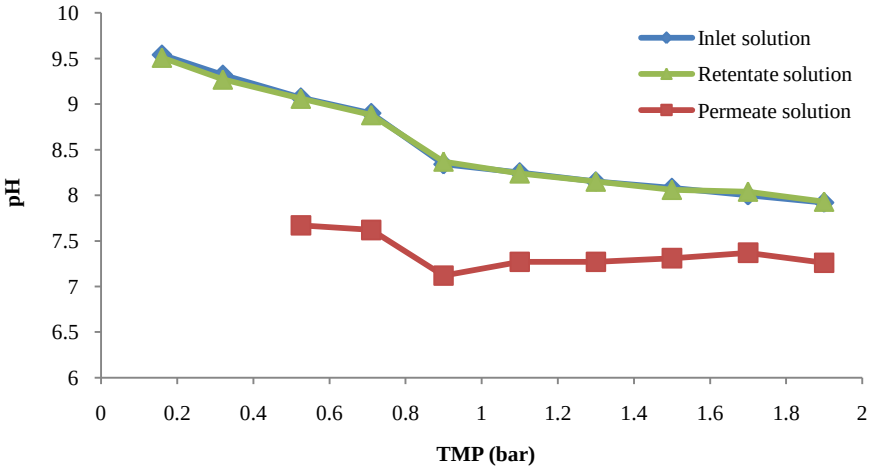

Figure 8-59. pH of Mixed salts solution versus TMP.

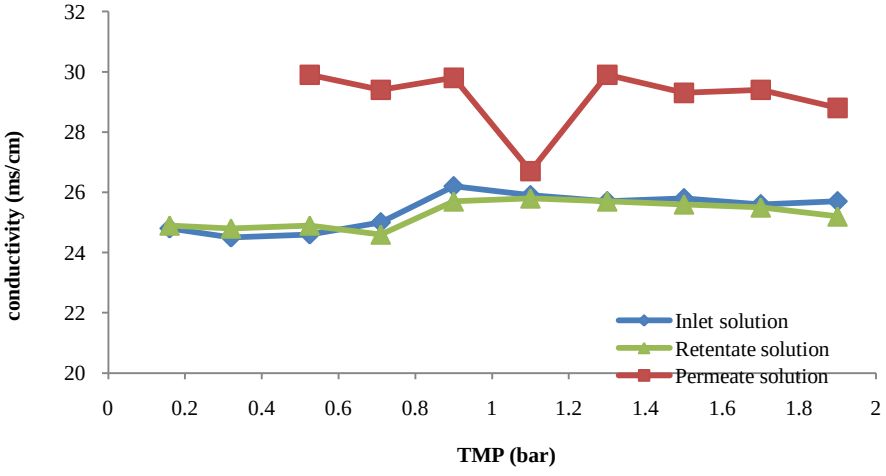

Figure 8-60. Conductivity of mixed salts solution versus TMP.

When comparing the separation of ions from a single salt solution and a mixed salt solution, it was noticed that the rejection of cation Mg^{2+} from a mixed salt solution was higher than its rejection from a single salt solution. For the Ca^{2+} ion case, its rejection from a single salt solution was lower than a mixed salt solution. For the Na^{1+} case, its rejection from a single salt solution was higher than a mixed salt solution. For Cl^{1-} ion case, its rejection from calcium chloride and a mixed salt solution was higher than its rejection from magnesium chloride and sodium chloride solutions. This implies that its rejection did depend on other ion types or its concentration in the solution.

8.5.4 Different concentration experiments

Another set of experiments was used for both 0.9 and 1.0nm membranes at different concentration. The used salts were magnesium chloride ($MgCl_2$) and sodium nitrate ($NaNO_3$), at a concentration value equal to 0.01 M. At first, a single salt solution of each salt was prepared at 0.01M concentration. Secondly, a mixed solution of both salts was prepared with 0.01M concentration for each salt. The experimental procedure used is the same procedure mentioned in section 8.3.2. This was done to study the effect of concentration on the separation of ions.

8.5.4.1 0.9 nm membrane

The first solution was prepared by diluting sodium nitrate ($NaNO_3$) in distilled water. $NaNO_3$ permeate flux (volume flux based on the membrane area) through the membrane increased from 1.1E-07 to 2.10E-06 $m^3/m^2/s$ as the TMP increased. When excluding the minimum TMP value, it was found that the rejection of nitrate (NO_3^{1-}) ions was lower than the rejection of sodium (Na^{1+}) ions. Also, the rejection of NO_3^{1-} and Na^{1+} remained constant as the TMP increased. The highest rejection for both ions was at the lowest TMP, where the rejection of NO_3^{1-} was about 46% and the rejection of Na^{1+} was about 42%. See Figure 8-61. When comparing this experiment (M = 0.01mol/l) with the previous one (M = 0.1mol/l), it was found that the rejection of both NO_3^{1-} and Na^{1+} from the lower concentration solution was higher than their rejection from the higher concentration solution. In the previous experiment (mentioned in section 8.3.3.1.1), the cation and anion had more negative values, which means that rejection did not take place and the ions were passing through the membrane, while for the lower concentration experiment, negative rejections barely excited. In general, for the lower concentration experiment, the rejection of Na^{1+} was higher than the rejection of NO_3^{1-}.

Rejections of NO_3^{1-} and Na^{1+} in the other experiment were almost similar. In addition, when comparing the permeation of distilled water through the membrane, before and after the $NaNO_3$ solution permeation through the membrane, it was found that distilled water permeation was higher than the $NaNO_3$ solution. This means that fouling did not occur and did not have an effect on separation. In addition, when comparing the permeation of distilled water through the membrane, before and after $NaNO_3$ solution permeation through the membrane, it was found that distilled water permeation was higher than the $NaNO_3$ solution. This means that fouling did not occur or it was weak and did not have an effect on separation. The pH and conductivity of the inlet, retentate and permeate were measured. The pH of the inlet, retentate and permeate increased as the TMP increased. See Figure 8-62. The conductivity of the inlet and retentate almost remained constant as the TMP increased. The permeate conductivity increased as the TMP increased, until the TMP reached 1.1 bar, then the permeate conductivity remained constant as the TMP increased. The permeate conductivity was lower than the inlet and the retentate conductivity. See Figure 8-63.

When excluding the rejections of NO_3^{1-} and Na^{1+} at the lowest TMP, it was found that the rejection of Na^{1+} was higher than the rejection of NO_3^{1-}; this cannot be explained by the ion charge effect or the ion size. Because Na^{1+} has an opposite charge of the membrane charge where attraction occurs, thus causing the Na^{1+} to pass more freely through the membrane but this did not happen. Also, it has a smaller ion size than NO_3^{1-} where it should pass more freely through the membrane, but in this case it had a higher rejection. Moreover, at the lowest TMP value, the rejection of NO_3^{1-} was higher than the rejection of Na^{1+}, which is because NO_3^{1-} has a bigger ion size than Na^{1+}, where the Na^{1+} ion can permeate more freely through the membrane. Moreover, because NO_3^{1-} ion has the same charge sign as the membrane, this would cause repulsion between them and forcing the NO_3^{1-} ion to move back to the solution. See Figure 8-61. Low rejection may be related to electro-neutrality condition, where NO_3^{1-} and Na^{1+} ions permeate through the membrane (from high concentration to low concentration) to stabilise the system. In addition, if membrane charge shielding occurred, this would cause low rejection of Na^{1+} and NO_3^{1-} because Donna exclusion would not have an effect on rejection. In general, the low rejection values for both NO_3^{1-} and Na^{1+} may be due to TMP, where rejection decreased as the TMP increased, which means that convection transport increased as TMP increased and had more effect on NO_3^{1-} and Na^{1+} rejections than ion charge and ion size.

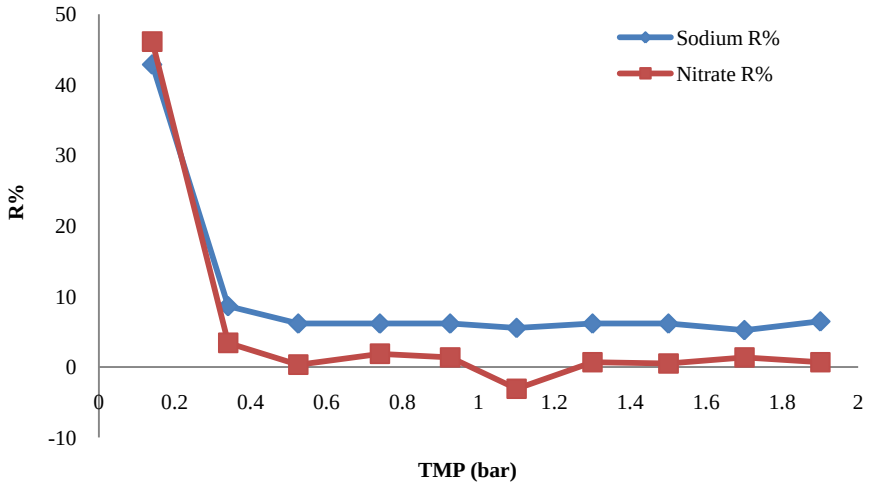

Figure 8-61. $NaNO_3$ rejection versus TMP, M = 0.01mol/l.

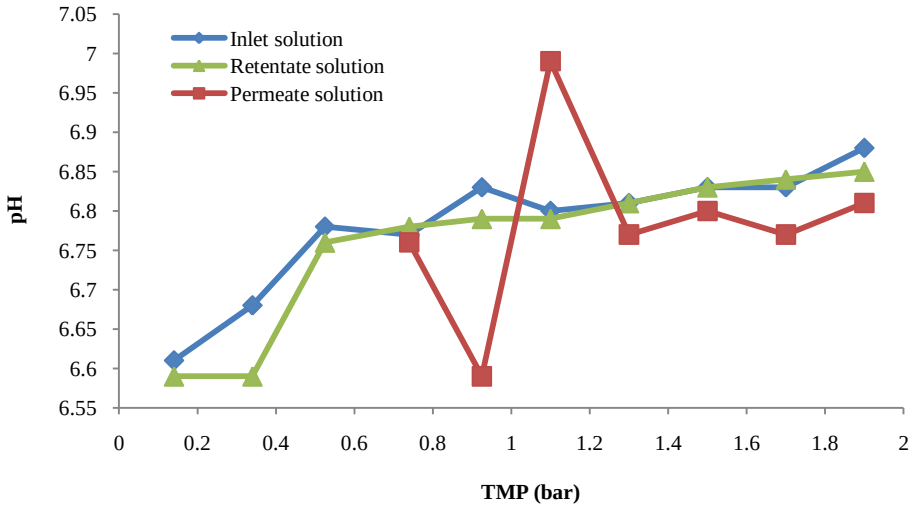

Figure 8-62. pH of $NaNO_3$ solution versus TMP.

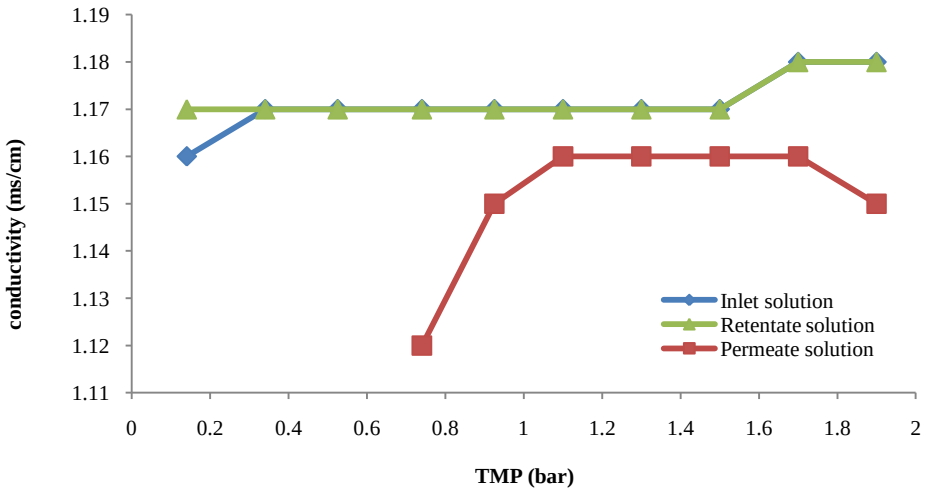

Figure 8-63. Conductivity of $NaNO_3$ solution versus TMP.

The second solution was prepared by diluting magnesium chloride ($MgCl_2$) in distilled water. $MgCl_2$ permeate flux (volume flux based on the membrane area) through the membrane increased from 1.25E-07 to 1.88E-06 $m^3/m^2/s$ as the TMP increased. The rejection of Mg^{2+} ions was slightly higher than the rejection of Cl^{1-} ions. The highest rejection for both ions was at the lowest TMP, where the rejection of Cl^{1-} was about 13% and the rejection of Mg^{2+} was about 36%. When excluding the minimum TMP value, in general it can be noticed that the rejection of Cl^{1-} and Mg^{2+} increased slightly as the TMP increased. See Figure 8-64. Also, when comparing the permeation of distilled water through the membrane, before and after $MgCl_2$ solution permeation through the membrane it was found that distilled water permeation was higher than the $MgCl_2$ solution. This means that fouling did not occur or it was weak and did not have an effect on separation. The pH and conductivity of the inlet, retentate and permeate were measured. The pH of the inlet and retentate increased as the TMP increased, while the pH of the permeate decreased as TMP increased. See Figure 8-65. The conductivity of the inlet and retentate almost remained constant as the TMP increased. The permeate conductivity decreased as the TMP increased. The permeate conductivity was lower than the inlet and the retentate conductivity. See Figure 8-66.

The rejection of Mg^{2+} was higher than the rejection of Cl^{1-}; this cannot be explained by the ion charge effect or the ion size because Mg^{2+} has an opposite sign of the membrane charge where attraction should occur, which causes Mg^{2+} to permeate more freely through the membrane, but this did not happen. Also, it has a smaller ion size than Cl^{1-} where it should pass more freely through the membrane, but in this case it had a higher rejection. These results might be explained by the permeation of H^{1+} and OH^{1-} through the membrane to obtain electro-neutral condition at both sides of the membrane. From Figure 8-65, it can be noticed that the permeate pH decreased as TMP increased, which means that more H^{1+} ions were permeating through the membrane; as a result, Mg^{2+} rejection increased and was higher than Cl^{1-} rejection. In general, the low rejection values for both Cl^{1-} and Mg^{2+} might be due to electro-neutrality condition. In order to reach the electro-neutral condition at both sides of the membrane, Cl^{1-} and Mg^{2+} ions had to pass through the membrane, thus they had low rejection values. When comparing this experiment (M = 0.01mol/l) with the previous one (M = 0.1mol/l), it was found that the rejection of both Mg^{2+} and Cl^{1-} from a lower concentration solution was higher than their rejection from a higher concentration solution. In the previous experiment (mentioned in section 8.3.3.1.2), the cation had more negative values, which means that rejection did not take place and the ions were passing through the membrane. This

means that membrane charge shielding was more effective as the ion concentration increased, which decreased ion rejection. In general, for the lower concentration experiment, the rejection of Mg^{2+} was higher than the rejection of Cl^{1-}. On the other hand, for the higher concentration experiment, the rejection of Cl^{1-} was higher than the rejection of Mg^{2+}.

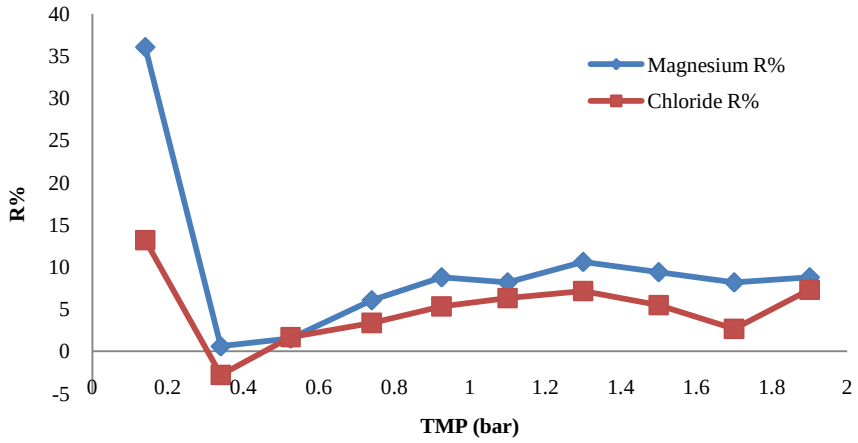

Figure 8-64. $MgCl_2$ rejection versus TM, M = 0.01mol/l.

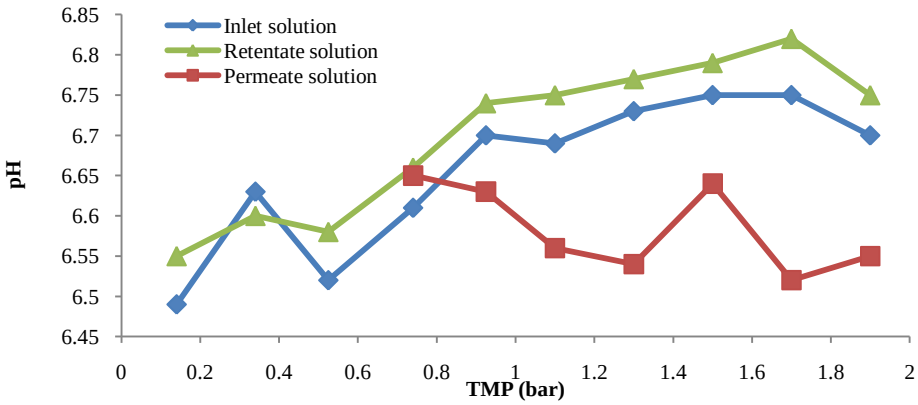

Figure 8-65. pH of $MgCl_2$ solution versus TMP.

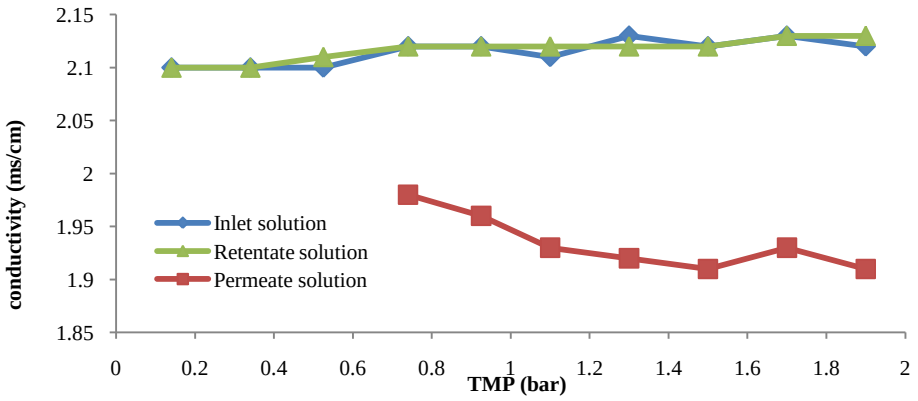

Figure 8-66. Conductivity of $MgCl_2$ solution versus TMP.

The third solution was prepared by diluting magnesium chloride ($MgCl_2$) and sodium nitrate ($NaNO_3$) in distilled water. The mixed salt solution permeates flux (volume flux based on the membrane area) through the membrane increased from 1.07E-07 to 1.80E-06 $m^3/m^2/s$ as the TMP increased. The rejection of ions took the following trend: R of magnesium (Mg^{2+}) > R of nitrate (NO_3^{1-}) > R of chloride (Cl^{1-}) > R of sodium (Na^{1+}). See Figure 8-67. This is true except at the lowest TMP, where the rejection of the Na^{1+} ion was higher than the rejection of the Cl^{1-} ion. The highest rejection for all ions was at the lowest TMP, where the rejection of Cl^{1-} was about 45.3%, the rejection of NO_3^{1-} 55.4%, the rejection of Na^{1+} 47.4% and the rejection of Mg^{2+} was about 55.5%. When excluding the minimum TMP value, it can be noticed that the rejection of Cl^{1-}, NO_3^{1-}, Na^{1+} and Mg^{2+} remained constant as the TMP increased. In addition, when comparing the permeation of distilled water through the membrane, before and after mixed salt solution permeation through the membrane, it was found that distilled water permeation was higher than the mixed salt solution. This means that fouling did not occur or was weak and did not have an effect on separation. The pH and conductivity of the inlet, retentate and permeate were measured. The pH of the inlet and retentate increased as the TMP increased, while the pH of permeate decreased as TMP increased, but when TMP reached 1.1 bar, the permeate pH increased as TMP increased. See Figure 8-68. The conductivity of the inlet, retentate and permeate almost remained constant as the TMP increased. See Figure 8-69.

In general, the low rejection values of the anions and cations may be due to Donnan exclusion and electro-neutrality condition. Because of the electro-neutrality at both sides of the membrane, Cl^{1-}, NO_3^{1-}, Na^{1+} and Mg^{2+} ions had to pass through the membrane in order to reach electro-neutrality condition at both sides of the membrane, which might explain the low rejection values. Since Cl^{1-} and NO_3^{1-} have the same charge sign as the membrane, both ions would repel away from the membrane and back to the solution. On the other hand, Mg^{2+} and Na^{1+} had an opposite sign of the membrane, which would cause attraction between Mg^{2+} and Na^{1+} and the membrane, and as a result, they would pass freely through the membrane. This is known as Donnan exclusion. This is true when comparing Cl^{1-} and NO_3^{1-} rejections with Na^{1+} rejection but not with Mg^{2+} rejection. Also when comparing the rejection of Cl^{1-} with the rejection of NO_3^{1-}, it was found the rejection of Cl^{1-} was lower than the rejection of NO_3^{1-}. This result might be due to the ion size, where Cl^{1-} ion size is smaller than NO_3^{1-} ion size; as a result, the Cl^{1-} ion would be able to pass through the membrane more freely. When comparing the rejection of Na^{1+} and Mg^{2+}, it was found that the rejection of Mg^{2+} was higher

than the rejection of Na^{1+}. This cannot be explained by ion size because Mg^{2+} ion has a smaller ion-size than Na^{1+}, where Mg^{2+} rejection should have been lower than Na^{1+}. This rejection result might be related to Mg^{2+} ability to diffuse through the membrane; if Mg^{2+} diffusivity through the membrane is lower than Na^{1+} then as a result its rejection would be low. If H^{1+} and OH^{1-} permeation through the membrane is included, Mg^{2+} rejection behaviour might be explained. The permeation of H^{1+} through the membrane is high; see Figure 8-68, where the inlet and retentate pH increased as TMP increased, which means that the solution is more basic. As H^{1+} permeation through the membrane increases, either Mg^{2+} or Na^{1+} rejection would decrease. In this case, it was Mg^{2+} because it has a smaller ion size.

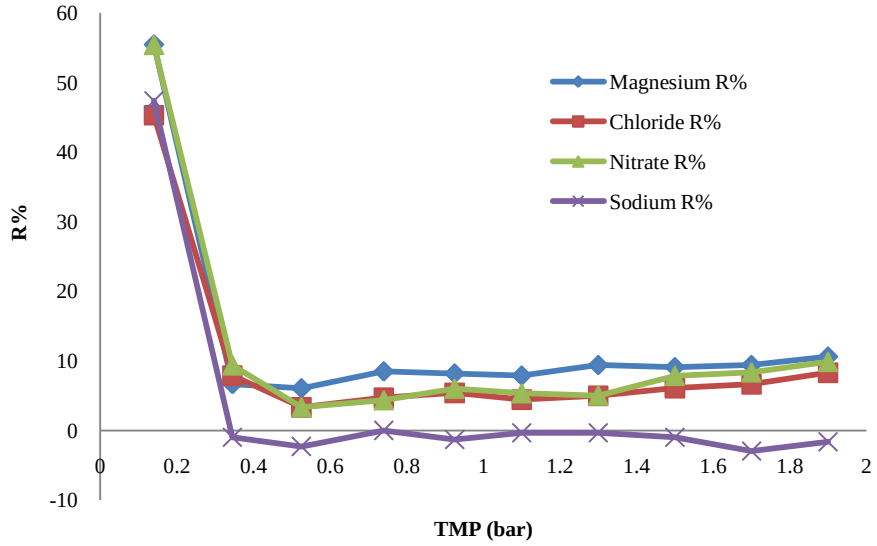

Figure 8-67. Mixed salt solution rejection versus TMP, M = 0.01mol/l for each salt.

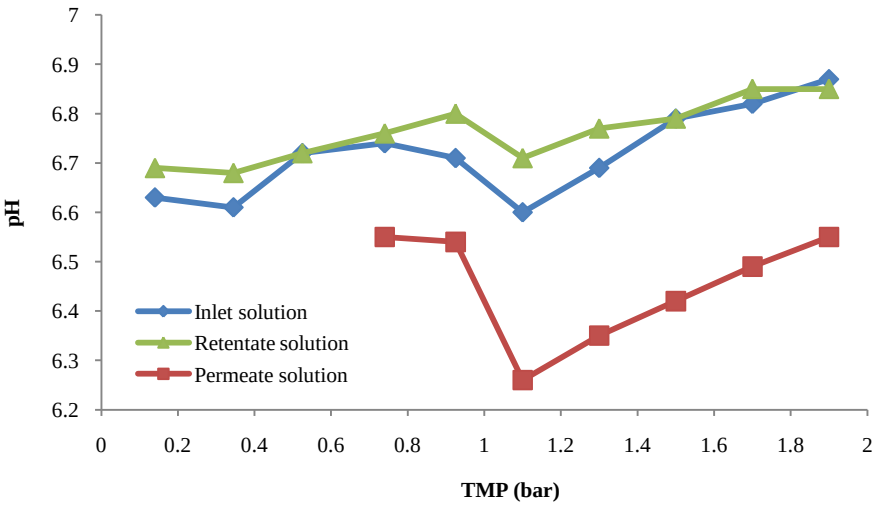

Figure 8-68. pH of mixed salts solution versus TMP.

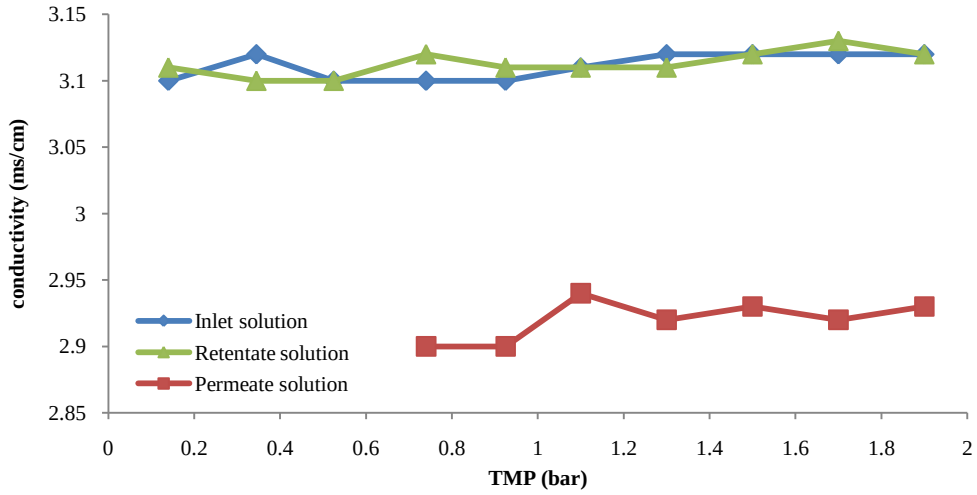

Figure 8-69. Conductivity of mixed salts solution versus TMP.

8.5.4.2 1.0 nm membrane

The first solution was prepared by diluting sodium nitrate ($NaNO_3$) in distilled water. $NaNO_3$ solution permeate flux (volume flux based on the membrane area) through the membrane increased from 9.1E-07 to 1.5E-05 $m^3/m^2/s$ as the TMP increased. The rejection of nitrate (NO_3^{1-}) ions was higher than the rejection of sodium (Na^{1+}) ions. The rejection of NO_3^{1-} decreased as the TMP increased, until TMP reached 0.735 bar value, then the rejection of NO_3^{1-} slightly increased and almost remained constant as the TMP increased. The rejection of Na^{1+} decreased as the TMP increased, until TMP reached 0.9 bar, then it started to increase as the TMP increased. The highest rejection for both ions was at the lowest TMP, where the rejection of NO_3^{1-} was about 15.3% and the rejection of Na^{1+} was about 11.6%. The pH and conductivity of the inlet, retentate and permeate were measured. The pH of the inlet and retentate increased as the TMP increased, while the permeate pH slightly decreased as TMP increased. See Figure 8-71. The conductivity of the inlet, retentate and permeate almost remained constant as the TMP increased. See Figure 8-72.

The rejection of Na^{1+} was lower than the rejection of NO_3^{1-}; this can be explained by the ion charge effect and ion size. Na^{1+} has an opposite charge of that of the membrane charge, where attraction occurred and caused the cation to pass more freely through the membrane. On the other hand, NO_3^{1-} has the same charge sign as the membrane, which caused repulsion between them and resulted in the rejection of NO_3^{1-} ions. In addition, Na^{1+} has a smaller ion size than NO_3^{1-}, where it could pass more freely through the membrane, and as a result, it had lower rejection than the rejection of NO_3^{1-}. See Figure 8-70. Furthermore, low rejection may

be related to electro-neutrality condition, where NO_3^{1-} and Na^{1+} ions permeate through the membrane (from high concentration to low concentration) to stabilise the system. When comparing this experiment (M = 0.01mol/l) with the previous one (M = 0.1mol/l), it was found that the rejections of Na^{1+} from both solutions were similar and lower than NO_3^{1-}, while the rejection of NO_3^{1-} from a higher concentration solution was higher than its rejection from a lower concentration solution (see section 8.5.3.2.1). In general, the rejection decreased as the TMP increased, which means that convection transport increased as the TMP and had more effect on NO_3^{1-} and Na^{1+} rejections than ion charge and ion size. Even though, as the TMP reached 0.9 bar, the rejection of ions increased as the TMP increased, which means that convective transport decreased as the TMP increased, still the rejection values were small and convective transport played a major role on rejection.

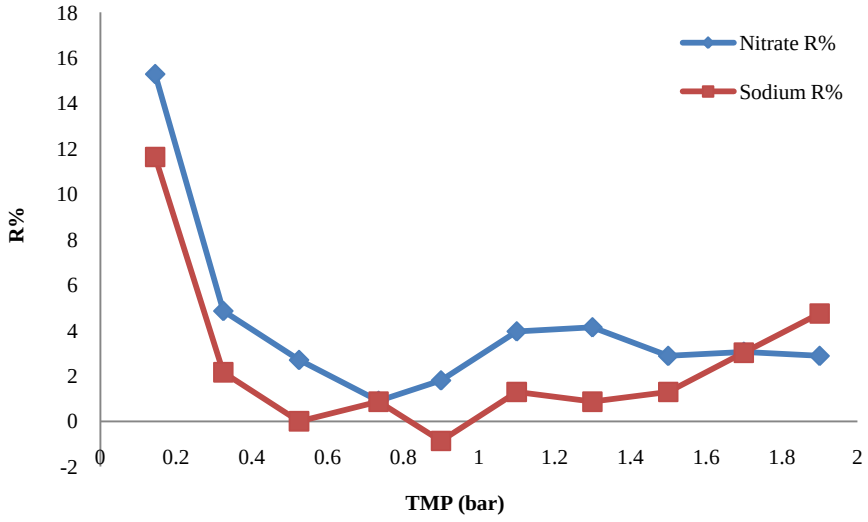

Figure 8-70. $NaNO_3$ rejection versus TMP, M = 0.01mol/l.

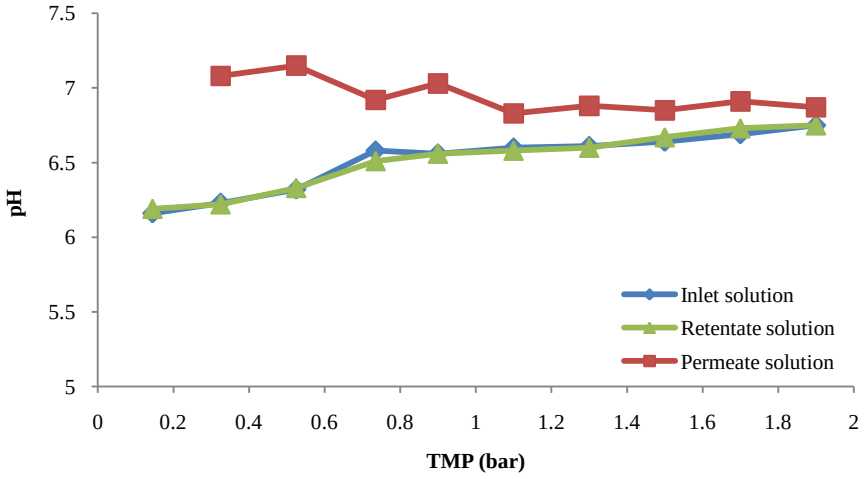

Figure 8-71. pH of $NaNO_3$ solution versus TMP.

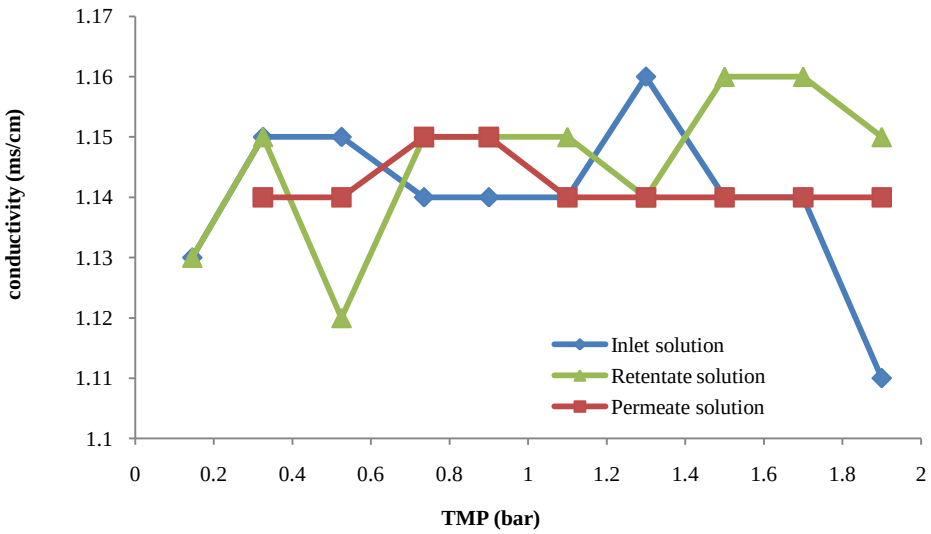

Figure 8-72. Conductivity of $NaNO_3$ solution versus TMP.

The second solution was prepared by diluting magnesium chloride ($MgCl_2$) in distilled water. $MgCl_2$ solution permeates flux (volume flux based on the membrane area) through the membrane increased from 6.6E-07 to 1.30E-05 $m^3/m^2/s$ as the TMP increased. The rejection of Cl^{1-} ions was slightly higher than the rejection of Mg^{2+} ions. The highest rejection for both ions was at the lowest TMP, where the rejection of Cl^{1-} was about 14.4% and the rejection of Mg^{2+} was about 11%. When excluding the minimum TMP value, in general it can be noticed that the rejection of Cl^{1-} and Mg^{2+} increased slightly as the TMP increased. See Figure 8-73. When comparing the permeation of distilled water through the membrane, before and after $MgCl_2$ solution permeation through the membrane, it was found that distilled water permeation was higher than $MgCl_2$ solution. This means that fouling did not occur or it was weak and did not have an effect on separation. The pH and conductivity of the inlet, retentate and permeate were measured. The pH of the inlet and retentate remained constant as the TMP increased, except when TMP was equal to 1.1 bar where they decreased. The pH of permeate remained constant as TMP increased, except when TMP was equal to 0.335 and 0.925 bar where it increased. See Figure 8-74. In general, the conductivity of the inlet and retentate increased as the TMP increased. On the other hand, the permeate conductivity decreased as the TMP increased, and it was lower than the inlet and retentate conductivity. See Figure 8-75.

In general, the low rejection values for both Cl^{1-} and Mg^{2+} may be due to the electro-neutrality condition, where Cl^{1-} and Mg^{2+} ions had to pass through the membrane in order to attain the electro-neutrality condition at both sides of the membrane. When excluding the

lowest TMP, the rejection of both Cl^{1-} and Mg^{2+} ions increased slightly as TMP increased, which indicates that convective transport decreased as TMP increased. Moreover, the rejection of Mg^{2+} was lower than the rejection of Cl^{1-}, which can be explained by the ion charge effect and ion size. Since Mg^{2+} has an opposite sign of the membrane charge, as a result, attraction occurred and caused the cation to pass more freely through the membrane, while Cl^{1-} has the same charge sign as the membrane, which caused Cl^{1-} to repulse away from the membrane and back to solution, thus, it had higher rejection than the rejection of Mg^{2+}. Beside this, Mg^{2+} has a smaller ion size than Cl^{1-} where it increased Mg^{2+} ability to permeate more freely through the membrane. This means that Donnan exclusion and ion size had an effect on the rejection of Mg^{2+} and Cl^{1-}. The permeation of H^{1+} and OH^{1-} can be considered to be negligible because the pH of the inlet, retentate and permeate remained constant as the TMP increased, and the pH values were similar. See Figure 8-74.

When comparing this experiment (M = 0.01mol/l) with the previous one (M = 0.1mol/l), it was found that the rejection of both Mg^{2+} and Cl^{1-} from the lower concentration solution was higher than their rejection from the higher concentration solution. In the previous experiment (mentioned in section 8.3.3.1.2), Mg^{2+} had more negative values, which means that rejection did not take place and the ions were permeating through the membrane. The lower rejection at a higher concentration might be due to membrane charge shielding by the ions, where the membrane charge would be neutralised by the ions consequently, the membrane rejection ability decreases. In general, for both concentration experiments, the rejection of Mg^{2+} was lower than the rejection of Cl^{1-}.

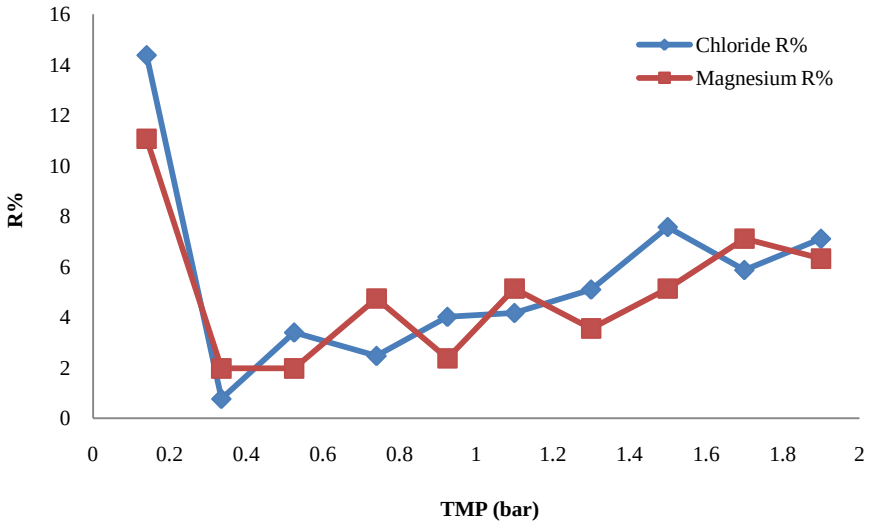

Figure 8-73. $MgCl_2$ rejection versus TMP, M = 0.01mol/l.

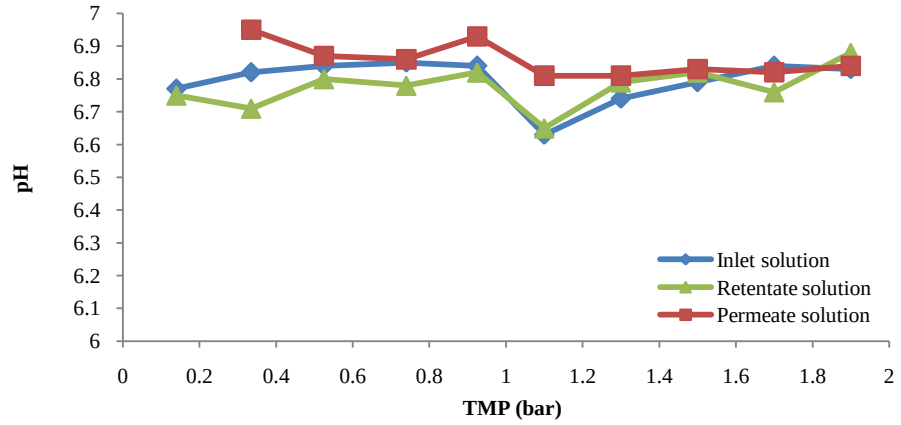

Figure 8-74. pH of $MgCl_2$ solution versus TMP.

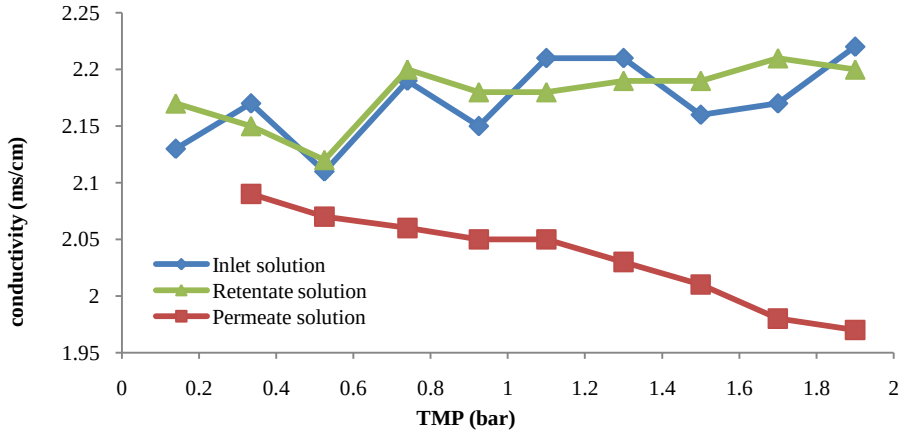

Figure 8-75. Conductivity of $MgCl_2$ solution versus TMP.

The third solution was prepared by diluting magnesium chloride ($MgCl_2$) and sodium nitrate ($NaNO_3$) in distilled water. The mixed salt solution permeates flux (volume flux based on the membrane area) through the membrane increased from 6.5E-07 to 1.30E-05 $m^3/m^2/s$ as the TMP increased. It was found that the rejection of ions took the following trend: R of magnesium (Mg^{2+}) > R of nitrate (NO_3^{1-}) > R of chloride (Cl^{1-}) > R of sodium (Na^{1+}). See Figure 8-76. The highest rejection for all the ions was at the lowest TMP, where the rejection of Cl^{1-} was about 16.4%, the rejection of NO_3^{1-} was about 19.8%, the rejection of Na^{1+} was about 4.8% and the rejection of Mg^{2+} was about 20.0%. When excluding the minimum TMP value, the rejection of Cl^{1-}, NO_3^{1-}, Na^{1+} and Mg^{2+} remained constant as the TMP increased. An exception for this result is at the TMP value equal to 1.1 bar for Mg^{2+}. When comparing the permeation of distilled water through the membrane, before and after the mixed salt solution permeation through the membrane, it was found that distilled water permeation was higher than the mixed salt solution. This means that fouling did not occur or it was weak and

did not have an effect on separation. The pH and the conductivity of the inlet, retentate and permeate were measured. The pH of the inlet, retentate and permeate almost remained constant as the TMP increased. See Figure 8-77. In general, the conductivity of the inlet and retentate did not have a specific trend as the TMP increased, but the difference between the highest and smallest readings was small. On the other hand, the permeate conductivity remained constant as the TMP increased. See Figure 8-78. In general, the low rejection values of the anions and cations may be due to the electro-neutrality condition. Because the electro-neutrality condition at both sides of the membrane must be maintained all the time, Cl^{1-}, NO_3^{1-}, Na^{1+} and Mg^{2+} ions had to pass through the membrane in order to reach electro-neutrality at both sides of the membrane. The rejection result for these ions can be explained by Donnan exclusion and ion size except for Mg^{2+}. When comparing the rejection of Na^{1+} and Mg^{2+}, it was found that the rejection of Mg^{2+} was higher than the rejection of Na^{1+}. This cannot be explained by ion size because Mg^{2+} ion has smaller ion size than Na^{1+}, where Mg^{2+} rejection should have been lower than Na^{1+}. This rejection result might be related to Mg^{2+} ability to diffuse through the membrane. If Mg^{2+} diffusivity through the membrane was low then as a result, its rejection would be high. In addition, when comparing the rejection of Cl^{1-} with the rejection of NO_3^{1-}, it was found the rejection of Cl^{1-} was lower than the rejection of NO_3^{1-}. This result might be due to the ion size, where Cl^{1-} ion size is smaller than NO_3^{1-} ion size; as a result, the Cl^{1-} ion would be able to pass through the membrane more freely. NO_3^{1-} and Cl^{1-} have higher rejection than Na^{1+}, which is due to their charge and ion size. Since both ions have the same charge sign as the membrane, repulsion occurred between them and the membrane, hence a higher rejection than Na^{1+}. In addition, NO_3^{1-} and Cl^{1-} have a bigger ion size than Na^{1+}, which increased their rejection by membrane more than Na^{1+} rejection.

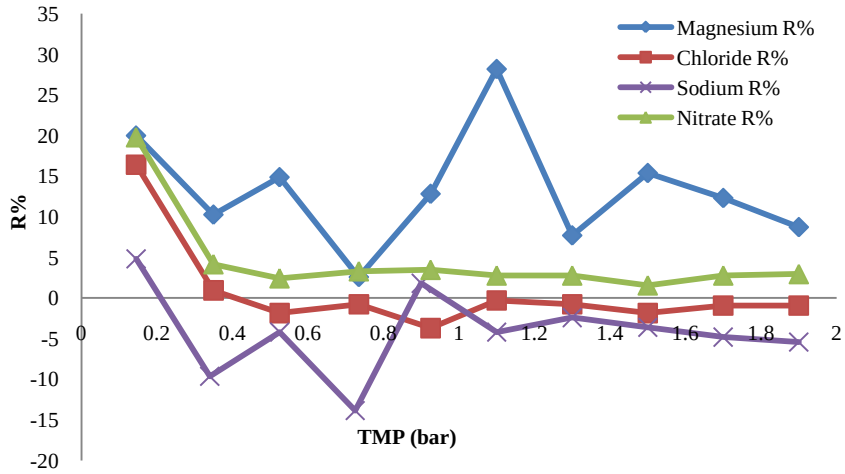

Figure 8-76. Mixed salt solution rejection versus TMP, M = 0.01mol/l for each salt.

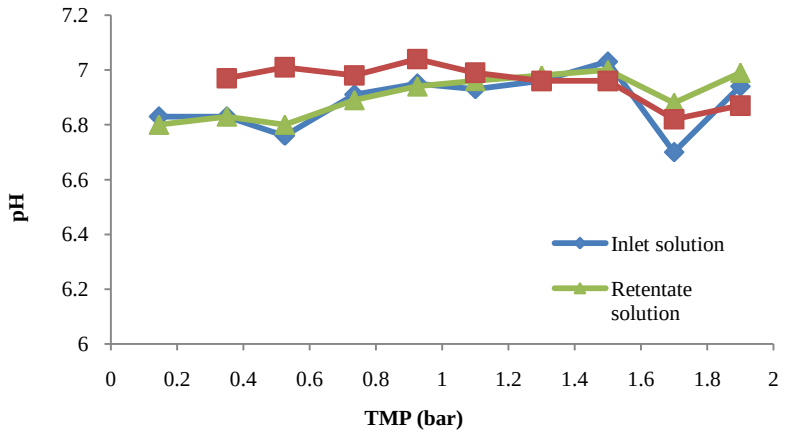

Figure 8-77. pH of mixed salt solution versus TMP.

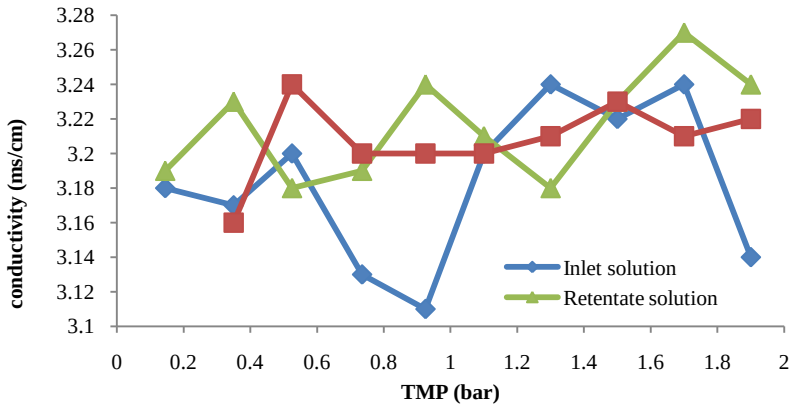

Figure 8-78. Conductivity of mixed salt solution versus TMP.

8.6 pH-controlled experiments

The effect of pH on the separation behaviour of the nanofiltration membrane was studied for single and mixed salt solutions (cation was the common ion). Three different pH values were used, which are 3, 7 and 10. The membrane that was used was a ceramic nanofiltration membrane (the membrane made of TiO_2, with 7.00 mm I.D, 10 mm O.D and length of 190 mm, with 1.0 nm mean pore radius, from Inopor Company).

8.6.1 Materials

The used salts used were sodium chloride (NaCl) and sodium sulphate (Na_2SO_4), where the cation Na^{1+} was the common ion. For single and mixed salt solution, a solution with a concentration of 0.1M for each salt was prepared at each pH value. The pH was controlled by an acidic and basic solution. The studied pH values were pH3, pH7 and pH10. The acid solution was 0.1M HCl, which was prepared from 5M HCl laboratory solution. The base

solution was 0.1M NaOH, which was prepared by diluting 2 g of NaOH in 500 ml of distilled water. To obtain pH 3, the solution was controlled with 0.1M HCl solution. Moreover, to obtain pH 7 and 10, the solutions were controlled with 0.1M NaOH solutions.

8.6.2 Experimental procedure

At the start of each experiment, distilled water was used at first in order to make sure that the membrane properties did not change. The results of distilled and brackish water were compared to describe the separation behaviour and to find out if fouling or concentration polarisation took place. At first, distilled water passed through the membrane at constant inlet volumetric flow rate equal to 2.78E-5 m^3/s (100 l/h). The inlet pressure was increased from 0.2 bar to 2.0 bar, which gives a TMP value between 0.15 bar to 1.9 bar. The pressure was increased at 0.5 intervals and run for 30 minutes for each TMP value. Permeate of distilled water was collected for 25 minutes. The pH and conductivity of the feed distilled water and the retentate was measured for each TMP value. The same procedure for single and mixed salt solutions was followed but the inlet pressure was increased each 60 minutes, where the permeate sample was collected for 55 minutes. The pH and conductivity at each TMP value were measured for the feed salt solution and the retentate to make sure that the process was stable and that the feed concentration did not change. After each experiment, the membrane was cleaned by 0.1M NaOH solution for 2 hours, and then cleaned by distilled water for at least 18 hours.

8.6.3 Results

8.6.3.1 pH 3

The first solution was prepared by diluting sodium chloride (NaCl) in distilled water, where the concentration was about 0.1M. Then the solution pH was adjusted to the value of 3 by using 0.1M HCl solution. NaCl permeate flux (volume flux based on the membrane area) through the membrane increased from 4.5E-07 to 8.1E-06 $m^3/m^2/s$ as the TMP increased. It was found that the rejection of chloride (Cl^{1-}) ions was lower than the rejection of sodium (Na^{1+}) ions. The highest rejection of both ions was at the lowest TMP, where the rejection of Cl^{1-} was about 24.9% and the rejection of Na^{1+} was about 25.4%. When excluding the lowest TMP value, the rejection of Na^{1+} slightly increased as the TMP increased. Whilst the rejection of Cl^{1-} remained constant as the TMP increased. When comparing the permeation of distilled water through the membrane, before and after sodium chloride (NaCl) solution

permeation through the membrane, it was found that distilled water permeation was higher than the sodium chloride (NaCl) solution. This means that fouling did not occur or it was weak and did not have an effect on separation. See Figure 8-79. The pH and conductivity of the inlet, retentate and permeate were measured. The pH of the inlet, retentate and permeate remained constant as the TMP increased. See Figure 8-80. The conductivity of the inlet decreased then increased as the TMP increased. Retentate conductivity did not have a specific trend as the TMP increased, but the difference between the highest and smallest readings was small. On the other hand, the permeate conductivity decreased as the TMP increased. The permeate conductivity was higher than the inlet and the retentate conductivity. See Figure 8-81.

In the case of sodium chloride (NaCl), the rejection of Na^{1+} was higher than the rejection of Cl^{1-}. These results cannot be explained by the ion size, because Cl^{1-} has a bigger ion size than Na^{1+} where Cl^{1-} should have a higher rejection than Na^{1+}. However, these results can be explained by the Donnan exclusion, which is the interaction between the membrane and ion charge. In this pH range, the membrane charge is considered to be positive; see section 8.3. Since Cl^{1-} has an opposite charge sign of the membrane charge, attraction would occur causing the Cl^{1-} ion to permeate easily through the membrane, resulting in low rejection. On the other hand, Na^{1+} has the same charge as the membrane charge, which caused repulsion between them, thus the membrane rejected the Na^{1+} ion. Because of the Donnan exclusion, Na^{1+} rejection was higher than Cl^{1-} rejection. The low rejection values for both ions might be due to the electro-neutrality condition and the membrane charge shielding. Due to the electro-neutrality condition, the ions had to move from the higher charge concentration area to the lower charge concentration area until the electro-neutrality condition at both sides of the membrane was reached. As the concentration of ions near the membrane surface starts to build up, as a result a membrane charge shielding by the ions would occur, which would decrease the rejection of Na^{1+} and Cl^{1-} because the Donnan exclusion effect would decrease? The membrane charge shielding effect might be very effective at the highest TMP because Na^{1+} rejection decreased and was lower than Cl^{1-}.

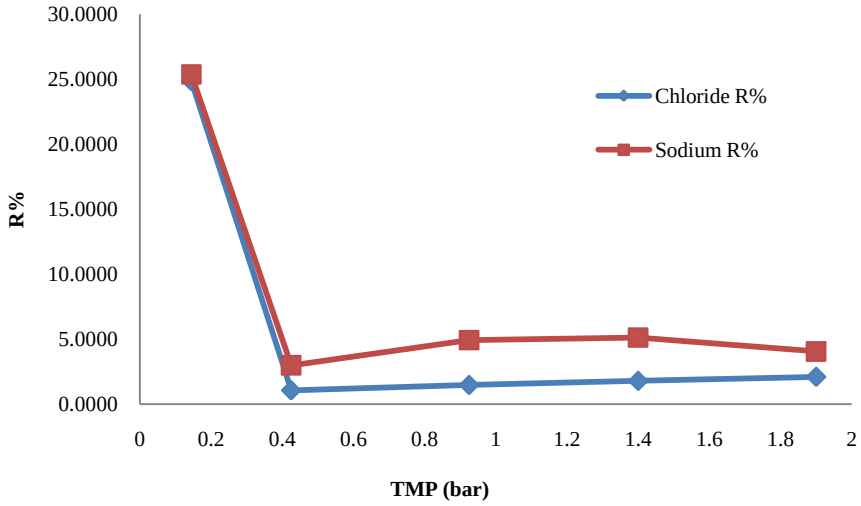

Figure 8-79. NaCl solution rejection versus TMP at pH = 3.

The second solution was prepared by diluting sodium sulphate (Na_2SO_4) in distilled water, where the concentration was about 0.1M. Then the solution pH was adjusted to the value of 3 by using 0.1M HCl solution. Na_2SO_4 permeate flux (volume flux based on the membrane area) through the membrane increased from 2.7E-07 to 5.8E-06 $m^3/m^2/s$ as the TMP increased. It was found that the rejection of sulphate (SO_4^{2-}) ions was lower than the rejection of sodium (Na^{1+}) ions. The highest rejection of both ions was at the lowest TMP, where the rejection of SO_4^{2-} was about 39.6% and the rejection of Na^{1+} was about 46.5%. When excluding the lowest TMP value, the rejection of SO_4^{2-} and Na^{1+} remained constant as the TMP increased. When comparing the permeation of distilled water through the membrane, before and after sodium sulphate (Na_2SO_4) solution permeation through the membrane, it was

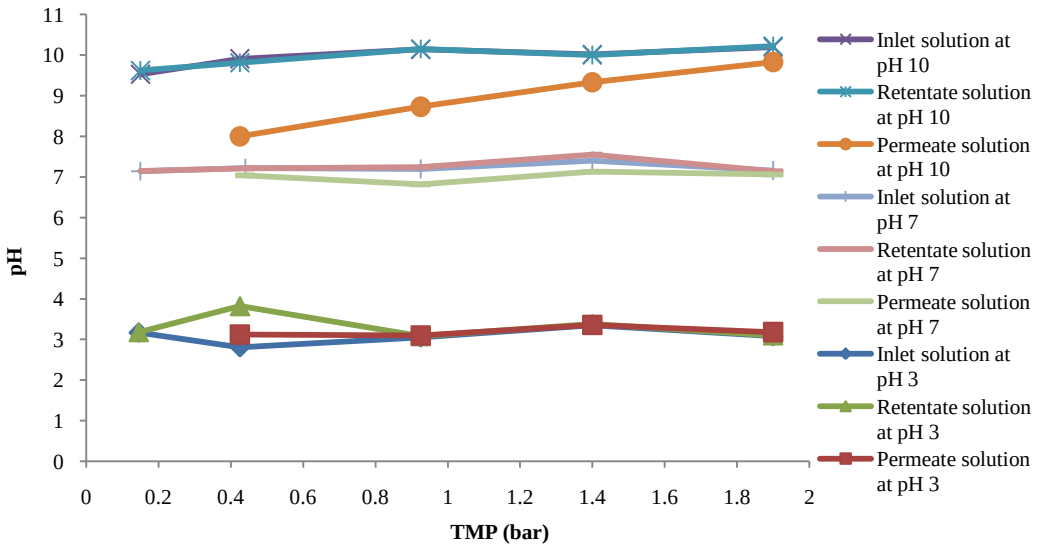

Figure 8-80. pH of NaCl solution versus TMP.

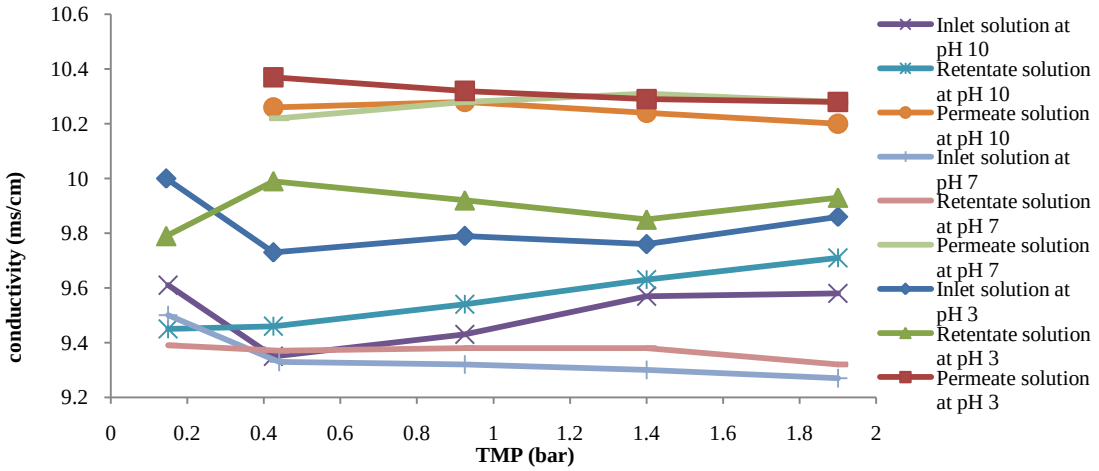

Figure 8-81. Conductivity of NaCl solution versus TMP.

found that distilled water permeation was higher than that of the sodium sulphate (Na_2SO_4) solution. This means that fouling did not occur or was weak and did not have an effect on separation. See Figure 8-82. The pH and conductivity of the inlet, retentate and permeate were measured. The pH of the inlet, retentate and permeate remained constant as the TMP increased. See Figure 8-83. The conductivity of the inlet and retentate remained constant as the TMP increased. On the other hand, the permeate conductivity decreased as the TMP increased. The permeate conductivity was higher than the inlet and the retentate conductivity. See Figure 8-84.

For the sodium sulphate (Na_2SO_4) solution, the rejection of Na^{1+} was higher than the rejection of SO_4^{2-}. This cannot be explained by the ion size because SO_4^{2-} has a bigger ion size than Na^{1+}; as a result, SO_4^{2-} should have a higher rejection than Na^{1+}. On the other hand, these results can be explained by Donnan exclusion. Since the membrane charge is considered positive in the pH 3 regions — see section 8.3 — then repulsion between Na^{1+} ion and the membrane charge would occur, moving Na^{1+} away from the membrane and back to the solution. While attraction between the membrane charge and SO_4^{2-} occurs, allowing SO_4^{2-} to permeate through the membrane. As a result, Na^{1+} rejection would increase and SO_4^{2-} rejection would decrease. The low rejection values for both ions can be explained by the electro-neutrality condition, were the ions had to move from the higher charge concentration area to the lower charge concentration area until electro-neutrality condition at both sides of the membrane was reached. In this case, Na^{1+} and SO_4^{2-} had to permeate from the feed side to the permeate side until the electro-neutrality condition is reached at both sides of the membrane, which caused their rejection to decrease. In addition, low ion rejection might be

due to membrane charge shielding, as the ion concentration at the membrane surface increases then counter-ions would interact with the membrane charge decreasing the membrane ability to reject co-ions, thus decreasing ion rejection.

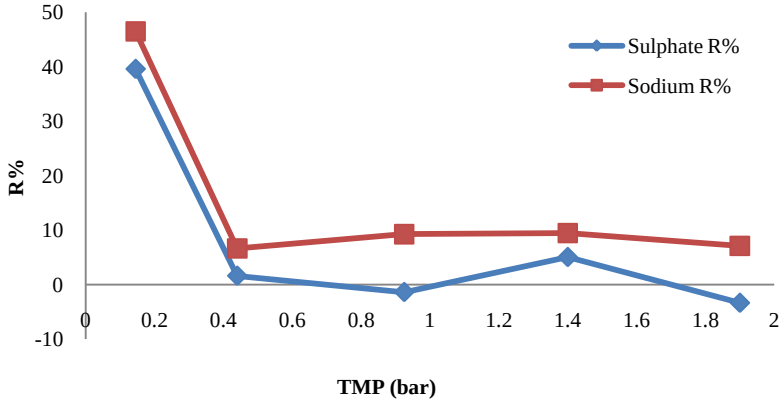

Figure 8-82. Na_2SO_4 solution rejection versus TMP at pH = 3.

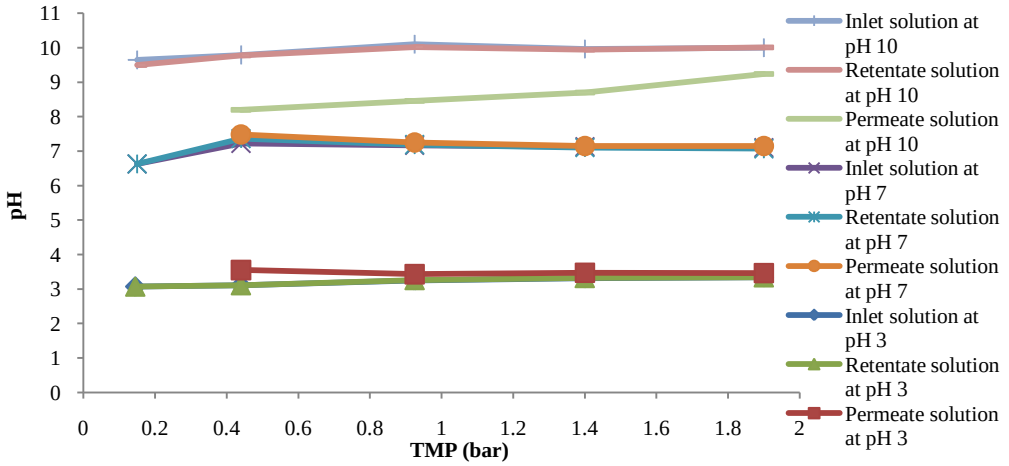

Figure 8-83. pH of Na_2SO_4 solution versus TMP.

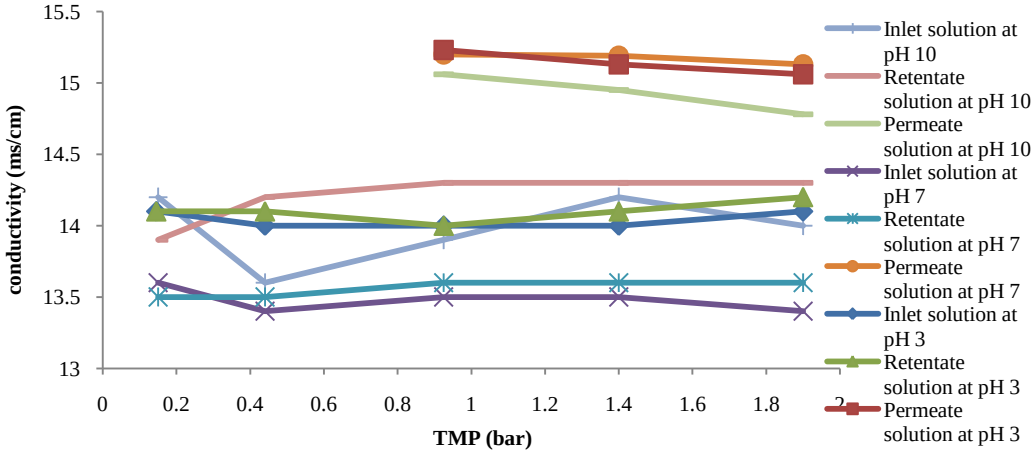

Figure 8-84. Conductivity of Na_2SO_4 solution versus TMP.

The third solution was prepared by diluting sodium chloride (NaCl) and sodium sulphate (Na_2SO_4) in distilled water, where the concentration of each salt was about 0.1M. Then the solution pH was adjusted to the value of 3 by using 0.1M HCl solution. The mixed salt solution permeates flux (volume flux based on the membrane area) through the membrane increased from 2.4E-07 to 5.5E-06 $m^3/m^2/s$ as the TMP increased. It was found that the rejection of sulphate (SO_4^{2-}) ions was higher than the rejection of chloride (Cl^{1-}) ions. The highest rejection of all ions was at the lowest TMP, where the rejection of SO_4^{2-} was about 50.0%, the rejection of Cl^{1-} was about 39.0% and the rejection of Na^{1+} was about 49.9%. When excluding the lowest TMP value, the rejection of Na^{1+} remained constant as the TMP increased. On the other hand, the rejection of SO_4^{2-} and Cl^{1-} decreased then increased as the TMP increased. See Figure 8-85. When comparing the permeation of distilled water through the membrane, before and after mixed salt solution permeation through the membrane, it was found that distilled water permeation was higher than that of the mixed salt solution. This means that fouling did not occur or it was weak and did not have an effect on separation. The pH and the conductivity of the inlet, retentate and permeate were measured. The pH of the inlet, retentate and permeate remained constant as the TMP increased. See Figure 8-86. The conductivity of the inlet and retentate remained constant as the TMP increased. On the other hand, the permeate conductivity increased as the TMP increased. The permeate conductivity was lower than the inlet and the retentate conductivity. See Figure 8-87.

The rejection of Na^{1+} was higher than Cl^{1-} rejection and was higher than SO_4^{2-} rejection when TMP is lower than 1.4 bar, even though Na^{1+} has the smallest ion size. Where Na^{1+} rejection is a result of Donnan exclusion, where it has the same charge sign as the membrane charge, which caused repulsion between Na^{1+} and the membrane charge, thus increasing its rejection. While SO_4^{2-} and Cl^{1-} have an opposite charge of the membrane, which caused attraction between them and increased their permeation through the membrane, causing their rejection to decrease. The rejection of SO_4^{2-} was higher than the rejection of Cl^{1-}. This might be due to the ion size, where SO_4^{2-} has a bigger ion size than Cl^{1-}, thus SO_4^{2-} had higher rejection. Furthermore, SO_4^{2-} had a higher rejection than Cl^{1-} due to ion speciation. Where HSO_4^{1-} may have formed, and since it has a bigger ion size than Cl^{1-}, consequently its rejection would be higher. The low rejection values for all ions might be because of electro-neutrality condition and membrane charge shielding. For the electro-neutrality condition, the ions have to move from the higher charge concentration area to the lower charge concentration area until electro-neutrality condition at both sides of the membrane is reached, thus ion rejection

would decrease. As the concentration of ions in the area near the membrane surface area increases, the membrane charge becomes neutralised by SO_4^{2-} and Cl^{1-}, which would affect the membrane ability to reject ions. As a result, the ion rejection would decrease because it can permeate more freely through the membrane.

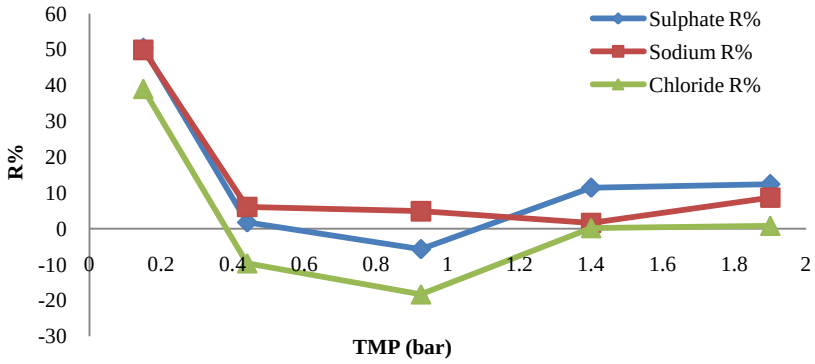

Figure 8-85. Mixed salts solution rejection versus TMP at pH = 3.

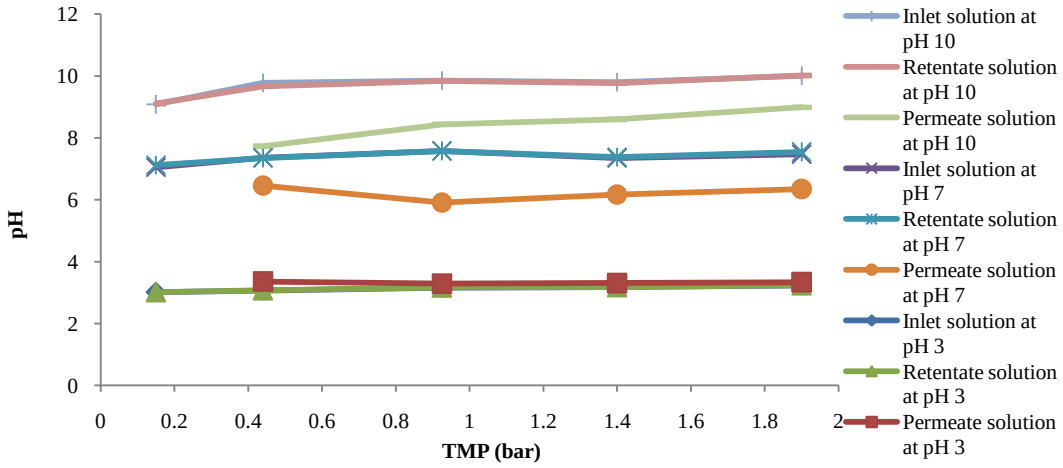

Figure 8-86. pH of mixed salt solution versus TMP.

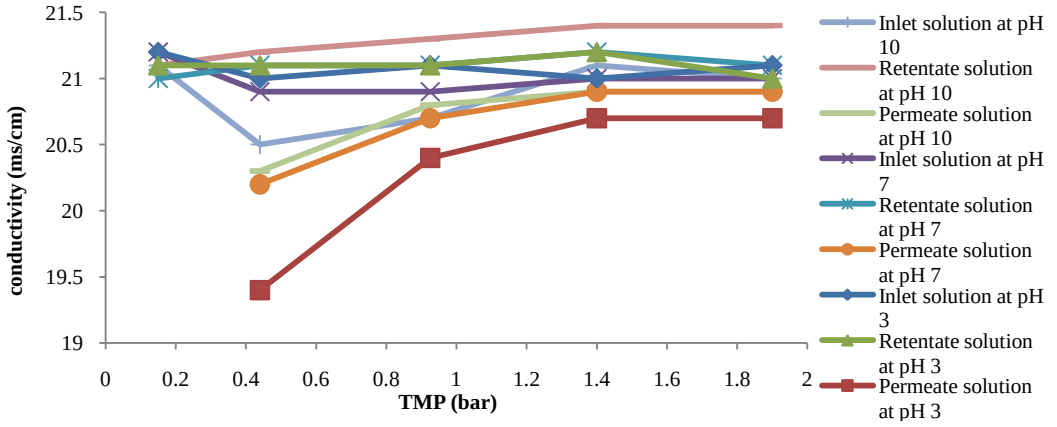

Figure 8-87. Conductivity of mixed salt solution versus TMP.

8.6.3.2 pH 7

The first solution was prepared by diluting sodium chloride (NaCl) in distilled water, where the concentration was about 0.1M. Then the solution pH was adjusted to the value of 7 by using 0.1M NaOH solution. NaCl permeate flux (volume flux based on the membrane area) through the membrane increased from 3.0E-07 to 5.6E-06 $m^3/m^2/s$ as the TMP increased. It was found that the rejection of chloride (Cl^{1-}) ions was lower than the rejection of sodium (Na^{1+}) ions. The highest rejection of both ions was at the lowest TMP, where the rejection of Cl^{1-} was about 38.8% and the rejection of Na^{1+} was about 42.3%. When excluding the lowest TMP value, the rejections of Cl^{1-} and Na^{1+} remained constant as the TMP increased. See Figure 8-88. When comparing the permeation of distilled water through the membrane, before and after sodium chloride (NaCl) solution permeation through the membrane, it was found that distilled water permeation was higher than that of sodium chloride (NaCl) solution. This means that fouling did not occur or was weak and did not have an effect on separation. The pH of the inlet, retentate and permeate remained constant as the TMP increased. See Figure 8-80. The conductivity of the inlet and the retentate decreased as the TMP increased. On the other hand, the permeate conductivity increased as the TMP increased. The permeate conductivity was higher than the inlet and the retentate conductivity. See Figure 8-81.

In the case of sodium chloride (NaCl), the rejection of Na^{1+} was higher than the rejection of Cl^{1-}. This cannot be explained by the ion size because Cl^{1-} has a bigger ion size than Na^{1+}, thus Cl^{1-} should have a higher rejection. Also, these results cannot be explained by the ion charge, since Cl^{1-} has the same charge sign as that of the membrane where repulsion occurs, causing Cl^{1-} ions to diffuse back to the solution, resulting in higher Cl^{1-} rejection, but Na^{1+} rejection was higher than Cl^{1-} rejection. These results might be explained by ion diffusivity through the membrane material. If Cl^{1-} has a higher diffusivity coefficient through the membrane material than Na^{1+}, it would pass more easily through the membrane thus resulting in lower rejection than Na^{1+}. The low rejection values for both ions can be explained by the electro-neutrality condition, where the ions had to move from the higher charge concentration area to the lower charge concentration area until electro-neutrality condition at both sides of the membrane was reached, and as result, their rejection would decrease. As the concentration of Na^{1+} in the area near the membrane surface area increases, the membrane charge becomes neutralised, which would affect the membrane ability to reject ions. As a

result, the ion rejection would decrease because it can permeate more freely through the membrane.

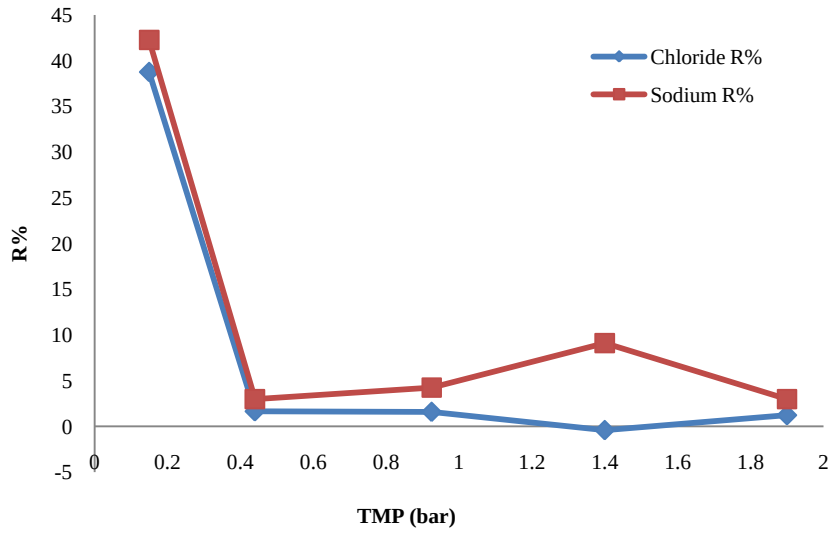

Figure 8-88. NaCl solution rejection versus TMP at pH = 7.

The second solution was prepared by diluting sodium sulphate (Na_2SO_4) in distilled water, where the concentration was about 0.1M. Then the solution pH was adjusted to the value of 7 by using 0.1M NaOH solution. Na_2SO_4 permeate flux (volume flux based on the membrane area) through the membrane increased from 2.5E-07 to 4.5E-06 $m^3/m^2/s$ as the TMP increased. It was found that the rejection of sulphate (SO_4^{2-}) ions was higher than the rejection of sodium (Na^{1+}) ions. The highest rejection of both ions was at the lowest TMP, where the rejection of SO_4^{2-} was about 55.2% and the rejection of Na^{1+} was about 48.0%. When excluding the lowest TMP value, the rejection of SO_4^{2-} and Na^{1+} remained constant as the TMP increased. See Figure 8-89. When comparing the permeation of distilled water through the membrane, before and after sodium sulphate (Na_2SO_4) solution permeation through the membrane, it was found that distilled water permeation was higher than that of the sodium sulphate (Na_2SO_4) solution. This means that fouling did not occur or was weak and did not have an effect on separation. The pH and conductivity of the inlet, retentate and permeate were measured. The pH of the inlet, retentate and permeate remained constant as the TMP increased. See Figure 8-83. The conductivity of the inlet, retentate and permeate remained constant as the TMP increased. The permeate conductivity was higher than the inlet and the retentate conductivities. See Figure 8-84.

For the sodium sulphate (Na_2SO_4) solution, the rejection of Na^{1+} was lower than the rejection

of SO_4^{2-}. This might be related to the ion size and Donnan exclusion. Where SO_4^{2-} ion has a bigger ion size than Na^{1+} where it would be harder for SO_4^{2-} to permeate through the membrane than Na^{1+}, thus SO_4^{2-} has a higher rejection. Also, these results can be explained by the ion charge, since SO_4^{2-} has the same charge sign as that of the membrane. Therefore, repulsion occurs, causing the SO_4^{2-} ion to diffuse back to the solution resulting in higher SO_4^{2-} rejection than Na^{1+} rejection. If ion speciation was taken into consideration, it would have increased the SO_4^{2-} rejection. Where SO_4^{2-} would react with H^{1+} forming HSO_4^{1-}, and since it has the same charge as the membrane, the membrane would reject HSO_4^{1-} because of the repulsion interaction between them, and because it has a big ion size, its rejection would increase. The low rejection values for both ions can be explained by the electro-neutrality condition, were Na^{1+} and SO_4^{2-} had to move from the higher charge concentration area to the lower charge concentration area until the electro-neutrality condition at both sides of the membrane was reached. Low rejection might also be caused by the increase in Na^{1+} concentration near the membrane surface, where the membrane charge becomes neutralised, which would affect the membrane ability to reject ions. As a result, the ion rejection would decrease because it can permeate more freely through the membrane.

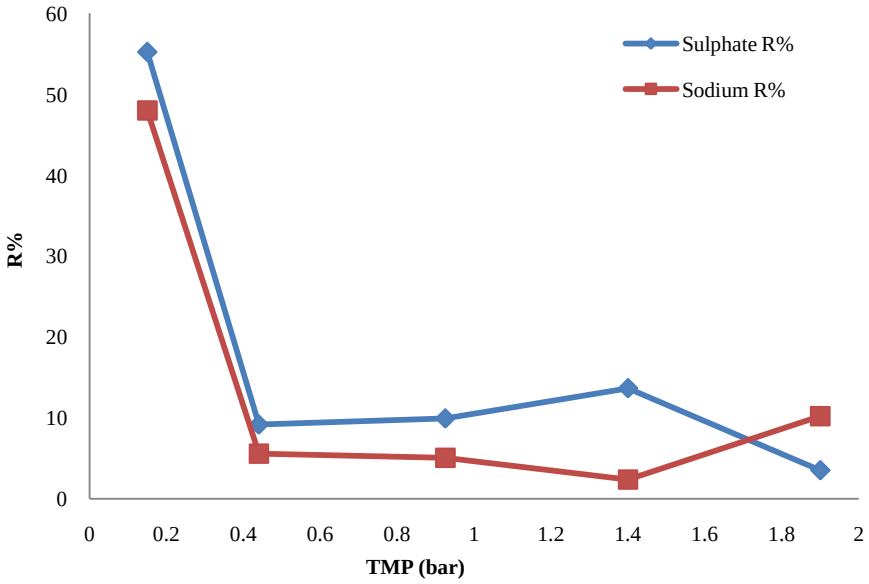

Figure 8-89. Na2SO4 solution rejection versus TMP at pH = 7.

The third solution was prepared by diluting sodium chloride (NaCl) and sodium sulphate (Na_2SO_4) in distilled water, where the concentration of each salt was about 0.1M. Then the solution pH was adjusted to the value of 7 by using 0.1M NaOH solution. The mixed salt solution permeates flux (volume flux based on the membrane area) through the membrane

increased from 4.4E-07 to 6.8E-06 $m^3/m^2/s$ as the TMP increased. The highest rejection of all ions was at the lowest TMP, where the rejection of SO_4^{2-} was about 28.4%, the rejection of Cl^{1-} was about 24.1% and the rejection of Na^{1+} was about 32.0%. When excluding the lowest TMP value, the rejection of the three ions remained constant as the TMP increased. It was found that the rejection of sodium (Na^{1+}) was the highest of them all, then the rejection of sulphate (SO_4^{2-}) ions, and the lowest rejection was the rejection of chloride (Cl^{1-}) ions. See Figure 8-90. When comparing the permeation of distilled water through the membrane, before and after mixed salt solution permeation through the membrane, it was found that distilled water permeation was higher than that of mixed salt solution. This means that fouling did not occur or it was weak and did not have an effect on separation. The pH of the inlet, retentate and permeate remained constant as the TMP increased. See Figure 8-86. The conductivity of the inlet did not have a specific trend as the TMP increased, but in general, the difference between the highest and lowest reading was small. The conductivity of retentate and permeate increased as the TMP increased. The permeate conductivity was lower than the inlet and the retentate conductivity. See Figure 8-87.

The rejection of SO_4^{2-} was higher than the rejection of Cl^{1-}. This might be due to the ion size, where SO_4^{2-} has a bigger ion size than Cl^{1-} thus SO_4^{2-} had a higher rejection. Also, the SO_4^{2-} ion has a higher ion charge than the Cl^{1-} ion, thus its repulsion away from the membrane would be stronger resulting in higher rejection. Ion speciation may have an effect on the rejection of SO_4^{2-}, where it reacts with H^{1+} forming HSO_4^{1-}. Since it has a negative charge, repulsion between HSO_4^{1-} and the membrane charge (which is negative in this case) forcing HSO_4^{1-} to move away from the membrane and back to the feed solution. Also, HSO_4^{1-} rejection would be higher than Cl^{1-} because it has a bigger ion size, where it will be difficult to diffuse through the membrane pores. The rejection of Na^{1+} was higher than the rejection of Cl^{1-} and SO_4^{2-}. Even though Na^{1+} has, the smallest ion size and the opposite charge sign of that of the membrane charge, for these reasons it should have the lowest rejection but this was not the case. The low rejection values for all ions might be due to the electro-neutrality condition and membrane charge shielding. In the case of electro-neutrality condition, Na^{1+}, Cl^{1-} and SO_4^{1-} had to move from the higher charge concentration area to the lower charge concentration area until the electro-neutrality condition at both sides of the membrane was reached. Since attraction between the membrane charge and Na^{1+} occurred, the concentration of Na^{1+} near the membrane would start to build up. As a result, the membrane charge would be shielded by Na^{1+} charge and consequently the membrane charge would be neutralised.

Because of the membrane charge neutralisation, the permeation of ions through the membrane would be easier; as a result, the rejection of ions by the membrane would decrease.

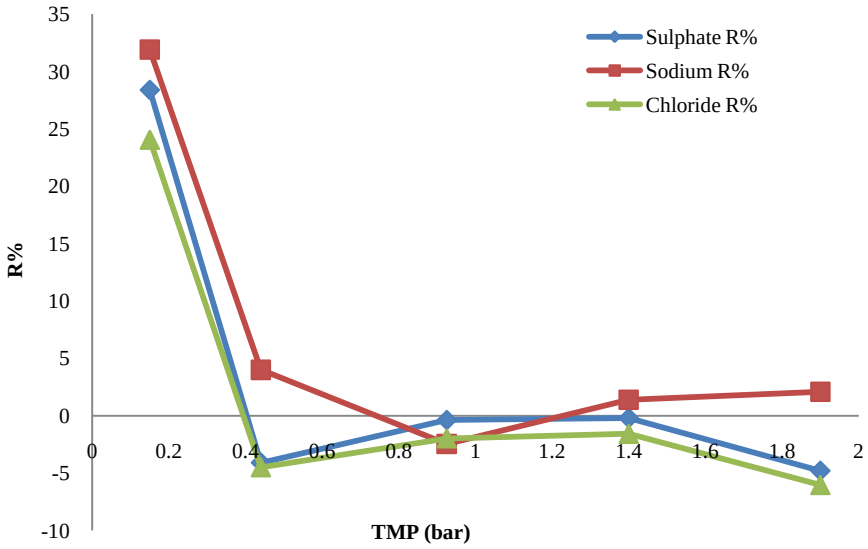

Figure 8-90. Mixed salts solution rejection versus TMP at pH = 7.

8.6.3.3 pH 10

The first solution was prepared by diluting sodium chloride (NaCl) in distilled water, where the concentration was about 0.1M. Then the solution pH was adjusted to the value of 10 by using 0.1M NaOH solution. NaCl permeate flux (volume flux based on the membrane area) through the membrane increased from 4.19E-07 to 8.67E-06 $m^3/m^2/s$ as the TMP increased. It was found that the rejection of chloride (Cl^{1-}) ions was higher than the rejection of sodium (Na^{1+}) ions. The highest rejection of both ions was at the lowest TMP, where the rejection of Cl^{1-} was about 27.5% and the rejection of Na^{1+} was about 25.5%. When excluding the lowest TMP value, the rejection of Cl^{1-} increased as the TMP increased. On the other hand, the rejection of Na^{1+} decreased as the TMP increased until it reached 0.925 bar, then it started to increase as the TMP increased. See Figure 8-91. When comparing the permeation of distilled water through the membrane, before and after sodium chloride (NaCl) solution permeation through the membrane, it was found that distilled water permeation was higher than that of the sodium chloride (NaCl) solution. This means that fouling did not occur or it was weak and did not have an effect on separation. The pH of the inlet and retentate remained constant as the TMP increased, while the permeate pH increased as TMP increased. See Figure 8-80. The inlet and the retentate conductivities increased as the TMP increased. On the other hand,

the permeate conductivity decreased as the TMP increased. The permeate conductivity was higher than the inlet and retentate conductivities. See Figure 8-81.

The rejection of Na^{1+} was lower than the rejection of Cl^{1-}. This can be explained by the ion size, since Cl^{1-} has a bigger ion size than Na^{1+}, thus Cl^{1-} permeating through the membrane pores would be more difficult causing a higher rejection. Also, these results can be explained by the ion charge, where Cl^{1-} has the same charge sign as that of the membrane, thus repulsion occurs causing the Cl^{1-} ion to diffuse back to the solution resulting in higher Cl^{1-} rejection. The low rejection values for both ions might be due to the electro-neutrality condition, were Na^{1+} and Cl^{1-} had to move from the higher charge concentration area to the lower charge concentration area until the electro-neutrality condition at both sides of the membrane was reached. Also, lower rejection might be due to the neutralisation of the membrane charge by Na^{1+}, which would affect the membrane ability to reject ions. As a result, the ion rejection would decrease because it can permeate more freely through the membrane. The rejection of Na^{1+} and Cl^{1-} might have been affected by the permeation of H^{1+} and OH^{-1} through the membrane. It can be noticed that OH^{-1} ion permeation through the membrane increased as the TMP increased because the permeate pH increased as the TMP increased. In addition, according to the electro-neutrality condition, a specific amount of ions permeates through the membrane, thus the rejection of Cl^{1-} increased. As a result of the increase in the permeation of OH^{1-}, the rejection of Na^{1+} decreased because Na^{1+} had to permeate through the membrane to obtain the electro-neutrality condition. On the other hand, H^{1+} ion should have permeated through the membrane rather than Na^{1+} because it had a smaller ion size. Nevertheless, because of ion speciation, H^{1+} would react with Cl^{1-} forming HCl; as a result, Na^{1+} ions permeated through the membrane to obtain the electro-neutrality condition.

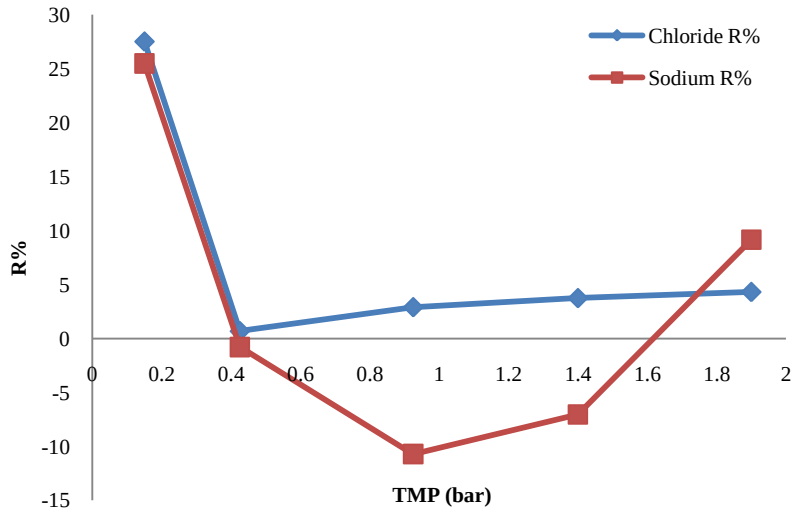

Figure 8-91. NaCl solution rejection versus TMP at pH = 10.

The second solution was prepared by diluting sodium sulphate (Na_2SO_4) in distilled water, where the concentration was about 0.1M. Then the solution pH was adjusted to the value of 10 by using 0.1M NaOH solution. Na_2SO_4 permeate flux (volume flux based on the membrane area) through the membrane increased from 2.5E-07 to 5.80E-06 $m^3/m^2/s$ as the TMP increased. In general, it can be said that the rejection of sulphate (SO_4^{2-}) ions was higher than the rejection of sodium (Na^{1+}) ions. The highest rejection of both ions was at the lowest TMP, where the rejection of SO_4^{2-} was about 54.6% and the rejection of Na^{1+} was about 48.8%. When excluding the lowest TMP value, the rejection of SO_4^{2-} and Na^{1+} remained constant as the TMP increased. See Figure 8-92. When comparing the permeation of distilled water through the membrane, before and after sodium sulphate (Na_2SO_4) solution permeation through the membrane, it was found that distilled water permeation was higher than that of the sodium sulphate (Na_2SO_4) solution. This means that fouling did not occur or it was weak and did not have an effect on separation. The pH of the inlet and retentate remained constant as the TMP increased, while permeate pH increased as the TMP increased. See Figure 8-83. The conductivity of the inlet did not have a specific trend as the TMP increased, but the difference between the highest and lowest reading was small. The retentate conductivity remained constant as the TMP increased. On the other hand, the permeate conductivity decreased as the TMP increased. The permeate conductivity was higher than the inlet and the retentate conductivity. See Figure 8-84.

The rejection of Na^{1+} was lower than the rejection of SO_4^{2-}, which may be due to the ion size and charge. Where the SO_4^{2-} ion has a bigger ion size than Na^{1+} , thus SO_4^{2-} has a higher

rejection. Since SO_4^{2-} has the same charge sign as that of the membrane, repulsion occurs, causing the SO_4^{2-} ion to diffuse back to the feeding solution resulting in higher SO_4^{2-} rejection than Na^{1+} rejection. Na^{1+} has an opposite charge of the membrane charge, which caused attraction between Na^{1+} and the membrane charge, resulting in the permeation of Na^{1+} through the membrane. Low rejection values for both ions can be explained by the electro-neutrality condition and membrane charge neutralisation. Na^{1+} and SO_4^{2-} ions had to move from the higher charge concentration area to the lower charge concentration area until electro-neutrality condition at both sides of the membrane was reached. Additionally, lower rejection might be due to the neutralisation of the membrane charge by Na^{1+}, which would affect the membrane ability to reject ions. As a result, the ions rejection would decrease because they can permeate more freely through the membrane. The rejection of Na^{1+} and SO_4^{2-} might have been affected by the behaviour of H^{1+} and OH^{-1}. Because of ion speciation, H^{1+} would react with SO_4^{2-} forming HSO_4^{1-}; since it has a big ion size and negative charge it would be rejected by the membrane, thus increasing the rejection of SO_4^{2-}. In addition, it can be noticed that OH^{1-} ion permeation through the membrane increased as the TMP increased because the permeate pH increased as the TMP increased. Moreover, according to the electro-neutrality condition, a specific amount of ions permeates through the membrane; consequently, the rejection of SO_4^{2-} increased. Because of the increase in the permeation of OH^{1-} and the decrease in the permeation of H^{1+}, the rejection of Na^{1+} decreased because Na^{1+} had to permeate through the membrane to obtain the electro-neutrality condition.

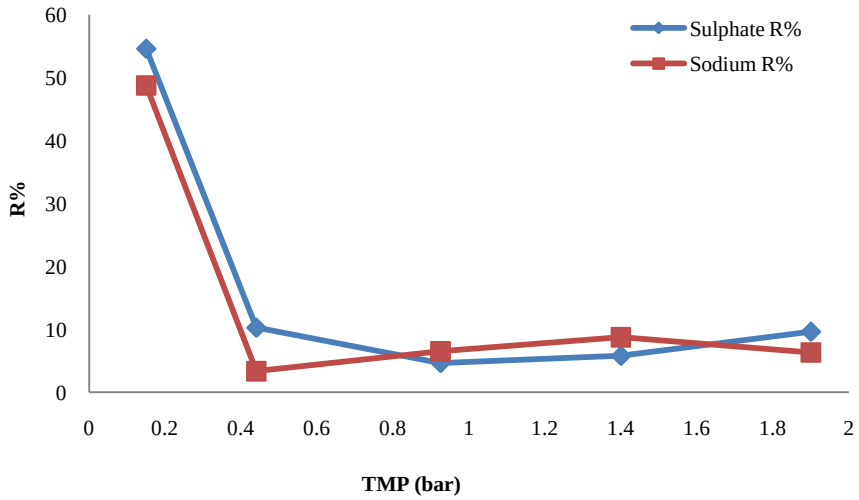

Figure 8-92. Na_2SO_4 solution rejection versus TMP at pH = 10.

The third solution was prepared by diluting sodium chloride (NaCl) and sodium sulphate

(Na_2SO_4) in distilled water, where the concentration of each salt was about 0.1M. Then the solution pH was adjusted to the value of 10 by using 0.1M NaOH solution. The mixed salt solution permeates flux (volume flux based on the membrane area) through the membrane increased from 4.6E-07 to 8.3E-06 $m^3/m^2/s$ as the TMP increased. The highest rejection of all ions was at the lowest TMP, where the rejection of SO_4^{2-} was about 34.1%, the rejection of Cl^{1-} was about 28.8% and the rejection of Na^{1+} was about 38.5%. When excluding the lowest TMP value, the rejection of Na^{1+} ions remained constant as the TMP increased, while the rejections of SO_4^{2-} and Cl^{1-} increased then decreased as the TMP increased. It was found that the rejection of sodium (Na^{1+}) was the highest of them all, and then was the rejection of sulphate (SO_4^{2-}) ions, and the lowest rejection of them all was the rejection of chloride (Cl^{1-}) ions. See Figure 8-93. When comparing the permeation of distilled water through the membrane, before and after mixed salt solution permeation through the membrane, it was found that distilled water permeation was higher than that of the mixed salt solution. This means that fouling did not occur or it was weak and did not have an effect on separation. The pH of the inlet and retentate remained constant as the TMP increased, while the pH of permeate increased as the TMP increased. See Figure 8-86. The conductivity of the retentate and permeate increased as the TMP increased. On the other hand, the inlet conductivity did not have a specific trend as the TMP increased, but in general, the difference between the highest and lowest values was small. The permeate conductivity was lower than the inlet and the retentate conductivity. See Figure 8-87.

Na^{1+} had the highest rejection of all ions, and the rejection of SO_4^{2-} was higher than the rejection of Cl^{1-}. Higher rejection of SO_4^{2-} than the rejection of Cl^{1-} might be due to the ion size and charge, where SO_4^{2-} has a bigger ion size than Cl^{1-}; as a result, SO_4^{2-} had higher rejection. Since SO_4^{2-} and Cl^{1-} had, the same charge as the membrane, repulsion would occur resulting in rejecting SO_4^{2-} and Cl^{1-} ions to permeate through the membrane. In addition, the SO_4^{2-} ion has a higher ion charge than the Cl^{1-} ion, thus its repulsion away from the membrane would be stronger, resulting in higher rejection. Despite the fact that Na^{1+} has the smallest ion size and opposite charge sign of that of the membrane charge, the rejection of Na^{1+} was higher than the rejections of Cl^{1-} and SO_4^{2-}. Na^{1+} rejection result might be due to ion speciation, which will be explained later. Low ion rejection values can be explained by the electro-neutrality condition and membrane charge neutralisation, where Na^{1+}, Cl^{1-} and SO_4^{2-} ions had to move from the higher charge concentration area to the lower charge concentration area until the electro-neutrality condition at both sides of the membrane was

reached. In addition, lower rejection might be due to the neutralisation of the membrane charge by Na^{1+}, which would affect the membrane ability to reject ions. As a result, the ion rejection would decrease because it can permeate more freely through the membrane. The rejection of Na^{1+}, Cl^{1-} and SO_4^{2-} ions might have been affected by the behaviour of H^{1+} and OH^{-1}. Because of ion speciation, H^{1+} would react with SO_4^{2-} forming HSO_4^{1-}; since it has a big ion size and negative charge, it would be rejected by the membrane, thus increasing the rejection of SO_4^{2-}. Moreover, this explains the higher rejection of SO_4^{2-} than Cl^{1-} rejection. In addition, it can be noticed that OH^{1-} ion permeation through the membrane increased as the TMP increased because the permeate pH increased as the TMP increased. Moreover, according to the electro-neutrality condition, a specific amount of ions permeates through the membrane; consequently, the rejections of Cl^{1-} and SO_4^{2-} increased. As a result of the increase in the permeation of OH^{1-} and the decrease in permeation of H^{1+}, the rejection of Na^{1+} should have decreased because Na^{1+} had to permeate through the membrane to obtain the electro-neutrality condition, but in this case, it increased. The only explanation for Na^{1+} high rejection would be the increase of H^{1+} concentration near the membrane surface. The increase in the concentration of H^{1+} would have shielded the membrane charge, and as a result, repulsion between Na^{1+} and H^{1+} would have occurred, which would increase the rejection of Na^{1+} and decrease the rejections of Cl^{1-} and SO_4^{2-}.

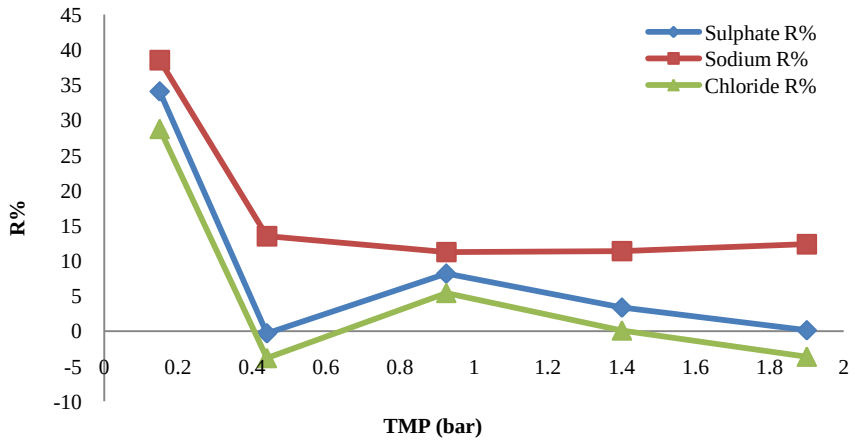

Figure 8-93. Mixed salts solution rejection versus TMP at pH = 10.

8.6.4 Discussion

Three different pH values were investigated which were 3, 7 and 10. For each pH value, two single salt and one binary salt solutions were prepared and their pH values were adjusted using 0.1M HCl and 0.1M NaOH solutions. In the case of pH 3, for NaCl solution it was

noticed that the rejection of Cl^{1-} ions was lower than the rejection of Na^{1+} ions, and the highest rejection of both ions was at the lowest TMP. For Na_2SO_4 solution, it was noticed that the rejection of SO_4^{2-} ions was lower than the rejection of Na^{1+} ions, and the highest rejection of both ions was at the lowest TMP. For NaCl and Na_2SO_4 solution, it was noticed that the rejection of SO_4^{2-} ions was higher than the rejection of Cl^{1-} ions, and the highest rejection of all ions was at the lowest TMP. The rejection of Na^{1+} was higher than the rejection of Cl^{1-}, and was higher than the rejection of SO_4^{2-} when TMP is lower than 1.4 bar, even though Na^{1+} has the smallest ion size. In the case of pH 7, for NaCl solution, it was noticed that the rejection of Cl^{1-} ions was lower than the rejection of Na^{1+} ions. The highest rejection of both ions was at the lowest TMP. For Na_2SO_4 solution, it was noticed that the rejection of SO_4^{2-} ions was higher than the rejection of Na^{1+} ions. The highest rejection of both ions was at the lowest TMP. For NaCl and Na_2SO_4 solution it was noticed that the highest rejection of all ions was at the lowest TMP, and if the lowest TMP was excluded then the rejection of the three ions remained constant as the TMP increased. The rejection of Na^{1+} was higher than the rejections of Cl^{1-} and SO_4^{2-}. The rejection of SO_4^{2-} was higher than the rejection of Cl^{1-}. The permeate flux increased as the TMP increased, on the hand the rejection decreased as the TMP increased. In the case of pH 10, for NaCl solution it was noticed that the rejection of Cl^{1-} ions was higher than the rejection of Na^{1+} ions. The highest rejection for both ions was at the lowest TMP. The rejection of Na^{1+} was lower than the rejection of Cl^{1-}. For Na_2SO_4 solution, it was noticed that the rejection of SO_4^{2-} ions was higher than the rejection of Na^{1+} ions. The highest rejection of both ions was at the lowest TMP, but if the lowest TMP was excluded then the rejection of SO_4^{2-} and Na^{1+} remained constant as the TMP increased. For NaCl and Na_2SO_4 solution it was noticed that Na^{1+} ions had the highest rejection of them all, and then was the rejection of SO_4^{2-} ions, and Cl^{1-} ions had the lowest rejection. In general, the ions rejection was not affected by the change in the pH of the solution. For an example, the rejections of NaCl from a pH controlled solution around pH 3 and 7 and non-controlled pH solutions were similar, but the rejection from a pH 10 solution differed. Where the rejection from pH 10 solution was lower than the rest of the rejection values and the rejection of Cl^{1-} was higher than the rejection of Na^{1+}. The pH had an effect on the behaviour of the cation and the anion rejection but not the rejections value.

8.7 Flux-step method

In this work, a ceramic nanofiltration membrane was used (the membrane made of TiO_2, with

7.00 mm I.D, 10 mm O.D and length of 190 mm, with 1.0 nm mean pore radius, from inopor company). It was used to desalinate water samples containing magnesium chloride and magnesium sulphate. The salt concentration value that was used is 0.1 M. To study the separation behaviour of the membrane, distilled water was used at first, and then followed by distilled water with a single or mixed salt solution. The results of distilled and brackish water were compared to describe the separation behaviour and to find out if fouling took place.

8.7.1 Materials

One set of solutions was used, where the cation Mg^{2+} was the common ion. The salts that were used were magnesium sulphate ($MgSO_4$) and magnesium chloride ($MgCl_2$). At first, a single solution of each salt was prepared with 0.1M concentration. Then a mixed solution of both salts was prepared at 0.1M concentration for each salt. Single and binary salt solutions were used to compare the effect of ion type and charge on separation.

8.7.2 Experimental procedure

At first distilled water was desalinated using 1.0 nm membrane at constant feed flow rate, which was equal to 1.22E-5 m^3/s (44 l/h). Then the inlet pressure was recorded and monitored for 60 minutes to see if any changes occurred to the TMP, and the final TMP was recorded. Afterwards, the inlet flow rate was increased each 60 minutes, and during this, the TMP was monitored. The inlet flow rate was controlled by changing the pump speed. During the experiments, for each different feed flow rate, the permeate sample was collected for 55 minutes. The pH and conductivity for each sample were measured to make sure that the process was stable and there was nothing affecting the process. The same procedure for the single and binary salt solutions was followed. After each experiment, the membrane was cleaned continuously for at least 18 hours with distilled water.

8.7.3 Results

The first solution that was used was prepared by diluting magnesium sulphate ($MgSO_4$) in distilled water. During the experiment, it was noticed that for each different flux used, the TMP for that specific flux did not change with time, which means that fouling did not occur and the process was stable. As a result, the rate of increase in TMP (see equation 8.2) would be equal to zero. When comparing the ion rejection with TMP, it was found that the rejection

of sulphate ions (SO_4^{2-}) was slightly higher than the rejection of magnesium ions (Mg^{2+}). The highest rejection for both ions was at the lowest TMP, where the rejection of SO_4^{2-} was about 72.4% and the rejection of Mg^{2+} was about 72.1%. The rejection of SO_4^{2-} and Mg^{2+} decreased as the TMP increased. See Figure 8-94. $MgSO_4$ permeate flux (volume flux based on the membrane area) through the membrane increased from 1.4E-07 to 2.30E-06 $m^3/m^2/s$ as the inlet flow rate increased. In addition, when comparing the permeation of distilled water through the membrane, before and after $MgSO_4$ solution permeation through the membrane, it was found that distilled water permeation through the membrane was higher than the $MgSO_4$ solution permeation through the membrane. This means that fouling did not occur or was weak and did not have an effect on separation.

It was found that several factors affect the rejection of ions such as the ion size, the electrostatic interaction between the membrane charge and the ion charge, and the electro-neutrality condition. In the case of magnesium sulphate ($MgSO_4$), the rejection of SO_4^{2-} was higher than the rejection of Mg^{2+}. This might be explained by the electrostatic interaction between the membrane and ion charge. Where the membrane charge is negative and Mg^{2+} charge is positive, which causes attraction between them; as a result, Mg^{2+} passes more freely through the membrane than SO_4^{2-}. On the other hand, SO_4^{2-} has a negative charge, which is the same as the membrane charge. This would cause repulsion between the membrane and SO_4^{2-} causing the rejection of SO_4^{2-} and not allowing it to pass through the membrane. Also, ion size played a role in rejection, where SO_4^{2-} ion size is bigger than the Mg^{2+} ion size, which would cause Mg^{2+} to pass more freely through the membrane pores than SO_4^{2-}. In addition, a higher rejection of SO_4^{2-} might be due to acid-based behaviour, where SO_4^{2-} would react with H^{1+} forming HSO_4^{1-}. Since HSO_4^{1-} has a negative charge, then repulsion between HSO_4^{1-} and the membrane charge would occur, resulting in the increase of SO_4^{2-} rejection. The electro-neutrality condition might explain the low rejection values. According to this condition, SO_4^{2-} and Mg^{2+} ions move from the higher concentration to the lower concentration side until equilibrium is reached. As a result, SO_4^{2-} and Mg^{2+} ions would move from the high concentration side of the membrane to the permeate side of the membrane until electro-neutrality at both sides of the membrane is reached.

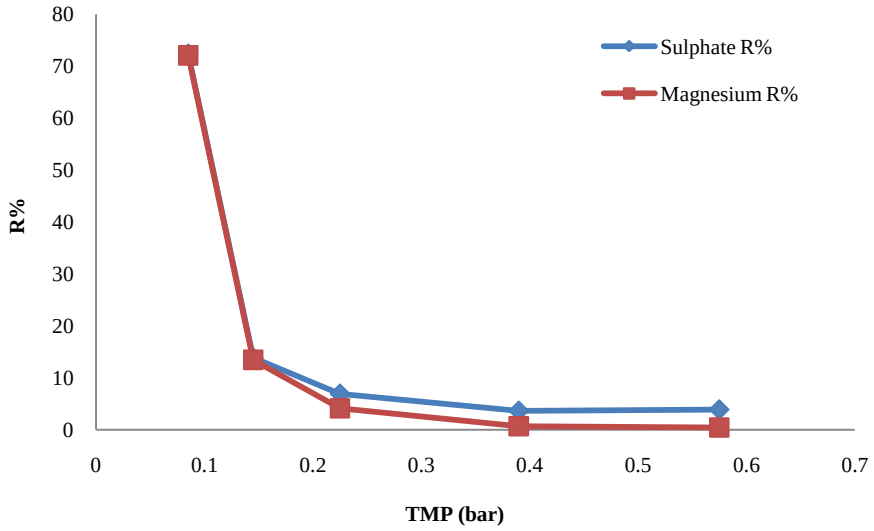

Figure 8-94. Magnesium sulphate solution rejection versus TMP.

The second solution was prepared by diluting magnesium chloride ($MgCl_2$) in distilled water. It was noticed that for each different flux used, the TMP for that specific flux did not change with time, which means that fouling did not occur and the process was stable. As a result, the rate of increase in TMP (see equation 8.2) would be equal to zero. When comparing the ion rejection with TMP, it was found that the rejection of chloride ions (Cl^{1-}) was slightly higher than the rejection of magnesium ions (Mg^{2+}). The highest rejection for both ions was at the lowest TMP, where the rejection of Cl^{1-} was about 76.0% and the rejection of Mg^{2+} was about 76.3%. The rejection of Cl^{1-} and Mg^{2+} decreased as the TMP increased. See Figure 8-95. $MgCl_2$ permeate flux (volume flux based on the membrane area) through the membrane increased from 1.1E-07 to 1.7E-06 $m^3/m^2/s$ as the inlet flow rate increased. Also, when comparing the permeation of distilled water through the membrane, before and after $MgCl_2$ solution permeation through the membrane, it was found that distilled water permeation through the membrane was higher than $MgCl_2$ solution permeation through the membrane. This means that fouling did not occur or was weak and did not have an effect on separation.

Several factors would affect the rejection of ions such as the ion size, the electrostatic interaction between the membrane and ion charge and the electro neutrality condition. In the case of magnesium chloride ($MgCl_2$), the rejection of Cl^{1-} was higher than the rejection of Mg^{2+}. This might be explained by the electrostatic interaction between the membrane and ion charge. Since the membrane charge is negative and Mg^{2+} charge is positive, as a result an attraction would occur between them causing Mg^{2+} ions to permeate more freely through the membrane than Cl^{1-}. On the other hand, Cl^{1-} has a negative charge, which is the same as the

membrane charge. This would cause repulsion between the membrane and Cl^{1-} causing the rejection of Cl^{1-} and not allowing it to permeate through the membrane. In addition, ion size played a role in the rejection, where Cl^{1-} ion size is bigger than Mg^{2+} ion size, which would cause Mg^{2+} to pass more freely through the membrane pores than Cl^{1-}. The electro-neutrality condition might explain the low rejection values. According to this condition, the ions move from the higher concentration to the lower concentration side until equilibrium is reached. As a result, Mg^{2+} and Cl^{1-} would move from the high concentration side of the membrane to the permeate side of the membrane until electro-neutrality at both sides of the membrane is reached. Also, membrane charge shielding would decrease the rejection of Mg^{2+} and Cl^{1-}. Since the Mg^{2+} ion has the same charge as the membrane, Mg^{2+} ions would be attracted by the membrane, thus the concentration of Mg^{2+} near the membrane would increase. As the concentration of Mg^{2+} ions near the membrane build up, the membrane charge would be neutralised. Consequently, the Mg^{2+} and Cl^{1-} ions would permeate through the membrane easily, which decreased their rejection.

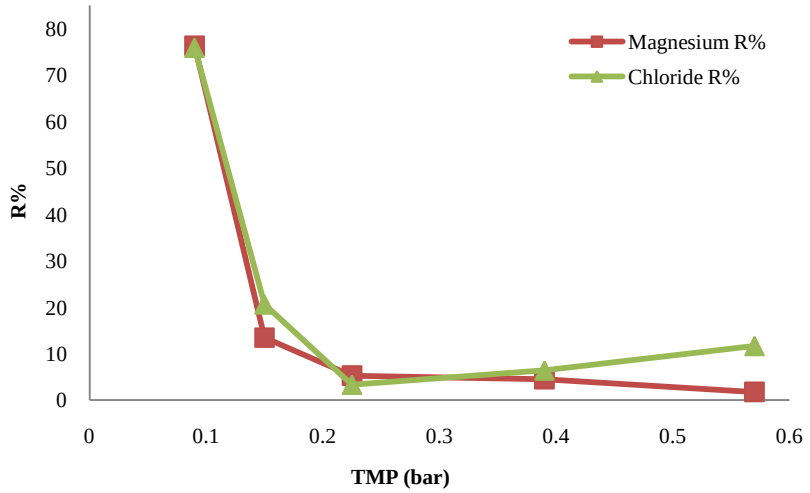

Figure 8-95. Magnesium chloride solution versus TMP.

The third solution was prepared by diluting magnesium chloride ($MgCl_2$) and magnesium sulphate ($MgSO_4$) in distilled water. In general, the rejection of ions took the following trend: except at the lowest TMP, R of sulphate (SO_4^{2-}) > R of chloride (Cl^{1-}) > R of magnesium (Mg^{2+}). See Figure 8-96. The highest rejection for all the ions was at the lowest TMP, where the rejection of Cl^{1-} was about 50.8%, the rejection of SO_4^{2-} was about 57.4%, and the rejection of Mg^{2+} was about 52.3%. When excluding the minimum TMP value, in general it can be noticed that the rejection of Cl^{1-}, SO_4^{2-} and Mg^{2+} stayed constant as the TMP increased. The mixed salt solution permeates flux (volume flux based on the membrane area)

through the membrane increased from 1.7E-07 to 2.7E-06$m^3/m^2/s$ as the inlet flow rate increased. Also, when comparing the permeation of distilled water through the membrane, before and after mixed salt solution permeation through the membrane, it was found that distilled water permeation was higher than the mixed salt solution. This means that fouling did not occur or it was weak and did not have an effect on separation.

The rejection of SO_4^{2-} was higher than the rejection of Cl^{1-}, which can be explained by the ion size and the repulsion force between the ions and the membrane. Where the ion size of SO_4^{2-} is bigger than the ion size of Cl^{1-} and as a result, it would be more difficult for SO_4^{2-} ions to diffuse through the membrane pores and as a result, they would have higher rejection. SO_4^{2-} and Cl^{1-} have the same charge as the membrane, which would cause repulsion between SO_4^{2-} and Cl^{1-} ions and the membrane charge, thus SO_4^{2-} and Cl^{1-} ions would be rejected by the membrane. Since SO_4^{2-} has a higher ion charge than Cl^{1-} ions, this would cause higher repulsion force between SO_4^{2-} ions and the membrane charge than between Cl^{1-} ions and the membrane, resulting in higher rejection of SO_4^{2-} ions than Cl^{1-} ions. Mg^{2+} had the lowest rejection value (excluding the lowest TMP) and opposite ion charge than that of the membrane charge. Because it had the smallest ion size, this helped the ions to diffuse more freely through the membrane. Moreover, since it had the opposite charge sign of that of the membrane, this caused attraction between Mg^{2+} and the membrane causing it to diffuse more freely through the membrane. At the lowest TMP, the rejection of ions followed the following trend: R of sulphate (SO_4^{2-}) > R of magnesium (Mg^{2+}) > R of chloride (Cl^{1-}). The rejection of Mg^{2+} cannot be explained by the ion size because it has a smaller ion size than Cl^{1-}. This might be related to the membrane material, where if Cl^{1-} had higher diffusivity coefficient than Mg^{2+}; as a result, it would diffuse more freely through the membrane and would have lower rejection. In general, the low rejection of Mg^{2+}, SO_4^{2-} and Cl^{1-} ions may be due to the electro-neutrality condition. Because of the electro-neutrality Cl^{1-}, SO_4^{2-} and Mg^{2+} ions had to permeate through the membrane in order to reach the electro-neutrality condition at both sides of the membrane, causing low rejection values. In addition, membrane charge shielding would decrease the rejection of Mg^{2+}, Cl^{1-} and SO_4^{2-}. Since Mg^{2+} ion has the same charge of the membrane; as a result, the concentration of Mg^{2+} near the membrane would increase because of the attraction between Mg^{2+} and the membrane charge; consequently, the concentration of Mg^{2+} ions near the membrane build-up, and the membrane charge would be neutralised. Consequently, the rejection of Mg^{2+}, Cl^{1-} and SO_4^{2-} decreased.

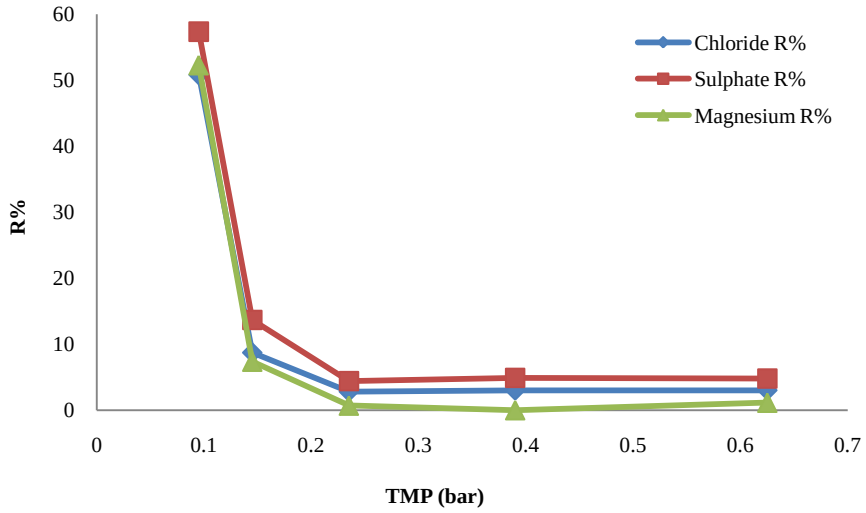

Figure 8-96. Mixed salt solution rejection versus TMP.

8.8 Critical flux

Another important parameter in characterising nanofiltration membrane is the critical flux. The critical flux is known as the flux where below it the flux does not decrease with time, and above it fouling can be observed. There are two forms of the critical flux: the strong critical flux and the weak critical flux. The strong critical flux is the flux where TMP starts to deviate from the distilled water flux, and the membrane resistance for the solution and distilled water is the same. The weak critical flux is the flux where all of its values are lower than that of the distilled water flux, where the membrane resistance for the solution is different from that of the distilled water. As a result, the critical flux is the flux where the TMP deviates from the distilled water flux or it is the flux at which irreversible fouling occurs.

The flux was found to be a critical flux, which was obtained by comparing the permeation of salt solution through 0.9nm and 1.0nm membranes with the permeation of distilled water. This was the case for the different salt solutions and different concentrations. The distilled water was permeated through the membrane before and after the permeation of salt solution, and for both cases, the flux was a weak critical flux. As an example, see figure 8-97. The permeation of distilled water before and after the permeation of salt solution was similar, which means fouling did not occur and the membrane was clean.

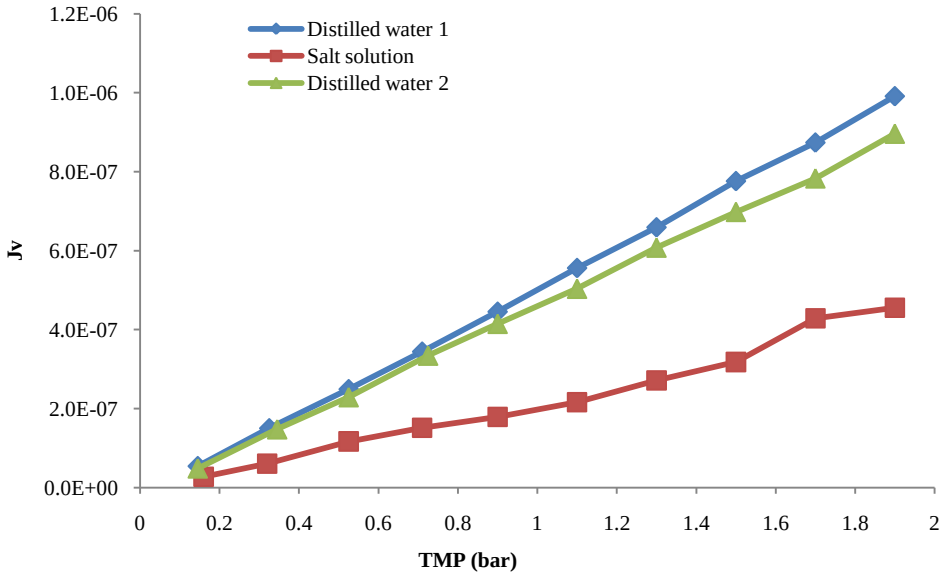

Figure 8-97. J_v ($m^3/m^2/s$) versus TMP.

8.9 Summary

This chapter discusses the different experimental procedures that were used to understand the separation behaviour of ions from brackish water using ceramic nanofiltration membrane. Ceramic (TiO_2) nanofiltration membrane with 0.9 and 1.0 nm pore radii were used. Ceramic nanofiltration membrane was chosen because it has longer life than other membrane types and can be restored to its original conditions by using simple cleaning methods. Another reason for choosing ceramic membranes was the obstacles that were encountered while using polymer flat sheet nanofiltration membranes and the unsatisfactory obtained results. The membrane ISP point was gained by measuring the membrane zeta-potential. The membrane active layer thickness was obtained by using SEM-EDXS equipment. The rejection of different types of cations and anion was measured for different feed concentrations, pH values of the feed solution and TMP. Membrane fouling was monitored and the type of the critical flux was obtained by comparing the permeation of distilled water with the permeation of solution through the membrane.

Chapter 9 Modelling

A model is very important in predicting the membrane performance, understanding the separation mechanism for various substances, selecting the appropriate membrane for a specific application and process design and optimization. The permeation of ions through nanofiltration membrane can be described by using the extended Nernst-Planck equation, where it describes the solute concentration change inside the membrane and the change between the feed and the permeate concentrations, (refs. 7, 14, 97, 103, 138, 169, 170, 289, 290, 295, 297). The extended Nernst-Planck equation describes the transport of ions through nanofiltration membrane in terms of concentration gradient, electrical potential gradient and pressure difference across the membrane, (refs. 68, 219, 319, 321, 323, 325, 326, 336, 348). This chapter discusses the mathematical modelling of the extended Nernst-Planck equation was used due to its description of the ionic transport mechanisms through nanofiltration membranes. The mathematical model was developed for a negatively charged membrane and one type of electrolyte system, i.e. charged solutes. The charged electrolyte system is in the form of a salt solution containing one anion and one cation species. The existence of a cation and an anion will cause the Donnan effect and consequently affect the separation performance together with the steric effect.

The extended Nernst-Planck equation covers all of the three important aspects in transport mechanisms through nanofiltration membrane: diffusion, electro-migration and convection. Four assumptions were made

- The solution is assumed ideal.
- The membrane charge capacity is uniform.
- All the ions that exist in the membrane are transportable.
- The Donnan equilibrium takes place at the membrane/feed interface, and the membrane/permeate interface.

The model development is based on two approaches: the irreversible thermodynamic approach and the hydrodynamic approach, which are governed by both the steric and the charge effects, which in turn govern the ion transport through nanofiltration membrane. The steric effect is caused by the difference between the membrane pore radius and the solute ion radius, while the Donnan effect is actually the result of the charge polarities between the

membrane and the solute. These combined effects influence the selectivity of the membrane. The concentration gradient and the electrical potential gradient cause ion diffusion across nanofiltration membranes, whilst the pressure difference causes convection of ions across nanofiltration membrane.

The derivation of the extended Nernst-Planck equation is explained in chapter 7. The extended Nernst-Planck equation is given as

$$j_i = K_{i,c} c_i J_v - D_{i,p} \frac{dc_i}{dx} - \frac{z_i c_i D_{i,p}}{RT} F \frac{d\Psi}{dx} \qquad (9.1)$$

where j_i is the flux of ion (i) based on the membrane area (mol/m².s), $D_{i,p}$ is the hindered diffusivity (m²/s), c_i is the concentration in the membrane (mol/m³), z_i is the valence of ion (i), $K_{i,c}$ is the hindrance factor for convection inside the membrane, J_v is the volume flux based on the membrane area ($m^3/m^2/s$), R is the gas constant (J/mol.K), T is the absolute temperature (K), F is Faraday constant (C/mol) and Ψ is the electrical potential (V). Transport of ions through the membrane is obtained by implying a set of boundary conditions. The ions rejection is calculated by writing the Nernst-Planck equation in the form of concentration and potential gradients. To obtain the concentration gradient, the ion flux is related to its concentration as

$$j_i = C_{i,p} J_v \qquad (9.2)$$

where $C_{i,p}$ is the concentration of ion (i) in the permeate (mol/m³). Substituting equation (9.2) into equation (9.1) and rearranging it gives the concentration gradient as follows

$$\frac{dc_i}{dx} = \frac{J_v}{D_{i,p}} \left(K_{i,c} c_i - C_{i,p} \right) - \frac{z_i c_i}{RT} F \frac{d\Psi}{dx} \qquad (9.3)$$

To obtain the potential gradient, several conditions were implied. The electro-neutrality conditions are fulfilled in the following order: the feed, the membrane and the permeate, as in equations (9.4) and (9.5). The membrane effective charge (X_d) is assumed to be constant and is given as

$$\sum_{i=1}^{n} z_i c_i = -X_d \qquad (9.4)$$

where X_d is the effective membrane charge density (mol/m³). The electro-neutrality condition in the bulk solution is given as

$$\sum_{i=1}^{n} z_i C_i = 0 \qquad (9.5)$$

The electro-neutrality condition in the permeate solution is given as

$$\sum_{i=1}^{n} z_i C_{i,p} = 0 \qquad (9.6)$$

By applying the conditions in equations (9.4), (9.5) and (9.6) for equation (9.3) and rearranging it, gives the electrical potential gradient as follows

$$\frac{d\Psi}{dx} = \frac{\sum_{i=1}^{n} \frac{z_i J_v}{D_{i,p}} \left(K_{i,c} c_i - C_{i,p} \right)}{\frac{F}{RT} \sum_{i=1}^{n} z_i^2 c_i} \qquad (9.7)$$

The Donnan equilibrium was assumed to apply at the feed/membrane interface and at the membrane/permeate interface. The Donnan equilibrium is given as

$$\left(\frac{\gamma_i c_i}{\gamma_i^o C_i} \right) = \phi \exp\left(- \frac{z_i F}{RT} \Delta\Psi_D \right) \qquad (9.8)$$

where γ_i is the activity coefficient of ion (i) in the membrane, γ_i^o is the activity of ion (i) in the bulk solution and ϕ is the steric partitioning term. Where equation (9.8) defines the boundary conditions at both sides of the membrane. The steric partitioning term (ref. 323) can be calculated by using the following equation

$$\phi = (1 - \lambda)^2 \qquad (9.9)$$

where λ is the ratio of ionic or solute radius/pore radius. Assuming an ideal conditions then the steric partitioning was dropped from Donnan equation. Assuming that the solution is dilute then the activity coefficient, to be accounted for inside the membrane by the effective

membrane charge density, would be equal to unity. Thus, the Donnan equilibrium becomes as

$$\left(\frac{c_i}{C_i}\right) = \exp\left(-\frac{z_i F}{RT}\Delta\Psi_D\right) \qquad (9.10)$$

where $\Delta\Psi_D$ is the Donnan potential (V) and C_i is the ion concentration in the solution (mol/m³). Then equations (9.3) and (9.7) can be solved over the following conditions

$$at \quad x = 0 \longrightarrow C_i = C_{i,f}$$
$$at \quad x = \Delta x \longrightarrow C_i = C_{i,p}$$

where $C_{i,p}$ is the concentration of ion (i) in the permeate (mol/m³) and $C_{i,f}$ is the concentration of ion (i) in the feed (mol/m³). The rejection (R) of ion (i) is given as

$$R = 1 - \frac{C_{i,p}}{C_{i,f}} \qquad (9.11)$$

The hindered diffusivity ($D_{i,p}$) and the hindrance factor for convection ($K_{i,c}$) in Nernst-Planck can be obtained from the following equations. The hindered diffusivity is given as follows

$$D_{i,p} = K_{i,d} \cdot D_{i,\infty} \qquad (9.12)$$

where $D_{i,\infty}$ is the bulk diffusivity (m²/s) and $K_{i,d}$ is the hindrance factor for diffusion. If the solute velocity inside the membrane pores is taken into consideration then the hindrance factor for convection ($K_{i,c}$) (refs. 6, 125, 201, 312, 324, 325, 326) is given as follows

$$K_{i,c} = (2 - \phi_i)G(\lambda_i, 0) \qquad (9.13)$$

where G is the hydrodynamic drag coefficient and ϕ is steric partitioning term (given in equation 9.9). The hindrance factor for diffusion (refs. 6, 125, 201, 312, 325, 326) is given as follows

$$K_{i,d} = K^{-1}(\lambda_i, 0) \qquad (9.14)$$

where K is the hydrodynamic drag coefficient and λ is the stokes radius of component (i) to pore radius ratio. The hydrodynamic drag coefficients (K) and (G) are given as follows (refs.

321, 323)

$$K^{-1}(\lambda_i,0) = 1.0 - 2.30\lambda_i + 1.154\lambda_i^2 + 0.224\lambda_i^3 \qquad (9.15\text{-a})$$

$$G(\lambda_i,0) = 1.0 + 0.054\lambda_i - 0.988\lambda_i^2 + 0.441\lambda_i^3 \qquad (9.15\text{-b})$$

The ratio of the stokes radius of component (i) to the pore radius ratio (λ) is given as follows (refs. 6, 236)

$$\lambda_i = \frac{r_i}{r_p} \qquad (9.16)$$

where r_p is the effective pore radius and r_i is the stokes radius of component (i). By substituting equations (8.9), (8.14), (8.13), (8.15-a), (8.15-b) and (8.15) into equation (8.3) and (8.7) gives the following

$$\frac{dc_i}{dx} = \frac{J_v}{\left(1.0 - 2.30\lambda_i + 1.154\lambda_i^2 + 0.224\lambda_i^3\right)D_{i,p}}\left(\left(2-(1-\lambda_i)^2\right)\left(1.0 + 0.054\lambda_i - 0.988\lambda_i^2 + 0.441\lambda_i^3\right)c_i - C_{i,p}\right) - \frac{z_i c_i}{RT}F\frac{d\Psi}{dx} \qquad (8.17\text{-a})$$

$$\frac{d\Psi}{dx} = \frac{\sum_{i=1}^{n}\frac{z_i J_v}{\left(1.0 - 2.30\lambda_i + 1.154\lambda_i^2 + 0.224\lambda_i^3\right)D_{i,p}}\left(\left(2-(1-\lambda_i)^2\right)\left(1.0 + 0.054\lambda_i - 0.988\lambda_i^2 + 0.441\lambda_i^3\right)c_i - C_{i,p}\right)}{\frac{F}{RT}\sum_{i=1}^{n} z_i^2 c_i} \qquad (8.16\text{-b})$$

The above equation describes the concentration change inside the membrane depending on the effective pore radius and the ion (i) stokes radius.

9.1 Numerical solution

Ion permeation through nanofiltration membrane was described by equations (9.3), (9.7) and (9.10). Equations (9.3) and (9.7) were integrated across the membrane active layer thickness and the internal solute concentrations ($c_{i,1}$) is related to the bulk feed concentration ($C_{i,f}$) at the feed/membrane interface and the internal solute concentration ($c_{i,N}$) is related to the permeate concentration ($C_{i,p}$) at the membrane/permeate interface through equation (9.10). Two mathematical methods were used to integrate equations (9.3) and (9.7): Euler and Runge-Kutta. The feed concentration ($C_{i,f}$) with equation (9.10) was used to calculate the initial concentration inside the membrane ($c_{i,1}$) and the integration of equations (9.3) and

(9.7). Then from the estimate of ($c_{i,N}$) and the application of equation (9.10) the estimate of the permeate concentration ($C_{i,p}$) was calculated. Then the ion rejection was calculated using equation (9.11). In-order to integrate equation (9.3), it needs to have a value for $d\Psi/dx$, a calculation which requires a value of the permeate concentration ($C_{i,p}$). It is therefore reasoning to solve the model in an iterative function using an initial guess for the value of the permeate concentration ($C_{i,p}$). Therefore it was assumed that the initial permeate concentration ($C_{i,p}$) was equal to the feed concentration ($C_{i,f}$) which implies that rejection does not take place. The feed concentration assumed to be equal to the initial feed concentration used in the experiments. The hindered diffusivity ($D_{i,p}$), the hindrance factor for convection inside the membrane ($K_{i,c}$) and the Donnan potential ($\Delta\Psi_D$) were obtained from literature (refs. 125, 325). The solution was assumed to be dilute, as a result the activity coefficient, to be accounted for inside the membrane by the effective membrane charge density, would be equal to unity. The membrane thickness and the membrane pore size were obtained from the membranes used in the experiments.

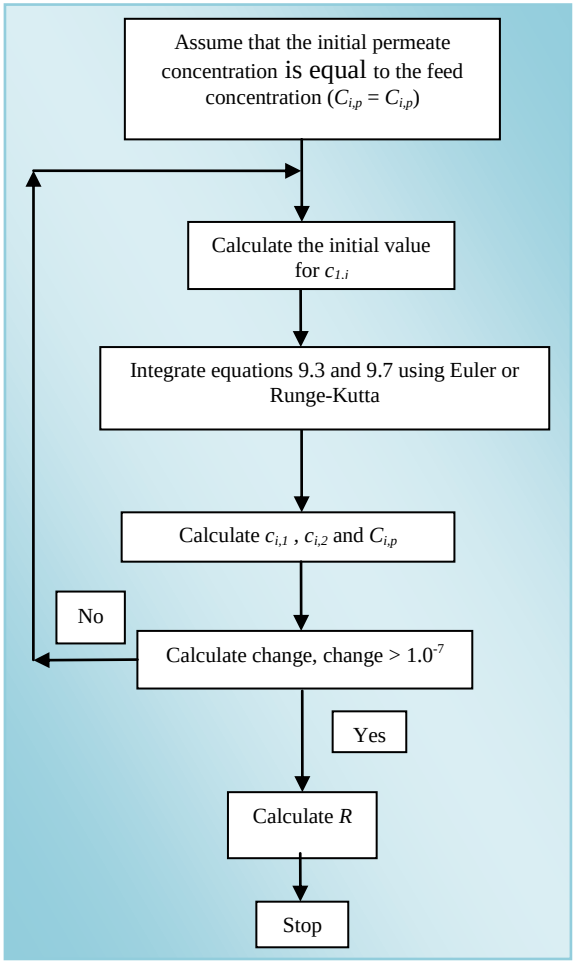

Figure 9-1. The programme flowchart.

9.1.1 Euler's numerical method

At the beginning, the initial permeate concentration ($C_{i,p}$) was assumed to be equal to the feed concentration ($C_{i,f}$) to be able to calculate the initial value of the concentration inside the membrane (c_i). Then equation (9.9) was rearranged and written as

$$c_i = C_{i,f} \exp\left(-\frac{z_i F}{RT} \Delta\Psi_D \right) \qquad (9.18)$$

where $C_{i,f}$ is the solute concentration in the feed solution. Equation (9.17) was used to determine the initial solute concentration inside the membrane (c_i) - at the feed/membrane interface - by using the solute feed concentration. Then equation (9.3) was written according to Euler's method as follows

$$\frac{c_{i,N+1} - c_{i,N}}{\Delta x} = \frac{J_v}{D_{i,p}} \left(K_{i,c} c_{i,N} - C_{i,p} \right) - \frac{z_i c_{i,N}}{RT} F \frac{d\Psi}{dx} \qquad (9.19)$$

Equation (9.18) was used to calculate the concentration inside the membrane. Then equation (9.7) was used to calculate the potential gradient ($d\Psi/dx$), where it was substituted into equation (9.18) to calculate a new value for the solute concentration inside the membrane. After that, the step-size was assumed to be equal to the membrane active layer thickness over the number of steps (node), where the number of steps (node) was equal to 200, as in the following equation

$$xstep = \frac{x_2 - x_1}{node} \qquad (9.20)$$

where *xstep* is the step-size, *node* is the number of steps and x is the membrane active layer thickness. The ion concentration inside the membrane active layer changes from $c_{i,1}$ at the feed-solution interface side to $c_{i,200}$ at the permeate-solution interface side. Afterwards, the final concentration inside the membrane was used to calculate the permeate concentration. The new value of the solute concentration inside the membrane was used to calculate the solute permeate concentration by substituting it into equation (9.20). The solute concentration in the permeate is given as

$$C_{i,p} = \frac{c_i}{\exp\left(-\frac{z_i F}{RT}\Delta\Psi_D\right)} \qquad (9.21)$$

where $C_{i,p}$ is the solute concentration in the permeate solution. Then the rejection of ions was calculated using equation (9.10). The program used (program-1) is given in Appendix-1. The permeation of ions through the membrane active layer is illustrated in figure 9-2. The programme would keep running until the difference (change) between the initial and final permeate concentration would be greater than 1.0^{-7}, the change is given as follows

$$change = \frac{c_{i,p} - c_{i+1,p}}{c_{i,p}} \qquad (9.22)$$

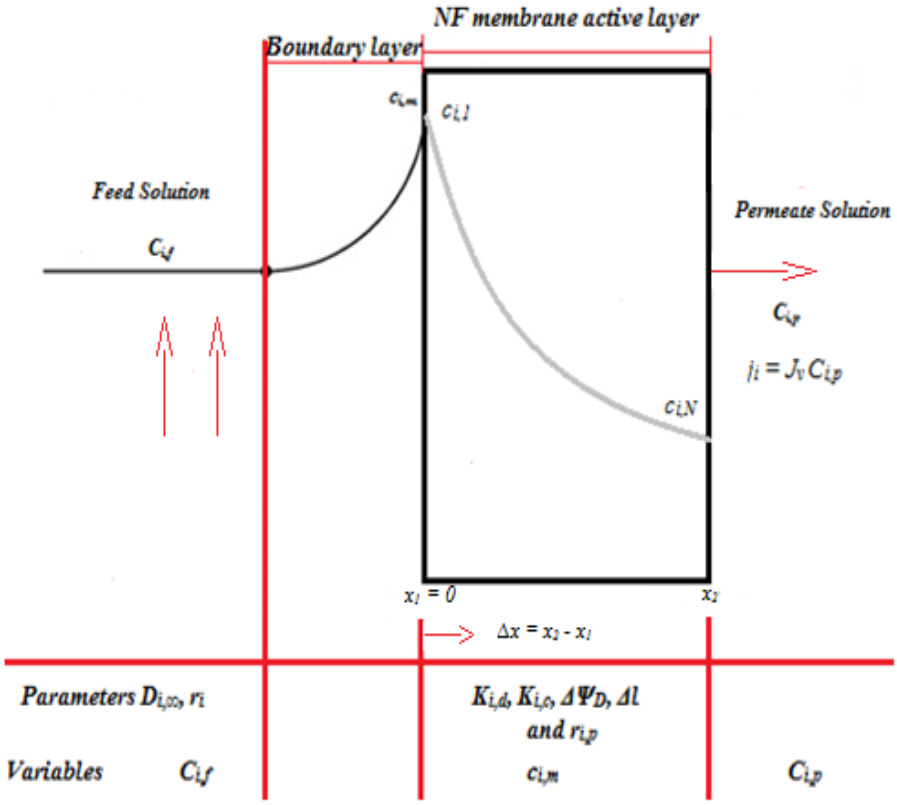

Figure 9-2. Ion transport across a NF membrane, (ref. 317).

9.1.2 Runge-Kutta numerical method

The Runge-Kutta method was used to calculate the concentration change inside the membrane. At first, the initial permeate concentration was assumed to be equal to the feed concentration in order to calculate the initial value of the concentration inside the membrane.

Then the initial concentration inside the membrane was calculated by using equation (9.17). Afterwards, the potential gradient was calculated by using equation (9.7). Then the initial concentration inside the membrane and the potential gradient were substituted into equation (9.3), where it was integrated and gave a new value for the concentration inside the membrane. After that, the step-size was assumed to be equal to the membrane active layer thickness over the number of steps, where the number of steps was equal to 200. The step-size is given as follows

$$h = \frac{x_2 - x_1}{nstep} \qquad (9.23)$$

where h is the step-size, $nstep$ is equal to 200 and x is the membrane active layer thickness. Where the ion concentration inside the membrane active layer changes from $c_{i,1}$ at the feed-solution side to $c_{i,200}$ at the permeate-solution side. Afterwards, the final concentration inside the membrane ($c_{i,200}$) was used to calculate the permeate concentration. The new value of the solute concentration inside the membrane was used to calculate the solute permeate concentration by substituting it into equation (9.20). Figure 9-2 illustrates the permeation of ions through the membrane active layer. The program used (program-2) is given in Appendix-2. The programme would keep running until the difference (change) between the initial and final permeate concentration would be greater than 0.0000001, as in equation (9.21).

9.2 Results

The programs have been run for sodium chloride (NaCl) for two different feed concentration values at a different volume flux based on the membrane area ($m^3/m^2/s$) values. The used concentration values were the same as the values used in the experiments. The model was only run for NaCl because it has some limitations for being solved for other types of ions and it was hard to obtain any values of the Donnan potential ($\Delta\Psi_D$) for other types of salts.

9.2.1 First program (Euler method)

Two different concentrations were used at different volume fluxes (based on the membrane area). The concentration values that were used are 10 and 100 mol/m^3, and the volume flux ranged between 1.0E-7 to 9.0E-6 $m^3/m^2/s$. The membrane active layer thickness was assumed

equal to 20.0E-6 m. The initial feed concentration, the volumetric flux and the membrane active layer thickness values were obtained from the experiments.

In the first case, when the concentration was equal to 10 mol/m^3, it was found that the rejection of Na^{1+} and Cl^{1-} ions increased as the volume flux increased. In addition, the rejection of Cl^{1-} was slightly higher than the rejection of Na^{1+}. See Figures 9-3 and 9-4. Such results are supported by the Nernst-Planck equation, where the membrane effective charge (X_d) would have played a role in causing a difference in the rejection between a cation and an anion. The membrane effective charge (X_d) is used as a condition to integrate equation (9.3) to obtain the electrical potential gradient, also the electrical potential gradient is used to integrate the Nernst-Planck equation to obtain the ions concentration inside the membrane and the permeate solution. It was noticed that the ions rejection increased as the permeate volume flux (based on the membrane area) increased, such observation supports the trans-membrane pressure (TMP) where the theory suggests that the ions rejection would increase as the TMP increases (refs. 7, 266, 283, 289, 314, 321, 325). The concentration of Na^{1+} and Cl^{1-} inside the membrane decreased as the ions moved through the membrane active layer from the feed side to the permeate side. It was noticed that the concentration of Na^{1+} ion inside the membrane active layer was lower than the concentration of Cl^{1-} ion. See Figures 9-5 and 9-6. These results are supported by theory where it suggests that the ions concentration decreases as the ions moves through the membrane active layer from the feed/membrane interface to the membrane/permeate interface (refs. 317, 325).

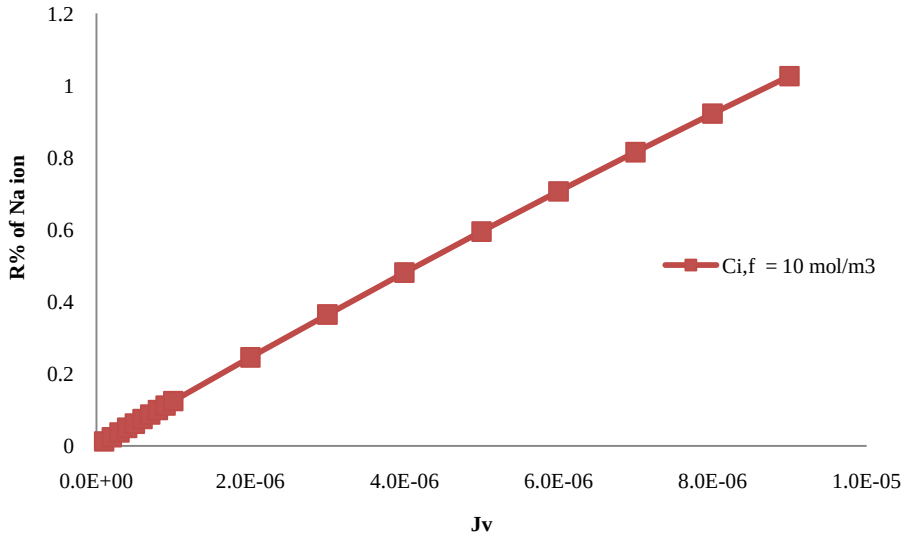

Figure 9-3. Rejection of Na^{1+} ion versus J_v (m^3/m^2/s).

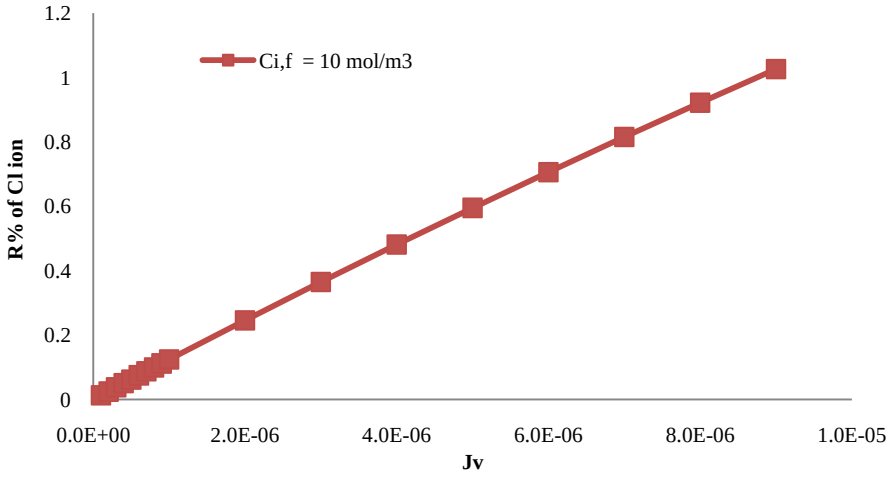

Figure 9-4. Rejection of Cl^{1-} ion versus J_v ($m^3/m^2/s$).

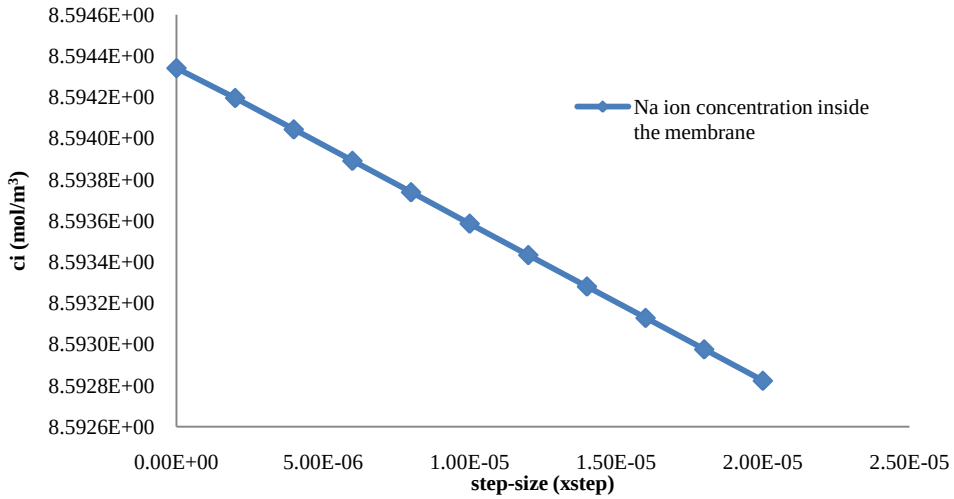

Figure 9-5. Na^{1+} ion concentration inside the membrane active layer versus the step-size.

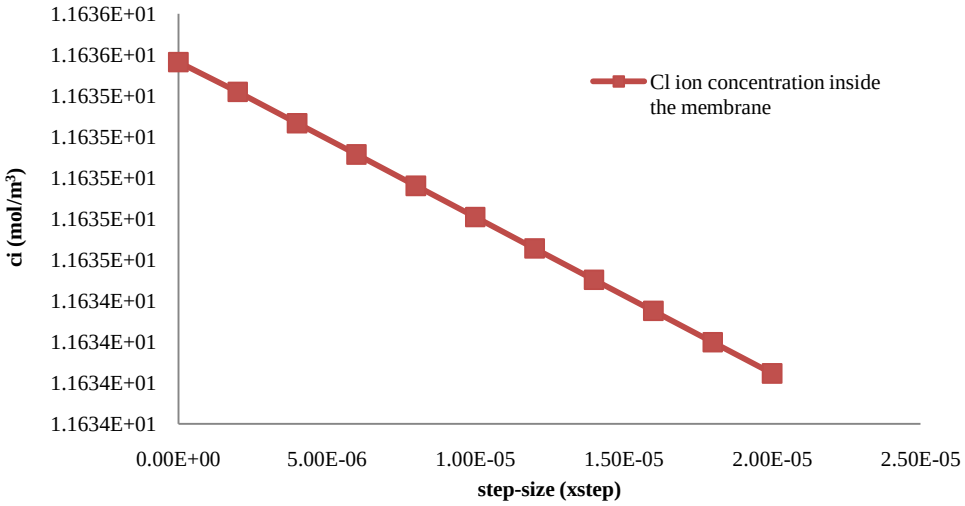

Figure 9-6. Cl^{1-} ion concentration inside the membrane active layer versus the step-size.

In the second case, when the concentration was equal to 100 mol/m^3, it was found that the rejection of Na^{1+} and Cl^{1-} ions increased as the volume flux increased. In addition, the rejection of Cl^{1-} was slightly higher than the rejection of Na^{1+}. See Figures 9-7 and 9-8. The concentration of Na^{1+} and Cl^{1-} ions inside the membrane active layer decreased as the ions moved through the membrane active layer from the feed side to the permeate side. It was noticed that the concentration of Na^{1+} ion inside the membrane active layer was lower than the concentration of Cl^{1-} ion inside the membrane active layer. See Figures 9-9 and 9-10.

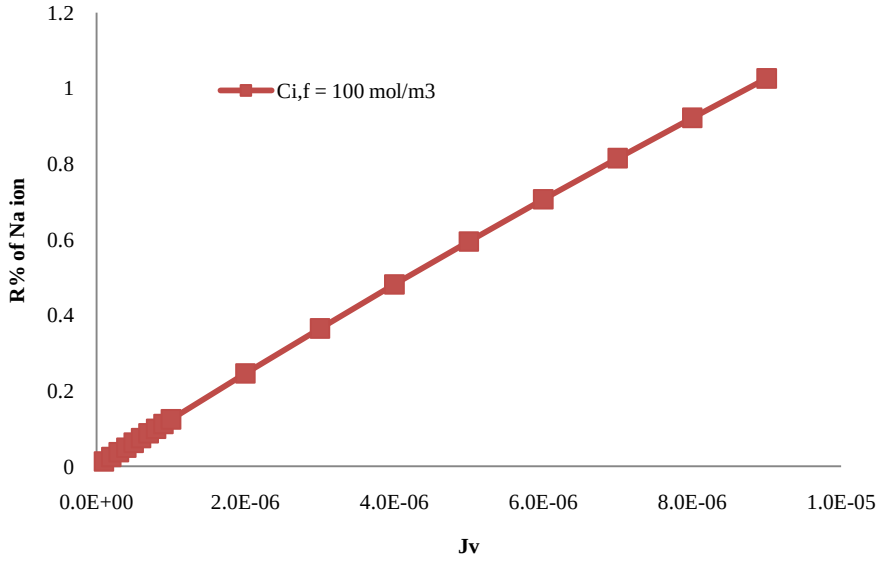

Figure 9-7. Rejection of Na^{1+} ion versus J_v ($m^3/m^2/s$).

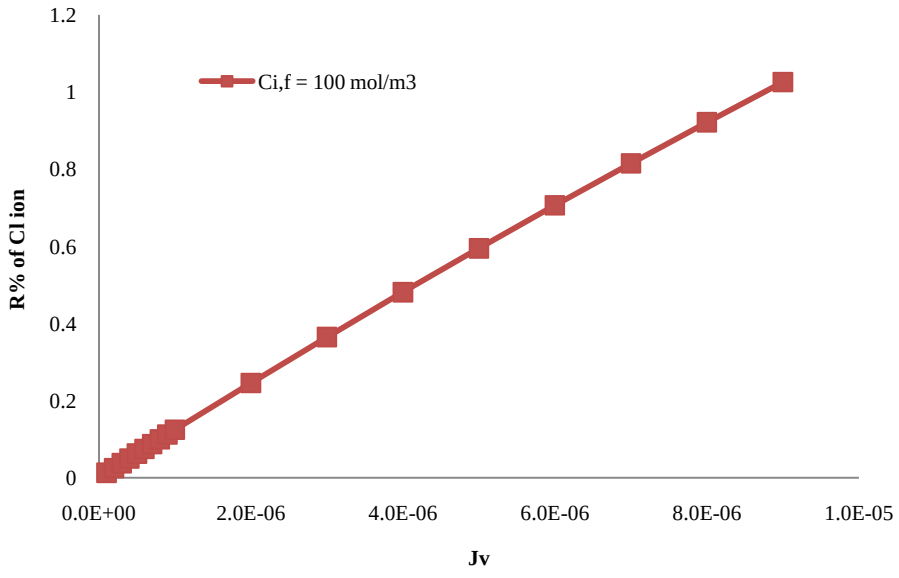

Figure 9-8. Rejection of Cl^{1-} ion versus J_v ($m^3/m^2/s$).

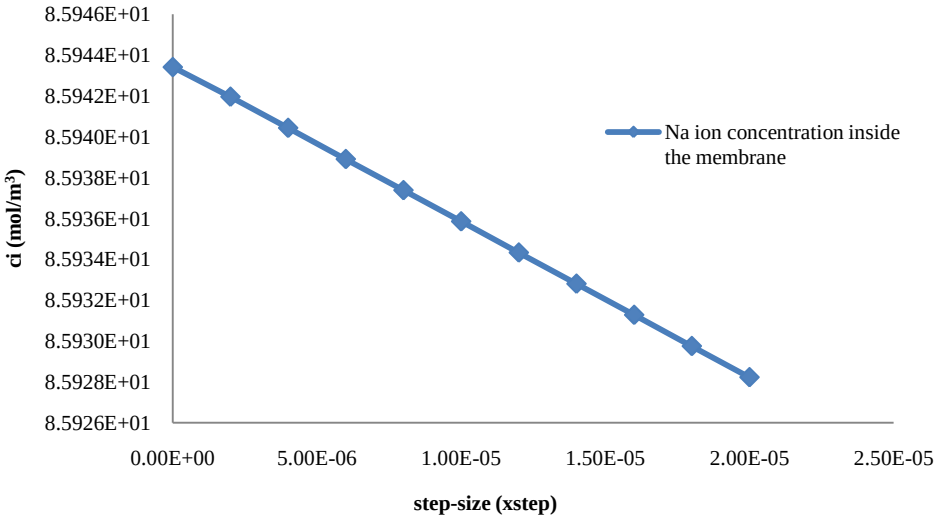

Figure 9-9. Na^{1+} ion concentration inside the membrane active layer versus the step-size.

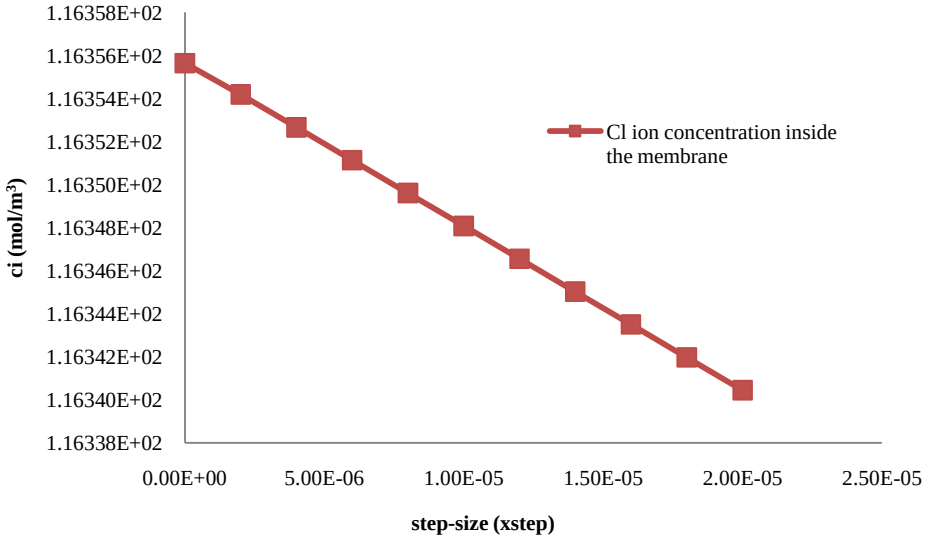

Figure 9-10. Cl^{1-} ion concentration inside the membrane active layer versus the step-size.

It was noticed that the rejection of Na^{+1} and Cl^{-1} ions increased as the volumetric flux based on membrane area (J_v) increased. In addition, the rejection of Na^{+1} and Cl^{-1} ions decreased as the feed concentration increased, (ref. 125). The rejection of Cl^{1-} was higher than the rejection of Na^{1+}. Such rejection behaviour is related to the membrane charge, which is a negative charge. The membrane charge effect would appear in the module in the electrical potential gradient (see equations 9.4 and 9.6), which would explain the difference between the rejection of Na^{1+} and Cl^{1-}. Where repulsion between the membrane charge and the Cl^{1-} ions occurs while attraction between the membrane charge and the Na^{1+} ions occurs, which means that Na^{1+} ions would pass more freely through the membrane active layer and the Cl^{1-} ions would be rejected. For the two initial feed concentration values (10 and 100 mol/m^3), it

was noticed that the concentration of Na^{1+} and Cl^{1-} ions inside the membrane active layer decreased as the ions moved through the membrane active layer from the feed side to the permeate side, moreover the concentration of the ions inside the membrane active layer decreased as the volumetric flux based on membrane area (J_v) increased, as an example see figure 9-11, (refs. 317, 325, 326).

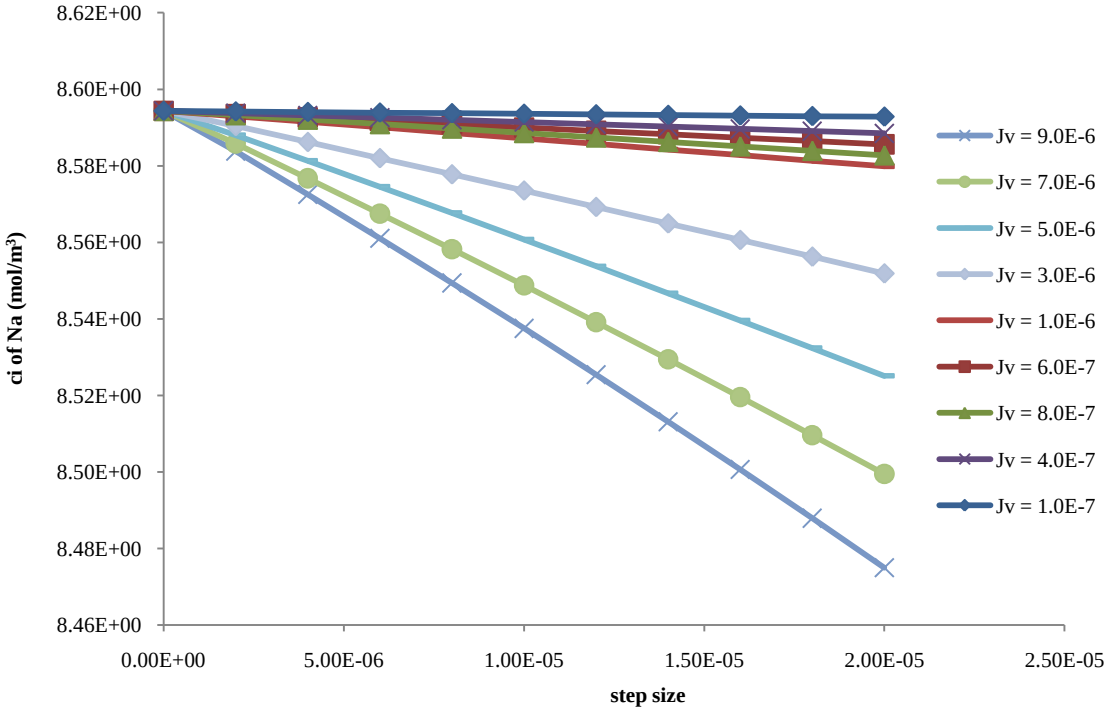

Figure 9-11. Na^{1+} ion concentration inside the membrane active layer versus the step-size (for different volumetric flux (J_v)).

9.2.2 Second program (Runge-Kutta method)

In this program, the Runge-Kutta method was used to solve equations (9.3), (9.6) and (9.9) to calculate the ion's concentration change inside the membrane and the ion's concentration in the permeate solution. After calculating the ions permeate concentration, the ions rejection was calculated. The calculation of the ion rejection would help in trying to understand the conditions that would affect the ion rejection and which parameter can be adjusted in the experiments. The step-size (h) which was used in the programme is given as follows

$$h = \frac{x_2 - x_1}{nstep} \qquad (9.24)$$

where *nstep* is the number of steps and (x_2-x_1) is the membrane thickness. In the program, the

Nernst-Planck equation was solved for two different initial feed ion concentrations over different volume fluxes (based on the membrane area). The initial feed ion concentrations were 10 and 100 mol/m^3. The volume fluxes (based on the membrane area) that were used ranged between 1.0E-7 and 9.0E-6 $m^3/m^2/s$. The membrane thickness was assumed to be equal to 20.0E-6 m.

In the first case, when the concentration was equal to 10 mol/m^3, it was found that the rejection of Na^{1+} and Cl^{1-} ions increased as the volume flux increased. See Figures 9-12 and 9-13. The rejection of Cl^{1-} was slightly higher than the rejection of Na^{1+}. The concentration of Na^{1+} and Cl^{1-} inside the membrane decreased as the ions moved through the membrane active layer from the feed side to the permeate side. See Figures 9-14 and 9-15. It was noticed that the concentration of Na^{1+} ion inside the membrane active layer was lower than the concentration of Cl^{1-} ion inside the membrane active layer (refs. 325, 326).

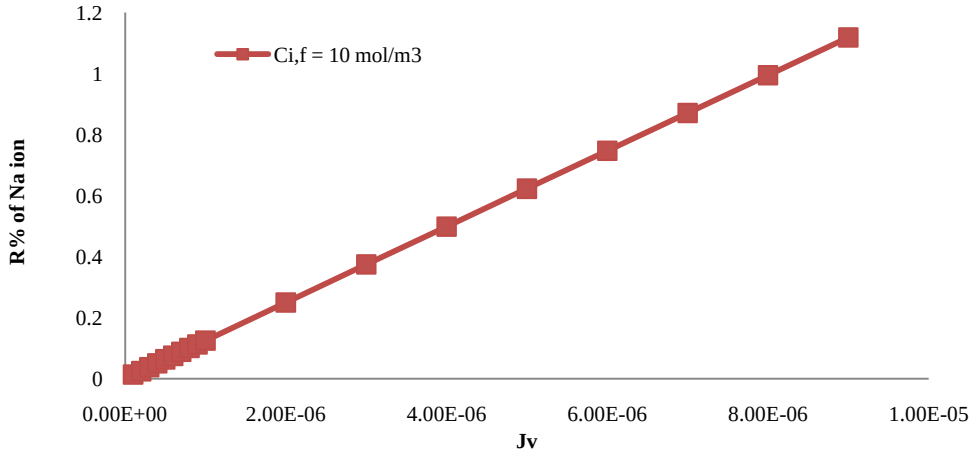

Figure 9-12. Rejection of Na^{1+} ion versus J_v ($m^3/m^2/s$).

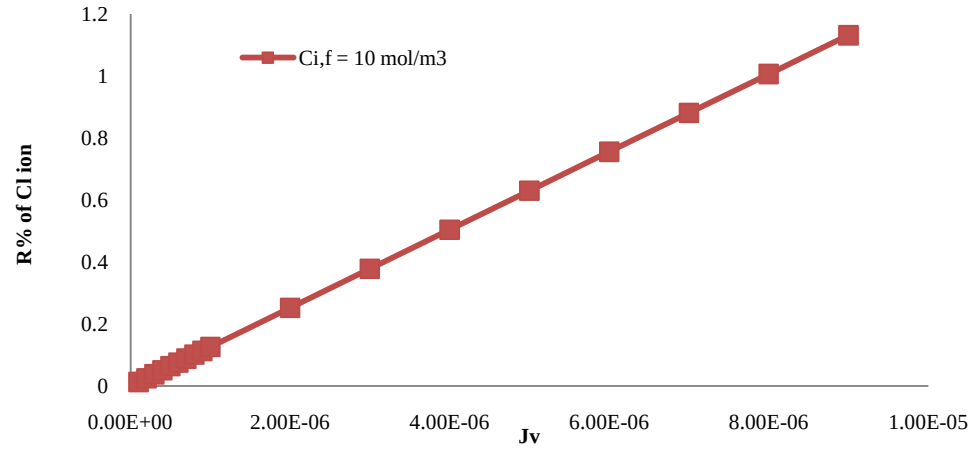

Figure 9-13. Rejection of Cl^{1-} ion versus J_v ($m^3/m^2/s$).

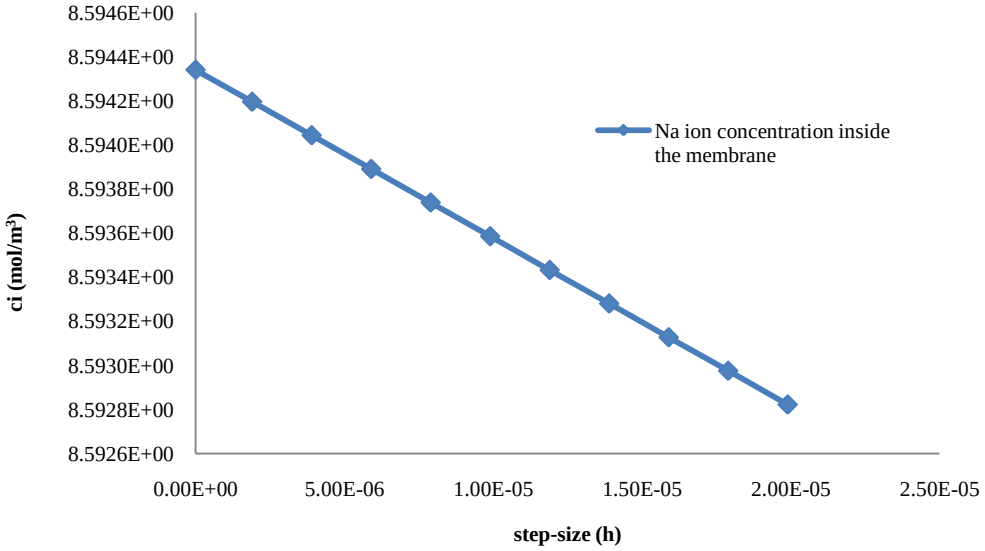

Figure 9-14. Na^{1+} ion concentration inside the membrane active layer versus the step-size.

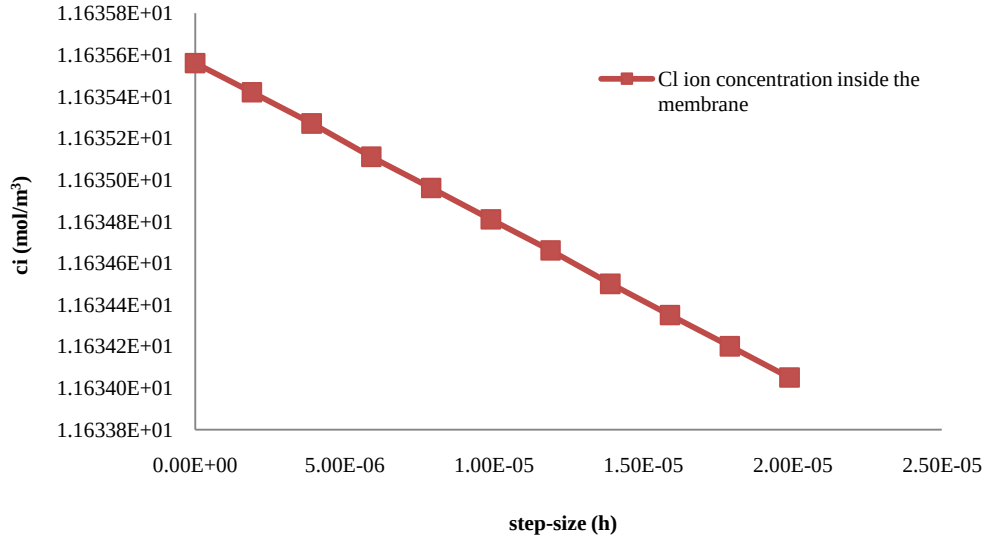

Figure 9-15. Cl^{1-} ion concentration inside the membrane active layer versus the step-size.

In the second case, when the concentration was equal to 100 mol/m^3, it was found that the rejection of Na^{1+} and Cl^{1-} ions increased as the volume flux increased. See Figures 9-16 and 9-17. The rejection of Cl^{1-} was slightly higher than the rejection of Na^{1+}. The concentration of Na^{1+} and Cl^{1-} inside the membrane decreased as the ions moved through the membrane active layer from the feed side to the permeate side. See Figures 9-18 and 9-19. It was noticed that the concentration of the Na^{1+} ion inside the membrane active layer was lower than the concentration of Cl^{1-} ion inside the membrane active layer.

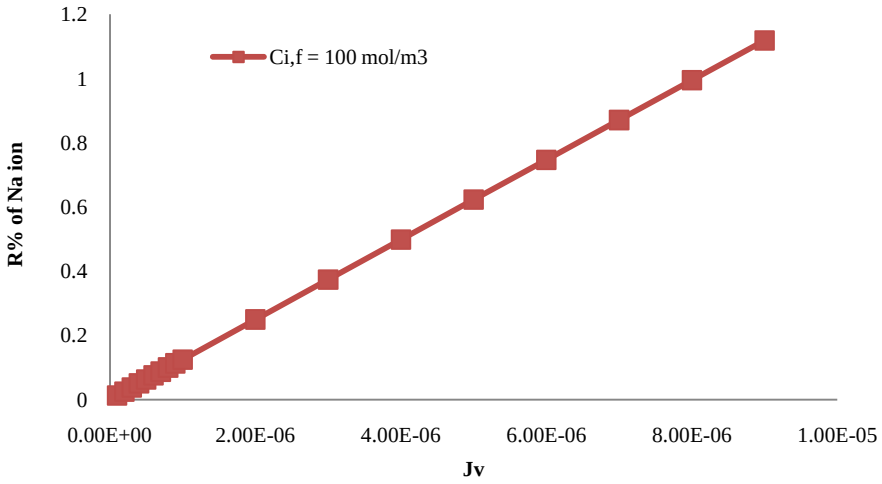

Figure 9-16. Rejection of Na^{1+} ion versus J_v ($m^3/m^2/s$).

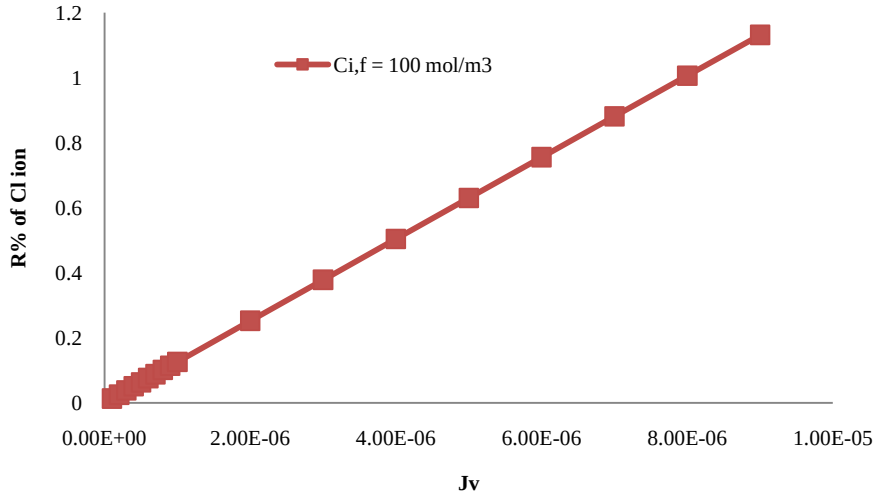

Figure 9-17. Rejection of Cl^{1-} ion versus J_v ($m^3/m^2/s$).

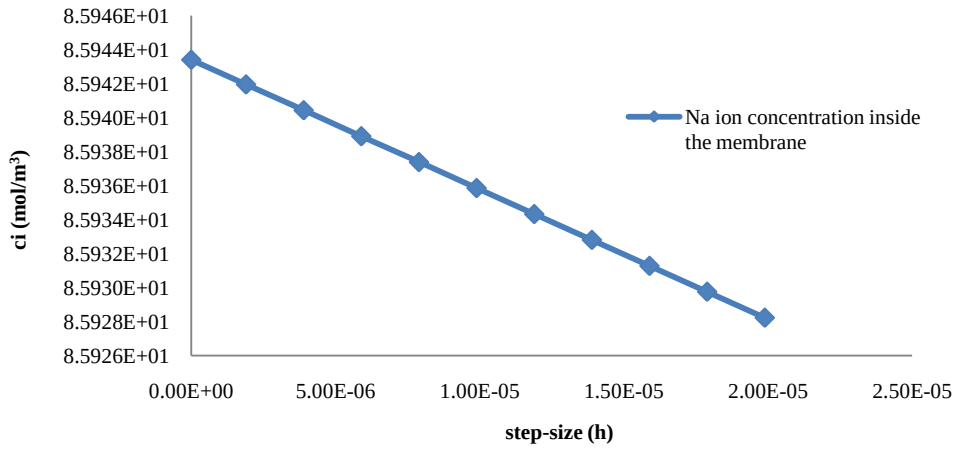

Figure 9-18. Na^{1+} ion concentration inside the membrane active layer versus the step-size.

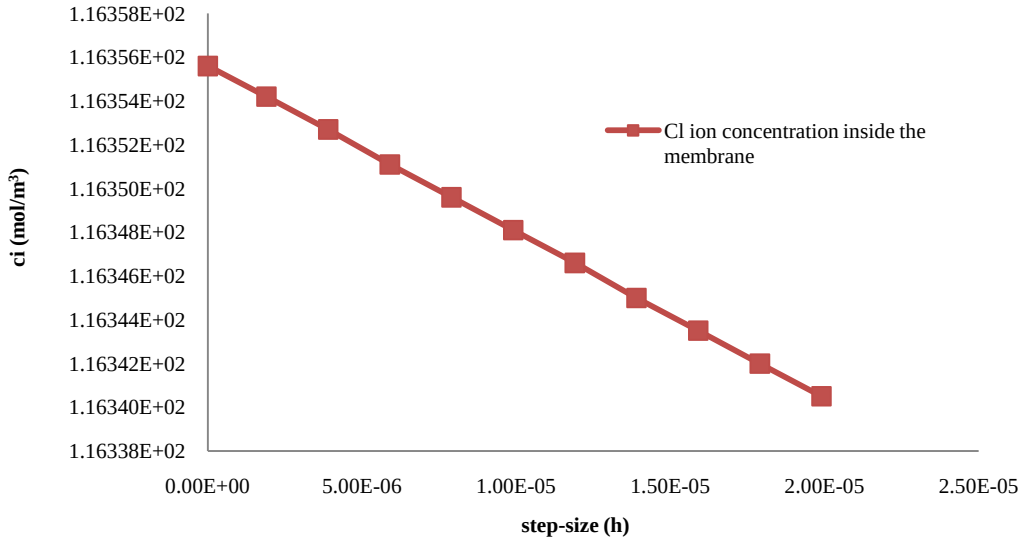

Figure 9-19. Cl^{1-} ion concentration inside the membrane active layer versus the step-size.

The ion's rejection from lower feed ion concentration was slightly higher than the ion's rejection from higher feed ion concentration. This agrees with the theory, because as the ions concentration in the feed solution increases then the ions accumulation on the feed/membrane interface would increase causing the membrane charge effect to decrease and the permeation of ions through the membrane active layer would increase. The rejection of Cl^{1-} was higher than the rejection of Na^{1+}; these results are supported by the Nernst-Planck equation, where the membrane effective charge (X_d) would have played a role in causing a difference in the rejection between a cation and an anion. It was noticed that the ions rejection increased as the permeate volume flux (based on the membrane area) increased, such observation supports the trans-membrane pressure (TMP) where the theory suggests that the ions rejection would increase as the TMP increases. For both values of the feed concentration, it was noticed that the concentration of Na^{1+} and Cl^{1-} inside the membrane decreased as the ions moved through the membrane active layer from the feed side to the permeate side. It was noticed that the concentration of Na^{1+} ion inside the membrane active layer was lower than the concentration of Cl^{1-} ion. For the two initial feed concentration values (10 and 100 mol/m^3) that were assumed, it was noticed that the concentration of Na^{1+} and Cl^{1-} ions inside the membrane active layer decreased as the ions moved through the membrane active layer from the feed side to the permeate side, beside that the concentration of the Na^{1+} and Cl^{1-} ions inside the membrane active layer decreased as the volumetric flux based on membrane area (J_v) increased, see figure 9-20, (refs. 317, 325).

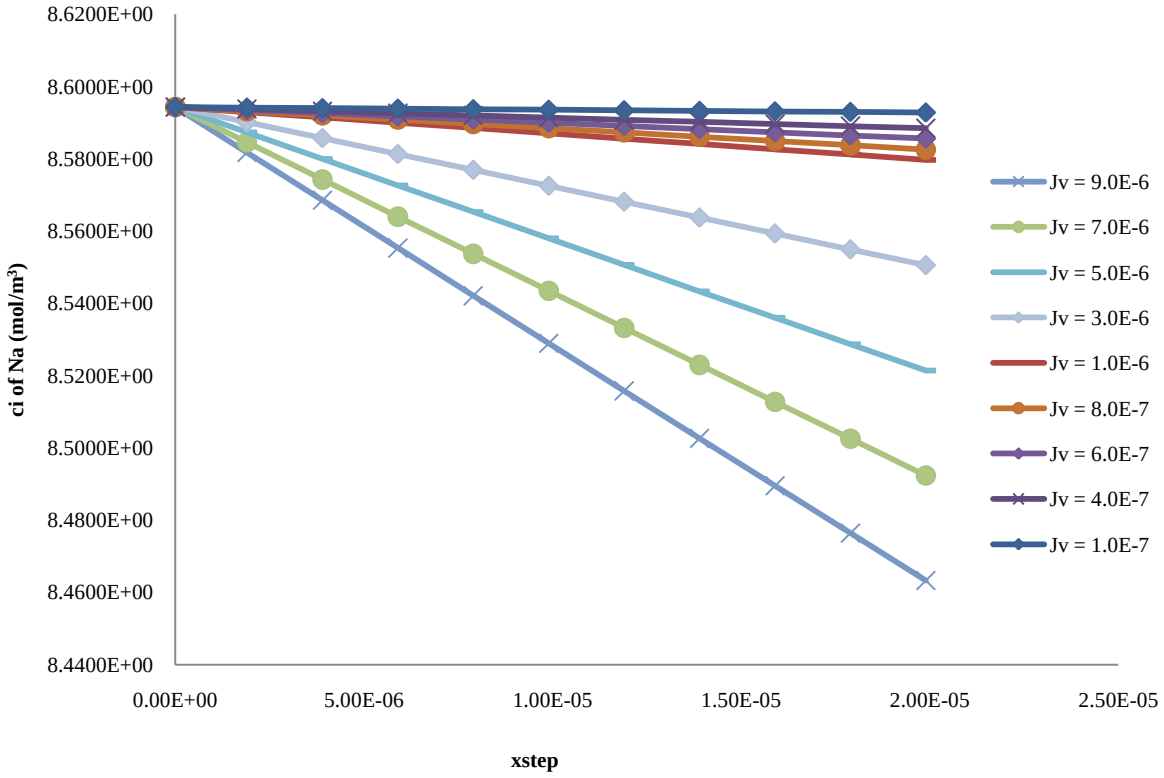

Figure 9-20. Na^{1+} ion concentration inside the membrane active layer versus the step-size (for different volumetric flux (J_v)).

9.3 Discussion

The same results were obtained when using the Euler and Runge-Kutta methods. The difference between the two methods is that the ion's rejection values obtained by using the Runge-Kutta method were slightly higher than the values obtained by the Euler method. From Euler and Runge-Kutta mathematical methods, it was noticed that the rejection of Na^{+1} and Cl^{-1} ions increased as the volumetric flux based on membrane area (J_v) increased. Also the concentration of Na^{+1} and Cl^{-1} ions inside the membrane active layer decreased as the volumetric flux based on membrane area (J_v) increased (ref. 317), which supports the increase in the ions rejection as the volumetric flux based (J_v) increased. These results are related to the TMP, where the theory suggests that the ions rejection would increase as the TMP increases (ref. 7). In addition, the rejection of Na^{+1} and Cl^{-1} ions decreased as the feed concentration increased (refs. 125, 325), which was similar to results obtained from the experiments. The rejection of Cl^{1-} was higher than the rejection of Na^{1+}, which agrees with the results obtained from the experiments. Such rejection behaviour is related to the membrane charge, which is a negative charge. Where the membrane effective charge (X_d) was used as a condition to integrate equation (9.3) to obtain the electrical potential gradient,

as well the electrical potential gradient is used to integrate the Nernst-Planck equation to obtain the ions concentration inside the membrane and the permeate solution (see equations 9.4 and 9.6). Repulsion between the membrane charge and the Cl^{1-} ions would occur while attraction between the membrane charge and the Na^{1+} ions would occur, which means that Na^{1+} ions would pass more freely through the membrane active layer and the Cl^{1-} ions would be rejected. Another parameter that would affect the ions rejection is the membrane active layer pore size which appears in the hindrance factor for diffusion ($K_{i,d}$) and the hindrance factor for convection ($K_{i,c}$) as have been explained in equations (9.8), (9.12) and (9.13) (See appendix-3 and appendix-4). However, the hindrance factor for diffusion ($K_{i,d}$) and the hindrance factor for convection ($K_{i,c}$) that were used in the model were assumed a constant parameters in-order to try to understand other parameters such as the change in the concentration feed on the rejection of ions. Similar results were obtained by W. Richard Bowen et. al. (refs. 325, 326) over the boundary conditions that were used, where the rejection increased as the volumetric flux based on membrane area (J_v) increased. The rejection values the found agrees with values obtained in this work. Moreover when applying the volumetric flux based on membrane area (J_v) that were used in W. Richard Bowen et. al. work, similar results were obtained with the model that was used in this work. Increasing the membrane thickness increased ions rejection, where rejection was higher than 40%, which agrees with several works that have been for nanofiltration membrane. Nevertheless, in this work, the thickness of the membrane active layer was considered as the membrane thickness because it is the main part of the membrane where ions separation occurs. In addition, the pore radius of the support layer is larger than the ions radius thus the ions would pass easily through the support layer; as a result, the support layer thickness can be neglected. However, if large molecules were used with such model then the support layer thickness cannot be neglected because it would have an impact on the rejection of molecules. Runge-Kutta method could solve equation (9.3) when the membrane thickness was assumed to be equal to 1.40E-3 m, which is the actual membrane thickness including the active layer and the support layer. On the other hand, Euler method could not solve equation (9.3) for a membrane thickness higher than 6.0E-4 m. Same results were obtained by increasing the step-size for both mathematical methods, but as the step-size was further increased Euler method stopped working and no results were obtained. The accuracy of both models was checked by doubling the step-size, were similar results were obtained.

9.4 Summary

This chapter described the calculation methods for the Nernst-Planck equation. In this chapter, the extended Nernst-Planck equation was solved using Euler and Runge-Kutta mathematical methods. FORTRAN programme was used to solve the model. This model is known for its limitation and for being more descriptive than predictive, and in-order to overcome these limitations experimental parameters were used. The chosen ions were Na^{1+} and Cl^{1-} ions. The model was solved for two different feed concentrations, which were 10 and 100 mol/m^3. The membrane active layer thickness was assumed to be equal to 20.0E-6 m, which was obtained from the experiments, see section 8-7 in chapter 8. For each concentration value, the model was solved for different volume flux values that ranged between 1.0E-7 to 9.0E-6 $m^3/m^2/s$. More work need to be done in-order to improve this method such understanding the physics of solutions and the properties of ions because they have great effect on the nanofiltration separation process. Moreover, more experimental work need to be done to try to understand separation behaviour of nanofiltration membrane in-order to compare it to theoretical model and try to improve the theory so that it would be more predictive.

Chapter 10 Conclusion and further work

The aim of this work was to try to understand the separation behaviour and the permeation properties of a TiO_2 ceramic nanofiltration membrane for an aqueous solution containing inorganic electrolytes. The influences of ion concentration, electrolyte type, feed pH and concentration polarisation on the membrane separation behaviour were investigated.

10.1 Conclusion

Two different membranes were investigated with pore radii of 0.9 and 1.0nm. The separation behaviour of sodium chloride (NaCl), sodium nitrate ($NaNO_3$), sodium sulphate (Na_2SO_4), magnesium chloride ($MgCl_2$), and calcium chloride ($CaCl_2$) was observed in single salt solutions and two combinations of mixed salts solutions. The first combination consisted of sodium chloride (NaCl), sodium nitrate ($NaNO_3$), sodium sulphate (Na_2SO_4), whilst the second combination consisted of sodium chloride (NaCl), magnesium chloride ($MgCl_2$), and calcium chloride ($CaCl_2$). The feed concentration was 0.1M. In general, the highest rejection was found at the lowest TMP value for both single and mixed salt solutions. Rejection of all salts declined rapidly as TMP was increased, the maximum rejections where at approximately at 0.2bar TMP. It was found that the ion charge and the ion size had an effect on its rejection. In addition, the electrostatic interaction between the membrane charge and the ions' charge plays a significant role.

- Common cation and mixed anions

The rejection of the common Na^{1+} cation from single and mixed salt solutions by 0.9nm membrane was found to be independent of the anion type and the electrolyte concentration. Where Na^{1+} cation had the lowest rejection from single salt and mixed salts solutions. The rejections of SO_4^{2-} and Cl^{1-} anions from single and mixed salts solutions by 0.9nm membrane were found to be independent of the anion type. The rejection of the NO_3^{1-} anion from mixed salt solution, on the other hand, was found to be higher than from single salt solution. Except at the lowest TMP were the rejection of the NO_3^{1-} anion from mixed salt solution, on the other hand, was found to be lower than from single salt solution.

The rejection of the common Na^{1+} cation from single and mixed salt solution by 1.0nm membrane was found to be dependent of the anion type and the electrolyte concentration.

The rejection of Na^{1+} cation from $NaNO_3$ and Na_2SO_4 solutions was lower than the anions rejection, but Na^{1+} rejection from NaCl and mixed salts solutions was higher than the anions rejection. The rejection of Cl^{1-} ions by 1.0 nm membrane from single salt and mixed salts solution was independent of the anions type. Except at the lowest TMP, the rejection of Cl^{1-} from mixed salts solution was higher than Cl^{1-} rejection from NaCl solution. On the other hand, the rejections of NO_3^{1-} and SO_4^{2-} anions from mixed salts solution were lower than their rejection from single salt solution, which concludes that the rejections of NO_3^{1-} and SO_4^{2-} was affected by the existence of anther types of anions. At the lowest TMP, the rejections of NO_3^{1-} and SO_4^{2-} from mixed salts solution were higher than their rejections from $NaNO_3$ and Na_2SO_4 solutions.

When comparing the rejections of NO_3^{1-} from $NaNO_3$ solution by 0.9 and 1.0nm membranes, it was noticed that the rejection by 1.0nm membrane was higher than the rejection by 0.9 except at the lowest TMP. The rejections of SO_4^{2-} from $NaSO_4$ solution and Cl^{1-} from NaCl solution by 0.9 and 1.0nm membranes were similar. The rejection of Na^{1+} from the single salts solution by 0.9 and 1.0nm were similar, except that the rejection of Cl^{1-} from NaCl solution by 0.9nm membrane was higher than the rejection of Na^{1+}, and vice versa by 1.0nm membrane. The common cation rejection from the mixed salts solution by 0.9nm membrane was lower than the anions rejections. On the other hand, the common cation rejection from the mixed salts solution by 1.0nm membrane was higher than the anions rejections

- Common anion and mixed cations

For 0.9nm membrane, the rejection of Ca^{2+} cation from single salt solution was higher than its rejection from mixed salt solution. The rejection of Mg^{2+} cation from single salts solution was lower than its rejection from mixed salt solution. The rejection of Na^{1+} cation from single and mixed salt solutions was found to be independent of the anion type and the electrolyte concentration. The rejection of Cl^{1-} from $MgCl_2$ solution was higher than the rejection of Mg^{2+}. The rejection of Cl^{1-} from NaCl solution was higher than the rejection of Na^{1+}. The rejection of Cl^{1-} from $CaCl_2$ solution was lower than the rejection of Ca^{2+}. The rejection of Cl^{1-} from mixed salt solution was higher than the rejection of Mg^{2+}, Ca^{2+} and Na^{1+}, where the rejection took the following trend R of Cl^{1-} > R of Ca^{2+} > R of Mg^{2+} > R of Na^{1+}, except at the TMP where the rejection of Cl^{1-} was lower the rejections of cations. Thus, the rejections

of Cl^{1-} anion, Ca^{2+} and Mg^{2+} cations were dependent of the cation type and the electrolyte concentration.

For 1.0nm membrane, he rejections of Mg^{2+} and Ca^{2+} cations from mixed salts solution were higher than their rejection from single salt solution. The rejection of Na^{1+} cation from mixed salt solution was lower than its rejection from single salt solution. The rejection of Cl^{1-} from $MgCl_2$ solution was higher than the rejection of Mg^{2+}. The rejection of Cl^{1-} from NaCl solution was lower than the rejection of Na^{1+}. The rejection of Cl^{1-} from $CaCl_2$ solution was higher than the rejection of Ca^{2+}. The rejection of Cl^{1-} from mixed salt solution was higher than the rejection of Mg^{2+}, Ca^{2+} and Na^{1+}, where the rejection took the following trend R of Cl^{1-} > R of Ca^{2+} > R of Mg^{2+} > R of Na^{1+}. The rejection of Cl^{1-} anion from $CaCl_2$ and mixed salts solutions was higher than its rejection from $MgCl_2$ and NaCl solutions, where its rejection depended on the ions type and electrolyte concentration.

Comparing rejections of 0.9 and 1.0nm membranes, it was found that the rejections of Cl^{1-} from $MgCl_2$ and NaCl solutions by were similar. The rejections of Cl^{1-} from $CaCl_2$ by 0.9nm membrane were lower than the rejection by 1.0nm membranes. The rejection of Cl^{1-} from NaCl solution by 0.9nm membrane was higher than the rejection of Na^{1+}, and vice versa by 1.0nm membrane. The rejections of Cl^{1-} from $MgCl_2$ solution by both 0.9 and 1.0nm membranes were higher than the rejection of Mg^{2+}. The rejection of Cl^{1-} from $CaCl_2$ solution by 0.9nm membrane was lower than the rejection of Ca^{2+}, and vice versa by 1.0nm membrane. The common anion rejection from the mixed salts solution by 0.9nm membrane was lower than the catios rejections. On the other hand, the common anion rejection from the mixed salts solution by 1.0nm membrane was higher than the anions rejections

- Mixed anions and cations

The separation behavior of magnesium chloride ($MgCl_2$) and sodium nitrate ($NaNO_3$), with feed concentration equal to 0.01M, was observed in single salt and mixed salts solution for 0.9 and 1.0nm membrane.

In the case of 0.9nm membrane, the rejection of Cl^{1-} from single salt solution was higher than the reject cation of NO_3^{1-}. Moreover, the rejection of Mg^{2+} from single salt solution was higher than the rejection of Na^{1+}. For $NaNO_3$ solution, when excluding the minimum TMP value, the rejection of NO_3^{1-} ion was lower than the rejection of Na^{1+} ion. The highest

rejection for Na^{1+} and NO_3^{1-} was at the lowest TMP, and the rejection of NO_3^{1-} was higher than the rejection of Na^{1+}. For $MgCl_2$ solution, the rejection of Mg^{2+} was higher than the rejection of Cl^{1-}. The rejection of cations and anions from a mixed solution ($MgCl_2$ and $NaNO_3$) took the following trend, R of Mg^{2+} > R of NO_3^{1-} > R of Cl^{1-} > R of Na^{1+}. However, at the lowest TMP the rejection took the following trend R of Mg^{2+} > R of NO_3^{1-} > R of Na^{1+} > R of Cl^{1-}. The rejection of Mg^{2+} and Cl^{1-} were independent of electrolyte concentration, anions and cations type. Whilst the rejections of Na^{1+} and NO_3^{1-} were dependant on the anions type and the electrolyte concentration, their rejections from single salt solution was higher than their rejection from mixed salts solution.

For 1.0 nm membrane, the rejection of NO_3^{1-} ions from $NaNO_3$ solution was higher than the rejection of Na^{1+} ions, and the highest rejection for both ions was at the lowest TMP. The rejection of Cl^{1-} ion from $MgCl_2$ solution was higher than the rejection of Mg^{2+} ions, and the highest rejection for both ions was at the lowest TMP. The rejection of ions from mixed salt solution of $MgCl_2$ and $NaNO_3$ took the following trend, R of Mg^{2+} > R of NO_3^{1-} > R of Cl^{1-} > R of Na^{1+}, and the highest rejection for all the ions was at the lowest TMP. When excluding the minimum TMP value, the rejection of Cl^{1-}, NO_3^{1-}, Na^{1+} and Mg^{2+} remained constant as the TMP increased. The rejection of Cl^{1-} from single salt solution was higher than the reject cation of NO_3^{1-}. Moreover, the rejection of Mg^{2+} from single salt solution was higher than the rejection of Na^{1+}. The rejection of Mg^{2+} and Cl^{1-} were dependant of electrolyte concentration, anions and cations type. Whilst the rejection of Na^{1+} and NO_3^{1-} were independent on the anions type and electrolyte concentration, their rejections from single salt solution were similar to their rejections from mixed salts solution.

By comparing the rejection of cations and anions by 0.9 and 1.0nm membranes, it was notice that the rejection of Na^{1+} by 0.9nm membrane was higher than the rejection of NO_3^{1-}, whilst the rejection of Na^{1+} by 1.0nm membrane was lower than the rejection of NO_3^{1-}. The rejection of Mg^{2+} by 0.9nm membrane from single salt was higher than the rejection of Cl^{1-}. Whilst the rejection of Mg^{2+} from single salt solution by 1.0nm membrane was lower than the rejection of Cl^{1-}. Thus, the ions rejection from single salt solutions was dependant on ions type, electrolyte concentration and membrane pore size. The rejection of ions from mixed salts solution by both membranes took the following trend: R of Mg^{2+} > R of NO_3^{1-} > R of Cl^{1-} > R of Na^{1+}, thus the cations and anions were independent of ions type, electrolyte concentration and membrane pore size.

- Concentration effect

For 0.9nm membrane, the rejection of NO_3^{1-} and Na^{1+} from 0.01M single salt solution was higher than their rejection from 0.1M solution. In the case of 0.01M solution, the rejection of Na^{1+} was higher than the rejection of NO_3^{1-}. Whilst, in the case of 0.1M solution, the rejections of NO_3^{1-} and Na^{1+} were similar. The rejection of Mg^{2+} and Cl^{1-} from 0.01M single salt solution was higher than their rejection from 0.1M solution. The rejection of Mg^{2+} from 0.01M solution was higher than the rejection of Cl^{1-}. On the other hand, the rejection of Mg^{2+} from 0.1M solution was lower than the rejection of Cl^{1-}.

For 1.0nm membrane, the rejections of Na^{1+} from 0.01 and 0.1M mixed salt solutions were similar and lower than the rejection of NO_3^{1-}. While the rejection of NO_3^{1-} from 0.1M mixed salt solution was higher than its rejection from 0.01M mixed salt solution. The rejection of Mg^{2+} and Cl^{1-} from 0.01M mixed salt solution was higher than their rejection from 0.1M mixed salt solution. The rejection of Mg^{2+} from 0.01 and 0.1M solutions was lower than the rejection of Cl^{1-}.

During the experimental work, it was noticed that rejection of ions decreased as the TMP increased, while in Maria Diná Afonso et al. (ref. 201) work it was noticed that rejection of ions increased as the TMP increased. This might be due to the difference in the used TMP, where in Maria Diná Afonso et al. (ref. 201) work TMP had values between 10-25 bar, where in this work TMP was between 0.2-1.9 bar. The reason for using low TMP values is due to the instability in the used system when the TMP was increased for higher values. In addition, it was noticed that the permeate volume flux based on the membrane area for distilled water and salt solutions increased as the TMP increased. Also, the permeate volume flux based on the membrane area for distilled water was higher than that of the salt solution, (Carolina Mazzoni et al. (ref. 72)). For 0.9 and 1.0nm membranes, the rejection of ions decreased as TMP increased for different electrolyte concentrations and mixtures. On the other hand, the rejection behaviours of cations and anions by 0.9nm membrane were different from that by 1.0nm membrane. Where the rejection of Na^{1+} by 0.9nm membrane was lower than the rejection of Cl^{1-}. Whilst the rejection of Na^{1+} by 1.0nm membrane was higher than the rejection of Cl^{1-}. In addition, the rejection of Ca^{2+} by 0.9nm membrane was higher than the rejection of Cl^{1-}. Moreover, the rejection of Ca^{2+} by 1.0nm membrane was, lower than the rejection of Cl^{1-}. Nevertheless, the rejections of SO_4^{2-} and NO_3^{1-} were higher than the

rejection of Na^{1+} for 0.9 and 1.0nm membrane.

When comparing theoretical and experimental results for sodium chloride (NaCl), it was noticed that they differ. For Na^{1+}, it was noticed from the experiments - if the lowest TMP was excluded for both membranes – that the rejection did not change as the TMP increased, while from the theoretical model it was noticed that the rejection increased as the permeate volumetric flux per unit area increased. The same results were noticed for Cl^{1-}, where in the experiments - if the lowest TMP was excluded for both membranes – the rejection did not change as the TMP increased, while from the theoretical model it was noticed that the rejection increased as the permeate volumetric flux per unit area increased. In addition, in the experiments the rejection of Na^{1+} by 1.0 nm membrane was higher than the rejection of Cl^{1-} but the rejection of Na^{1+} by 0.9nm membrane was lower than the rejection of Cl^{1-}, while in the theoretical modelling the rejection of Na^{1+} was lower than the rejection of Cl^{1-}. Moreover, the change in concentration did not have an effect on the rejection of Na^{1+} either in the theoretical modelling or in the experiments, which means that they agree. While for Cl^{1-} case, the concentration did not have an effect on its rejection in the theoretical part but in the experiments, it was found that Cl^{1-} rejection from lower concentration solution was higher than their rejection from higher concentration solution.

- pH

Another set of experiments were done by controlling the pH of the feed solution, the used pH values where pH3, pH7 and pH10. In these experiments, sodium chloride (NaCl) and sodium sulphate (Na_2SO_4) salts were use, where the Na^{1+} was the common ion. The membrane that was used was a ceramic nanofiltration membrane (the membrane made of TiO_2, with 7.00 mm I.D, 10 mm O.D and length of 190 mm, and the mean pore radius was 1.0 nm).

  - pH 3

The rejection of Cl^{1-} ions from NaCl solution was lower than the rejection of Na^{1+} ions, and the highest rejection of both ions was at the lowest TMP. If the lowest TMP value was excluded, then the rejection of Cl^{1-} remained constant as the TMP increased, while the rejection of Na^{1+} increased as TMP increased.

The rejection of SO_4^{2-} ions from Na_2SO_4s solution was lower than the rejection of Na^{1+} ions,

and the highest rejection of both ions was at the lowest TMP. If the lowest TMP value was excluded, then the rejection of SO_4^{2-} and Na^{1+} remained constant as the TMP increased.

The rejection of SO_4^{2-} ions from NaCl and Na_2SO_4 solution was higher than the rejection of Cl^{1-} ions, and the highest rejection of all ions was at the lowest TMP. By excluding the lowest TMP value, the rejection of Na^{1+} remained constant as the TMP increased. On the other hand, the rejections of SO_4^{2-} and Cl^{1-} decreased then increased as the TMP increased. The rejection of Na^{1+} was higher than the rejections of Cl^{1-}, and SO_4^{2-}. In addition, the rejection of SO_4^{2-} was higher than the rejection of Cl^{1-}.

The rejection of Na^{1+} from Na_2SO_4 solution was higher than its rejection from NaCl and mixed salts solution. In addition, the rejection of Na^{1+} from NaCl and mixed salts solutions were similar. At the lowest TMP, the rejections of Na^{1+} from NaCl solution was 25.0%, from Na_2SO_4 solution was 46.0% and from mixed salt solutions was 50.0%. This means the highest rejection of Na^{1+} was from mixed salts solution. The rejection of Cl^{1-} from mixed salt solution (39.0%) was lower than its rejection from NaCl solution (25.0%). As a result, Na^{1+} and Cl^{1-} rejections were dependent on ions type and electrolytes concentrations. On the other hand, the rejection of SO_4^{2-} was independent on ions type and electrolyte concentration.

- pH 7

The rejection of Cl^{1-} ions from NaCl solution was lower than the rejection of Na^{1+} ions. The highest rejection of both ions was at the lowest TMP. Moreover, if the lowest TMP value is excluded, then the rejections of Cl^{1-} and Na^{1+} remained constant as the TMP increased and the rejection of Na^{1+} was higher than the rejection of Cl^{1-}.

The rejection of SO_4^{2-} ions from Na_2SO_4 solution was higher than the rejection of Na^{1+} ions. The highest rejection of both ions was at the lowest TMP, and by excluding the lowest TMP value, the rejection of SO_4^{2-} and Na^{1+} remained constant as the TMP increased and the rejection of Na^{1+} was lower than the rejection of SO_4^{2-}.

The rejection of Na^{1+} ion from mixed salt (NaCl and Na_2SO_4) solution was the higher than the rejection of Cl^{1-} and SO_4^{2-}. In addition, the rejection of SO_4^{2-} ion was higher than the rejection of Cl^{1-} ion. The highest rejection of all ions was at the lowest TMP, and if the lowest TMP was excluded then the rejection of the three ions remained constant as the TMP

increased.

- pH 10

For NaCl solution, the rejection of Cl^{1-} ions was higher than the rejection of Na^{1+} ions. The highest rejection for both ions was at the lowest TMP. For Na_2SO_4 solution, the rejection of SO_4^{2-} ions was higher than the rejection of Na^{1+} ions. The highest rejection of both ions was at the lowest TMP. For NaCl and Na_2SO_4 solution, the rejection had the following trend: R of Na^{1+} > R of SO_4^{2-} > R of Cl^{1-}.

The rejection of Na^{1+} from mixed salts solution was higher than its rejection from single salt solutions. In additions, the rejection of Na^{1+} from Na_2SO_4 solution was higher than its rejection from NaCl solution. The rejection of Cl^{1-} from mixed salts solution was higher than its rejection from NaCl solution. The rejection of SO_4^{2-} from mixed salts solution was lower than its rejection from Na_2SO_4 solution.

In general, the ions rejection was affected by changing the solution pH. For an example, the rejections of NaCl from a pH controlled solution around pH 3 and 7 and non-controlled pH solutions were similar, but the rejection from a pH 10 solution differed. Where the rejection from pH 10 solution was lower than the rest of the rejection values and the rejection of Cl^{1-} was higher than the rejection of Na^{1+}. Similar results were obtained by P. Puhlfürß et al (ref. 240), where the pH had an effect on the behaviour of the cation and the anion rejection but not the rejections value. However, in G. Hagmeyer et al. (ref. 97) it was found that the lowest rejection was around the ISP, but in this work, the rejection of ions around the ISP was higher. This might be due to the difference in the membrane pore radius, where in this work the membrane pore radius was 1.0E-9m but in G. Hagmeyer et al. (ref. 97) work, it was 0.7E-9 and 3.32E-9m. Which support the different rejection results obtained by 0.9 and 1.0nm membranes.

The obtained results were compared with G. Hagmeyer and R. Gimbel work (ref. 97), it was noticed that they differed. Where the rejection of NaCl in G. Hagmeyer and R. Gimbel increased as the permeate flux increased, while in this work the rejection of NaCl decreased as the permeate flux increased. The permeate flux increased as the TMP increased, on the hand the rejection decreased as the TMP increased. This might be due to the difference in the volume flux based on the membrane area values (which is related to the TMP), where the

volume flux ranged between 3.0E-7 to 9.0E-6 $m^3/m^2/s$ but in G. Hagmeyer and R. Gimbel work the volume flux ranged between 2.0E-6 to 22.0E-6 $m^3/m^2/s$. The differences between the rejections might be due to the membrane charge, which can be explained through the difference in the zeta potential. In this work, the zeta potential had negative values around pH 5, while in G. Hagmeyer et al. (ref. 97) work the zeta potential had negative values at pH 4. This may increase the negative membrane charge as a result would increase the ions rejection as was noticed in the work of G. Hagmeyer et al. (ref. 97).

- Theoretical section

In the theoretical part, nanofiltration membrane was characterised by the Nernst-Planck equation. Euler and Runge-Kutta methods were used to solve the Nernst-Planck equation by using FORTRAN (F77) program. The two programs were run for sodium chloride (NaCl) for two different feed concentrations at various volumetric fluxes (based on the membrane area). The boundary conditions that were used to solve the modelling were similar to the conditions used in the experiments. The two different concentrations and the volume (based on the membrane area) fluxes values were used in order to observe their effects on the membrane rejection. In addition, volume (based on the membrane area) fluxes were considered because they are related to the TMP, which does not appear in Nernst-Planck equation but has an effect on rejection.

When Euler's method was used, it was found that nanofiltration membrane rejection increased as the volume flux increased. For the two different concentration values, which are 0.01 and 0.1M, the rejection of Cl^{1-} was slightly higher than the rejection of Na^{1+}. In addition, the concentration of Na^{1+} ion inside the membrane active layer was lower than the concentration of Cl^{1-} ion. Moreover, the concentration of the ions inside the membrane active layer decreased as the volumetric flux based on membrane area (J_v) increased (ref. 317). The ion's rejection from lower feed ion concentration was slightly higher than the ion's rejection from higher feed ion concentration. When Runge-Kutta method was used, it was found that the rejection increased as the volume flux through the membrane increased. For the two different concentrations, the rejection of Na^{1+} and Cl^{1-} ions increased as the volume flux increased. The rejection of Cl^{1-} was slightly higher than the rejection of Na^{1+}. Also, the concentration of Na^{1+} and Cl^{1-} inside the membrane decreased as the ions move through the membrane active layer from the feed side to the permeate side (ref. 317). In addition, the

concentration of Na^{1+} ion inside the membrane active layer was lower than the concentration of Cl^{1-} ion inside the membrane active layer. It was noticed, that the rejection of ions from the lower initial concentration was slightly higher than the ions rejection from higher initial ion concentration. The initial ion concentration effect on the rejection of ions was very small that it can be neglected. As a result, the initial ion concentration did not have an effect on the ion rejection. Similar results were obtained by using Euler method and Runge-Kutta method, the difference between the two methods that the ions rejection values obtained by using Runge-Kutta method were slightly higher than the values obtained by Euler method. W. Richard Bowen et. al. work (refs. 325, 326) supported the obtained results, where they got low rejection values for similar conditions. In addition, the volumetric flux based on membrane area (J_v) was increased to the same values that were used by Richard Bowen et. al, where both models obtained similar results. Ions rejection increased as the membrane thickness was increased - to be equal to the whole membrane thickness.

From the experiments and by including the lowest TMP, the rejection deceased rapidly then remained constant as TMP increased, while in the theoretical modelling the rejection increased as TMP increased. On the other hand, the low rejections obtained from the theoretical modelling agree with the low rejections obtained from the experiments. Thus, the difference in the rejection behaviour because of the TMP might be due

10.2 Further work

- Ceramic nanofiltration membrane is a promising method that has a good separation mechanism especially for a mixed ions solution. Thus, further work should be done for higher concentrations and more mixed salts similar to the one found in nature such as seawater.
- Ceramic nanofiltration membrane is made from different materials such as TiO_2 and ZrO_2, where the membrane material affects ions rejection. TiO_2 nanofiltration membrane has been used, thus a good approach would be investigating ZrO_2 nanofiltration membrane for similar conditions in order to compare these two membranes and investigate the membrane material effect on the rejection of ions.
- Nanofiltration membrane pore size ranges between 0.5-8nm. In this work 0.9 and 1.0nm were investigated, which would be a good approach investigating the separation behaviour of electrolyte solutions using membrane with lower pore radius. This approach would give a better understanding of the effect of the membrane pore size on the rejection of ions, because it was noticed that the rejection behaviour of ions such as Na^{1+} and Cl^{1-} differed

from 0.9 to 1.0nm membranes and better conclusion would be obtained by comparing the obtained results with different type of membrane.

- In the theoretical modelling, include parameters such as the ion activity coefficient (γ_i) as in Lawrence Dresner work (ref. 170).
- In the modelling work, the used Donnan potential assumed that the dielectric constant in the bulk was equal to the dielectric constant in the membrane pores. Thus, it would be a good approach to account for the change in the dialectical constant between the bulk and the pores by considering the change of electrostatic free energy (ΔW).
- In the theoretical modelling, it was assumed that the osmotic pressure to be negligible. Nevertheless, in fact it does exist which might be the reason for the highest rejection that was obtained at the lowest TMP in the experiments. Thus, it would be a good approach to add the osmotic pressure variable to the theoretical modelling to study the effect of the osmotic pressure on the rejection of ions.
- Solve the model for different types of ions and for mixed ions such as tertiary and quaternary ions.
- Use other theories such as the electrostatic and the steric-hindrance model, and the Spiegler-Kedem model to predict the separation behaviour of nanofiltration membrane.
- Apply an electrical current on the membrane surface to enhance the separation of ions mechanism.

Appendix 1

```
      PROGRAM membrane
      IMPLICIT REAL (A-H,O-Z)
      DOUBLE PRECISION vpm,diff,hidc,hidf,temp,umem,con,edon
      DOUBLE PRECISION deex,xstep,farad,gascon ,dydx
      COMMON/aleph/vpm(10,2),diff(10,2),hidc(10,2),hidf(10,2),con(10,2)
      COMMON/ale/edon(10,2)
      COMMON/a/c(20001,2),conf(20001,2),dydx(20001,2)
      COMMON/beth/farad,gascon,deex,umem,nep,xstep,temp,node

      OPEN(unit=5,file='memb.dat',status='unknown')
      OPEN(unit=6,file='memb.res',status='unknown')
      farad=96485.3383
      gascon=8.3145
!     convrg=1.0D-5
!     PRINT*,' auto 1 other 0'
!     read*,iauto
      iauto = 1
      IF(iauto.EQ.1)THEN
        READ(5,*)nep
        print*, nep
        write(6,*) nep
        READ(5,*)temp,umem
        print*,temp,umem
        write(6,*)temp,umem
       Print*,'temp',temp
      Print*,'umem',umem

        DO i = 1,nep
          DO j = 1,2
            READ(5,*)vpm(i,j),diff(i,j),hidc(i,j),hidf(i,j)
            READ(5,*)con(i,j),edon(i,j)
            PRINT*,i,j,vpm(i,j),diff(i,j),hidc(i,j),hidf(i,j)
            PRINT*,con(i,j),edon(i,j)
            WRITE(6,*)i,j,vpm(i,j),diff(i,j),hidc(i,j),hidf(i,j)
            WRITE(6,*)i,j,con(i,j),edon(i,j)
          END DO
          vpm(i,1)=DABS(vpm(i,1))
          vpm(i,2)=-DABS(vpm(i,2))
        END DO
      ELSE
        Print*,' Where is the data??'
        stop
      END IF
      node=200
!     thick = membrane thickness in micron
      deex = 20.0
      deex = deex*1.0D-6
      xstep = deex/(DFLOAT(node))
      print*,'xstep',xstep
      print*,'node',node
      print*,' '
      print*,'*****************************************************'
      print*,' '
      print*,'              ALL UNITS ARE S.I. '
      print*,' '
      print*,'*****************************************************'
      print*,' '
```

```
      CALL euler
      CALL output
      STOP
      END

      SUBROUTINE EULER
      IMPLICIT REAL (A-H,O-Z)
      DOUBLE PRECISION conf,vpm,diff,hidc,hidf,temp,umem,con,edon
      DOUBLE PRECISION deex,xstep,farad,gascon
      DOUBLE PRECISION change,dydx
      COMMON/aleph/vpm(10,2),diff(10,2),hidc(10,2),hidf(10,2),con(10,2)
      COMMON/ale/edon(10,2)
      COMMON/a/c(20001,2),conf(20001,2),dydx(20001,2)
      COMMON/beth/farad,gascon,deex,umem,nep,xstep,temp,node
      change = 1.0
!     set initial conditions
      conf(1,1)=con(1,1)/1.0
      conf(1,2)=con(1,2)/1.0
      while(dabs(change).GT.0.0000001)DO

      c(1,1)=con(1,1)*exp(-vpm(1,1)*farad*edon(1,1)/gascon/temp)
      c(1,2)=con(1,2)*exp(-vpm(1,2)*farad*edon(1,2)/gascon/temp)

       DO i=2,node
       const1= (vpm(1,1)*umem/diff(1,1))*(hidc(1,1)*c(i-1,1)-conf(1,1))
       const2= (vpm(1,2)*umem/diff(1,2))*(hidc(1,2)*c(i-1,2)-conf(1,2))
       const3= vpm(1,1)*vpm(1,1)*c(i-1,1)
       const4= vpm(1,2)*vpm(1,2)*c(i-1,2)

       cons=(const1+const2)/((farad/gascon/temp)*(const3+const4))

       const5 = (umem/diff(1,1))*(hidc(1,1)*c(i-1,1)-conf(1,1))
       const6 = (vpm(1,1)*c(i-1,1)*farad/gascon/temp)*cons

       const7 = (umem/diff(1,2))*(hidc(1,2)*c(i-1,2)-conf(1,2))
       const8 = (vpm(1,2)*c(i-1,2)*farad/gascon/temp)*cons

       dydx(i-1,1) = (const5-const6)
       dydx(i-1,2) = (const7-const8)

       c(i,1) = c(i-1,1) + xstep*(const5-const6)
       c(i,2) = c(i-1,2) + xstep*(const7-const8)

      end do

       conf(2,1)=c(200,1)/(exp(-vpm(1,1)*farad*edon(1,1)/gascon/temp))
       conf(2,2)=c(200,2)/(exp(-vpm(1,2)*farad*edon(1,2)/gascon/temp))
       change = ((conf(1,1) - conf(2,1))/conf(1,1))
       change = ((conf(1,2) - conf(2,2))/conf(1,2))
       relax=0.9
       conf(1,1)=relax*conf(1,1)+(1-relax)*conf(2,1)
       conf(1,2)=relax*conf(1,2)+(1-relax)*conf(2,2)

       IF(dabs(change).gt.0.0000001)then

       print*, conf(1,1),conf(1,2),change,dydx(1,1)
       end if

       END DO
```

```
      RETURN
      END

      SUBROUTINE output
      IMPLICIT REAL (A-H,O-Z)
      DOUBLE PRECISION conf,vpm,diff,hidc,temp,umem,con,edon
      DOUBLE PRECISION deex,xstep,farad,gascon,dydx
      COMMON/aleph/vpm(10,2),diff(10,2),hidc(10,2),hidf(10,2),con(10,2)
      COMMON/ale/edon(10,2)
      COMMON/a/c(20001,2),conf(20001,2),dydx(20001,2)
      COMMON/beth/farad,gascon,deex,umem,nep,xstep,temp,node
      i = 1
      write(6,10)  i,c(i,1),c(i,2),xstep
      DO i = 2,node
        iz = i/50
        ii = 50*iz
        IF(i.eq.ii)THEN
          print*, i,c(i,1),c(i,2),xstep
          write(6,10) i,c(i,1),c(i,2),xstep
        END IF
      END DO
   10  FORMAT(i6,8(8x,e13.8))
      RETURN
      END
```

Appendix 2

```
      PROGRAM membrane runge kutta
C     driver for routine membrane
      IMPLICIT REAL (A-H,O-Z)
      DOUBLE PRECISION con,conf
      DOUBLE PRECISION vpm,diff,hidc,temp,umem,farad,gascon,edon
      COMMON/aleph/con(10,2),vpm(10,2),diff(10,2),hidc(10,2),edon(10,2)
      COMMON/ale/conf(2000,2)
      COMMON/beth/farad,gascon,umem,nep,temp,node
      INTEGER NSTEP,NVAR
      PARAMETER(NVAR=2,NSTEP=200)
      INTEGER i,j
      REAL xx(2000),x1,x2,y(2,2000),vstart(NVAR)
      COMMON /path/ xx,y
      EXTERNAL derivs

      OPEN(unit=5,file='memb.dat',status='unknown')
      OPEN(unit=6,file='memb.res',status='unknown')

      farad=96485.3383
      gascon=8.3145
!     convrg=1.0D-5
!     PRINT*,' auto 1 other 0'
!     read*,iauto
      iauto = 1
      IF(iauto.EQ.1)THEN
!       READ(5,*)nep
        READ(5,*)nep
        print*, nep
        write(6,*) nep
        READ(5,*)temp,umem
        print*,temp,umem
        write(6,*)temp,umem
        DO i = 1,nep
          DO j = 1,2
            READ(5,*)vpm(i,j),diff(i,j),hidc(i,j)
            READ(5,*)con(i,j),edon(i,j)
            PRINT*,i,j,vpm(i,j),diff(i,j),hidc(i,j)
            PRINT*,con(i,j),edon(i,j)
            WRITE(6,*)i,j,vpm(i,j),diff(i,j),hidc(i,j)
            WRITE(6,*)i,j,con(i,j),edon(i,j)
          END DO
          vpm(i,1)=DABS(vpm(i,1))
          vpm(i,2)=-DABS(vpm(i,2))
        END DO
      ELSE
        Print*,' Where is the data??'
        stop
      END IF
      node=200

      conf(1,1)=con(1,1)/1.0
      conf(1,2)=con(1,2)/1.0

!     set intial value of y

      y(1,1)=con(1,1)*exp(-vpm(1,1)*farad*edon(1,1)/gascon/temp)
      y(2,1)=con(1,2)*exp(-vpm(1,2)*farad*edon(1,2)/gascon/temp)
```

```
!    thick = membrane thickness in micron
     x1=0.0D-6
     vstart(1)=y(1,1)
     vstart(2)=y(2,1)
     x2=20.0D-6
     call membrane(vstart,NVAR,x1,x2,NSTEP,derivs)
     call output
     do 11 i=1,200
       print*,i,xx(i),y(1,i),y(2,i)
11    continue
     END

     SUBROUTINE derivs(x,y,dydx)
     REAL x,y(*),dydx(*)
     DOUBLE PRECISION con,conf
     DOUBLE PRECISION vpm,diff,hidc,temp,umem,farad,gascon,edon
     COMMON/aleph/con(10,2),vpm(10,2),diff(10,2),hidc(10,2),edon(10,2)
     COMMON/ale/conf(2000,2)
     COMMON/beth/farad,gascon,umem,nep,temp,node

       const1= (vpm(1,1)*umem/diff(1,1))*(hidc(1,1)*y(1)-conf(1,1))
       const2= (vpm(1,2)*umem/diff(1,2))*(hidc(1,2)*y(2)-conf(1,2))
       const3= vpm(1,1)*vpm(1,1)*y(1)
       const4= vpm(1,2)*vpm(1,2)*y(2)
       cons=(const1+const2)/((farad/gascon/temp)*(const3+const4))
       const5 = (umem/diff(1,1))*(hidc(1,1)*y(1)-conf(1,1))
       const6 = (vpm(1,1)*y(1)*farad/gascon/temp)*cons
       const7 = (umem/diff(1,2))*(hidc(1,2)*y(2)-conf(1,2))
       const8 = (vpm(1,2)*y(2)*farad/gascon/temp)*cons
       dydx(1) = (const5-const6)
       dydx(2) = (const7-const8)

       conf(2,1)=y(1)/((exp(-vpm(1,1)*farad*edon(1,1)/gascon/temp)))
       conf(2,2)=y(2)/((exp(-vpm(1,2)*farad*edon(1,2)/gascon/temp)))

       change = ((conf(1,1) - conf(2,1))/conf(1,1))
       change = ((conf(1,2) - conf(2,2))/conf(1,2))

       relax=0.9

       conf(1,1)=relax*conf(1,1)+(1-relax)*conf(2,1)
       conf(1,2)=relax*conf(1,2)+(1-relax)*conf(2,2)

     print*,change,y(1),y(1),cons,conf(1,1)
     return
     END

     SUBROUTINE membrane(vstart,nvar,x1,x2,nstep,derivs)
     DOUBLE PRECISION con,conf
     DOUBLE PRECISION vpm,diff,hidc,temp,umem,farad,gascon,edon
     COMMON/aleph/con(10,2),vpm(10,2),diff(10,2),hidc(10,2),edon(10,2)
     COMMON/ale/conf(2000,2)
     COMMON/beth/farad,gascon,umem,nep,temp,node
     INTEGER nstep,nvar,NMAX,NSTPMX
     PARAMETER (NMAX=2,NSTPMX=2000)
     REAL x1,x2,vstart(nvar),xx(NSTPMX),y(NMAX,NSTPMX)
     EXTERNAL derivs
     COMMON /path/ xx,y
CU   USES rk4
     INTEGER i,k
```

```
      REAL h,x,dv(NMAX),v(NMAX)
      do 11 i=1,nvar
        v(i)=vstart(i)
        y(i,1)=v(i)
11    continue
      xx(1)=x1
      x=x1
      h=(x2-x1)/nstep
      do 13 k=1,nstep
       call derivs(x,v,dv)
       call rk4(v,dv,nvar,x,h,v,derivs)
      if(x+h.eq.x)pause 'stepsize not significant in membrane'
       x=x+h
       xx(k+1)=x
       do 12 i=1,nvar
         y(i,k+1)=v(i)
12     continue
      print*,xx(k+1),y(1,k+1),y(2,k+1)
13    continue
      return
      END

      SUBROUTINE rk4(y,dydx,n,x,h,yout,derivs)
      DOUBLE PRECISION con,conf
      DOUBLE PRECISION vpm,diff,hidc,temp,umem,farad,gascon,edon
      COMMON/aleph/con(10,2),vpm(10,2),diff(10,2),hidc(10,2),edon(10,2)
      COMMON/ale/conf(2000,2)
      COMMON/beth/farad,gascon,umem,nep,temp,node
      INTEGER n,NMAX
      REAL h,x,dydx(n),y(n),yout(n)
      EXTERNAL derivs
      PARAMETER (NMAX=2)
      INTEGER i
      REAL h6,hh,xh,dym(NMAX),dyt(NMAX),yt(NMAX)
      hh=h*0.5
      h6=h/6.
      xh=x+hh
      do 11 i=1,n
        yt(i)=y(i)+hh*dydx(i)
11    continue
      call derivs(xh,yt,dyt)
      do 12 i=1,n
        yt(i)=y(i)+hh*dyt(i)
12    continue
      call derivs(xh,yt,dym)
      do 13 i=1,n
        yt(i)=y(i)+h*dym(i)
        dym(i)=dyt(i)+dym(i)
13    continue
      call derivs(x+h,yt,dyt)
      do 14 i=1,n
        yout(i)=y(i)+h6*(dydx(i)+dyt(i)+2.*dym(i))
14    continue
      return
      END

      SUBROUTINE output
      IMPLICIT REAL (A-H,O-Z)
      DOUBLE PRECISION con,conf
      DOUBLE PRECISION vpm,diff,hidc,temp,umem,farad,gascon,edon
```

```
      COMMON/aleph/con(10,2),vpm(10,2),diff(10,2),hidc(10,2),edon(10,2)
      COMMON/ale/conf(2000,2)
      COMMON/beth/farad,gascon,umem,nep,temp,node
      INTEGER NSTEP,NVAR
      PARAMETER(NVAR=2,NSTEP=200)
      INTEGER i,j
      REAL xx(2000),x1,x2,y(2,2000),vstart(NVAR)
      COMMON /path/ xx,y
      i = 1
      write(6,10) i,xx(i),y(1,i),y(2,i)
      DO i = 2,node
        iz = i/50
        ii = 50*iz
        IF(i.eq.ii)THEN
          print*, i,xx(i),y(1,i),y(2,i)
          write(6,10)i,xx(i),y(1,i),y(2,i)
        END IF
      END DO
10    FORMAT(i6,5(8x,e13.7))
      RETURN
      END
```

Appendix 3

```
      PROGRAM membrane
      IMPLICIT REAL (A-H,O-Z)
      DOUBLE PRECISION vpm,diff,hidc,temp,umem,hidd,radis,radip
      DOUBLE PRECISION deex,xstep,con,edon,farad,gascon
      DOUBLE PRECISION change,dydx,conf
      COMMON/aleph/vpm(10,2),diff(10,2),hidc(10,2),hidd(10,2)
      COMMON/ale/radis(10,2),radip,con(10,2),edon(10,2)
      COMMON/a/c(20001,2),conf(20001,2),dydx(20001,2)
      COMMON/beth/farad,gascon,deex,umem,nep,xstep,temp,node

      OPEN(unit=5,file='memb.dat',status='unknown')
      OPEN(unit=6,file='memb.res',status='unknown')
      farad=96485.3383
      gascon=8.3145
!     convrg=1.0D-5
!     PRINT*,' auto 1 other 0'
!     read*,iauto
      iauto = 1
      IF(iauto.EQ.1)THEN
        READ(5,*)nep
        print*, nep
        write(6,*) nep
        READ(5,*)temp,umem,radip
        print*,temp,umem,radip
        write(6,*)temp,umem,radip
       Print*,'temp',temp
      Print*,'umem',umem

        DO i = 1,nep
          DO j = 1,2
            READ(5,*)vpm(i,j),diff(i,j),radis(i,j)
            READ(5,*)con(i,j),edon(i,j)
            PRINT*,i,j,vpm(i,j),diff(i,j),radis(i,j)
            PRINT*,con(i,j),edon(i,j)
            WRITE(6,*)i,j,vpm(i,j),diff(i,j),radis(i,j)
            WRITE(6,*)i,j,con(i,j),edon(i,j)
          END DO
          vpm(i,1)=DABS(vpm(i,1))
          vpm(i,2)=-DABS(vpm(i,2))
        END DO
      ELSE
        Print*,' Where is the data??'
        stop
      END IF
      node=200
!     thick = membrane thickness in micron
      deex = 20.0
      deex = deex*1.0D-6
      xstep = deex/(DFLOAT(node))
      print*,'xstep',xstep
      print*,'node',node
      print*,' '
      print*,'**************************************************'
      print*,' '
      print*,'              ALL UNITS ARE S.I. '
      print*,' '
      print*,'**************************************************'
```

```
      print*,' '
      CALL euler
      CALL output
      STOP
      END

      SUBROUTINE EULER
      IMPLICIT REAL (A-H,O-Z)
      DOUBLE PRECISION vpm,diff,hidc,temp,umem,hidd,radis,radip
      DOUBLE PRECISION deex,xstep,con,edon,farad,gascon
      DOUBLE PRECISION change,dydx,conf
      COMMON/aleph/vpm(10,2),diff(10,2),hidc(10,2),hidd(10,2)
      COMMON/ale/radis(10,2),radip,con(10,2),edon(10,2)
      COMMON/a/c(20001,2),conf(20001,2),dydx(20001,2)
      COMMON/beth/farad,gascon,deex,umem,nep,xstep,temp,node

      change = 1.0
!     set initial conditions
      conf(1,1)=con(1,1)/1.0
      conf(1,2)=con(1,2)/1.0
      while(dabs(change).GT.0.0000001)DO

!     calculate hidd
       con1 = 2.30*(radis(1,1)/radip)
       con2 = 1.154*((radis(1,1)/radip)**2)
       con3 = 0.224*((radis(1,1)/radip)**3)
       hidd(1,1) = (1.0-con1+con2+con3)
       con4 = 2.30*(radis(1,2)/radip)
       con5 = 1.154*(radis(1,2)/radip)**2
       con6 = 0.224*(radis(1,2)/radip)**3
       hidd(1,2) = (1.0-con4+con5+con6)

!     calculate hidc
       cons1 = 0.054*(radis(1,1)/radip)
       cons2 = 0.988*((radis(1,1)/radip)**2)
       cons3 = 0.441*((radis(1,1)/radip)**3)
       hidc(1,1) = (2-(1-(radis(1,1)/radip))**2)*(1.0+cons1-cons2+cons3)
       cons4 = 0.054*(radis(1,2)/radip)
       cons5 = 0.988*((radis(1,2)/radip)**2)
       cons6 = 0.441*((radis(1,2)/radip)**3)
       hidc(1,2) = (2-(1-(radis(1,2)/radip))**2)*(1.0+cons4-cons5+cons6)

       co1=(1-(radis(1,1)/radip))*(1-(radis(1,1)/radip))
       c(1,1)=con(1,1)*co1*exp(-vpm(1,1)*farad*edon(1,1)/gascon/temp)
       co2=(1-(radis(1,2)/radip))*(1-(radis(1,2)/radip))
       c(1,2)=con(1,2)*co2*exp(-vpm(1,2)*farad*edon(1,2)/gascon/temp)

       DO i=2,node
        constant1=vpm(1,1)*umem/diff(1,1)/hidd(1,1)
        const1= (constant1)*(hidc(1,1)*c(i-1,1)-conf(1,1))
        constant2=vpm(1,2)*umem/diff(1,2)/hidd(1,2)
        const2= (constant2)*(hidc(1,2)*c(i-1,2)-conf(1,2))
        const3= vpm(1,1)*vpm(1,1)*c(i-1,1)
        const4= vpm(1,2)*vpm(1,2)*c(i-1,2)

        cons=(const1+const2)/((farad/gascon/temp)*(const3+const4))

        constant3=umem/diff(1,1)/hidd(1,1)
        const5 = (constant3)*(hidc(1,1)*c(i-1,1)-conf(1,1))
        const6 = (vpm(1,1)*c(i-1,1)*farad/gascon/temp)*cons
```

```
 constant4=umem/diff(1,2)/hidd(1,2)
 const7 = (constant4)*(hidc(1,2)*c(i-1,2)-conf(1,2))
 const8 = (vpm(1,2)*c(i-1,2)*farad/gascon/temp)*cons

 dydx(i-1,1) = (const5-const6)
 dydx(i-1,2) = (const7-const8)

 c(i,1) = c(i-1,1) + xstep*(const5-const6)
 c(i,2) = c(i-1,2) + xstep*(const7-const8)

 end do

 co3=(1-(radis(1,1)/radip))*(1-(radis(1,1)/radip))
 constan1=(co3*exp(-vpm(1,1)*farad*edon(1,1)/gascon/temp))
 conf(2,1)=c(200,1)/constan1
 co4=(1-(radis(1,2)/radip))*(1-(radis(1,2)/radip))
 constan2=(co4*exp(-vpm(1,2)*farad*edon(1,2)/gascon/temp))
 conf(2,2)=c(200,2)/constan2

 change = ((conf(1,1) - conf(2,1))/conf(1,1))
 change = ((conf(1,2) - conf(2,2))/conf(1,2))
 relax=0.9
 conf(1,1)=relax*conf(1,1)+(1-relax)*conf(2,1)
 conf(1,2)=relax*conf(1,2)+(1-relax)*conf(2,2)

 IF(dabs(change).gt.0.0000001)then
 print*, conf(1,1),conf(1,2),change,dydx(1,1)
 end if
 END DO

RETURN
END

SUBROUTINE output
IMPLICIT REAL (A-H,O-Z)
DOUBLE PRECISION vpm,diff,hidc,temp,umem,hidd,radis,radip
DOUBLE PRECISION deex,xstep,con,edon,farad,gascon
DOUBLE PRECISION change,dydx,conf
COMMON/aleph/vpm(10,2),diff(10,2),hidc(10,2),hidd(10,2)
COMMON/ale/radis(10,2),radip,con(10,2),edon(10,2)
COMMON/a/c(20001,2),conf(20001,2),dydx(20001,2)
COMMON/beth/farad,gascon,deex,umem,nep,xstep,temp,node
i = 1
write(6,10)  i,c(i,1),c(i,2),xstep,radis(1,1),radis(1,2)
DO i = 2,node
  iz = i/50
  ii = 50*iz
  IF(i.eq.ii)THEN
    print*, i,c(i,1),c(i,2),xstep,radis(1,1),radis(1,2)
    write(6,10) i,c(i,1),c(i,2),xstep,radis(1,1),radis(1,2)
  END IF
END DO
10  FORMAT(i6,8(8x,e13.8))
RETURN
END
```

Appendix 4

```
      PROGRAM membrane runge kutta
C     driver for routine membrane
      IMPLICIT REAL (A-H,O-Z)
      DOUBLE PRECISION con,conf,hidd,radis,radip
      DOUBLE PRECISION vpm,diff,hidc,temp,umem,farad,gascon,edon
      COMMON/aleph/con(10,2),vpm(10,2),diff(10,2),edon(10,2)
      COMMON/alep/hidc(10,2),hidd(10,2),radis(10,2),radip
      COMMON/ale/conf(2000,2)
      COMMON/beth/farad,gascon,umem,nep,temp,node
      INTEGER NSTEP,NVAR
      PARAMETER(NVAR=2,NSTEP=200)
      INTEGER i,j
      REAL xx(2000),x1,x2,y(2,2000),vstart(NVAR)
      COMMON /path/ xx,y
      EXTERNAL derivs


      OPEN(unit=5,file='memb.dat',status='unknown')
      OPEN(unit=6,file='memb.res',status='unknown')

      farad=96485.3383
      gascon=8.3145
!     convrg=1.0D-5
!     PRINT*,' auto 1 other 0'
!     read*,iauto
      iauto = 1
      IF(iauto.EQ.1)THEN
!       READ(5,*)nep
        READ(5,*)nep
        print*, nep
        write(6,*) nep
        READ(5,*)temp,umem,radip
        print*,temp,umem,radip
        write(6,*)temp,umem,radip
        DO i = 1,nep
          DO j = 1,2
            READ(5,*)vpm(i,j),diff(i,j),radis(i,j)
            READ(5,*)con(i,j),edon(i,j)
            PRINT*,i,j,vpm(i,j),diff(i,j),radis(i,j)
            PRINT*,con(i,j),edon(i,j)
            WRITE(6,*)i,j,vpm(i,j),diff(i,j),radis(i,j)
            WRITE(6,*)i,j,con(i,j),edon(i,j)
          END DO
          vpm(i,1)=DABS(vpm(i,1))
          vpm(i,2)=-DABS(vpm(i,2))
        END DO
      ELSE
        Print*,' Where is the data??'
        stop
      END IF
      node=200

      conf(1,1)=con(1,1)/1.0
      conf(1,2)=con(1,2)/1.0

!     set intial value of y
```

```
      y(1,1)=con(1,1)*exp(-vpm(1,1)*farad*edon(1,1)/gascon/temp)
      y(2,1)=con(1,2)*exp(-vpm(1,2)*farad*edon(1,2)/gascon/temp)

!     thick = membrane thickness in micron
      x1=0.0D-6
      vstart(1)=y(1,1)
      vstart(2)=y(2,1)
      x2=20.0D-6
      call membrane(vstart,NVAR,x1,x2,NSTEP,derivs)
      call output
      do 11 i=1,200
        print*,i,xx(i),y(1,i),y(2,i)
11    continue
      END

      SUBROUTINE derivs(x,y,dydx)
      REAL x,y(*),dydx(*)
      DOUBLE PRECISION con,conf,hidd,radis,radip
      DOUBLE PRECISION vpm,diff,hidc,temp,umem,farad,gascon,edon
      COMMON/aleph/con(10,2),vpm(10,2),diff(10,2),edon(10,2)
      COMMON/alep/hidc(10,2),hidd(10,2),radis(10,2),radip
      COMMON/ale/conf(2000,2)
      COMMON/beth/farad,gascon,umem,nep,temp,node

!     calculate hidd
       con1 = 2.30*(radis(1,1)/radip)
       con2 = 1.154*((radis(1,1)/radip)**2)
       con3 = 0.224*((radis(1,1)/radip)**3)
       hidd(1,1) = (1.0-con1+con2+con3)
       con4 = 2.30*(radis(1,2)/radip)
       con5 = 1.154*(radis(1,2)/radip)**2
       con6 = 0.224*(radis(1,2)/radip)**3
       hidd(1,2) = (1.0-con4+con5+con6)

!     calculate hidc
       cons1 = 0.054*(radis(1,1)/radip)
       cons2 = 0.988*((radis(1,1)/radip)**2)
       cons3 = 0.441*((radis(1,1)/radip)**3)
       hidc(1,1) = (2-(1-(radis(1,1)/radip))**2)*(1.0+cons1-cons2+cons3)
       cons4 = 0.054*(radis(1,2)/radip)
       cons5 = 0.988*((radis(1,2)/radip)**2)
       cons6 = 0.441*((radis(1,2)/radip)**3)
       hidc(1,2) = (2-(1-(radis(1,2)/radip))**2)*(1.0+cons4-cons5+cons6)


        constant1=vpm(1,1)*umem/diff(1,1)/hidd(1,1)
        const1= (constant1)*(hidc(1,1)*y(1)-conf(1,1))
        constant2=vpm(1,2)*umem/diff(1,2)/hidd(1,2)
        const2= (constant2)*(hidc(1,2)*y(2)-conf(1,2))
        const3= vpm(1,1)*vpm(1,1)*y(1)
        const4= vpm(1,2)*vpm(1,2)*y(2)

        cons=(const1+const2)/((farad/gascon/temp)*(const3+const4))

        constant3=umem/diff(1,1)/hidd(1,1)
        const5 = (constant3)*(hidc(1,1)*y(1)-conf(1,1))
        const6 = (vpm(1,1)*y(1)*farad/gascon/temp)*cons

        constant4=umem/diff(1,2)/hidd(1,2)
        const7 = (constant4)*(hidc(1,2)*y(2)-conf(1,2))
```

```
      const8 = (vpm(1,2)*y(2)*farad/gascon/temp)*cons

      dydx(1) = (const5-const6)
      dydx(2) = (const7-const8)

      conf(2,1)=y(1)/((exp(-vpm(1,1)*farad*edon(1,1)/gascon/temp)))
      conf(2,2)=y(2)/((exp(-vpm(1,2)*farad*edon(1,2)/gascon/temp)))

      change = ((conf(1,1) - conf(2,1))/conf(1,1))
      change = ((conf(1,2) - conf(2,2))/conf(1,2))

      relax=0.9

      conf(1,1)=relax*conf(1,1)+(1-relax)*conf(2,1)
      conf(1,2)=relax*conf(1,2)+(1-relax)*conf(2,2)


     print*,change,y(1),y(1),cons,conf(1,1)
     return
     END

     SUBROUTINE membrane(vstart,nvar,x1,x2,nstep,derivs)
     DOUBLE PRECISION con,conf,hidd,radis,radip
     DOUBLE PRECISION vpm,diff,hidc,temp,umem,farad,gascon,edon
     COMMON/aleph/con(10,2),vpm(10,2),diff(10,2),edon(10,2)
     COMMON/alep/hidc(10,2),hidd(10,2),radis(10,2),radip
     COMMON/ale/conf(2000,2)
     COMMON/beth/farad,gascon,umem,nep,temp,node
     INTEGER nstep,nvar,NMAX,NSTPMX
     PARAMETER (NMAX=2,NSTPMX=2000)
     REAL x1,x2,vstart(nvar),xx(NSTPMX),y(NMAX,NSTPMX)
     EXTERNAL derivs
     COMMON /path/ xx,y
CU    USES rk4
     INTEGER i,k
     REAL h,x,dv(NMAX),v(NMAX)
     do 11 i=1,nvar
       v(i)=vstart(i)
       y(i,1)=v(i)
11    continue
     xx(1)=x1
     x=x1
     h=(x2-x1)/nstep
     do 13 k=1,nstep
      call derivs(x,v,dv)
      call rk4(v,dv,nvar,x,h,v,derivs)
     if(x+h.eq.x)pause 'stepsize not significant in membrane'
      x=x+h
      xx(k+1)=x
      do 12 i=1,nvar
        y(i,k+1)=v(i)
12      continue
     print*,xx(k+1),y(1,k+1),y(2,k+1)
13    continue
     return
     END

     SUBROUTINE rk4(y,dydx,n,x,h,yout,derivs)
     DOUBLE PRECISION con,conf,hidd,radis,radip
     DOUBLE PRECISION vpm,diff,hidc,temp,umem,farad,gascon,edon
```

```
      COMMON/aleph/con(10,2),vpm(10,2),diff(10,2),edon(10,2)
      COMMON/alep/hidc(10,2),hidd(10,2),radis(10,2),radip
      COMMON/ale/conf(2000,2)
      COMMON/beth/farad,gascon,umem,nep,temp,node
      INTEGER n,NMAX
      REAL h,x,dydx(n),y(n),yout(n)
      EXTERNAL derivs
      PARAMETER (NMAX=2)
      INTEGER i
      REAL h6,hh,xh,dym(NMAX),dyt(NMAX),yt(NMAX)
      hh=h*0.5
      h6=h/6.
      xh=x+hh
      do 11 i=1,n
        yt(i)=y(i)+hh*dydx(i)
11    continue
      call derivs(xh,yt,dyt)
      do 12 i=1,n
        yt(i)=y(i)+hh*dyt(i)
12    continue
      call derivs(xh,yt,dym)
      do 13 i=1,n
        yt(i)=y(i)+h*dym(i)
        dym(i)=dyt(i)+dym(i)
13    continue
      call derivs(x+h,yt,dyt)
      do 14 i=1,n
        yout(i)=y(i)+h6*(dydx(i)+dyt(i)+2.*dym(i))
14    continue
      return
      END

      SUBROUTINE output
      IMPLICIT REAL (A-H,O-Z)
      DOUBLE PRECISION con,conf,radis,radip
      DOUBLE PRECISION vpm,diff,hidc,temp,umem,farad,gascon,edon
      COMMON/aleph/con(10,2),vpm(10,2),diff(10,2),edon(10,2)
      COMMON/alep/hidc(10,2),hidd(10,2),radis(10,2),radip
      COMMON/ale/conf(2000,2)
      COMMON/beth/farad,gascon,umem,nep,temp,node
      INTEGER NSTEP,NVAR
      PARAMETER(NVAR=2,NSTEP=200)
      INTEGER i,j
      REAL xx(2000),x1,x2,y(2,2000),vstart(NVAR)
      COMMON /path/ xx,y
      i = 1
      write(6,10) i,xx(i),y(1,i),y(2,i)
      DO i = 2,node
        iz = i/50
        ii = 50*iz
        IF(i.eq.ii)THEN
          print*, i,xx(i),y(1,i),y(2,i)
          write(6,10)i,xx(i),y(1,i),y(2,i)
        END IF
      END DO
 10   FORMAT(i6,5(8x,e13.7))
      RETURN
      END
```

Appendix 5

0.9nm membrane active layer and its supporting layer.

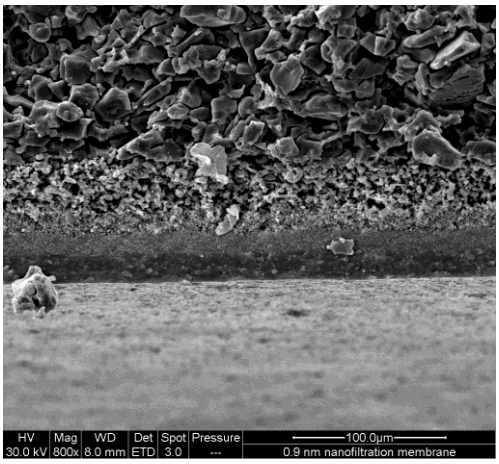

Figure 1. 0.9nm membrane at 100.0µm.

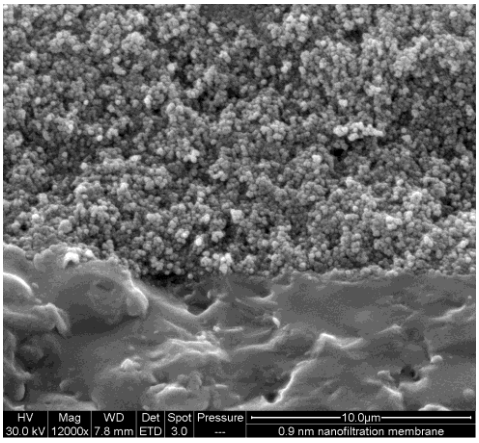

Figure 2. 0.9nm membrane at 10.0µm.

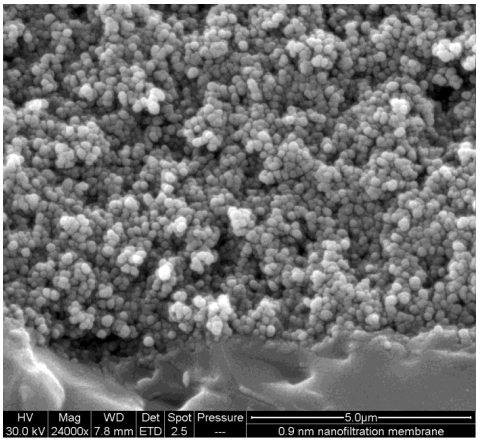

Figure 3. 0.9nm membrane at 5.0µm.

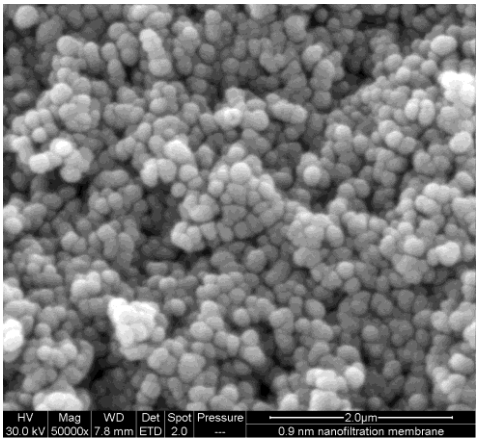

Figure 4. 0.9nm membrane at 2.0µm.

Appendix 6

1.0nm membrane active layer and its supporting layer.

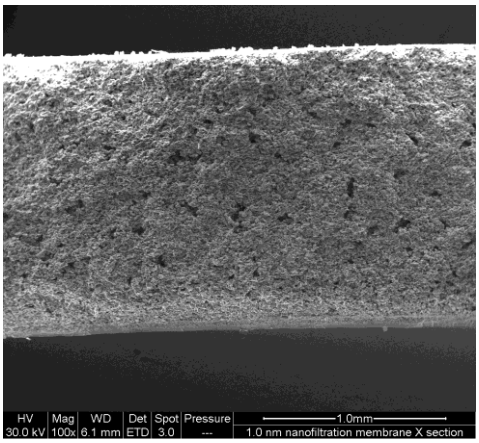

Figure 1. 1.0nm membrane at 1.0mm.

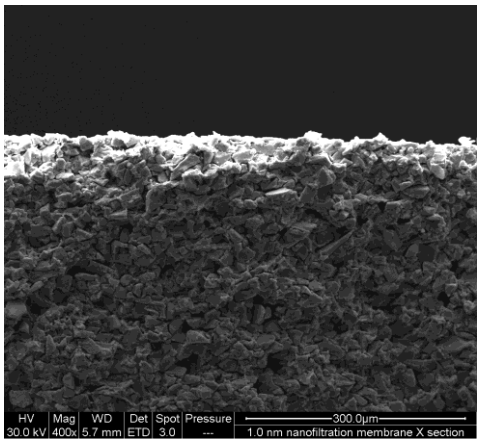

Figure 2. 1.0nm membrane at 300.0µm.

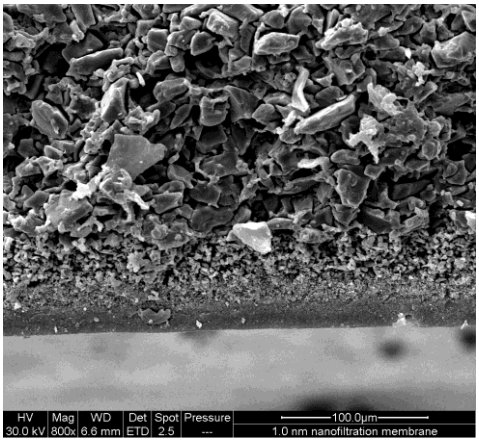

Figure 3. 1.0nm membrane at 100.0 µm.

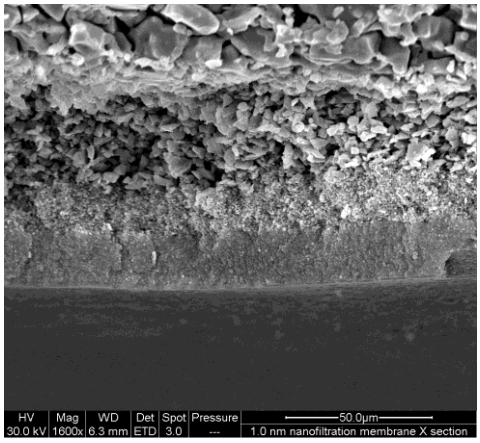

Figure 4. 1.0nm membrane at 50.0µm.

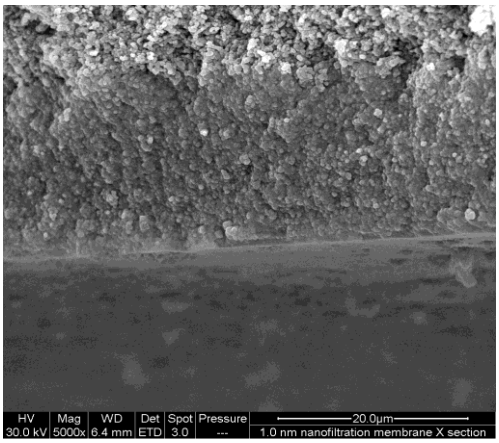

Figure 5. 1.0nm membrane at 20.0µm.

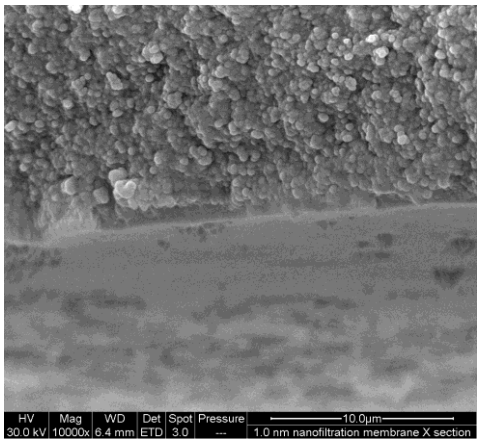

Figure 6. 1.0nm membrane at 10.0µm.

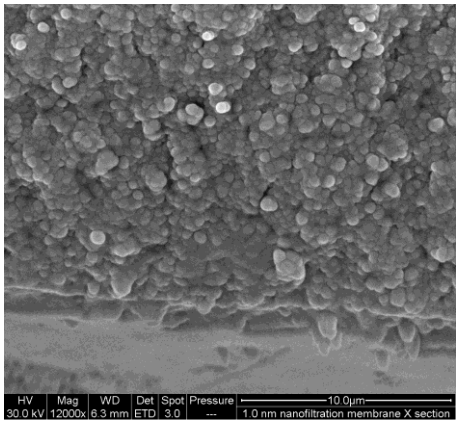

Figure 7. 1.0nm membrane at 10.0µm.

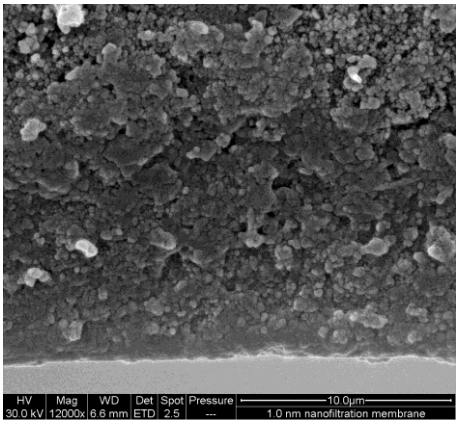

Figure 8. 1.0nm membrane at 10.0µm.

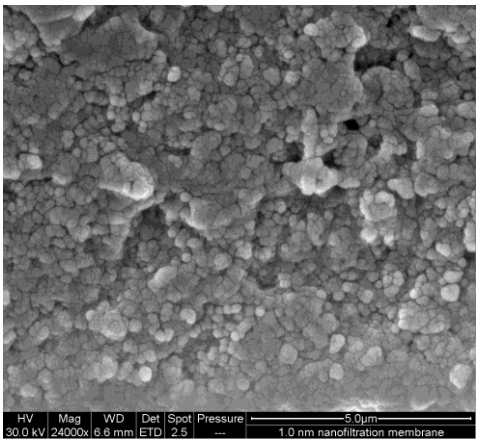

Figure 9. 1.0nm membrane at 5.0µm.

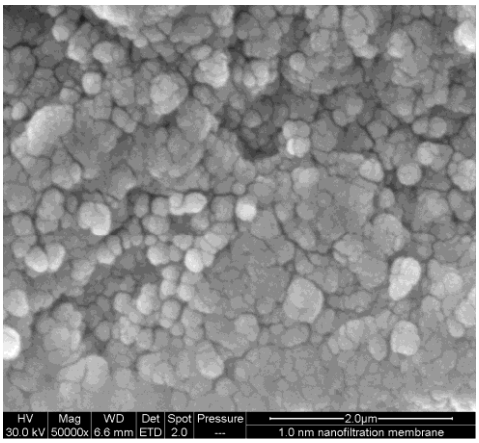

Figure 10. 1.0nm membrane at 2.0µm.

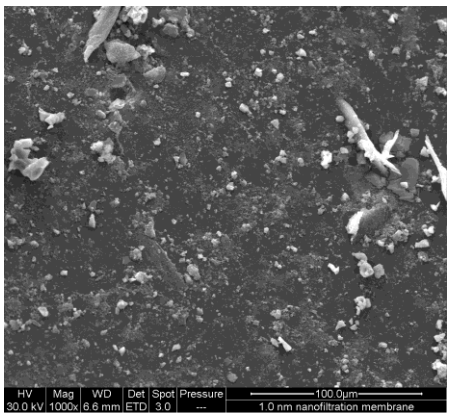

Figure 11. Surface of 1.0nm membrane at 100.0µm.

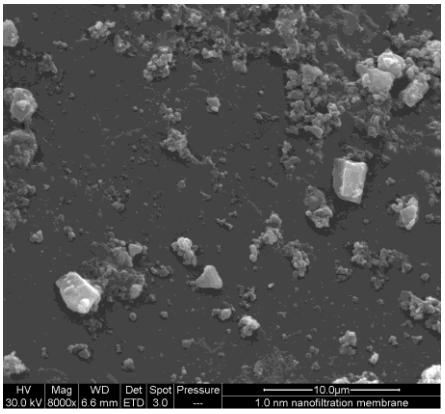

Figure 12. Surface of 1.0nm membrane at 10.0µm.

Appendix 7

Equipment used during the experiments.

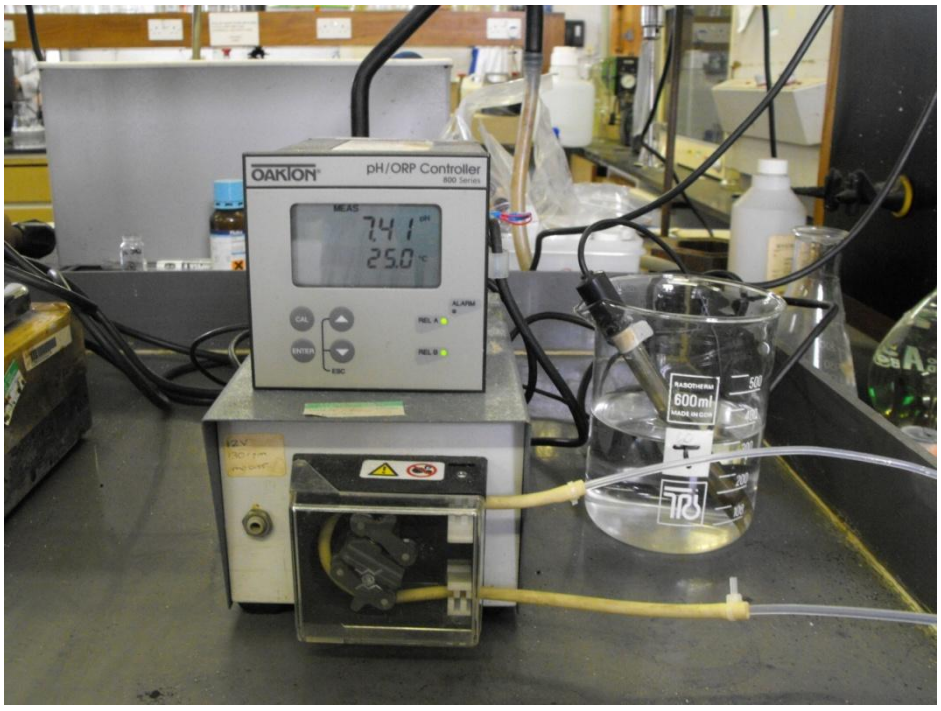

Figure 1. Oakton pH/ORP controller, 1000 series.

Figure 2. Accumet pH/Ion/Conductivity Meter (Fisher Scientific, Model 50).

Figure 3. Fistreem Cyclon.

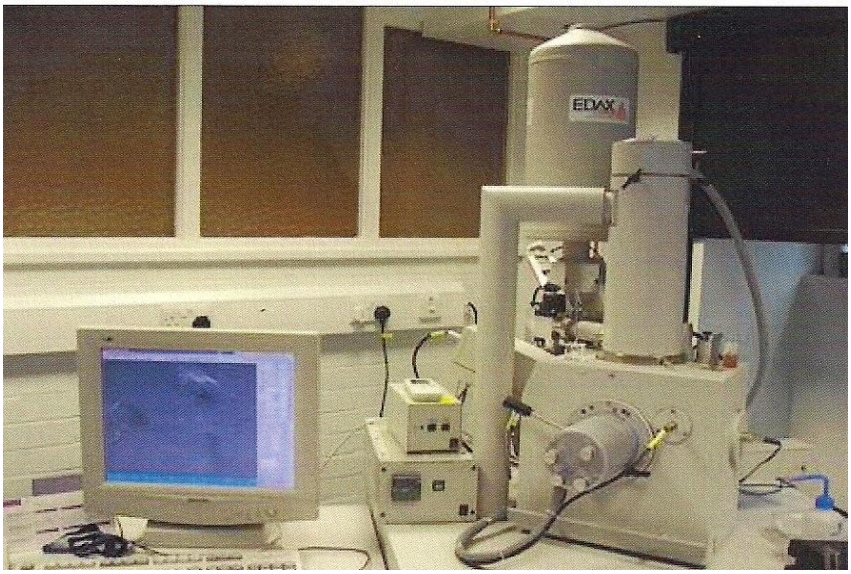

Figure 4. SEM (FEI Quanta 200, Purge, Czech Republic) and EDXS equipment (EDXS, Amertek Inc, Paoli, PA, USA).

Figure 5. Laser Doppler Velocimeter, Zetasizer 3000HS advance, Malvern instrument GmbH, UK.

Figure 6. Mistral 1000 (MSE), centrifuge device.

Figure 7. Experimental setup of the NF membrane rig.

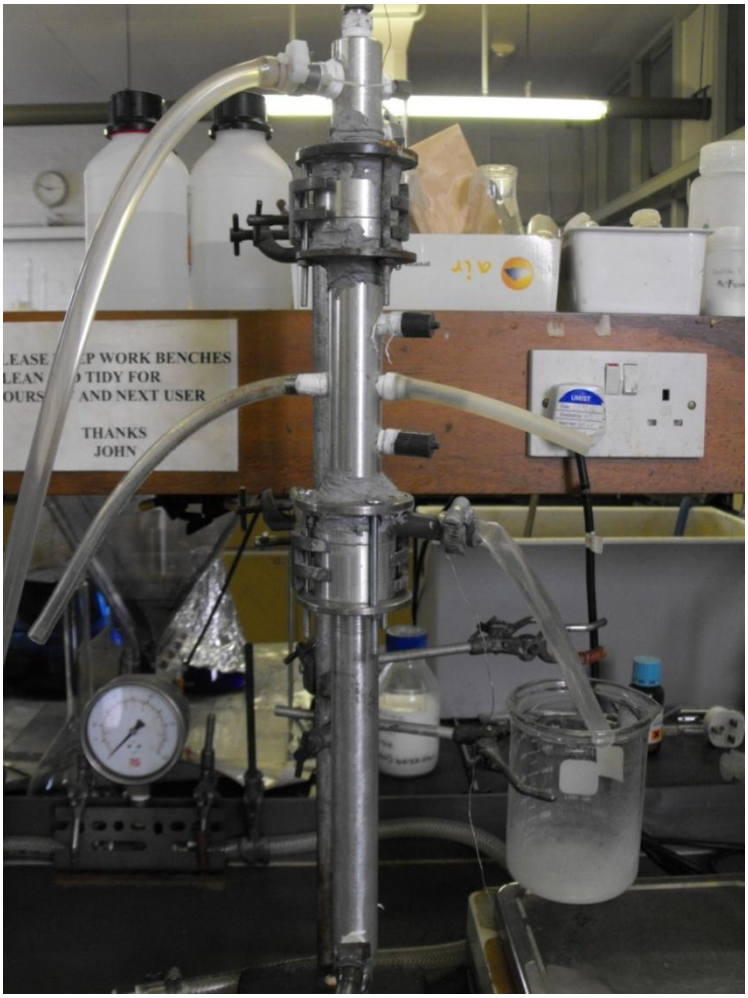

Figure 8. Membrane module.

References

A

1) A. A. Hussain, M. E. E. Abashar, I. S. Al-Mutaz. *Influence of ion size on the prediction of nanofiltration membrane systems.* Desalination 214 (2007) 150–166.
2) A. E. Simpson, C.A. Kerri and C.A. Buckley. *The effect of pH on the nanofiltration of the carbonate system in solution.* Desalination 64 (1987) 305–319.
3) A. E. Simpson and C. A. Buckley. *The treatrent of industrial effluents containing sodium hydroxide to enable the reuse of chemicals and water.* Desalination 67 (1987) 409–429.
4) A. E. Yaroshchuk. *Asymptotic behaviour in the pressure-driven separations of ions of different mobilities in charged porous membranes.* Journal of Membrane Science 167 (2000) 163–185.
5) A. E. Yaroshchuk. *Dielectric exclusion of ions from membranes.* Advances in Colloid and Interface Science 85 (2000) 193–230.
6) A. I. Cavaco Morão, A. Szymczyk, P. Fievet, A. M. Brites Alves. *Modelling the separation by nanofiltration of a multi-ionic solution relevant to an industrial process*. Journal of Membrane Science 322 (2008) 320–330.
7) A. I. Schäfer, A. G. Fane and T. D. Waite. *Nanofiltration principles and applications.* Published by Elsevier Ltd.
8) A. I. Schäfer, A. G. Fane and T. D. Waite. *Nanofiltration of natural organic matter: Removal, fouling and the influence of multivalent ions*. Desalination 118 (1998) 109–122.
9) A. I. Schäfer , A. G. Fane, T. D. Waite. *Fouling effects on rejection in the membrane filtration of natural waters.* Desalination 131 (2000) 215–224.
10) A. I. Schäfer, A. Pihlajamäki, A. G. Fane, T. D. Waite and M. Nyström *Natural organic matter removal by nanofiltration: effects of solution chemistry on retention of low molar mass acids versus bulk organic matter.* Journal of Membrane Science 242 (2004) 73–85.
11) A. J. Rachwal, J. Khow, J. S. Colbourne and J. O'Donnell. *Water treatment for public supply in the 1990's - a role for membrane technology*. Desalination 97 (1994) 427–436.
12) A. L. Ahmad and A. Mariadas. *Baffled micro filtration membrane and its fouling control for feed water of desalination*. Desalination 168 (2004) 223–230.
13) A. L. Ahmad, B. S. Ooi. *Optimisation of composite nanofiltration membrane through pH control: Application in $CuSO_4$ removal.* Separation and purification technology 47 (2006) 162-172.
14) A. L. Ahmad, M. F. Chong and S. Bhatia. *Mathematical modelling and simulation of the multiple solutes system for Nanofiltration process*. Journal of membrane science, 253 (2005) 103–115.
15) A. M. Hassan, A. M. Farooque, A. T. M. Jamaluddin, A. S. Al-Amoudi, M. AK. Al-Sofi, A. F. Al-Rubaian, N. M. Kither. I. A. R. Al-Tisan and A. Rowaili. *A demonstration plant based on the new NF-SWRO process*. Desalination 131 (2000) 157–171.
16) A. M. Hassan, A. M. Farooque, A. T. M. Jamaluddin, A. S. Al-Amoudi, M. A. K. Al-Sofi, A. F. Al-Rubaian, N. M. Kither, I. A. R. Al-Tisan and A. Rowaili. *A demonstration plant based on the new NF-SWRO process.* Desalination 131 (2000) 157–171.
17) A. W. Mohammad, N. Hilal, H. Al-Zoubi, N.A. Darwish. *Prediction of permeate fluxes and rejections of highly concentrated salts in nanofiltration membranes*. Journal of membrane science 289 (2007) 40–50.
18) A. Bindoff, C. J. Davies, C. A. Kerr and C. A. Buckley. *The nanofiltration and reuse of effluent from the caustic extraction stage of wood pulping.* Desalination 67 (1987) 455–465.

19) A. Bes-Pi, A. Iborra-Clar, C. García-Figueruelo, S. Barredo-Damas, M. I. Alcaina-Miranda, J. A. Mendoza-Roca and M. I. Iborra-Clar. *Comparison of three NF membranes for the reuse of secondary textile effluents*. Desalination 241 (2009) 1–7.
20) A. Favre-Réguillona, G. Lebuzit, D. Murat, J. Foos, C. Mansour, M. Draye. *Selective removal of dissolved uranium in drinking water by nanofiltration*. Water Research 42 (2008) 1160–1166.
21) A. Larbot, S. Alami-Younssi, M. Persin, J. Sarrazin, L. Cot. *Preparation of a γ-alumina nanofiltration membrane.* Journal of Membrane Science 97 (1994) 167–173.
22) A. Lhassani, M. Rumeau, D. Benjelloun and M. Pontie. *Selective demineralisation of water by Nanofiltration application to the de-fluorination of brackish water.* Water Research Volume 35, No. 13 (2001) 3260–3264.
23) A. Malek, M. N. A. Hawlader and J. C. Ho. A. Malek, M. N. A. Hawlader and J. C. Ho. *A lumped transport parameter approach in predicting B10 RO permeator performance.* Desalination 99 (1994) 19–38.
24) A. Santafé-Moros, J. M. Gozálvez-Zafrilla, J. Lora-García. *Nitrate removal from ternary ionic solutions by a tight nanofiltration membrane*. Desalination, 204 (2007) 63–71.
25) A. Santafé-Moros, J. M. Gozálvez-Zafrilla, J. Lora-García. *Applicability of the DSPM with dielectric exclusion to a high rejection nanofiltration membrane in the separation of nitrate solutions*. Desalination 221 (2008) 268–276.
26) A. Santafé-Moros, J. M. Gozálvez-Zafrilla, J. Lora-García, J. C. Garcia-Diaz. *Mixture design applied to describe the influence of ionic composition on the removal of nitrate ions using nanofiltration*. Desalination 185 (2005) 289–296.
27) A. Szymczyk, C. Labbez, P. Fievet, A. Vidonne, A. Foissy, J. Pagetti. *Contribution of convection, diffusion and migration to electrolyte transport through nanofiltration membranes*. Advances in Colloid and Interface Science 103 (2003) 77–94.
28) Abderrahim Abbas, Nader Al-Bastaki. *Performance decline in rakish water Film Tec spiral wound RO membranes*. Desalination 136 (2001) 281–286.
29) Abdul Sattar Kahdim, Alaa Abdulrazaq Jassim and Saleh Ismail. *Effect of different operation pressures for various membranes on the performance of RO plants*. Desalination 155 (2003) 287–291.
30) Abdul Wahab Mohammad, Mohd Sobri Takriff. *Predicting flux and rejection of multicomponent salts mixture in nanofiltration membranes*. Desalination 157 (2003) 105–111.
31) Abraham Sagiv, Raphael Semiat. *Analysis of parameters affecting boron permeation through reverse osmosis membranes*. Journal of Membrane Science 243 (2004) 79–87.
32) Ahmed Al-Amoudi, Paul Williams , A. S. Al-Hobaib, Robert W. Lovitt. *Cleaning results of new and fouled nanofiltration membrane characterized by contact angle, updated DSPM, flux and salts rejection*. Applied Surface Science 254 (2008) 3983–3992.
33) Ahmad Al-Amoudi, Paul Williams, Steve Mandale and Robert W. Lovitt. *Cleaning results of new and fouled nanofiltration membrane characterised by zeta potential and permeability*. Separation and purification technology 54 (2007) 234–240.
34) Alexander A. Rashin and Barry Honig. *Reevaluation of the Born Model of Ion Hydration.* J. Phys. Chem. 89 (1985) 5588–5593.
35) Alexander Caus, Stefaan Vanderhaegen, Leen Braeken and Bart Van der Bruggen. *Integrated nanofiltration cascades with low salt rejection for complete removal of pesticides in drinking water production*. Desalination 241 (2009) 111–117.
36) Alexei G. Pervov, Eugene V. Dudkin, Oleg A. Sidorenko, Victor V. Antipov, Sergei A. Khakhanov and Roman I. Makarov. *RO and NF membrane systems for drinking water production and their maintenance techniques.* Desalination 132 (2000) 315–321.

37) Altaf H. Basta, Houssni El-Saied and Mohamed M. Elberry. *Cellulose membranes for reverse osmosis. Part. II Improving RO membranes prepared from non-woody cellulose*. Desalination 159 (2003) 183–196.
38) Amy E. Childress, Menachem Elimelech. *Effect of solution chemistry on the surface charge of polymeric reverse osmosis and nanofiltration membranes*. Journal of Membrane Science 119 (1996) 253–268.
39) Ana I. Cavaco Morão, Ana M. Brites Alves, Maria Diná Afonso. *Concentration of clavulanic acid broths: Influence of the membrane surface charge density on NF operation*. Journal of Membrane Science 281 (2006) 417–428.
40) Andrew Porteous. *Desalination technology, developments and practice*.
41) Andrij E. Yaroshchuk. *Dielectric exclusion of ions from membranes*. Advances in Colloid and Interface Science 85 (2000) 193–230.
42) Andrij E. Yaroshchuk. *Rejection mechanisms of NF membranes*. Membrane Technology No.100 (1998) 9–11.
43) Andrij Yaroshchuk and Eberhard STAUDE. *Charged membranes for low pressure reverse osmosis properties and applications.* Desalination 86 (1992) 115–134.
44) Andriy E. Yaroshchuk. *Negative rejection of ions in pressure-driven membrane processess.* Advances in colloid and intrface science 139 (2008) 150–173.
45) Andriy E. Yaroshchuk, Alexander L. Makovetskiy, Yuriy P. Boiko, Eduard W. Galinker. *Non-steady-state membrane potential: theory and measurements by a novel technique to determine the ion transport numbers in active layers of nanofiltration membranes.* Journal of Membrane Science 172 (2000) 203–221.
46) Andras Roman, Jianming Wang, Jozsef Csanadic, Cecília Hodurc and Gyula Vatai. *Partial demineralization and concentration of acid whey by nanofiltration combined with diafiltration*. Desalination 241 (2009) 288–295.
47) Anthony Szymczyk, Patrick Fievet. *Investigating transport properties of nanofiltration membranes by means of a steric, electric and dielectric exclusion model*. Journal of Membrane Science 252 (2005) 77–88
48) Antoine Bouchoux, Helene Roux-de Balmann and Florence Lutin. *Nanofiltration of glucose and sodium lactate solutions variations of retention between single- and mixed-solute solutions*. Journal of membrane science 258 (2005) 123–132.
49) Arun Subramani, Eric M. V. Hoek. *Direct observation of initial microbial deposition onto reverse osmosis and nanofiltration membranes*. Journal of Membrane Science 319 (2008) 111–125.

B

50) B. M. Watson and C. D. Hornburg. *Low-energy membrane nanofiltration for removal of color, organics and hardness from drinking water supplies 6.M. Watson and C.D. Hornburg DSS Engineers, inc., Fort Landerdale, Florida ABSTRACT.* Desalination 72 (1989) 11–22.
51) B. Chaufer, M. Rabiller-Baudry, L. Guihard, and G. Daufin. *Retention of ions in nanofiltration at various ionic strength*. Desalination 104 (1996) 37–46.
52) B. Van der Bruggen, I. Hawrijk, E. Cornelissen, C. Vandecasteele. *Direct nanofiltration of surface water using capillary membranes: comparison with flat sheet membranes*. Separation and Purification Technology 31 (2003) 193–201.
53) B. Van der Bruggen, J. Schaep, W. Maes, D. Wilms, C. Vandecasteele. *Nanofiltration as a treatment method for the removal of pesticides from ground waters*. Desalination 117 (1998) 139–147.
54) B. Van der Bruggen, J. Schaep, D. Wilms, C. Vandecasteele. *Influence of molecular size, polarity and charge on the retention of organic molecules by nanofiltration*. Journal of Membrane Science 156 (1999) 29–41.

55) B. Van der Bruggen, R. Milis, C. Vandecasteele, P. Bielen, E. Van San, K. Huysman. *Electrodialysis and nanofiltration of surface water for subsequent use as infiltration water*. Water Research 37 (2003) 3867–3874.
56) Bart Van der Bruggen. *Desalination by distillation and by reverse osmosis - trends towards the future*. Membrane technology (February 2003) 6–9.
57) Bart Van der Bruggen and Carlo Vandecasteele. *Distillation vs. membrane filtration: overview of process evolutions in seawater desalination*. Desalination 143 (2002) 207–218.
58) Bart Van der Bruggen and Carlo Vandecasteele. *Removal of pollutants from surface water and groundwater by Nanofiltration: overview of possible applications in the drinking water industry*. Environmental Pollution 122 (2003) 435–445.
59) Bart. Van der Bruggen, K. Everaert, D. Wilms and C. Vandecasteele. *Application of Nanofiltration for removal of pesticides, nitrate and hardness from ground water: rejection properties and economic evaluation*. Journal of membrane science 193 (2001) 239–248.
60) Benoit Fradin and R. W. Field. *Crossflow microfiltration of magnesium hydroxide suspensions: determination of critical fluxes, measurement and modelling of fouling*. Separation and purification technology 16 (1999) 25–45.
61) Bernt Ericssonl, Magnus Hallberg and Jan Wachenfeldt. Desalination 108 (1996) 129–141.
62) Brian J. Rudie, Greg S. Ross, Steven J. Harrold and David J. Paulson. *Effects of surface force interactions on an NF/UF membrane.* Desalination 90 (1993) 107–118.
63) Bryce S. Richards and Andrea I. Schafer. *Design considerations for a solar-powered desalination system foe remote communities in Australia*. Desalination 144 (2002) 193–199.

C

64) C. J. M. van Rijin. *Nano amd micro engineered membrane technology*. Elsevier, first edetion 2004. ISBN: 0-444-51489-9. ISSN: 0927–5193.
65) C. Brent Cluff. *Slow sandhanofiltration treatment for secondary treated wastewater.* Desalination 88 (1992) 53–67.
66) C. Combe, C. Guizard, P. Aimar, V. Sanchez. *Experimental determination of four characteristics used to predict the retention of a ceramic nanofiltration membrane*. Journal of Membrane Science 129 (1997) 147–160.
67) C. Labbez, P. Fievet, A. Szymczyk, A. Vidonne, A. Foissy, J. Pagetti. *Retention of mineral salts by a polyamide nanofiltration membrane*. Separation and Purification Technology 30 (2003) 47–55.
68) C. Labbez, P. Fievet, F. Thomas, A. Szymczyk, A. Vidonne, A. Foissy, and P. Pagetti. *Evaluation of the "DSPM" model on a titania membrane: measurements of charged and uncharged solute retention, electrokinetic charge, pore size, and water permeability*. Journal of colloid and interface science 262 (2003) 200–211.
69) C. Martin-Orue, S. Bouhallab, A. Garem. *Nanofiltration of amino acid and peptide solutions: mechanisms of separation*. Journal of Membrane Science 142 (1998) 225–233.
70) C. Robert Reiss, James S. Taylor, Christophe Robert. *Surface water treatment using nanofiltration - pilot testing results and design considerations*. Desalination 125 (1999) 97–112.
71) C. Visvanathan, Bowo Djoko Marsono and Biswadeep Basu. *Removal of THMP by nanofiltration: effects of interfernce parameters*. Wat. Res. Vol. 32 No. 12 (1998) 3527–3538.
72) Carolina Mazzoni, Fiorenzo Orlandini and Serena Bandini. *Role of electrolyte type on TiO2-ZrO2 nanofiltration membranes performances*. Desalination 240 (2009) 227–235.

73) Che-Jen Lin, Pritesh Rao, Saqib Shirazi. *Effect of operating parameters on permeate flux decline caused by cake formation - a model study*. Desalination 171 (2004) 95–105.
74) Christopher Bellona, Jörg E. Drewes. *The role of membrane surface charge and solute physico-chemical properties in the rejection of organic acids by NF membranes*. Journal of Membrane Science 249 (2005) 227–234.
75) Christopher Bellona, Jörg E. Drewes, Pei Xu, Gary Amy. *Review Factors affecting the rejection of organic solutes during NF/RO treatment—a literature review.* Water Research 38 (2004) 2795–2809.
76) Claire Ventresque, Guy Bablon. *The integrated nanofiltration system of the Méry-sur-Oise surface water treatment plant (37 mgd)*. Desalination 113 (1997) 263–266.
77) Claire Ventresquea, Valérie Gisclon, Guy Bablon, Gérard Chagneau. *An outstanding feat of modem technology: the Mery-sur-Oise Nanofiltration Treatment Plant (340,000 ml/d).* Desalination 131 (2000) 1–16.
78) Courfia K. Diawara, Sidy M. Lô, Michel Rumeau, Maxime Pontie and Oumar Sarr. *A phenomenological mass transfer approach in Nanofiltration of halide ions for a selective defluorination of brackish drinking water*. Journal of membrane science 219 (2003) 103–112.
79) Craig Bartels, Mark Wilf, Warren Casey, Jeff Campbell. *New generation of low fouling nanofiltration membranes*. Desalination 221 (2008) 158–167.

D

80) D. R. Paul. *Reformulation of the solution-diffusion theory of reverse osmosis.* Journal of membrane science 241 (2004) 371–386.
81) D. Y. Kwon, S. Vigneswaran, A. G. Fane, R. Ben Aim. *Experimental determination of critical flux in cross-flow microfiltration*. Separation and purification technology 19 (2000) 169–181.
82) D. Prats, M. F. Chillon, M. Rubio and J. A. Reverter. *Alicante university, closed water cycle, reverse osmosis and water treatment plants*. Desalination 109 (1997) 315–321.
83) Daniela Szaniawskaa, H. G. Spencer. *Non-equilibrium thermodynamics analysis of the transport properties of formed-in-place Zr(IV) hydrous oxide-polyacrylate membranes: III. Ternary lactose-NaCl-water solutions*. Desalination 113 (1997) l–6.
84) Darío R. Machado, David Hasson, Raphael Semiat. *Effect of solvent properties on permeate flow through nanofiltration membranes. Part I: investigation of parameters affecting solvent flux*. Journal of Membrane Science 163 (1999) 93–102.
85) David Hasson, Bracha Limoni-Relis, Paphael Semiat and Philip Tob. *Fouling of RO membranes by phthalate esters concentration*. Desalination 105 (1996) 13–20.
86) Dengxi Wu, J. A. Howell, R. W. Field. *Critical flux measurements for model colloids*. Journal of membrane science 152 (1999) 89–98.

E

87) E. J. Hoffman. *Membrane separation technology*.
88) Eert Vellenga, Gun Trägådh. *Nanofiltration of combined salt and sugar solutions: coupling between retentions*. Desalination 120 (1998) 211–220.
89) Einar Mathiasson and Bjorn Sivik. *Concentration polarisation and fouling*. Desalination, 35 (1980) 59–103.
90) Essam El-Sayed, Mahmoud Abdel-Jawad, Sadeq Ebrahim, Ahmad Al-Saffar. *Performance of two RO membrane configurations in MSF/RO hybrid system*. Desalination 128 (2000) 231–245.
91) Eric M. Vrijenhoek, John J. Waypa. *Arsenic removal from drinking water by a "loose" nanofiltration membrane.* Desalination 130 (2000) 265–277.
92) Evgenia Chilyumova, Jorg Thöming. *Nanofiltration of bivalent nickel cations - model parameter determination and process simulation*. Desalination 224 (2008) 12–17.

F

93) F. N. Karelin, A. A. Askerniya, M. L. Gril, and O. F. Parilova. *Salt concentration and recovery from aqueous solutions using pressure-driven membrane processes*. Desalination 104 (1996) 69–74.

94) François Garcia, Delphine Ciceron, Abdellah Saboni and Silvia Alexandrova. *Nitrate ions elimination from drinking water by nanofiltration: Membrane choice*. Separation and purification technology 52 (2006) 196–200.

G

95) G. A. Schrader, A. Zwijnenburg, M. Wessling. *The effect of WWTP effluent zeta-potential on direct nanofiltration performance*. Journal of Membrane Science 266 (2005) 80–93.

96) G. M. Rios, R. Joulie, S. J. Sarrade and M. Carles. *Investigation of ion separation by micro porous Nanofiltration membranes*. AIChE journal volume 42, no. 9 (September 1996) 2521–2528.

97) G. Hagmeyer, R. Gimbel. *Modelling the salt rejection of nanofiltration membranes for ternary ion mixtures and for single salts at different pH values*. Desalination 117 (1998) 247–256.

98) G. Hagmeyer, R. Gimbel. *Modelling the rejection of nanofiltration membranes using zeta potential measurements*. Separation and Purification Technology 15 (1999) 19–30.

99) G. Ricea, A. Barberb, A. O'Connora, G. Stevensa and S. Kentish. *Fouling of NF membranes by dairy ultrafiltration permeates*. Journal of Membrane Science 330 (2009) 117–126

100) Gaëlle Ducom, Corinne Cabassud. *Interests and limitations of nanofiltration for the removal of volatile organic compounds in drinking water production*. Desalination 124 (1999) 115–123.

101) Gary D. Christian. *Analytical chemistry*. John Wiley and sons. Fifth edition. (1994).

102) Gaurav Bhalla and William M. Deen. *Effects of charge on osmotic reflection coefficients of macromolecules in porous membranes*. Journal of Colloid and Interface Science 333 (2009) 363–372.

103) George E. Forsythe. *Computer methods for mathematical computations*.

104) Gerhard Schmid, Hans Schwarz. *Electrochemistry of capillary systems with narrow pores V. streaming potential : Donnan hindrance of electrolyte transport.* Journal of membrane science 150 (1998) 197–209.

105) Greg Guillen and Eric M. V. Hoek. *Modelling the impacts of feed spacer geometry on reverse osmosis and nanofiltration processes*. Chemical Engineering Journal 149 (2009) 221–231.

106) Guohua Chen, Xijun Chai, Po-Lock Yue, Yongli Mi. *Treatment of textile desizing wastewater by pilot scale nanofiltration membrane separation*. Journal of Membrane Science 127 (1997) 93–99.

107) Gurdev Singh, Lianfa Song. *Impact of feed water acidification with weak and strong acids on colloidal silica fouling in ultrafiltration membrane processes*. Water Research 42 (2008) 707–713.

H

108) H. C. van der Horst, J. M. K. Timmer, T. Robbertsen and J. Leenders. *Use of nanofiltration for concentration and demineralisation in the diary industry: Model for mass transport*. Journal of membrane science 104 (1995) 205–218.

109) H. D. M. Sombekke, D. K. Voorhoeve, P. Hiemstra. *Environmental impact assessment of groundwater treatment with nanofiltration*. Desalination 113 (1997) 293–296.

110) H. K. Shon, S. Vigneswaran, In S. Kim, J. Chob, H. H. Ngo. *Effect of pretreatment on the fouling of membranes: application in biologically treated sewage effluent*. Journal of Membrane Science 234 (2004) 111–120.

111) H. K. Shona, S. Vigneswaran, In S. Kimb, J. Cho, H. H. Ngo. *Fouling of ultrafiltration membrane by effluent organic matter: A detailed characterization using different organic fractions in wastewater*. Journal of Membrane Science 278 (2006) 232–238.

112) H. Strathmann. *Asymmetric polymide membranes for filtration of non aqueous solution*. Desalination 26 (1978) 85–91.

113) H. Ivnitsky, I. Katz, D. Minz, E. Shimoni, Y. Chen, J. Tarchitzky, R. Semiat, C. G. Dosoretz. *Characterisation of membrane biofouling in nanofiltration processes of wastewater treatment*. Desalination 185 (2005) 255–268.

114) Houssni El-Saied, Altaf H. Basta, Barsoum N. Barsoum and Mohamed M. Elberry. *Cellulose membranes for reverse osmosis. Part. I RO cellulose acetate membrane including a composite with polypropylene*. Desalination 159 (2003) 171–181.

I

115) I. S. Han, M. Cheryan. *Nanofiltration of model acetate solutions*. Journal of Membrane Science 107 (1995) 107–113.

116) I. Atamanenko, A. Kryvoruchko and L. Yurlova. *Study of the scaling process on membranes*. Desalination 167 (2004) 327–334.

117) Ismail Koyuncu. *Influence of dyes, salts and auxiliary chemicals on the nanofiltration of reactive dye baths: experimental observations and model verification*. Desalination 154 (2003) 79–88.

J

118) J. A. Otero, G. Lena, J. M. Colina, P. Prádanos, F. Tejerina, A. Hernández. *Characterisation of nanofiltration membranes: Structural analysis by the DSP model and microscopical techniques*. Journal of Membrane Science 279 (2006) 410–417.

119) J. A. Redondo. *Brackish-, sea- and wastewater desalination*. Desalination 138 (2001) 29–40.

120) J. G. A. Bitter. *Transport mechanisms in membrane separation processes*. The plenum chemical engineering series. (1991) Plenum press, New York.

121) J. G. Wijmans, R. W. Baker. The solution-diffusion model: a review. Journal of Membrane Science 107 (1995) 1–21.

122) J. L. C. Santos, A. M. Hidalgo, R. Oliveira, S. Velizarov, J. G. Crespo. *Analysis of solvent flux through nanofiltration membranes by mechanistic, chemometric and hybrid modelling*. Journal of Membrane Science 300 (2007) 191–204.

123) J. M. K. Timmer, H. C van der Horst and T. Robbertsen. *Transport of lactic acid through reverse osmosis and nanofiltration membranes.* Journal of Membrane Science 85 (1993) 205–216.

124) J. M. K. Timmer, J. Kromkamp, T. Robbertsen. *Lactic acid separation from fermentation broths by reverse osmosis and nanofiltration.* Journal of Membrane Science 92 (1994) 185–197.

125) J. M. M. Peeters, J. P. Boom, M. H. V. Mulder and H. Strathmann. *Retention measurements of Nanofiltration membranes with electrolyte solutions*. Journal of membrane science 145 (1998) 199–209.

126) J. M. M. Peeters, M. H. V. Mulder, H. Strathmann. *Streaming potential measurements as a characterization method for nanofiltration membranes*. Colloids and Surfaces A: Physicochemical and Engineering Aspects 150 (1999) 247–259.

127) J. S. Vrouwenvelder, S. A. Manolarakis, H. R. Veenendaal, D. van der Kooij. *Biofouling potential of chemicals used for scale control in RO and NF membranes.* Desalination 132 (2000) 1–10.
128) J. Cadotte, R. Forester, M. Kim, R. Petersen, T. Stocker. *Nanofiltration membranes broaden the use of membrane separation technology.* Desalination 70 (1988) 77–88.
129) J. Etienne, A. Larbot, A. Julbe, C. Guizard and L. Cot, *A microporous zirconia membrane prepared by the sol-gel process from zirconyl oxalate.* Journal of Membrane Science 86 (1994) 95–102.
130) J. Gilron, N. Daltrophe, O. Kedem. *Trans-membrane pressure in nanofiltration*. Journal of Membrane Science 286 (2006) 69–76.
131) J. Palmeri, P. Blanc, A. Larbot, P. David. *Theory of pressure-driven transport of neutral solutes and ions in porous ceramic nanofiltration membranes*. Journal of Membrane Science 160 (1999) 141–170.
132) J. Palmeri, P. Blanc, A. Larbot, P. David. *Hafnia ceramic nanofiltration membranes Part II. Modeling of pressure-driven transport of neutral solutes and ions.* Journal of Membrane Science 179 (2000) 243–266.
133) Jae-Hoon Choi, Kensuke Fukushi, Kazuo Yamamoto. *A study on the removal of organic acids from wastewaters using nanofiltration membranes*. Separation and Purification Technology 59 (2008) 17–25.
134) Jae-Hyuk Kim, Pyung-Kyu Park, Chung-Hak Leea, Heock-Hoi Kwon. *Surface modification of nanofiltration membranes to improve the removal of organic micro-pollutants (EDCs and PhACs) in drinking water treatment: Graft polymerization and cross-linking followed by functional group substitution*. Journal of Membrane Science 321 (2008) 190–198.
135) James Kelly and Philip Kelly. *Desalination of Acid Casein Whey by Nanofiltration***.** Int. Dairy Journal 5 (1995) 291–303.
136) Jean de Witte. *New development in nanofiltration and reverse osmosis membrane manufacturing*. Desalination 113 (1997) 153–156.
137) Jean-Pierre De Witte. *Surface water potabilisation by means of a novel nanofiltration element*. Desalination 108 (1996) 153–157.
138) Jesus Garcia-Aleman and Jmaes M. Dickson. *Mathematical modelling of Nanofiltration membranes with mixed electrolyte solutions*. Journal of membrane science 235 (2004) 1–13.
139) Jian-Hua Xu, Xin-Hui Xing, Shinjiro Yamamoto, Yasunori Tanji ang Hajime Unno. *Effect of ion transport on its permeation through a Nanofiltration membrane*. Journal of chemical engineering of Japan, volume 30, No. 5 (1997) 806–812.
140) Jia-yu Tian, Heng Liang, Jun Nan, Yan-ling Yang, Shi-jie You and Gui-bai Li. *Submerged membrane bioreactor (sMBR) for the treatment of contaminated raw water*. Chemical Engineering Journal 148 (2009) 296–305.
141) Jia-Zhen Yang, Jun Liu. *Application of Pitzer's electrolyte solution theory to frictional model of charged nanofiltration membrane*. Thermochimica Acta 308 (1998) 177–182.
142) Jinwen Wang, Zhongren Yue, James Economy. *Novel method to make a continuous micro-mesopore membrane with tailored surface chemistry for use in nanofiltration*. Journal of Membrane Science 308 (2008) 191–197.
143) Jinwen Wang, Zhongren Yue, Jeffrey Scott Ince, James Economy. *Preparation of nanofiltration membranes from polyacrylonitrile ultrafiltration membranes*. Journal of Membrane Science 286 (2006) 333–341.

144) Joanna M. Skluzacek, M. Isabel Tejedor, Marc A. Anderson. *An iron-modified silica nanofiltration membrane: Effect of solution composition on salt rejection*. Microporous and Mesoporous Materials 94 (2006) 288–294.

145) Johan Schaep, Bart Van der Bruggen, Carlo Vandecasteele, Dirk Wilms. *Influence of ion size and charge in nanofiltration*. Separation and Purification Technology 14 (1998) 155–162.

146) Johan Schaep, Bart Van der Bruggen, Steven Uytterhoeven, Raf Croux, Carlo Vandecasteele, Dirk Wilms, Emmanuel Van Houtte, Frans Vanlerberghe. *Removal of hardness from groundwater by nanofiltration*. Desalination 119 (1998) 295–302.

147) Johan Schaep, Carlo Vandecasteele, Bart Peeters, Jan Luyten, Chris Dotremont, Davy Roels. *Characteristics and retention properties of a mesoporous γ-Al_2O_3 membrane for nanofiltration*. Journal of Membrane Science 163 (1999) 229–237.

148) Jolanta Bohdziewicz, Michal Bodzek, Ewa Wąsik. *The application of reverse osmosis and nanofiltration to the removal of nitrates from groundwater*. Desalination 121 (1999) 139–147.

149) Jonathan A. Brant, Kelly M. Johnson, Amy E. Childress. *Examining the electrochemical properties of a nanofiltration membrane with atomic force microscopy*. Journal of Membrane Science 276 (2006) 286–294.

150) Joo-Hwa Tay, Jianlin Liu, Darren Deli Sun. *Effect of solution physic-chemistry on the charge property of nanofiltration membranes*. Water Research 36 (2002) 585–598.

151) Junwen Lv, Kai Yu Wang, Tai-Shung Chung. *Investigation of amphoteric polybenzimidazole (PBI) nanofiltration hollow fiber membrane for both cation and anions removal*. Journal of Membrane Science 310 (2008) 557–566.

152) Jutta Nuortila-Jokinen, Marianne Nyström. *Comparison of membrane separation processes in the internal purification of paper mill water*. Journal of Membrane Science 119 (1996) 99–115.

K

153) K. S. Spiegler and A. D. K. Laird. *Principles of desalination, part A.*

154) K. V. Plakas, A. J. Karabelas. *Membrane retention of herbicides from single and multi-solute media: The effect of ionic environment*. Journal of Membrane Science 320 (2008) 325–334.

155) K. Boussua, B. Van der Bruggen, A. Volodin, C. Van Haesendonck, J. A. Delcourc, P. Van der Meeren, C. Vandecasteele. *Characterization of commercial nanofiltration membranes and comparison with self-made polyethersulfone membranes*. Desalination 191 (2006) 245–253.

156) K. Lang, G. Chowdhury, T. Matsuura and S. Sourirajan. *Reverse osmosis performance of modified polyvinyl alcohol thin-film composite membranes.* Journal of colloid and interface science 166 (1994) 239–244.

157) K. Mehiguene, S. Taha, N. Gondrexon, J. Cabon and G. Dorange. *Copper transfer modeling through a nanofiltration membrane in the case of ternary aqueous solution.* Desalination 127 (2000) 135–143.

158) K. Mehiguene, Y. Garba, S. Taha, N. Gondrexon, G. Dorange. *Influence of operating conditions on the retention of copper and cadmium in aqueous solutions by nanofiltration: experimental results and modelling*. Separation and Purification Technology 15 (1999) 181–187.

159) K. Scott and R. Hughes. *Industrial membrane separation technology*.

160) K. Treffry-Goatley and J. Gilron. *The Application of Nanofiltration Membra.nes to the Treatment of Industrial Effluent and Process Streams.* Filtration and Separation (1993) 63–66.

161) Kang Hu, James M. Dickson. *Nanofiltration membrane performance on fluoride removal from water*. Journal of Membrane Science 279 (2006) 529–538.
162) Keith Scott . *Handbook of industrial membranes*. First edition.
163) Kristina Linde, Ann-Soft Jönsson. *Nanofiltration of salt solutions and landfill leachate*. Desalination 103 (1995) 223–232.
164) Kwang-Je Kima, Geeta Chowdhury, Takeshi Matsuura. *Low pressure reverse osmosis performances of sulfonated poly(2,6-dimethyl-1,4-phenylene oxide) thin film composite membranes: effect of coating conditions and molecular weight of polymer*. Journal of Membrane Science 179 (2000) 43–52.
165) Kyu-Hong Ahn, Ho-Young Cha, Ick-Tae Yeom, Kyung-Guen Song. *Application of nanofiltration for recycling of paper regeneration wastewater and characterization of filtration resistance*. Desalination 119 (1998) 169–176.

L

166) L. Paugam, S. Taha, J. Cabon, G. Dorange. *Elimination of nitrate ions in drinking waters by nanofiltration*. Desalination 152 (2002) 271–274.
167) L. Paugam, S. Taha, G. Dorange and F. Quéméneur. *Influence of ionic composition on nitrate retention by nanofiltration*. Trans IChemE vol. 81 part A (October 2003) 1199–1205.
168) L. Vandanjon, P. Jaouen, N. Rossignol, F. Quéméneur, J. -M. Robert. *Concentration and desalting by membrane processes of a natural pigment produced by the marine diatom Haslea ostrearia Simonsen*. Journal of Biotechnology 70 (1999) 393–402.
169) Larry Nyhoff and Sanford Leestma. *Fortran 77 for engineers and scientists*. Third edition.
170) Lawrence Dresner. *Some remarks on the integration of the extended Nernst-Planck equations in hyper-filtration of multi-component solution.* Desalination 10 (1972) 27–46.
171) Lianxiong Li, Junhang Dong, Tina M. Nenoff, Robert Lee. *Desalination by reverse osmosis using MFI zeolite membranes*. Journal of Membrane Science 243 (2004) 401–404.
172) Lina M. Ortega, Rémi Lebrun, Jean-François Blais, Robert Hausler. *Removal of metal ions from an acidic leachate solution by nanofiltration membranes*. Desalination 227 (2008) 204–216.
173) Lu Ouyang, Ramamoorthy Malaisamy, Merlin L. Bruening. *Multilayer polyelectrolyte films as nanofiltration membranes for separating monovalent and divalent cations*. Journal of Membrane Science 310 (2008) 76–84.
174) Luigi Bruni, Serena Bandini. *The role of the electrolyte on the mechanism of charge formation in polyamide nanofiltration membranes*. Journal of Membrane Science 308 (2008) 136–151.
175) Luigi Bruni and Serena Bandini. *Studies on the role of site-binding and competitive adsorption in determining the charge of nanofiltration membranes*. Desalination 241 (2009) 315–330.

M

176) M. F. A. Goosen, S. S. Sablani, H. Al-Hinai, S. Al-Obeidani, R. Al-Blushi and D. Jackson. *Fouling of reverse osmosis and ultrafiltration membranes: a critical review*. Separation science and technology, vol. 39, no. 10 (2004) 2261–2297.
177) M. L. Sforça, S. P. Nunes, K. -V. Peinemann. Composite nanofiltration membranes prepared by in situ polycondensation of amines in a poly(ethylene oxide-b-amide) layer. Journal of Membrane Science 135 (1997) 179–186.
178) M. N. A. Hawlader, J. C. Ho and Chua Kok Teng. *Desalination of seawater: an experiment with RO membranes*. Desalination 132 (2000) 275–280.

179) M. S. H. Bader. *Analysis of the Paradox Valley brine desulfation by nanofiltration*. Desalination 229 (2008) 33–51.
180) M. S. H. Bader. *Innovative processes to desulfate the Paradox Valley brine*. Desalination 229 (2008) 52–67.
181) M. Gamal Khedr. *Membrane methods in tailoring simpler, more efficient, and cost effective wastewater treatment alternatives*. Desalination 222 (2008) 135–145.
182) M. Isabel González, Silvia Alvarez, Francisco A. Riera, Ricardo Álvarez. *Lactic acid recovery from whey ultrafiltrate fermentation broths and artificial solutions by nanofiltration*. Desalination 228 (2008) 84–96.
183) M. Khayet, M. P. Godino and J. I. Mengual. *Study of asymmetric polarisation in direct contact membrane distillation*. Separation science and technology, vol. 39, no. 1 (2004) 125–147.
184) M. Mänttäri, J. Nuortila-Jokinen and M. Nyström. Evaluation of Nanofiltration Membranes for Filtration of Paper Mill Total Effluent. Filtration and separation (April 1997) 275–280.
185) M. Mänttäri, J. Nuortila-Jokinen and M. Nyström. *Influence of filtration conditions on the performance of NF membranes in the filtration of paper mill total effluent*. Journal of Membrane Science 137 (1997) 187–199.
186) M. Mänttäri, M. Nyström. *Critical flux in NF of high molar mass polysaccharides and effluents from the paper industry*. Journal of membrane science 170 (2000) 257–273.
187) M. Nyström, S. Butylina and S. Platt. *NF retention and critical flux of small hydrophilic/hydrophobic molecules*. Membrane technology 10 (October 2004) 5–8.
188) M. Perry and C. Linder. *Intermediate Reverse Osmosis Ultrafiltration (RO UF) membranes for concentration and desalting of low molecular weight organic solutes.* Desalinatlon 71 (1989) 233–245.
189) M. Pontié, C. K. Diawara, M. Rumeau. *Streaming effect of single electrolyte mass transfer in nanofiltration: potential application for the selective defluorination of brackish drinking waters*. Desalination 15 l(2002) 267–274.
190) M. Soltanieh, M. Mousavi. *Application of charged membranes in water softening: modeling and experiments in the presence of polyelectrolytes*. Journal of Membrane Science 154 (1999) 53–60.
191) M. Starov, W. R. Bowen and J. S. Welfoot. *Flow of multi-component electrolyte solutions through narrow pores of Nanofiltration membrane*. Journal of colloid and interface science 240 (2001) 509–524.
192) M. Tahaikt, A. Ait Haddou, R. El-Habbania, Z. Amor, F. Elhannouni, M. Taky, M. Kharif, A. Boughriba, M. Hafsi and A. Elmidaoui. *Comparison of the performances of three commercial membranes in fluoride removal by nanofiltration continuous operations*. Desalination 225 (2008) 209–219.
193) M. Taleb Ahmed, T. Chaabanea, S. Taha, R. Maachi. *Treatment of heavy metals by nanofiltration present in the lake Reghaïa*. Desalination 221 (2008) 277–283.
194) Magdalena Szmukala and Daniela Szaniawska. *Application of ceramic membranes in water treatment for fish hatchery supplying purposes*. Desalination 240 (2009) 117–126.
195) Marcel Mulder. *Basic principles of membrane technology, second edition*. Kluwer academic publishers. 1997. ISBN: 0-7923-4247-X (HB). ISBN: 0-7923-4248-8 (PB).
196) Marco Stoller. *On the effect of flocculation as pretreatment process and particle size distribution for membrane fouling reduction*. Desalination 240 (2009) 209–217.
197) Marco Stoller, Angelo Chianese. *Optimisation of membrane batch processes by means of the critical flux theory.* Desalination 191 (2006) 62–70.

198) Margarida Ribau Teixeira, Maria João Rosa and Marianne Nyström. *The role of membrane charge on nanofiltratin performance.* Journal of membrane science, 265 (2005) 160–166.
199) Maria Diná Afonso. *Surface charge on loose nanofiltration membranes*. Desalination 191 (2006) 262–272.
200) Maria Dina Afonso, Jamal O. Jaber and Mousa S. Mohsen. *Brackish groundwater treatment by reverse osmosis in Jordan*. Desalination 164 (2004) 157–171.
201) Maria Diná Afonso and Maria Norberta de Pinho. *Transport of $MgSO_4$, $MgCl_2$ and Na_2SO_4 across an amphitricha Nanofiltration membrane*. Journal of membrane science 179 (2000) 137–154.
202) Maria Joã Rosa, Maria Norberta de Pinho. *Separation of organic solutes by membrane pressure-driven processes.* Journal of Membrane Science 89 (1994) 235–243.
203) Maria Joã Rosa, Maria Norberta de Pinho. *The role of ultrafiltration and nanofiltration on the minimisation of the environmental impact of bleached pulp effluents*. Journal of Membrane Science 102 (1995) 155–161.
204) Marian Turek. *Seawater desalination and salt production in a hybrid membrane-thermal process*. Desalination 153 (2002) 173–177.
205) Marian Turek and Maciej Gonet. *Nanofiltration in the utilization of coal-mine brines.* Desalination 108 (1996) 171–177.
206) Marianne Nyström, Jukka Tanninen and Mika Mänttäri. *Separation of metal sulfates and nitrates from their acids using nanofiltration.* Membrane Technology 117 (2000) 5–9.
207) Marianne Nyström, Lena Kaipia, Susana Luque. *Fouling and retention of nanofiltration membranes***.** Journal of Membrane Science 98 (1995) 249–262.
208) Mark E. Davis. *Numerical methods and modeling for chemical engineers*.
209) Maryam Alborzfar, Gunnar Jonsson and Christian Grøn. *Removal of natural organic matter from two types of humic ground waters by nanofiltration*. Wat. Res. Vol. 32 No. 10 (1998) 2983–2994.
210) Mathias Ernst, Alexander Bismarck, Jürgen Springer, Martin Jekel. *Zeta-potential and rejection rates of a polyethersulfone nanofiltration membrane in single salt solutions*. Journal of Membrane Science 165 (2000) 251–259.
211) Maxime Pontae, Hervé Buisson, Courfia K. Diawara, Hortense Essis-Tome. *Studies of halide ions mass transfer in nanofiltration application to selective defluorination of brackish drinking water*. Desalination 157 (2003) 127–134.
212) Meng Su, Da-Xin Wang, Xiao-Lin Wang, Masasski Ando and Takuji Shintani. *Rejection of ions by NF membranes for binary electrolyte solutions of NaCl, $NaNO_3$, $CaCl_2$ and $Ca(NO_3)_2$*. Desalination 191 (2006) 303–308.
213) Michael B. Cutlip. *Problem solving in chemical engineering with numerical methods*.
214) Michael J. H. Snow, Dirk de Winter, Robert Buckingham, Jeff Campbell, J. Wagner. *New techniques for extreme conditions: high temperature reverse osmosis and nanofiltration*. Desalination 105 (1996) 57–61.
215) Mika Mänttäri, Arto Pihlajamäki, Marianne Nyström. *Effect of pH on hydrophilicity and charge and their effect on the filtration efficiency of NF membranes at different pH*. Journal of Membrane Science 280 (2006) 311–320.
216) Mohammad AK. A1-Sofi, Ata M. Hassan, Osman A. Hamed, Abdul Ghani I. Dalvi, Mohammad N. M. Kither, Ghulam M. Mustafa and Khalid Bamardouf. *Optimization of hybridized seawater desalination process.* Desalination 131 (2000) 147–156.
217) Mohamed Siddiqui, Gary Amy, Joseph Ryan and Wilbert Odem. *Membranes for the control of natural organic matter from surface waters.* Water Research vol. 34, no. 13 (2000) 3355–3370.

218) Mohammadali Safavi and Toraj Mohammadi. *High-salinity water desalination using VMD*. Chemical Engineering Journal 149 (2009) 191–195.

N

219) N. Hilal, H. Al-Zoubi, N. A. Darwish, A. W. Mohammad and M. Abu Arabi. *A comprehensive review of Nanofiltration membranes: Treatment, pre-treatment, modelling, and atomic force microscopy*. Desalination 170 (2004) 281–308.

220) N. Lakshminarayaniah. *Transport phenomena in membranes*.

221) N. M. Al-Bastaki and H. I. Al-Qahtani. *Assessment of thermal effects on the reverse osmosis of salt/water solutions by using a spiral wound polyamide membrane*. Desalination 99 (1994) 159–168.

222) Namguk Her, Gary Amy, Chalor Jarusutthirak. *Seasonal variations of nanofiltration (NF) foulants: identification and control.* Desalination 132 (2000) 143–160.

223) *News and Views.* Membrane Technology 30 (1992) 2.

224) Nidal Hilal, A. Wahab Mohammad, Brian Atkin and Naif A. Darwish. *Using atomic force microscopy towards improvement in Nanofiltration membranes properties for desalination pre-treatment: a review*. Desalination 157 (2003) 137–144.

225) *Numerical algorithms group Ltd NAG Fortran library manual*. Mark 16. Vol.2 : D02. Oxford : NAG (1993).

226) *Numerical recipes in fortran 77: the art of scientific computing.*

O

227) O. Kedem, V. Freger. *Determination of concentration-dependent transport coefficients in nanofiltration: Defining an optimal set of coefficients*. Journal of Membrane Science 310 (March 2008) 586–593.

228) Olga Sallangos and Peter Moss. *Pilot plant study at the Dhekelia seawater plant: a review of the performance and operating data of the Koch membrane systems spiral-wound TFC 2832SS-540 magnum seawater elements and study and interpretation of the normalised data using NormPro software*. Desalination 139 (2001) 125–129.

229) Osamu Miyatake and Kotaro Tagawa. *Numerical and experimental analyses for RO desalination systems using a static pressure head*. Desalination 136 (2001) 233–242.

P

230) P. M. Bungay, H. K. Lonsdale and M. N. de Pinho. *Synthetic membranes: science, engineering and applications*.

231) P. Bacchin, P. Aimar and R. W. Field. *Critical and sustainable fluxes: Theory, experiments and applications.* Journal of membrane science 281 (2006) 42–69.

232) P. Baticle, C. Kiefer, N. Lakhchaf, A. Larbot, O. Leclerc, M. Persin, J. Sarrazin. *Salt filtration on gamma alumina nanofiltration membranes fired at two different temperatures*. Journal of Membrane Science 135 (1997) 1–8.

233) P. Berg, G. Hagmeyer and R. Gimbel. *Removal of pesticides and other micro pollutants by Nanofiltration*. Desalination 113 (1997) 205–208.

234) P. Blanc, A. Larbot, J. Palmeri, M. Lopez, L. Cot. *Hafnia ceramic nanofiltration membranes. Part I: Preparation and characterization*. Journal of Membrane Science 149 (1998) 151–161.

235) P. Canepa and A. Gradozzi. *Comtinuous starch fermentation process by nanofiltration membrane bioreactor*. Membrane Technology 37 (1993) 6–9.

236) P. Fievet, C. Labbez, A. Szymczyk, A. Vidonne, A. Foissy, J. Pagetti. *Electrolyte transport through amphoteric nanofiltration membranes*. Chemical Engineering Science 57 (2002) 2921–2931.

237) P. Fievet, M. Sbaï, A. Szymczyk. *Analysis of the pressure-induced potential arising across selective multilayer membranes*. Journal of Membrane Science 264 (2005) 1-12.

238) P. Glueckstern, Y. Kantor and M. Wilf. *Application of membrane processes for water supply in Israel*. Desalination 24 (1978) 365–376.
239) P. Hillis. *Membrane technology in water and waste water treatment*.
240) P. Puhlfürß, A. Voigt, R. Weber, M. Morbé. *Microporous TiO_2 membranes with a cut off <500 Da*. Journal of Membrane Science 174 (2000) 123–133.
241) P. Schirg and F. Widmer. *Characterisation of nanofiltration membranes for the separation of aqueous dye-salt solutions*. Desalination 89 (1992) 89–107.
242) Pakawadee Narong. *The influence of electrokinetics on membrane MICRO/ULTRA filtration of colloidal systems.* Thesis. School of Chemical Engineering and Analytical Science, The University of Manchester, 2005.
243) Parna Mukherjeea, Kimberly L. Jones, Joshua O. Abitoye. *Surface modification of nanofiltration membranes by ion implantation*. Journal of Membrane Science 254 (2005) 303–310.
244) Patrick Meares. *Membrane separation processes.* Elsevier scientific publishing company. (1976). ISBN: 0-444-414460.
245) Paul Fu, Hector Ruiz, Jim Lozier, Ken Thompson, and Carl Spangenberg. *A pilot study on groundwater natural organics removal by low-pressure membranes*. Desalination 102 (1995) 47–56.
246) Pei Xua, Jörg E. Drewes, Tae-Uk Kimb, Christopher Bellona, Gary Amy. *Effect of membrane fouling on transport of organic contaminants in NF/RO membrane applications*. Journal of Membrane Science 279 (2006) 165–175.
247) Pierre Le Clech, Bruce Jefferson, In Soung Chang, Simon J. Judd. Critical *flux determination by flux-step method in a submerged membrane bioreactor*. Journal of membrane science, 227 (2003) 81–93.
248) Pierre-Yves Pontalier, Ali Ismail, Mohamed Ghoul. *Mechanisms for the selective rejection of solutes in nanofiltration membranes.* Separation and purification technology 12 (1997) 175–181.
249) Piotr Dydo, Marian Turek, Jerzy Ciba. *Scaling analysis of nanofiltration systems fed with saturated calcium sulfate solutions in the presence of carbonate ions*. Desalination 159 (2003) 245–251.

Q

R

250) R. A. Peterson, M. A. Anderson and C. G. Hill Jr. *Development of TiO_2, membranes for gas phase nanofiltration.* Journal of Membrane Science 94 (1994) 103–109.
251) R. J. Petersen. *Composite reverse osmosis and nanofiltration membranes.* Journal of Membrane Science 83 (1993) 81–150.
252) R. Bian, K. Yamamoto, Y. Watanabe. *The effect of shear rate on controlling the concentration polarization and membrane* fouling. Desalination 131 (2000) 225–236.
253) R. Boussahel, S. Bouland, K. M. Moussaoui, A. Montiel. *Removal of pesticide residues in water using the nanofiltration process.* Desalination 132 (2000) 205–209.
254) R. Günther and J. Hapke. *Design of membrane separation plants using a module data base*. Desalination 104 (1996) 119–128.
255) R. Jeantet, J. L. Maubois, and P. Boyaval. *Semicontinuous production of lactic acid in a bioreactor coupled with nanofiltration membranes*. Enzyme and Microbial Technology 19 (1996) 614–619.
256) R. Levenstein, D. Hasson and R. Semiat. *Utilisation of the Donnan effect for improving electrolyte separation with Nanofiltration membranes*. Journal of membrane science 116 (1996) 77–92.
257) R. Rautenbach and A. Gröschl. *Separation Potential of Nanofiltration Membranes.* Desalination 77 (1990) 73–84.

258) R. Rautenbach and F. P. Helmus. *Some considerations on mass-transfer resistances in solution-diffusion-type membrane processes.* Journal of Membrane Science 87 (1994) 171–181.
259) R. Rautenbach, R. Knauf and M. Perry. *Chemically stable nanofiltration membranes and their applications.* Membrane Technology 51 (1994) 6–9.
260) R. Rautenbach and R. Mellis. *Waste water treatment by a combination of bioreactor and nanofiltration* Desalination 95 (1994) 171–188.
261) R. Simons. *Trace element removal from ash dam waters by nanofiltration and diffusion dialysis.* Desalination 89 (1993) 325–341.
262) R. Vacassy, C. Guizard, V. Thoraval, L. Cot. *Synthesis and characterization of microporous zirconia powders: Application in nanofilters and nanofiltration characteristics*. Journal of Membrane Science 132 (1997) 109–118.
263) R. Vacassy, J. Palmeri, C. Guizard, V. Thoraval, L. Cot. *Performance of stabilized zirconia nanofilters under dynamic conditions*. Separation and Purification Technology 12 (1997) 243–253.
264) Ramesh R. Sharma, Shankararaman Chellam. *Solute rejection by porous thin film composite nanofiltration membranes at high feed water recoveries*. Journal of Colloid and Interface Science, volume 328, issue 2 (December 2008) 353–366.
265) Ramesh R. Sharma, Shankararaman Chellam. *Temperature and concentration effects on electrolyte transport across porous thin-film composite nanofiltration membranes: Pore transport mechanisms and energetics of permeation*. Journal of Colloid and Interface Science, volume 298, issue 1 (June 2006) 327–340.
266) Richard Bowen and A. Wahab Mohammad.*Diafiltration by Nanofiltration: prediction and optimisation*. W AIChE journal, volume 44, no. 8 (August 1998) 1799–1812.
267) Richard W. Baker. *Membrane technology and applications*.
268) Riina Liikanen, Ilkka Miettinen, Risto Laukkanen. *Selection of NF membrane to improve quality of chemically treated surface water*. Water Research 37 (2003) 864–872.
269) Robert Blank, Karl-Heinz Muth, Sabine Proske-Gerhards, Eberhard Staude. *Electrokinetic investigations of charged porous membranes*. Colloids and Surfaces A: Physicochemical and Engineering Aspects 140 (1998) 3–11.
270) Robert E. Treybal. *Mass transfer operations*.
271) Robert H. Perry and Don W. Green. *Perry's chemical engineering handbook*. seventh edition.
272) Robert J. Petersen. Review: *Composite reverse osmosis and nanofiltration membranes*. Journal of Membrane Science 83 (1993) 81–150.
273) Rodolfo Vegas, Andrés Moure, Herminia Domínguez, Juan Carlos Parajó, José Ramón Alvarez and Susana Luque. *Evaluation of ultra- and nanofiltration for refining soluble products from rice husk xylan*. Bioresource Technology 99 (2008) 5341–5351.

S

274) S. P. Nunes and K. V. Peinemaan. *Membrane technology in the chemical industry*. WILEY-VCH. ISBN: 3-527-28485-0.
275) S. S. Madaeni, V. Kazemi. *Treatment of saturated brine in chlor-alkali process using membranes*. Separation and Purification Technology 61 (2008) 68–74.
276) S. Alami-Younssi, A. Larbort, M. Persin, J. Sarrazin, L. Cot. *Gamma alumina nanofiltration membrane Application to the rejection of metallic cations*. Journal of Membrane Science 91 (1994) 87–95.
277) S. Alami-Younssi, A. Larbort, M. Persin, J. Sarrazin, L. Cot. *Rejection of mineral salts on a gamma alumina nanofiltration membrane Application to environmental process***.** Journal of Membrane Science 102 (1995) 123–129.

278) S. Cartier, M. A. Theoleyre, M. Decloux. *Treatment of sugar decolorizing resin regeneration waste using nanofiltration*. Desalination 113 (1997) 7–17.
279) S. Condom, A. Larbot, Saad Alami Younssi and M. Persin. *Use of ultra- and Nanofiltration ceramic membranes for desalination*. Desalination 168 (2004) 207-213.
280) S. Sarrade, G. M. Rios, M. Carlfés. *Nanofiltration membrane behavior in a supercritical medium*. Journal of Membrane Science 114 (1996) 81–91.
281) S. Singh, K. C. Khulbe, T. Matsuura, P. Ramamurthy. *Membrane characterisation by solute transport and atomic force microscopy*. Journal of Membrane Science 142 (1998) 111–127.
282) S. Veríssimo, K. -V. Peinemann, J. Bordado. *Influence of the diamine structure on the nanofiltration performance, surface morphology and surface charge of the composite polyamide membranes*. Journal of Membrane Science 279 (2006) 266–275.
283) S. Wadley, C. J. Brouckaert, L. A. D. Baddock, C. A. Buckley. *Modelling of nanofiltration applied to the recovery of salt from waste brine at a sugar decolourisation plant*. Journal of Membrane Science 102 (1995) 163–175.
284) Saliha Bouranene, Anthony Szymczyk, Patrick Fievet and Alain Vidonne. Effect of salts on the retention of polyethyleneglycol by a nanofiltration ceramic membrane. Desalination 240 (2009) 94–98.
285) Saliha Bouranene, Patrick Fievet, Anthony Szymczyk, Mohamed El-Hadi Samar, Alain Vidonne. *Influence of operating conditions on the rejection of cobalt and lead ions in aqueous solutions by a nanofiltration polyamide membrane*. Journal of Membrane Science 325 (2008) 150–157.
286) Sanchuan Yu, Congjie Gao, Hexiang Su and Meihong Liu. *Nanofiltration used for desalination and concentration in dye production*. Desalination 140 (2001) 97–100.
287) Sangho Lee, Jaehong Kim, Chung-Hak Lee. *Analysis of $CaSO_4$ scale formation mechanism in various nanofiltration modules*. Journal of membrane science 163 (1999) 63-74.
288) Seong-Hoon Yoon, Chung-Hak Lee, Kyu-Jin Kim and Anthony G. Fane. *Effect of calcium ion on the fouling of nanofilter by humic acid in drinking water production*. Wat. Res. Vol. 32, no. 7 (1998) 2180–2186.
289) Serena Bandini. *Modelling the mechanism of charge formation in NF membranes: Theory and application*. Journal of membrane science 264 (2005) 75–86.
290) Serena Bandini, Daniele Vezzani. *Nanofiltration modeling: the role of dielectric exclusion in membrane characterization*. Chemical Engineering Science 58 (2003) 3303 –3326.
291) Serena Bandini, Jrnnifer Drei, Daniele Vezzani. *The role of pH and concentration on the ion rejection in polymide nanofiltration membranes.* Journal of membrane science 264 (2005) 65–74.
292) Seungkwan Hong, Menachem Elimelech. *Chemical and physical aspects of natural organic matter (NOM) fouling of nanofiltration membranes*. Journal of Membrane Science 132 (1997) 159–181.
293) Shiao-Shing Chen, Bao-Chrung Hsu, Chun-Han Ko, Pei-Chi Chuang. *Recovery of chromate from spent plating solutions by two-stage nanofiltration processes*. Desalination 229 (2008) 147–155.
294) Shin-ichi Nakao. *Review Determination of pore size and pore size distribution 3. Filtration* membranes. Journal of Membrane Science 96 (1994) 13 l–165.
295) Shoichiro Nakamura. *Applied numerical methods with software.*
296) Shu-Su Lin, Takuya Harada, Chiho Hata, Osato Miyawki and Kozo Nakamura. *Nanofiltration Membrane Bioreactor for Continuous Asymmetric Reduction of 2-*

Ketoglutarate to Produce L-Glutamate with NADH Regeneration. Journal of Fermentation and Bioengineering Vol. 83 (1997) 54–58.

297) Sidney Yakowitz and Ferenc Szidarov. *An introduction to numerical computations*.

298) Skand Saksena and Andrew L. Zydney. *Pore size distribution effects on electro-kinetic phenomena in semi permeable membranes*. Journal of membrane science 105 (1995) 203–215.

299) Stan Hightower, Kevin Price and Lisa Henthorne. *The US Bureau of Reclamation's research programs in water treatment and desalting technologies.* Desalination 99 (1994) 201–210.

300) Stanislaw Koter. *Determination of the parameters of the Spiegler-Kedem-Katchalsky model for nanofiltration of single electrolyte solutions*. Desalination 198 (2006) 335-345.

301) Stéphane Sarrade, Gilbert M. Rios, Maurice Carlès. *Dynamic characterization and transport mechanisms of two inorganic membranes for nanofiltration* Journal of Membrane Science 97 (1994) 155–156.

302) Sudipta Sarkar, Arup K. SenGupta. *A new hybrid ion exchange-nanofiltration (HIX-NF) separation process for energy-efficient desalination: Process concept and laboratory evaluation*. Journal of Membrane Science 324 (2008) 76–84.

303) Su-Hsia Lin, Ruey-Chang Hsiao, Ruey-Shin Juang. *Removal of soluble organics from water by a hybrid process of clay adsorption and membrane filtration*. Journal of Hazardous Materials B135 (2006) 134–140.

304) Szabolcs Szoke, Gyorgy Patzay, Laszlo Weiser. *Characteristics of thin-film nanofiltration membranes at various pH-values*. Desalination 151 (2002) 123–129.

305) Szilvia Bánvolgyi, Szabina Horváth, Éva Stefanovits-Bányai, Erika Békássy-Molnár, Gyula Vatai. *Integrated membrane process for blackcurrant* (*Ribes nigrum L.*) *juice concentration.* Desalination 241 (2009) 281–287.

T

306) T. K. Dey, V. Ramachandhran, B. M. Misra. *Selectivity of anionic species in binary mixed electrolyte systems for nanofiltration membranes.* Desalination 127 (2000) 165–175.

307) T. Chaabane, S. Taha, J. Cabon, G. Dorange, R. Maachi. *Dynamic modelling of mass transfer through a nanofiltration membrane using calcium slat in drinking water*. Desalination 152 (2002) 275–280.

308) Takeshi Matsuura. *Progress in membrane science and technology for seawater desalination - a review*. Desalination 134 (2001) 47–54.

309) Tak-Hyun Kim, Chulhwan Park and Sangyong Kim. *Water recycling from desalination and purification process of reactive dye manufacturing industry by combined membrane filtration*. Journal of cleaner production 13 (2005) 779–786.

310) Taro Urase, Jeong-ik Oh and Kazuo Yammoto. *Effect of pH on rejection of different species of arsenic by Nanofiltration*. Desalination 117 (1998) 11–18.

311) Thomas A. Davis, J. David Genders and Derek Pletcher. *A first course in ion permeable membranes.* The electrochemical consultancy. 1997. ISBN: 0951730738.

312) Tim Van Gestel, Carol Vandecasteele, Anita Buekenhoudt, Chris Dotremint, Jan Luyten, Roger Leysen, Bart Van der Bruggen, Guido Maes. *Salt retention in nanofiltration with multilayer ceramic TiO_2 membranes.* Journal of membrane science 209 (2002) 379–389.

313) Toshio Luis Baldeón. *Studies of electrically enhanced membrane processes*. Thesis. Department of Chemical Engineering, The University of Manchester Institute of Science and Technology, 2002.

314) Tsuru, Shin-Ichi Nakao and Shoji Kimura. *Calculation of ion rejection by extended Nernst-Planck equation with charged Reverse osmosis membranes for single and mixed*

electrolyte solutions. Journal of chemical engineering of Japan, volume 24, no. 4 (1991) 511–517.

U

V

315) V. J. Shah, C. V. Devmurari, S. V. Joshi. J. J. Trivedi, A. Prakash Rao and P. K. Ghosh. *Acase study of long-term RO plane operation without chemical pre-treatment*. Desalination 161 (2004) 137–144.

316) V. Silva, P. Prádanos, L. Palacio, J. I. Calvo and A. Hernández. *Relevance of hindrance factors and hydrodynamic pressure gradient in the modelization of the transport of neutral solutes across nanofiltration membranes*. Chemical Engineering Journal 149 (2009) 78–86.

317) Vítor Geraldes, Ana Maria Brites Alves. *Computer program for simulation of mass transport in nanofiltration membranes*. Journal of Membrane Science 321 (2008) 172–182.

W

318) W. B. Samuel de Lint, P. Maarten Biesheuvel and Henk Verweij. *Application of the charge regulation model to transport of ions through hydrophilic membranes: one-dimensional transport model for narrow pores (Nanofiltration).* Journal of colloid and interface science 251 (2002) 131–142.

319) W. G. J. van der Meer, C. W. Aeijelts Averink, J. C. van Dijk. *Mathematical model of nanofiltration systems*. Desalination 105 (1996) 25–31.

320) W. M. Deen. *Hindered transport of large molecules in liquid-filled pores*. AICHE journal vol. 33, no. 9 (September 1987) 1409–1425.

321) W. R. Bowen (Fellow) and A. W. Mohammad. *Characterization and prediction of nanofiltration membrane performance – A general assessment*. Trans IChemE Vol. 76 Part A (November 1998) 885–893.

322) W. Richard Bowen and Adel O. Sharif. *Transport through microfiltration membranes-particle hydrodynamics and flux reduction.* Journal of colloid and interface science 168 (1994) 414–421.

323) W. Richard Bowen and A. Wahab Mohammad. *A theoretical basis for specifyingnNanofiltration membranes - Dye/salt/water streams*. Desalination 117 (1998) 257-264.

324) W. Richard Bowen, A. Wahab Mohammad, Nidal Hilal. *Characterisation of Nanofiltration membranes for predictive purposes use of salts, uncharged solutes and atomic force microscopy*. Journal of membrane science 126 (1997) 91–105.

325) W. Richard Bowen and Hilmi Mukhtar. *Characterisation of prediction of separation performance of Nanofiltration membranes*. Journal of membrane science 112 (1996) 263-274.

326) W. Richard Bowen, Julian S. Welfoot. *Modelling the performance of membrane nanofiltration - critical assessment and model development*. Chemical engineering science 57 (2002) 1121–1137.

327) W. Richard Bowen, Julian S. Welfoot and Paul M. Williams. *Linearized transport model for Nanofiltration: development and assessment*. AIChE journal, volume 48, No. 4 (April 2002) 760–773.

328) W. Richard Bowen, Xiaowei Cao. *Electokinetic effects in membrane pores and the determination of zeta-potential*. Journal of membrane science 140 (1998) 267–273.

329) Warren L. McCabe, Julian C. Smith and Peter Harriott. *Unit operations of chemical engineering*.

330) Wayne Jiang, Ronald F. Childs, Alicja M. Mika, James M. Dickson. *Pore-filled cation-exchange membranes containing poly(styrenesulfonic acid) gels*. Desalination 159 (2003) 253–266.
331) Weihua Peng, Isabel C. Escobar, Donald B. White. *Effects of water chemistries and properties of membrane on the performance and fouling — a model development study.* Journal of Membrane Science 238 (2004) 33–46.
332) Wenrui Zuo, Guoliang Zhang, Qin Meng, Hongzi Zhang. *Characteristics and application of multiple membrane process in plating wastewater reutilization*. Desalination 222 (2008) 187–196.
333) William B. Suratt, Douglas R. Andrews, Victor J. Pujals, S. April Richards. *Design considerations for major membrane treatment facility for groundwater*. Desalination 131 (2000) 37–46.
334) William H. Press, Saul A. Teukolsky, William T. Vetterling and Brian P. Flannery.
335) Wolf R. Vieth. *Membrane systems: analysis and design, applications in biotechnology, biomedicine and polymer science*. Hanser publishers. (1988). ISBN: 0-19-520767.

X

336) X. Lefebvre, J. Palmeri, J. Sandeaux, R. Sandeaux, P. David, B. Maleyre, C. Guizard, P. Amblard, J. -F. Diaz, B. Lamaze. *Nanofiltration modeling: a comparative study of the salt filtration performance of a charged ceramic membrane and an organic nanofilter using the computer simulation program NANOFLUX*. Separation and Purification Technology 32 (2003) 117–126.
337) Xianting Xu, H. Garth Spencer. *Transport of electrolytes through a weak acid nanofiltration membrane: Effects of flux and crossflow velocity interprete using a fine-porous membrane model*. Desalination 113 (1997) 85–93.
338) Xianting Xu, H. Garth Spencer. Dye-salt separations by nanofiltration using weak acid polyelectrolyte membranes. Desalination 114 (1997) 129–137.
339) Xiao-Lin Wang, Toshinori Tsuru, Shin-ichi Nakao, Shoji Kimura. *The electrostatic and steric-hindrance model for the transport of charged solutes through nanofiltration membranes*. Journal of Membrane Science 135 (1997) 19–32.
340) Xio-Lin Wang, Chenghong Zhang and Pingkai Ouyang. *The possibility of separating saccharides from a NaCl solution by using Nanofiltration in Diafiltration mode*. Journal of membrane science 204 (2002) 271–281.
341) Xio-Lin Wang, Toshinori Tsuru, Masanori Togoh, Shin-Ichi Nakao and Shoji Kimura. *Evaluation of pore structure and electrical properties of Nanofiltration membranes*. Journal of chemical engineering of Japan, volume 28, no. 2 (1995) 186–192.
342) Xio-Lin Wang, Toshinori Tsuru, Masanori Togoh, Shin-Ichi Nakao and Shoji Kimura. T*ransport of organic electrolytes with electrostatic and steric-hindrance effects through Nanofiltration membranes*. Journal of chemical engineering of Japan, volume 28, no. 4 (1995) 372–380.
343) Xio-Lin Wang, Toshinori Tsuru, Shin-Ichi Nakao and Shoji Kimura. *Electrolyte transport through Nanofiltration membrane by the space-charge model and the comparison with Teorell-Meyer-Sievers model*. Journal of membrane science 103 (1995) 117–133.
344) Xio-Lin Wang, Toshinori Tsuru, Shin-Ichi Nakao and Shoji Kimura. *The electrostatic and steric-hindrance model for the transport of charged solute through Nanofiltration membranes*. Journal of membrane science 135 (1997) 19–32.
345) Xu-Min He, Quan-Ling Xie, Hai-Ping Xia, Wei-Guang Lan. *Application of nanofiltration process in 5'-GMP production*. Desalination 225 (2008) 322–328.

346) Xue Jin, Anna Jawor, Suhan Kim and Eric M.V. Hoek. *Effects of feed water temperature on separation performance and organic fouling of brackish water RO membranes*. Desalination 239 (2009) 346–359.

Y

347) Y. Garba, S. Taha, J. Cabon, G. Dorange. *Modeling of cadmium salts rejection through a nanofiltration membrane: relationships between solute concentration and transport parameters*. Journal of Membrane Science 211 (2003) 51–58.

348) Y. Garba, S. Taha, N. Gondrexon, G. Dorange. *Ion transport modelling through nanofiltration membranes*. Journal of Membrane Science 160 (1999) 187–200.

349) Yasemin Kaya, Coskun Aydiner, Hulusi Barlas, Bulent Keskinler. *Nanofiltration of single and misture solutions containing anionics and non-ionic surfactants below their critical micelle concentrations* (*CMCs*). Journal of Membrane Science 282 (2006) 401–412.

350) Yazhen Xu, Rémi E. Lebrun. *Comparison of nanofiltration properties of two membranes using electrolyte and non-electrolyte solutes*. Desalination 122 (1999) 95–106.

351) Yazhen Xu, Rémi E. Lebrun. *Investigation of the solute separation by charged nanofiltration membrane: effect of pH, ionic strength and solute type*. Journal of Membrane Science 158 (1999) 93–104.

352) Yousif K. Kharaka, Gil Ambats, Theresa S. Presser and Roy A. Davis. *Removal of selenium from contaminated agricultural drainage water by nanofiltration membranes*. Applied Geochemistry 11 (1996) 797–802.

Z

353) Z. V. P. Murthy, Sharad K. Gupta. *Estimation of mass transfer coefficient using a combined nonlinear membrane transport and film theory model*. Desalination 109 (1997) 39–49.

354) Z. V. P. Murthy, Latesh B. Chaudhari. *Application of nanofiltration for the rejection of nickel ions from aqueous solutions and estimation of membrane transport parameters*. Journal of Hazardous Materials, volume 160, issue 1 (December 2008) 70–77.

355) Zoltan Kovacs and Wolfgang Samhaber. *Nanofiltration of concentrated amino acid solutions*. Desalination 240 (2009) 78–88.